# DEVELOPMENT OF 3D TUMOR MODELS FOR INVESTIGATING DRUG EFFICACY OF SAPOGENOL DERIVATIVES

**A Thesis Submitted to**
**the Graduate School of Engineering and Sciences of**
**İzmir Institute of Technology**
**in Partial Fulfillment of the Requirements for the Degree of**

**MASTER OF SCIENCE**

**in Bioengineering**

**by**
**N. Arda PİŞİRİCİ**

**July 2024**
**İZMİR**

We approve the thesis of **Necmettin Arda PİŞİRİCİ**

**Examining Committee Members:**

**Assoc. Prof. Dr. Ahu ARSLAN YILDIZ**
Bioengineering, İzmir Institute of Technology

**Prof. Dr. Erdal BEDİR**
Bioengineering, İzmir Institute of Technology

**Prof. Dr. Özlem YEŞİL ÇELİKTAŞ**
Bioengineering, Ege University

**01 July 2024**

**Assoc. Prof. Dr. AHU ARSLAN YILDIZ**
Supervisor, Bioengineering, İzmir Institute of Technology

**Assoc. Prof. Dr. Ceyda ÖKSEL**
Head of the Department of Bioengineering

**Prof. Dr. Mehtap EANES**
Dean of the Graduate School of Engineering and Sciences

# ACKNOWLEDGMENTS

Firstly, I would like to mention my deep and sincere gratitude to my supervisor Assoc. Prof. Dr. Ahu ARSLAN YILDIZ for her patience, help, counseling, and support throughout my thesis studies. I acknowledge TUBITAK 2210/C National MSc Scholarship Program in the Priority Fields in Science and Technology for financial support. I would like to thank Göklem ÜNER, a member of Bedir Lab, for her contributions to the sapogenol derivative toxicity parts of the thesis.

I am very grateful to my colleague and friend Ece ÖZMEN for her guidance, valuable friendship, encouragement, and deep support throughout my graduation life and personal life. I especially thank Biomimetics Research Group members; Özüm YILDIRIM, Alper Baran SÖZMEN, Başak ÇOBAN, Zeynep ALTAN, Rümeysa BİLGİNER KARTAL, for their friendship, support, help, and patience. I also want to express special thanks to my friend Çiğdem TANRIKULU for her encouragement, and support.

Finally, I would like to show my deepest appreciation and love to my mother Hülya PİŞİRİCİ for her endless encouragement and support.

# ABSTRACT

## DEVELOPMENT OF 3D TUMOR MODELS FOR INVESTIGATING DRUG EFFICACY OF SAPOGENOL DERIVATIVES

In studies on the treatment of cancer, which is a common disease of the latest period, 3D cell culture models, which show high similarity to tissue physiology, attract attention in order to investigate the efficacy of potential drugs. These models are preferred in drug development studies by overcoming many problems in 2D cell culture studies**.** In the completed research, drug activity screenings of sapogenol-derived molecules and anticancer drug Ptx were performed on 3D tumor spheroid models produced using new generation magnetic levitation (MagLev) technology. The magnetic levitation is a scaffold free methodology which allows the cells magnetized by the effect of paramagnetic agents in the magnetic field created by two magnets to balance at a unique height (levitation height) depending on density, without requiring an external force. With this method, intercellular interactions with the same level of levitation heights can be increased and 3D spheroid structures can be obtained quickly without the need any scaffold. In the completed thesis; As a control group for MagLev spheroids, hanging drop methodology was preferred with the same cell lines. The activity of sapogenol-derived molecules and the Ptx were investigated. The expected toxic effect on spheroids was observed and comparative results were shared. MagLev based new drug activity screening model which overcomes the disadvantages of 2D cell culture studies, can imitate real tumor physiology much more closely, can provide easy, realistic and fast results in drug screenings and investigating the effects of different molecules before clinical studies has been devoloped.

# ÖZET

## SAPOGENOL TÜREVLERİNİN İLAÇ ETKİNLİKLERİNİN ARAŞTIRILMASI İÇİN 3B TÜMÖR MODELLERİNİN GELİŞTİRİLMESİ

Son dönemin hastalığı olan kanser tedavisi çalışmalarında potansiyel ilaçların etkinliklerinin araştırılması için doku fizyolojisine yüksek benzerlik gösteren 3 boyutlu (3B) hücre kültürü modelleri dikkat çekmektedir. Bu modeller 2B hücre kültürü çalışmalarındaki birçok problemin aşılmasını sağlayarak ilaç geliştirme çalışmalarında tercih edilmektedir. Bu çalışmada yeni nesil manyetik levitasyon (MagLev) kullanılarak üretilmiş 3B tümör sferoid modelleri üzerinde sapogenol türevi potansiyel kanser ilaçları ve FDA onaylı antikanser ilacı Paklitaksel'in (Ptx) ilaç aktivite taramaları yapılmıştır. Manyetik levitasyon yöntemi doku iskelesinden bağımsız olup, iki mıknatıs tarafından yaratılmış manyetik alan içerisinde paramanyetik ajanların etkisiyle manyetize edilmiş hücrelerin yoğunlarına bağlı olarak kendilerine has bir yükseklikte (levitasyon yüksekliği) harici bir kuvvet gerektirmeden asılı kalmalarını sağlamaktadır. Bu yöntemle, levitasyon yükseklikleri aynı seviyede olan hücreler arası etkileşimler artarak 3B sferoid yapıları doku iskelesine ihtiyaç duyulmadan hızlıca elde edilebilmektedir. Tamamlanan çalışmada; tümör sferoid modelleri her hücre hattı için ayrı şekilde elde edilmiştir. MagLev yöntemine ek, kontrol amaçlı, aynı hücre hatlarıyla asılı damlacık yöntemi kullanılarak 3B sferoid modelleri elde edilmiştir. Oluşturulan sferoid modelleri üzerinde 2B hücre kültüründe ilaç etkinliği belirlenmiş sapogenol türevi ilaç moleküllerinin ve Ptx'in aktivitesi araştırılmıştır. Sferoid modelleri üzerinde beklenen toksik etki görülmüş, karşılaştırmalı sonuçlar paylaşılmıştır. Bu sonuçlarla birlikte, 2B hücre kültürü kullanılarak yapılan tümör fizyolojisi araştırmaları yerine bu modellerin dezavantajlarını geride bırakan, gerçek tümör fizyolojisini çok daha yakın seviyede taklit edebilen, klinik araştırmalar öncesinde ilaç taramalarında ve farklı moleküllerin etkilerinin araştırılmışında kolay, gerçekçi ve hızlı sonuçlar sağlayabilecek manyetik levitasyon temelli yeni bir ilaç aktivite tarama modeli geliştirilmiştir.

# TABLE OF CONTENTS

# LIST OF FIGURES

**Figure** **Page**

**Figure** **Page**

**Figure** **Page**

**Figure** **Page**

**Figure** **Page**

**Figure** **Page**

**Figure** **Page**

**Figure** **Page**

**Figure** **Page**

# CHAPTER 1

# INTRODUCTION

## 1.1. Scope of Thesis

It is aimed to investigate potential anticancer effects of molecules which derived from a cycloartane-type sapogenol on 3D tumor spheroid models. (Jensen et al., 2022). For this purpose, hanging drop and magnetic levitation methods, which are scaffold free 3D cell culturing methods, were used. Tumor spheroid models were obtained from HeLa, Sh-Sy5y, HepG2 and Mcf-7 cell lines. Toxic effects caused by the FDA-approved anticancer drug paclitaxel and four different molecules derived from sapogenol were investigated on the obtained models.

## 1.2. Tissue Engineering

The tissue engineering discipline was developed by Prof. Dr. Robert Langer from the Massachusetts Institute of Technology and Prof. Dr. James Vacanti from Harvard University in 1993. Tissue engineering is based on the repair or replacement of tissues that fail to function. While there may be congenitally damaged tissues, they may lose their function later due to disease or accident, or tissue death, called necrosis due to trauma, may occur (Langer & Vacanti, 1993).

At this stage, tissue engineering aims to produce 3D models that can mimic real tissue physiology in the laboratory environment by making use of material science, medical architecture, and cellular studies. Different tissue models have been targeted in recent years. Intensive studies are carried out on bone tissue, cartilage tissue, and skin

tissue (Arslan-Yildiz et al., 2016; Ferreira et al., 2019; Marques et al., 2022; Özmen et al., 2023; Seo et al., 2023; Souza et al., 2010; Turker & Arslan-Yildiz, 2018; Yildirim-Semerci et al., 2024). Tissue engineering is used more effectively in drug screening studies. Also, personalized medicine helps determine whether certain drugs work better in some patients based on their genetic characteristics and also reduces animal testing and its costs.

## 1.3. 3D Cell Culture Studies

2D cell culture is one of the basic methods that has been used for many years to study cell behaviour (Fontoura et al., 2020; Lugert et al., 2019)and biology. With this method, basic biological processes have been extensively investigated, and cellular functions and mechanisms have been revealed. The aim of 2D cell culture is to multiply cells in a single layer while adhering to the surface. In this process, the nutrients and environmental conditions necessary for the cells to survive and grow are provided to them. 2D studies have an important place in many diseases that are still being researched and are seen as a basic step (Fontoura et al., 2020; Lugert et al., 2019). However, since 2D cell culture models cannot fully mimic the complex 3D structure and related microenvironment found in living tissues, in recent years alternative approaches such as 3D cell culture models and organoid structures have become more preferred for more accurate representation of in vivo conditions and understanding of tissue architecture and cell functionality, which has begun to be implemented (Fontoura et al., 2020; Marques et al., 2022;). While 3D cell culture models increase cell-cell and cell-ECM interactions, they clearly reveal the need for nutrients and oxygen in 3D cell structures and the cellular effects in cases of deficiency (Asghar et al., 2015). 3D cell culture methods are basically divided into scaffold-based and scaffold-independent methods as illustrated in Figure 1. ( 2020; Jeong et al., 2016; Türker et al., 2018)

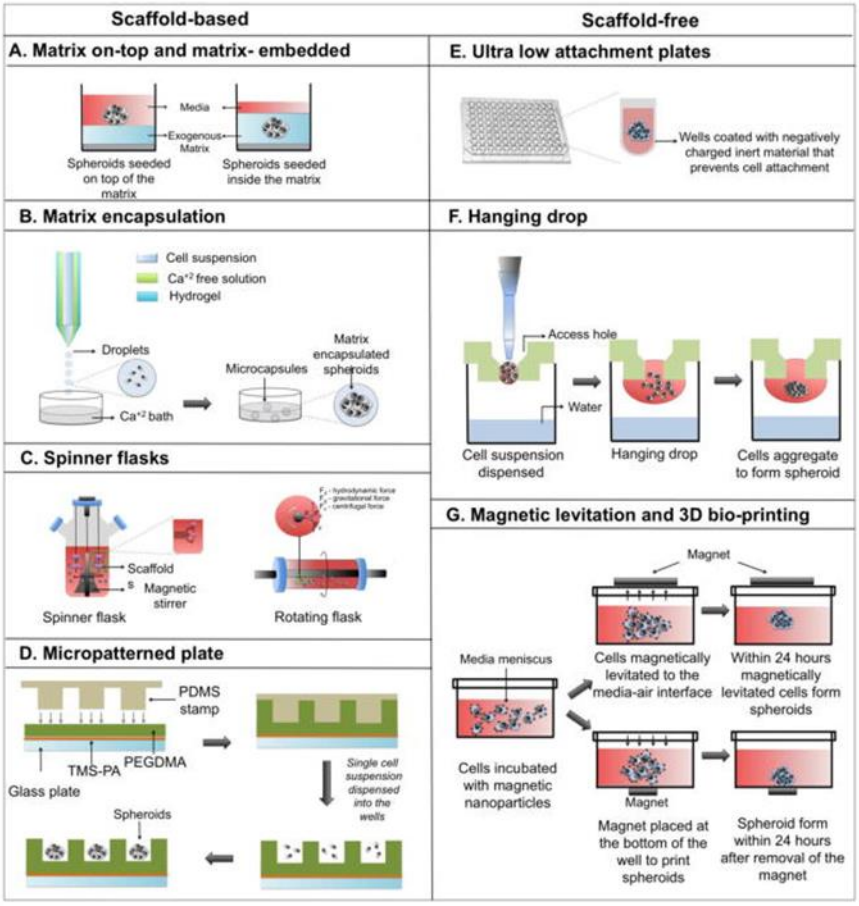


**Figure 1**. Various techniques are used to obtain 3D tumor spheroids; a-d) scaffold-based methods **e-g)** scaffold-independent methods(Nath & Devi, 2016).

## 1.3.1. Scaffold Based 3D Cell Culture Methodologies

Tissue scaffold-based cultures rely on the presence of a supporting material for cells to form tissue-like structures (Özmen et al., 2023). 3D scaffolds are important in supporting cell growth, tissue regeneration, and the transport of nutrients and waste (Tavafoghi et al., 2020). It is critical that the scaffold have mechanical properties compatible with the tissues in the region where it is implanted (Arslan-Yildiz et al., 2016; Yildirim & Arslan-Yildiz, 2022). The 3D scaffold model produced must be durable enough to resist structural collapse during implantation and should not damage the surrounding tissues (Yesil-Celiktas et al., 2018). Selecting the most appropriate scaffold

material is crucial to completing targeted drug screening and ensuring the successful implantation of the tissue model (Yesil-Celiktas et al., 2018). Tissue scaffolds can be produced with different techniques. Examples of tissue scaffold production methods include electrospinning, freeze drying, and bioprinting, which are frequently preferred in the literature (Arslan Yildiz et al., 2013; 2020; Özmen et al., 2023; Yildirim & Arslan-Yildiz, 2022; Yildirim-Semerci et al., 2024). Such methods are likely to require the use of organic solvents that may inhibit cell proliferation and differentiation, and it is not always possible to control the scaffold geometry. In addition, the scaffolds obtained by these methods are suitable for a single cell type and are generally homogeneous.

### 1.3.2. Scaffold Free 3D Cell Culture Methodologies

Scaffold-free methods enable the formation of spherical multicellular structures called "spheroids" by aggregating cells. (Fennema et al., 2013) While spheroids obtained by scaffold-free 3D culturing methods show high similarities to real tumor physiology, the methods are expected to be simple and reproducible (Crnogorac et al., 2021; Fennema et al., 2013; Nath & Devi, 2016). Examples of scaffold-free 3D culturing methods include the hanging drop method and the Magnectic Levation method.

#### 1.3.2.1 Magnetic Levitation Methodology

The Magnetic Levitation (MagLev) technique, which works on the principle of suspending cells in a weightless environment, is one of the scaffold-free 3D cell culture methods that has become frequently preferred in recent years (Anil-Inevi et al., 2018, 2021; Dabbagh et al., 2022; Jaganathan et al., 2014; Ozefe & Arslan Yildiz, 2020; Sabino et al., 2014; Sarigil et al., 2021; Souza et al., 2010; Tepe et al., 2023). In magnetic levitation technology, two magnets positioned in an anti-Helmholtz configuration are used, and due to the magnetic effect created by the same poles and the effect of the paramagnetic agent in the environment, magnetized objects are suspended at different

levels according to their density differences without requiring any external force (Figure 2) (Onbas & Arslan Yildiz, 2023; Ozefe & Arslan Yildiz, 2020; Souza et al., 2010). As cell-cell interactions increase in suspended cells, spheroid structures begin to form over time. (Türker et al., 2018)

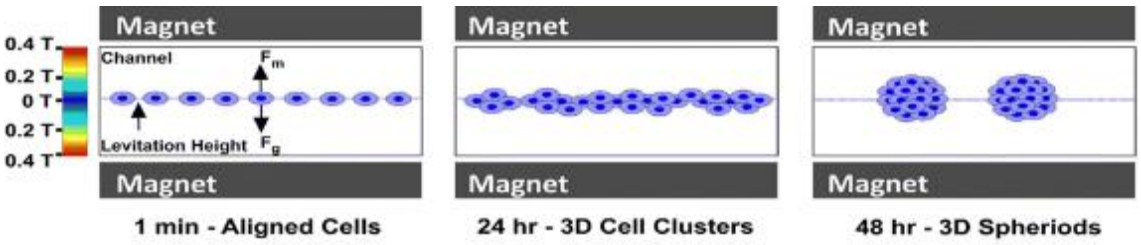


**Figure 2**. Schematic representation of 3D spheroid production with the MagLev method (Türker et al., 2018).

## 1.3.2.2 Hanging Drop Methodology

In the hanging drop method, suspended cells are cultured in droplets in an upside-down position on the culture plate lid by taking advantage of surface tension (Timmins & Nielsen, 2007). Cells that come together under the influence of gravity hold on to each other and form 3D spheroid structures (Wang et al., 2017). The size of the spheroids obtained by the method varies depending on the cell type and number of cells used (Banerjee & Bhonde, 2006). Although it is possible to obtain a large number of 3D spheroid models at once with this method, it has disadvantages such as not being able to culture the obtained spheroids for a long time, causing a lot of workloads in scanning, and not being able to add medium or other chemicals during the culturing process (Türker et al., 2018). (Huang et al., 2020)

## 1.4. Drug Screening

Drugs that play an important role in the diagnosis and treatment of existing diseases in the world have a long discovery period. Drug screening studies represent an important stage in the drug discovery process. This process aims to identify developable and reliable potential therapeutic agents. These studies enable systematic investigation of compounds in terms of their interactions with specific biological targets and modulation of molecular pathways. The effects of potential drug candidates at the molecular level are being examined by many research groups in different places of the world (Cortini et al., 2023; Sevimli-Gur et al., 2013; Yesil-Celiktas et al., 2010). Drug screening studies offer a diverse range of strategies to identify potential therapeutic candidates. Cellular studies are essential and frequently preferred in the literature. Cell-based assays are important for drug discovery and development as they have the ability to produce biomedically reliable information (Rimann et al., 2014). However, with developing technology, drug screening studies using 3D cell culture have accelerated recently due to the insufficiency of 2D cellular studies in terms of physiological mimicking (Bilginer & Arslan Yildiz, 2019; Bumpers et al., 2015;, 2021; Muguruma et al., 2020).

# CHAPTER 2

# MATERIALS AND METHODS

## 2.1. Materials

N-52 level neodymium (NdFeB) magnets, Different paramagnetic contrast agents containing gadolinium (Gd3+) ion; Gadobutrol (Gx) and Gadoteric acid (Dx) were preferred to provide magnetic effect in the magnetic levitation system. Cell culture experiments were performed by using Penicillin/Streptomycin (P/S), Trypsin-EDTA (sterile-filtered, 0.25%, BioReagent), high glucose Dulbecco's Modified Eagle's Medium (DMEM), Phosphate Buffered Saline (PBS, pH 7.4 10X); fetal bovine serum (FBS) from Gibco, and Dimethyl sulfoxide (DMSO) from AppliChem. HeLa (ATCC CCL-2), SH-SY5Y (ATCC CRL-2266), HepG2 (ATCC HB-8065) ve MCF-7 (ATCC HTB-22) were used for developing 3D tumor spheroid models and drug screening step. Propidium Iodide and CytoCalcein AM from (AAT Bioquest) were used for live/dead assay. MTT (3-(4,5-Dimethylthiazol-2-yl)-2,5-Diphenyltetrazolium Bromide), Actin Cytoskeleton/Focal Adhesion Staining Kit from Sigma-Aldrich, and Anti-collagen Type-I from Merck Millipore were used for immunostaining assay.

## 2.2. Methods

The flow of all studies planned to be carried out within the scope of the thesis step by step in this part.

## 2.2.1. Synthesis of Sapogenol Derivatives

Sapogenols planned to be used within the scope of the study have a cytotoxic effect on different cell types. It is AG-08 and its derivatives, demonstrated by BEDİR and his team, and was obtained by semi-synthesis in the group's further studies (within the scope of master's thesis number 554485). CG-03, which was determined to have similar activity to AG-08 in the group's previous studies, was chosen as another cytotoxic molecule to be studied in the 3D cell culture model (Üner et al., 2020). In order to fully evaluate the results, it was decided to use two molecules with similar chemistry but not cytotoxic as negative controls (AG-04 and CG-04) (Üner et al., 2022). Within the scope of step 1, 30 mg of each of the four sapogenol derivatives was produced. These molecules were obtained by following the method specified in the master's thesis numbered 554485, by reacting AG and CG with p-TsCl (p-tosyl chloride) and MsCl (Methane sulfonyl chloride) and purifying them by column chromatography. The chemical structures of the four different sapogenol derivatives used are shared in Figure 3.

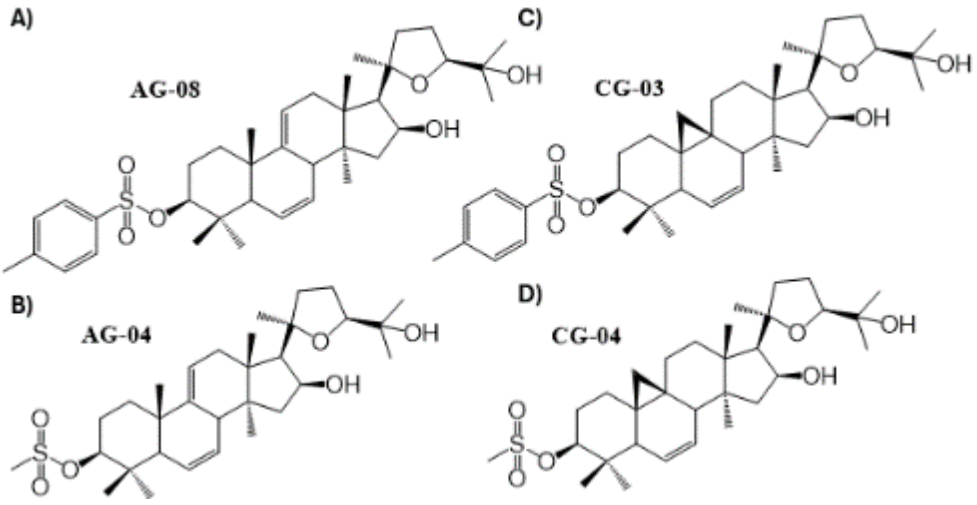


**Figure 3**. Sapogenol derivatives' chemical structures. a) AG-08 b) AG-04 c) CG-03 d) CG-04.

### 2.2.2. Paramagnetic Contrast Agent Optimization for Cell Culture Studies

#### 2.2.2.1 Standard 2D Cell Culture

To obtain 2D standard cell cultures, previously frozen HeLa, SH-SY5Y, HepG2, MCF-7, and THP-1 cell lines were thawed in flasks containing 5 ml cell medium with $1x10^6$ cells. Cells were incubated in a 37 °C, 5% $CO_2$ environment, and when cell confluency was 80-90%, they were passaged and brought to standard 2D cell culture conditions (Arora, 2013; Marin et al., 2001) .

#### 2.2.2.2. Determination of the Effects of Paramagnetic Contrast Agent Type and Concentration on Cell Viability, Growth and Morphology

With 2D standard cell cultures, viability tests were carried out to understand the toxic effects of paramagnetic contrast agents (Gadovist and Dotarem), which enable the effective operation of the magnetic levitation principle, on cell viability, cell morphology, and cell growth (Parant et al., 2019). Each experiment with paramagnetic agents tested at different concentrations (0-10-30-50-100 mM) was set up to have at least three repetitions (Türker et al., 2018). In experiments performed in 96-well plates, cells were incubated for a week at 37 °C with 5% CO2, and cell viability tests were performed on days 1, 3, 5, and 7 to understand the toxic effect of paramagnetic contrast agents on the cells. MTT and Alamar Blue methods were preferred to analyse cell viability quantitatively. For MTT analysis, cell medium containing 10% MTT (3-(4,5-dimethylthiazol-2-yl)-2,5-diphenyltetrazolium bromide) solution was added to each well in a volume of 200 µl. Formazan crystals formed after 4 hours of incubation were dissolved with DMSO, and absorbance was measured at wavelengths of 565-650 nm with a UV-Vis spectrophotometer (Van Tonder et al., 2015). For Alamar Blue analysis, cell medium

containing 1% Alamar Blue was added to each well in a volume of 100 µl. After 4 hours of incubation, absorbance was measured at wavelengths of 570-600 nm with a UV-Vis spectrophotometer (Longhin et al., 2022). Graphs showing the change in cell viability over time were drawn using the absorbance values obtained. In addition to quantitative measurement methods, a live/dead assay was applied to examine cell viability and morphology. Calcein Green and Propidium Iodide (PI) staining were performed, and cell viability was analysed in the images obtained using a fluorescence microscope. By comparing the results of the three methods, the types and concentrations of paramagnetic agents that do not cause toxic effects on cells were determined. The determined agent type and concentrations that did not cause toxic effects were used to create 3D tumor spheroid models, which was the next step of the study.

### 2.2.3. Creation and Characterization of In Vitro 3D Tumor Spheroid Model with Magnetic Levitation Method

In the 2.4 step, the necessary optimizations for the paramagnetic contrast agent type and concentration were completed for each cell line in 2D cell culture. Here, 3D culturing studies were started by determining the paramagnetic agent concentration below the toxicity threshold value. In this step, studies were continued with the paramagnetic agent Gadobutrol (Gx) due to its lower toxic effect. Optimization studies were carried out for four different cell lines for the number of cells, the incubation period required for spheroid formation, and the concentration of the paramagnetic agent.

#### 2.2.3.1 Optimization of Parameters for 3D Cell Culture Studies with the Magnetic Levitation Method and In Vitro 3D Cell Culturing

NdFeB magnets, 40×5 mm in size and placed in anti-Helmholtz configuration, providing a 0.4 T magnetic field, were used for 3D cell culture . Although it varies from cell to cell, cell numbers in the range of 5-25 x $10^3$ were tried to obtain the appropriate

spheroid structure (Onbas & Arslan Yildiz, 2021). Due to its low toxic effect, optimization was made for the concentration of Gx that would keep the cells suspended until they formed a spheroid, starting from a concentration of 10 mM and going up to a maximum of 50 mM. Culturing was continued for 7 days. Light images were taken on days 1, 2, 3, 4 and 7. At the end of the 7$^{th}$ day, the viability of the obtained spheroid/spheroid-like structures was checked by performing a live-dead test (Delikoyun et al., 2021).

#### 2.2.3.2 Characterization of in vitro 3D Tumor Spheroid Models Produced by Magnetic Levitation Method

The characterization of 3D tumor spheroid models obtained by the magnetic levitation method from HeLa, MCF7, SH-SY5Y, and HepG2 cell lines was carried out with comparisons made between the 1$^{st}$ and 7$^{th}$ days. Cell nuclei, cell scaffold formation, and extracellular matrix formation were observed using DAPI, Actin and Collagen I immunofluorescence staining methods (Bilginer et al., 2021; Onbas & Arslan Yildiz, 2023).

### 2.2.4. Creation and Characterization of 3D Tumor Spheroid Model with the Hanging Drop Method

The hanging drop method is preferred to the addition of Magnetic Levitation method to develop 3D tumor spheroid models. Firstly, for developing 3D models, cell number, incubation process, and drop size optimization were completed. In this method, cell medium exchange is a very difficult process. Spheroid structure might be lost or dispersed during this process. Therefore, to obtain the spheroid model, the ideal cell number and drop size that provide sufficient medium content must be determined (Raghavan et al., 2015). For this reason, the optimum cell number and drop size were determined. First, drops of 10 and 15 µl volumes were dropped into the petri dish and

incubated for 24 hours, with the drops remaining upside down on the surface. Since the 15 µl drops stuck to the surface because they did not have the required surface tension, the experiments were continued with 10 µl drops. Afterwards, the necessary optimizations to determine the appropriate number of cells for different cell lines were completed for values in range of 5-50 x $10^3$ (Yilmaz & Sakarya, 2018). It was concluded that 24-48 hours were sufficient for the culturing process. This process varies from cell to cell. The characterization of 3D tumor spheroid models obtained by the hanging drop method was carried out at the $24^{th}$ hour. Cell nuclei, cell scaffold formation, and extracellular matrix components were observed using DAPI, Actin, and Collagen I immunofluorescence staining methods. The obtained results were compared with the characterization results in spheroid models obtained with the MagLev method (Bilginer et al., 2021; Onbas & Arslan Yildiz, 2023).

### 2.2.5. Drug Activity Screening of Sapogenol Derived Molecules and Paclitaxel Anticancer Drug

In the last step of the thesis, drug activity screenings of the FDA-approved anticancer drug Paclitaxel (Ptx) whose chemical structures were shared in Figure 4 and sapogenol-derived molecules (structures were shared in Figure 3) were carried out in 2D cell culture and 3D tumor spheroid models, and the results were compared with each other. $IC_{50}$ values were determined from the results obtained in 2D cell culture.

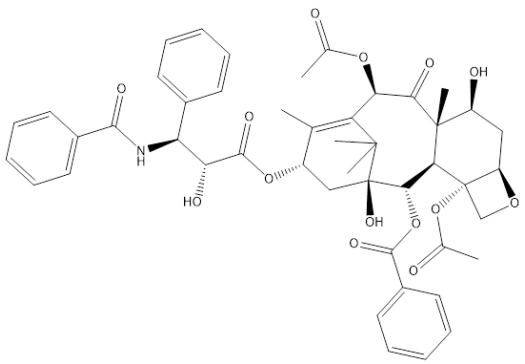


**Figure 4**. Chemical structure of Paclitaxel (Riccardi et al., 1995)

### 2.2.5.1 Drug Screening of Sapogenol Derived Molecules in Standard 2D Cell Culture

Here, viability tests were conducted to understand the toxic effects of the FDA-approved anticancer drug PTX and four different sapogenol-derived molecules on cell viability, cell morphology, and cell growth in cancer cell lines. In experiments carried out in 96-well plates, cells were incubated separately in the presence and absence of 10 mM paramagnetic agent Gx at 37 °C and 5% $CO_2$ environment for 24 hours. Then, the PTX and sapogenol-derived molecules were added separately at different concentrations (0-5-25-50-100-200 nM for Ptx; 0-1-5-10-20-30 μM for sapogenols) (Liebmann et al., 1993), and incubation was performed for 48 hours. Cell viability tests were performed at 24 and 48 hours to investigate the toxic effect of the molecules on the cells. MTT method was preferred to analyse cell viability quantitatively. For MTT analysis, cell medium containing 10% MTT (3-(4,5-dimethylthiazol-2-yl)-2,5-diphenyltetrazolium bromide) solution was added to each well in a volume of 200 μl. Formazan crystals formed after 4 hours of incubation were dissolved with DMSO, and absorbance was measured at wavelengths of 565-650 nm with a UV-Vis spectrophotometer. Graphs showing the change in cell viability over time were drawn using the absorbance values obtained. In addition to quantitative measurement methods, live/dead assay was applied to examine cell viability and morphology. Calcein Green and Propidium Iodide (PI) staining were performed, and cell viability was analyzed in the images obtained using a fluorescence microscope.

### 2.2.5.2 Drug Activity Screening in 3D Tumor Spheroids Produced by the Hanging Drop Method

After successfully obtaining tumor spheroids from different cell lines using the hanging drop method, the spheroids in the petri dish were transferred to 96-well plates via micropipettes in order to perform drug screening. After moving the spheroids, medium was added to make the total volume 190 μL. Concentration adjustment was made

with DMSO so that the Ptx to be tested was in the range of 0-400 nM (0-100-200-400 nM) and the s were in the range of 0-60 μM (0-20-40-60 μM). Drug/molecule solution was mixed with cell medium, and the total volume was added to the wells as 10 μL. After the 72-hour incubation period, the medium containing the molecules or drug was collected with the help of a micropipette without damaging the spheroids. For the live-dead test, the solution prepared as 0.1% was added to each well as 50 μL, and after 30 minutes of incubation, viability analysis was performed on a fluorescence microscope. For the MTT test, the solution prepared at 10% was added to each well as 200 μL, and after 3 hours of incubation, the formazan crystals formed on the spheroids were dissolved using DMSO. At this stage, spheroids were disrupted by pipetting. Absorbance was measured at wavelengths of 565-650 nm with a UV-Vis spectrophotometer. Graphs showing the change in cell viability over time were drawn using the absorbance values obtained.

#### 2.2.5.3 Drug Activity Screening in 3D Tumor Spheroids Produced by Magnetic Levitation Method

After successfully obtaining tumor spheroids/spheroid-like structures of different cell lines with the MagLev method, the petri dishes were removed from the MagLev devices to enable drug screening. The medium in the Petri dishes was collected without damaging the 3D structures. Concentration adjustment was made with DMSO so that the Ptx to be tested was in the range of 0-400 nM (0-100-200-400 nM) and the s were in the range of 0-60 μM (0-20-40-60 μM). The medium - molecule/drug suspension total volume was 800 μL and added slowly to the petri dishes without damaging the spheroids. After the 72-hour incubation period, the medium containing the molecules/drug was collected with the help of a micropipette without damaging the spheroids. For the live-dead test, the solution prepared as 0.1% was added to the petri dishes as 100 μL, and viability analysis was performed under a fluorescence microscope after 30 minutes of incubation. For the MTT test, the solution prepared as 10% was added to the petri dishes as 200 μL, and after 3 hours of incubation, the spheroids were moved separately to 96-well plates. Formazan crystals formed on the spheroids were dissolved using DMSO. At

this stage, the spheroids were broken up by pipetting. Absorbance was measured at wavelengths of 565-650 nm with a UV-Vis spectrophotometer. Graphs showing the change in cell viability over time were drawn using the absorbance values obtained.

### 2.2.6 Statistical Analyses

The data obtained within the scope of the thesis study is presented as "mean value ± standard deviation." The statistical test used was determined according to the convenience of the obtained data with normal distribution and variance homogeneity calculations, and the evaluation was made with the GraphPad Prism program. Bonferroni was used as a post hoc test, and the significance limit was evaluated based on the p value. $p^* \leq 0.05$, $p^{**} \leq 0.01$, $p^{***} \leq 0.001$ (Rice, 1989)

# CHAPTER 3

# RESULTS & DISCUSSIONS

## 3.1. Standard 2D Cell Culture

The purpose of this step was determined as the optimization of paramagnetic agent concentrations that can levitate the cells and also do not show any cytotoxic effects on the cells for the purpose of 3D culturing of the cells (HeLa, MCF-7, SH-SY5Y, and HepG2). For this goal, standard 2D cell cultures of the cells were obtained, and then studies were started with HeLa cells to determine the effects of paramagnetic contrast agent type and concentration on cell viability, growth, and morphology.

Firstly, standard 2D cell culturing of HeLa (human cervical epithelial adenocarcinoma cell, ATCC® CCL-2™), MCF-7 (human breast adenocarcinoma cell, ATCC® HTB-22™), SH-SY5Y (human neuroblastoma cell, ATCC® CRL-2266™) and HepG2 (human liver hepatocellular carcinoma cell, ATCC® HB-8065™) cells was performed. To obtain 2D standard cell cultures, frozen HeLa, MCF-7, SH-SY5Y, and HepG2 cell lines were thawed and planted individually in 25-T flasks containing 5 mL of cell medium. Within the scope of the culturing, DMEM containing 10% Fetal Bovine Serum and 1% antibiotics was used as cell medium for all cell lines. The cells were incubated in a 37 °C, 5% CO2 environment, and when they reached a confluency of 80-90%, they were passaged and standard 2D cell culture conditions were reached. Figure 5 shows light microscope images of standard 2D cell cultures of each cell line. All of the cell lines shared in Figure 5 are adherent and have epithelial characteristic. After adhering to the flask surface, the cells acquired their polygonal morphology in accordance with the character of epithelial cells.

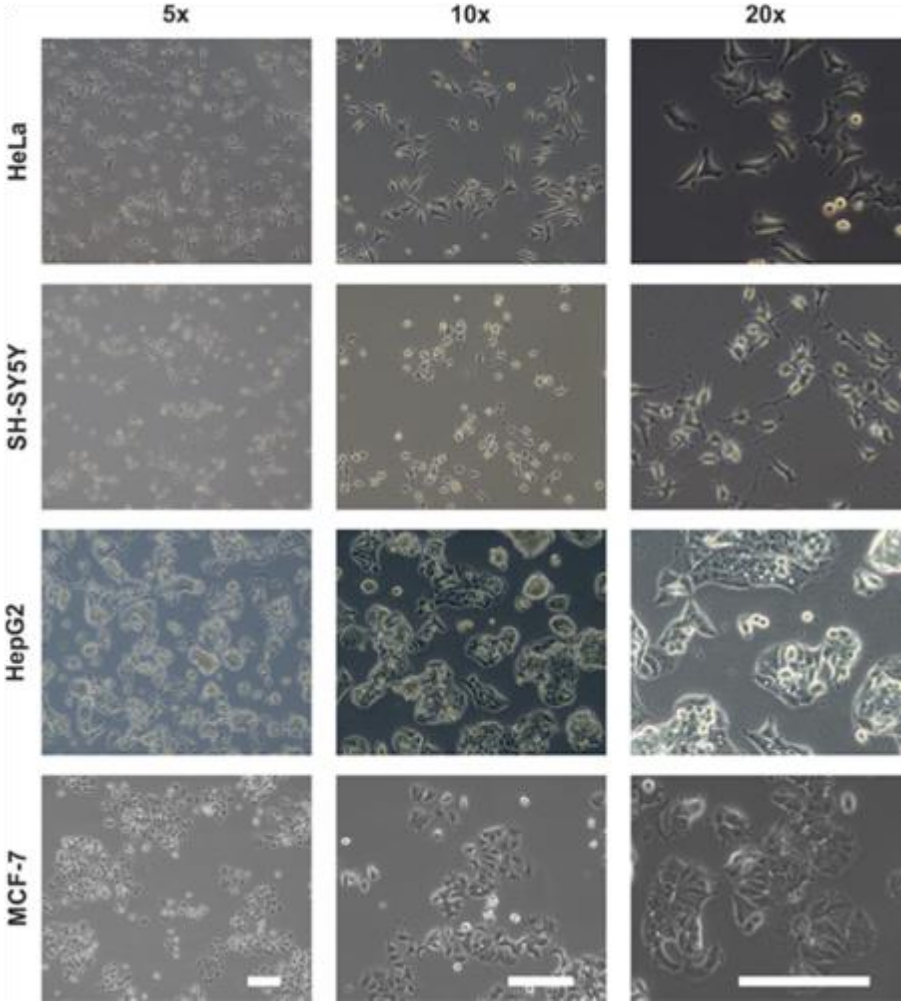


**Figure 5**. Light microscope images of standard 2D cell cultures of HeLa, SH-SY5Y, HepG2 and MCF-7 cell lines (scale size: 200 μm).

### 3.1.2. Determination of the Effects of Paramagnetic Contrast Agent Type and Concentration on Cell Viability, Growth and Morphology

After obtaining standard 2D cell cultures, the next step was to determine the effects of the type and concentration of the paramagnetic contrast agent used on cell viability, growth, and morphology. The studies started by investigating the effects of Gx and Dx paramagnetic contrast agents on HeLa cells. Accordingly, when HeLa cells cultured in 2D reached an 80-90% confluency, they were removed from the 2D cell

culture medium and planted in 96-well plates with 5000 cells in each well for each concentration value. Experiments were carried out in three repetitions for each concentration.

The plates were incubated for a week at 37 °C, 5% CO2, and cell viability tests were performed on the 1st, 3rd, 5th, and 7th days to understand the toxic effect of paramagnetic contrast agents on the cells. In this context, the viability of HeLa cells incubated in media containing Gx and Dx at various concentrations separately at the end of the 1st, 3rd, 5th, and 7th days was examined quantitatively using MTT analysis methods. According to the absorbance values obtained as a result of MTT analysis, cell viability graphs depending on paramagnetic agent concentration were obtained as shown in Figure 6.

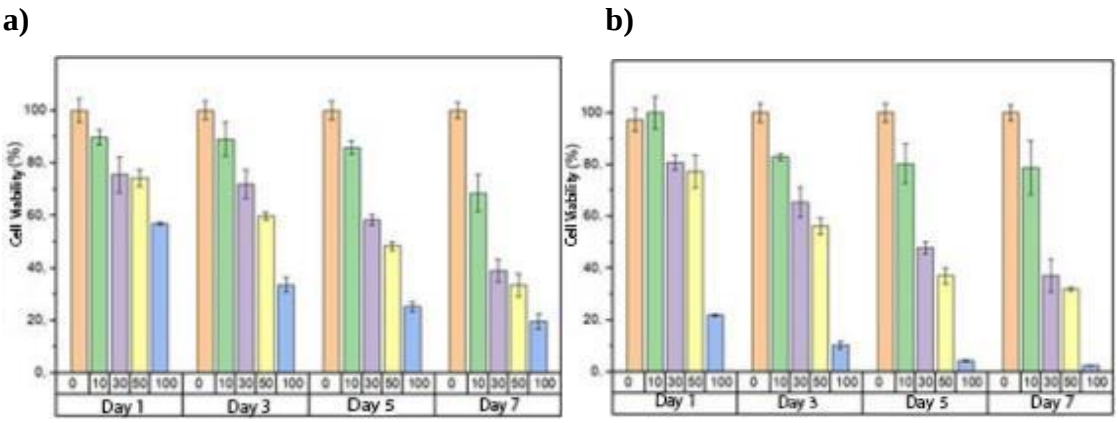


**Figure 6**. Effect of paramagnetic contrast agents on HeLa cell viability. Cell viability results obtained as a result of MTT analysis **a)** Gx effect **b)** Dx effect (Gx-Dx concentration unit: mM).

As shown in Figure 6, the increase in the concentration of paramagnetic agents caused a decrease in cell viability. However, when Gx and Dx paramagnetic contrast agents were compared, Dx was found to be more toxic than Gx. Especially when 100 mM Dx was used, cell viability dropped below 10% on the 3rd day. This situation is associated with the half-life of paramagnetic contrast agents in the literature. The half-life of the Gx agent is approximately 23 hours and is approximately 3 times slower than the Dx agent (Idée et al., 2008). This situation, which causes a decrease in the release of free Gd3+

ions, makes the Gx agent less toxic to cells. According to the MTT results obtained, the paramagnetic agent concentrations were determined as 10 and 30 mM, with 60% and above cell viability observed for HeLa cells after one week of incubation.

Figure 7 shows cell viability graphs with the results obtained from Alamar Blue (AB) analysis. According to the graphs, it was observed that there was a decreasing trend in cell viability as the paramagnetic agent concentration increased. In the comparison between the two agents, it can be said that Dx has a more toxic effect, especially by comparing the viability of the cells under the effect of the 100 mM drug. Viability values obtained in Alamar blue tests are higher than in MTT analysis. This result was also encountered in previous studies conducted by our group.

**a)** **b)**

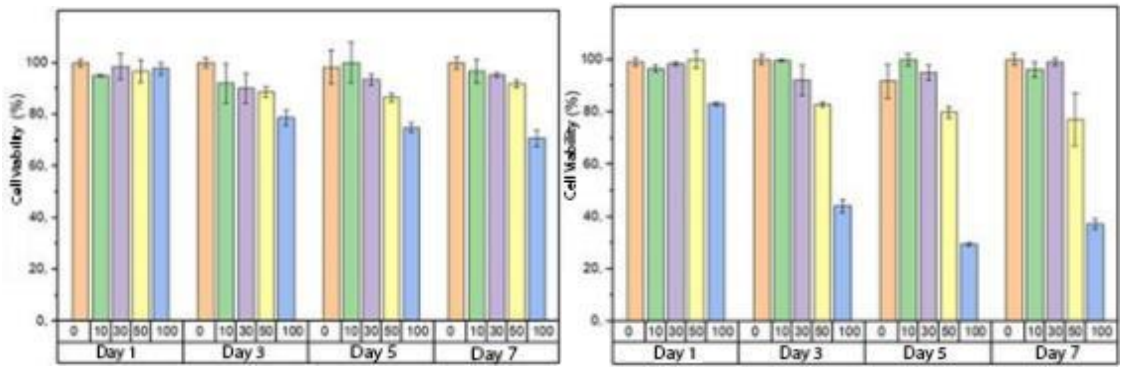


**Figure 7**. Effect of paramagnetic contrast agents on HeLa cell viability. Cell viability results obtained as a result of Alamar blue analysis **a)** Gx effect **b)** Dx effect (Gx-Dx concentration unit: mM).

In addition to MTT and AB analysis, cell viability and morphology were analysed by a live/dead assay. Figure 8 shows the effect of Gx and Dx paramagnetic contrast agents on cell viability and morphology. In the images, red dots show dead cells stained with PI (propidium iodide), and green dots show live cells stained with 'calcein green'.

As shown in Figure 8, live-dead analysis results are generally parallel to the MTT results. As in the MTT results, the highest viability in the live-dead analysis results was observed in the control groups that did not contain paramagnetic agents. The increase in paramagnetic contrast agent concentration caused a general decrease in cell viability. In

control groups and groups containing low concentrations of paramagnetic contrast agents, cells adhered to the surface of the well from day 1 and appeared morphologically normal. However, the cells in the groups containing 100 mM Dx were not able to adhere to the well surface and spread to the surface at the end of the first day, and the morphology remained circular, unlike normal. In addition, the vitality in these groups is quite low compared to other groups. Although some of the cells that could not adhere were alive at the end of the first day, they could not proliferate and died in the following days because they could not adhere to the surface. This confirms the low cell viability observed in MTT results from day 3 for 100 mM Dx and that Dx is much more toxic than Gx. For both paramagnetic contrast agents, the proliferation of experimental groups containing low concentrations of agents was faster, while at higher concentrations it was slower, which is interpreted as paramagnetic agents inhibiting proliferation even if they do not show immediate toxicity.

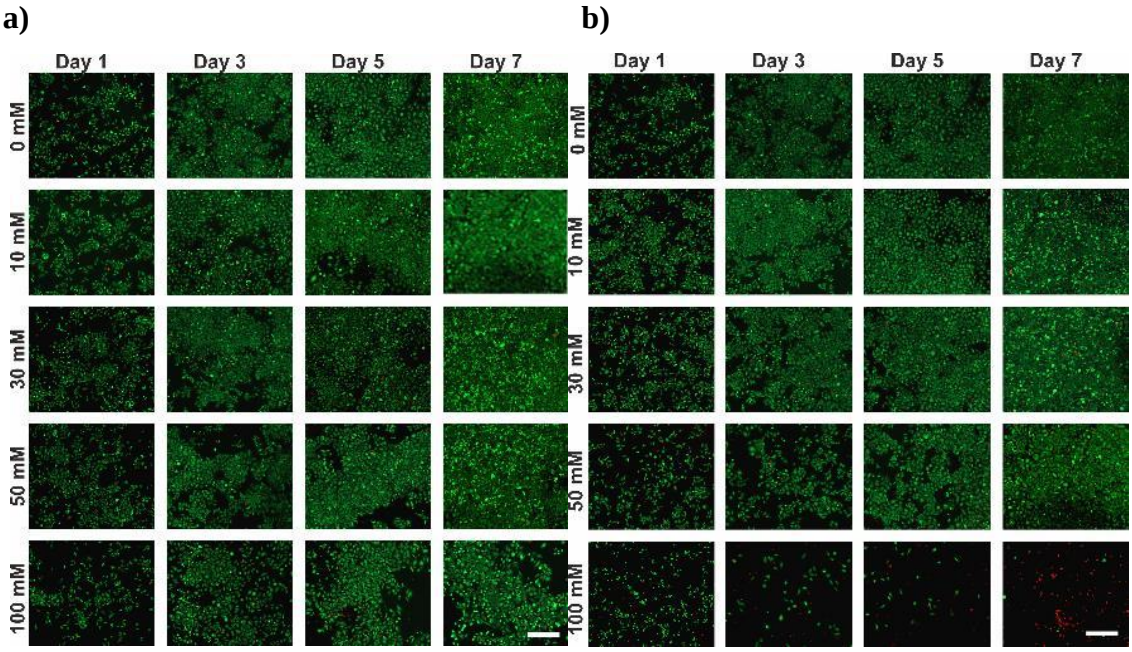


**Figure 8**. Effect of paramagnetic contrast agents on the viability of HeLa cells. Viability images obtained as a result of live-dead analysis **a)** Gx effect **b)** Dx effect (scale size: 200 μm).

After completion of the 2D cell culture experiments with HeLa, the same sets of experiments were repeated with the SH-SY5Y cell line. In this regard, when the SH-SY5Y cells cultured in 2D reached 80-90% confluency, they were removed from the flask and planted in 96-well plates with 15000 cells in each well for each concentration value. Experiments were carried out in at least 3 repetitions for each concentration. The plates were incubated for a week at 37 °C with 5% CO2, and cell viability tests were performed on days 1, 3, 5, and 7 to understand the toxic effect of paramagnetic contrast agents on the cells. In this context, the viability of SH-SY5Y cells incubated in media containing Gx and Dx at various concentrations separately at the end of the 1st, 3rd, 5th, and 7th days was examined quantitatively using MTT and Alamar blue analysis methods. According to the absorbance values obtained as a result of MTT analysis, cell viability graphs depending on paramagnetic agent concentration were obtained as shown in Figure 9.

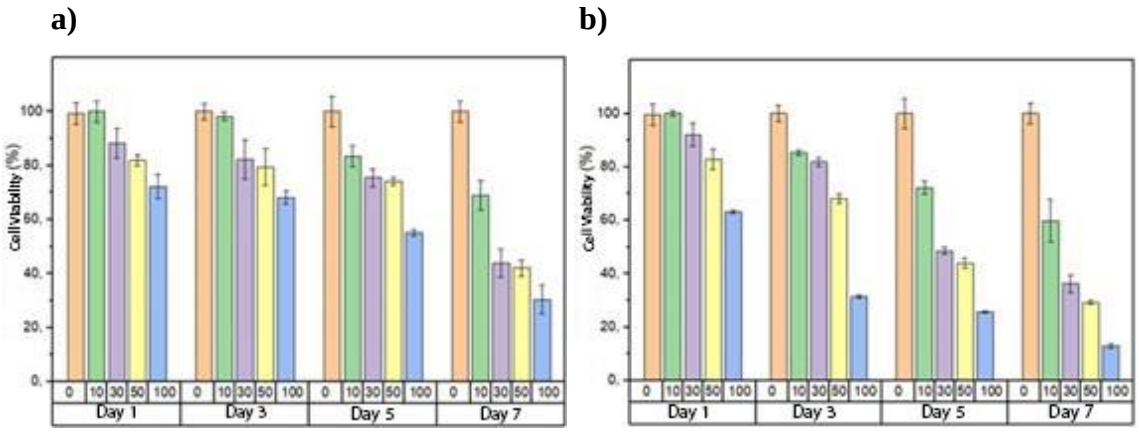


**Figure 9**. Effect of paramagnetic contrast agents on SH-SY5Y cell viability. Cell viability results obtained as a result of MTT analysis **a)** Gx effect **b)** Dx effect (Gx-Dx concentration unit: mM).

When the MTT graphs in Figure 9 are examined, it is seen that similar results were obtained for the SH-SY5Y cell line as for the HeLa cell. It was observed that the viability of the samples analysed on the same day decreased as the agent concentration increased. Additionally, it was observed that cell viability decreased day by day under constant agent concentrations. For the SH-SY5Y cell line, Dx has a more toxic effect than

Gx. The concentration of the paramagnetic agent that showed 60% and above viability in SH-SY5Y cells after one week of incubation was 10 mM.

Figure 10 shows cell viability values decreasing, day by day, as expected in the Alamar blue analysis graphs of the SH-SY5Y cell line. In addition, it was observed that as the agent concentration increased on the same day, cell viability decreased. This analysis also showed that the Dx effect is more toxic than Gx for the SH-SY5Y cell line. As with the results obtained from the Hela cell line, cell viabilities in the Alamar blue analysis are at higher levels compared to the viabilities in the MTT analysis. According to Alamar blue analysis, the concentration of a paramagnetic agent that provides 60% or more cell viability after 1 week of incubation for SH-SY5Y cell line is 10-50 mM.

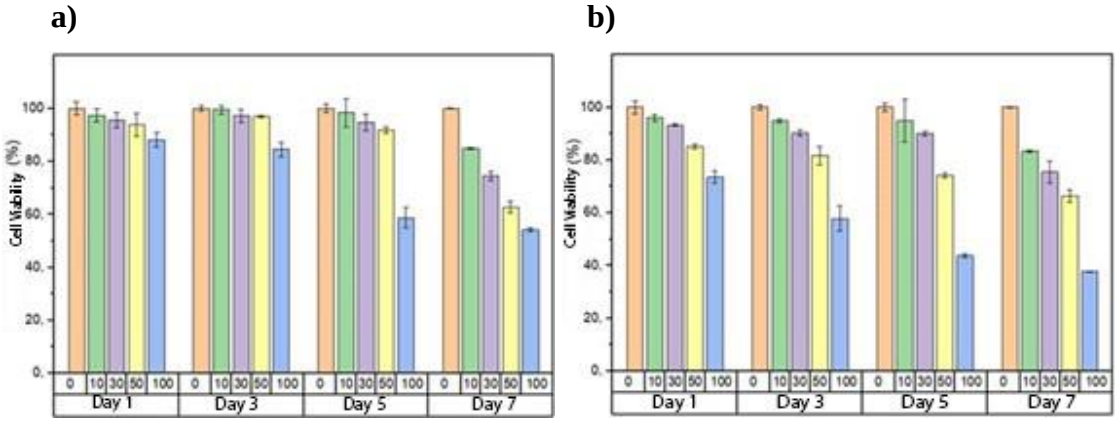


**Figure 10**. Effect of paramagnetic contrast agents on SH-SY5Y cell viability. Cell viability results obtained as a result of Alamar blue analysis **a)** Gx effect **b)** Dx effect (Gx-Dx concentration unit: mM).

After MTT and Alamar blue analysis, it was examined in terms of the effect of paramagnetic agents on the viability of the cells and morphology change with a live-dead assay. The obtained results are shared in figure 11. Similar results were seen at both paramagnetic agent concentrations. At 100 mM agent concentration, cells could not adhere to the surface or adhered to a very small amount and could not gain morphology. Cells incubated with a paramagnetic agent of 50 mM or less adhered to the surface from the first day, and it was observed that their amount increased day by day. In the analyses

performed with both agents, maximum cell viability was obtained in the control group. It was observed that as the amount of agent increased, the number of living cells decreased.

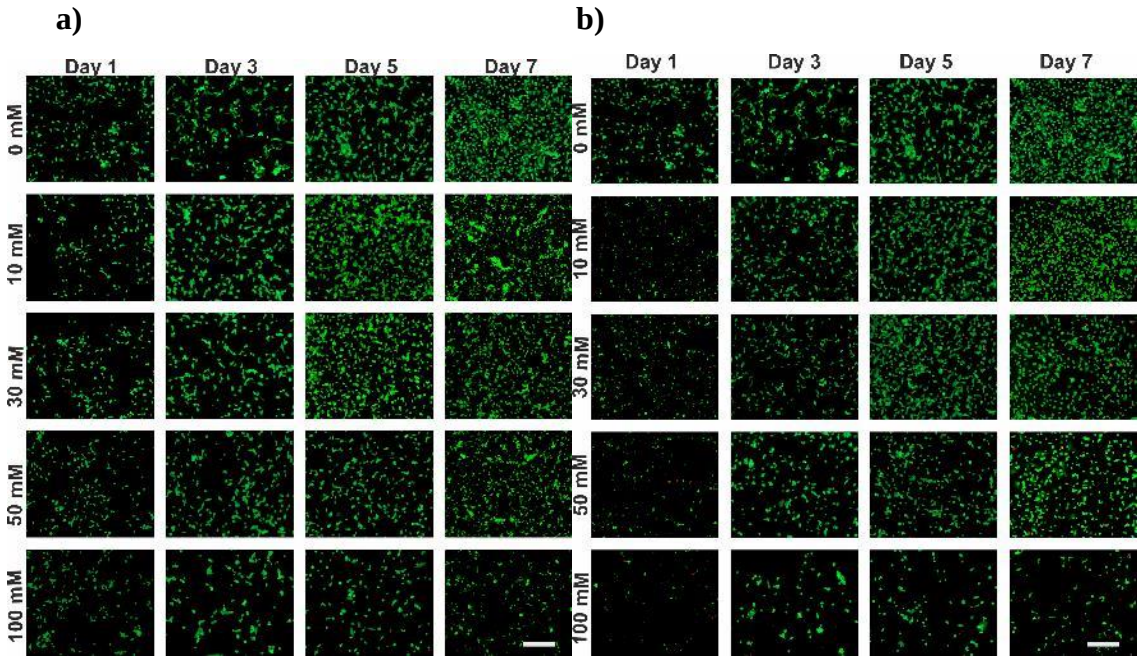


**Figure 11**. Effect of paramagnetic contrast agents on the viability of SH-SY5Y cells. Viability images obtained as a result of live-dead analysis **a)** Gx effect **b)** Dx effect (scale size: 200 μm)

After completion of the 2D cell culture experiments with SH-SY5Y, the same sets of experiments were repeated with the HepG2 cell line. In this regard, when the HepG2 cells cultured in 2D reached 80-90% confluency, they were removed from the flask and planted in 96-well plates with 10000 cells in each well for each concentration value. Experiments were carried out in at least 3 repetitions for each concentration. The plates were incubated for a week at 37 °C with 5% CO2, and cell viability tests were performed on days 1, 3, 5, and 7 to understand the toxic effect of paramagnetic contrast agents on the cells. In this context, the viability of HepG2 cells incubated in media containing Gx and Dx at various concentrations separately at the end of the 1$^{st}$, 3$^{rd}$, 5$^{th}$, and 7$^{th}$ days was examined quantitatively using MTT and Alamar blue analysis methods. According to the

absorbance values obtained as a result of MTT analysis, cell viability graphs depending on paramagnetic agent concentration were obtained as shown in Figure 12.

The MTT test results are consistent with expectations. As in the MTT results of Hela and SH-SY5Y cell lines, it was observed that the viability decreased as the amount of agent contained in the samples analysed on the same day increased (Figure 12). Additionally, cell viability was observed to decrease day by day under constant agent concentration. For the HepG2 cell line, Dx has a more toxic effect than Gx. The concentration of the paramagnetic agent that showed 60% or more viability in HepG2 cells after one week of incubation was 10 mM. In the $7^{th}$ day results of the Gx effect, it is seen that there is an increase in cell viability compared to day 5. However, this situation is at a tolerable level. Since, there is no incompatibility on the same day, it is also known that the HepG2 cell line clusters during the culturing process. It is thought that clustered cell groups grow very rapidly after contact with each other. In this percentage, cell viability values are higher in the results of day 7 compared to day 5.

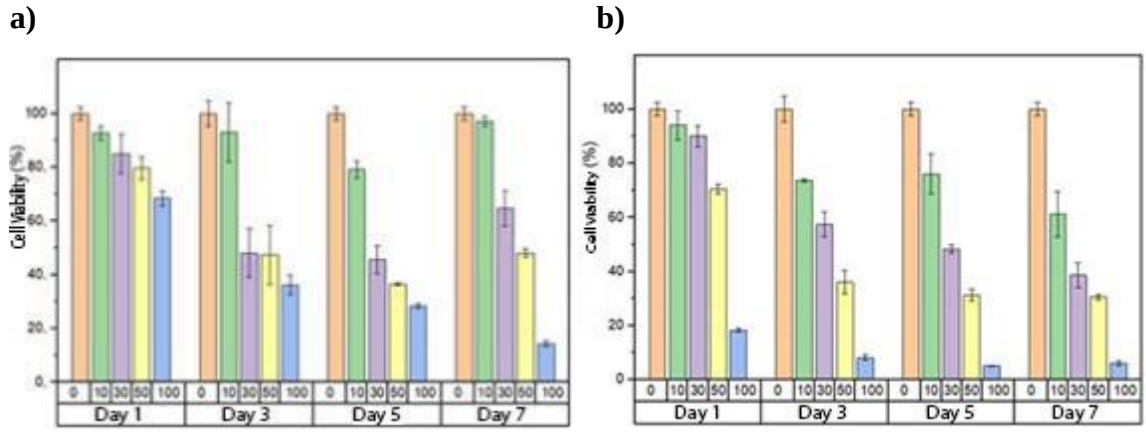


**Figure 12**. Effect of paramagnetic contrast agents on HepG2 cell viability. Cell viability results obtained as a result of MTT analysis **a)** Gx effect **b)** Dx effect (Gx-Dx concentration unit: mM).

Alamar blue analysis graphs of the HepG2 cell line showed cell viability values decreasing, day by day, as expected (Figure 13). In addition, it was observed that as the agent concentration increased on the same day, cell viability decreased conversely. This analysis also showed that the Dx effect is more toxic than Gx for the HepG2 cell line. In

Alamar blue analysis, the viability rates for the HepG2 cell line are quite high, as in other cell lines. According to Alamar blue analyses, the paramagnetic agent concentration that provides 60% or more cell viability after 1 week of incubation for the HepG2 cell line is all concentrations for Gx, while 50 mM and lower concentrations are for Dx.

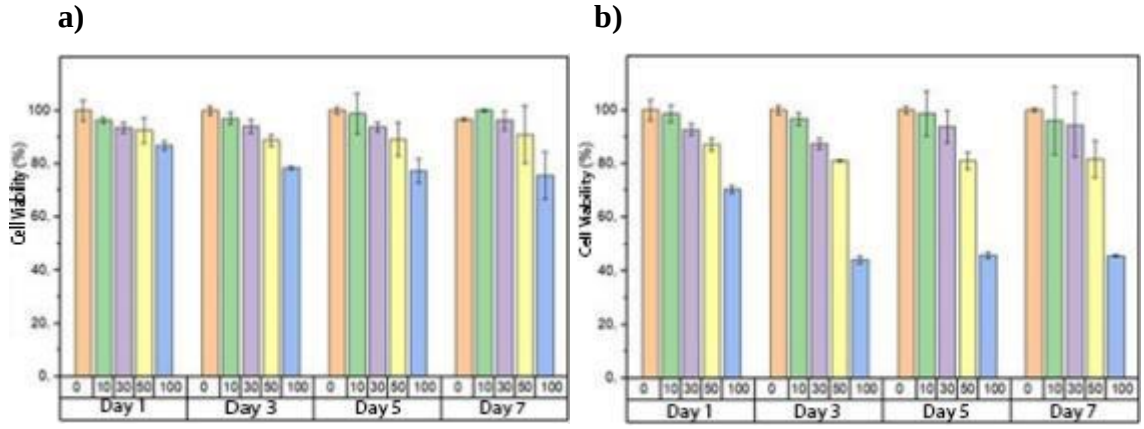


**Figure 13**. Effect of paramagnetic contrast agents on HepG2 cell viability. Cell viability results obtained as a result of Alamar blue analysis **a)** Gx effect **b)** Dx effect (Gx-Dx concentration unit: mM).

The live-dead test results given in Figure 14 are compatible with MTT and Alamar blue analysis. Like the results obtained in other cell lines, the highest cell viability was seen in the control groups that did not contain paramagnetic agents. The increase in paramagnetic contrast agent concentration caused a general decrease in cell viability. It is known from the light microscope images that the cell morphologies in Figure 27 are shared and that the HepG2 cell line forms colony-like structures due to proliferation. It is known that the cells remaining in the inner parts of these islets die due to a lack of diffusion. In the images obtained in Figure 14, it was observed that there was an increase in cell death due to the growth of the islet structures formed by the cells, starting from the $5^{th}$ day, in the trials performed with both types of agents. Like the results obtained in Hela and SH-SY5Y cell lines, it can be said in these test results that Dx is more toxic than Gx by looking at the viability of the cells exposed to 100 mM agent concentration.

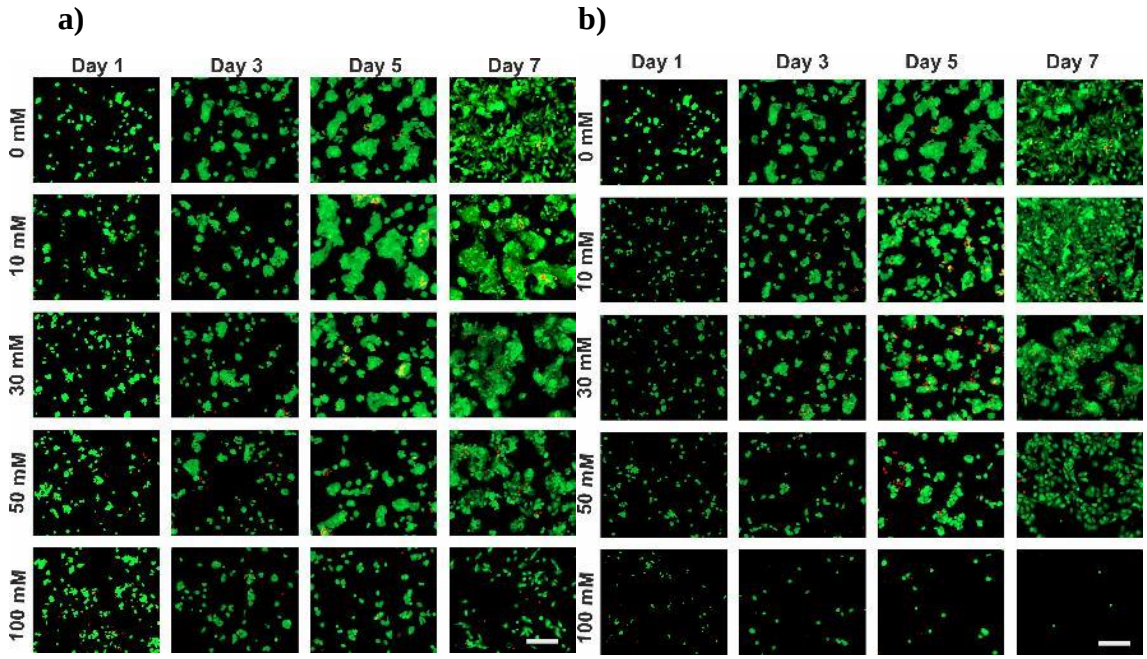


**Figure 14**. Effect of paramagnetic contrast agents on the viability of HepG2 cells. Viability images obtained as a result of live-dead analysis **a)** Gx effect **b)** Dx effect (scale size: 200 μm).

After the completion of the 2D cell culture experiments with HepG2, the same sets of experiments were repeated with the MCF-7 cell line. In this regard, when the MCF-7 cells cultured in 2D reached 80-90% confluency, they were removed from the flask and planted in 96-well plates with 10000 cells in each well for each concentration value. Experiments were carried out in at least 3 repetitions for each concentration. The plates were incubated for a week at 37 °C with 5% CO2, and cell viability tests were performed on days 1, 3, 5, and 7 to understand the toxic effect of paramagnetic contrast agents on the cells. In this context, the viability of MCF-7 cells incubated in media containing Gx and Dx at various concentrations separately at the end of the $1^{st}$, $3^{rd}$, $5^{th}$, and $7^{th}$ days was examined quantitatively using MTT and AB analysis methods. According to the absorbance values obtained as a result of MTT analysis, cell viability graphs depending on paramagnetic agent concentration were obtained as shown in Figure 15.

The MTT test result for the MCF-7 cell line is proportional to the previous MTT test results. In the samples analysed on the same day, it was observed that the viability decreased as the amount of agent contained increased (Figure 15). Additionally, cell

viability was observed to decrease day by day under constant agent concentration. For the MCF-7 cell line, Dx has a more toxic effect than Gx. The concentration of the paramagnetic agent that showed 60% and above viability in Mcf-7 cells after one week of incubation was 10 mM.

**a)** **b)**

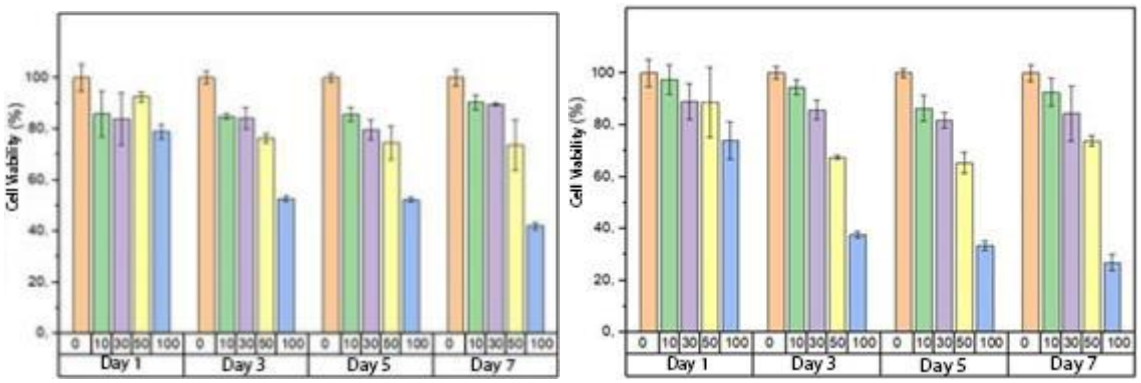


**Figure 15**. Effect of paramagnetic contrast agents on MCF-7 cell viability. Cell viability results obtained as a result of MTT analysis **a)** Gx effect **b)** Dx effect (Gx-Dx concentration unit: mM).

Alamar blue analysis graphs of the MCF-7 cell line show that cell viability is at high levels and values close to the control group. (Figure 16). It has also been shown by this analysis, based on the results of the 100 mM paramagnetic agent effect, that the Dx effect is more toxic than Gx for the MCF-7 cell line. According to Alamar blue analysis, the paramagnetic agent concentration that provides 60% or more cell viability after 1 week of incubation for the MCF-7 cell line is all concentrations for Gx, while it is 50 mM and below for Dx.

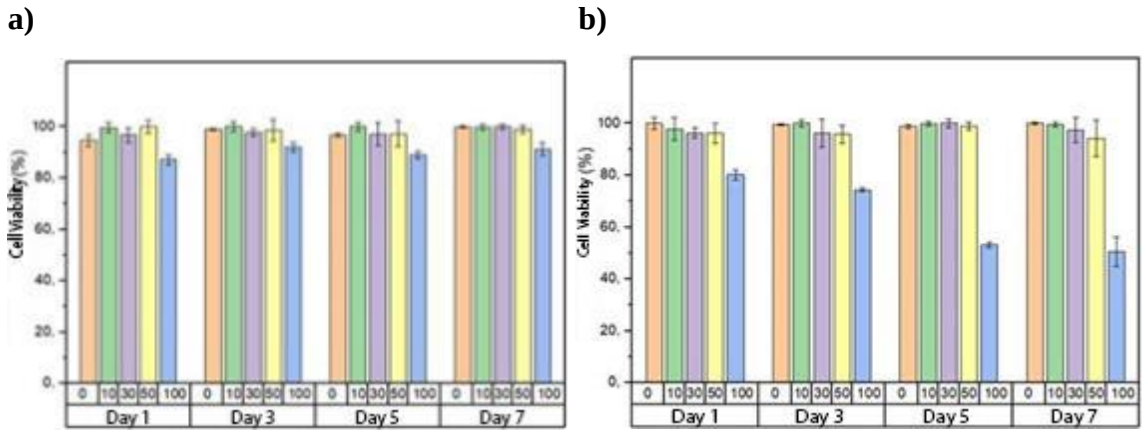


**Figure 16**. Effect of paramagnetic contrast agents on MCF-7 cell viability. Cell viability results obtained as a result of Alamar blue analysis **a)** Gx effect **b)** Dx effect (Gx-Dx concentration unit: mM).

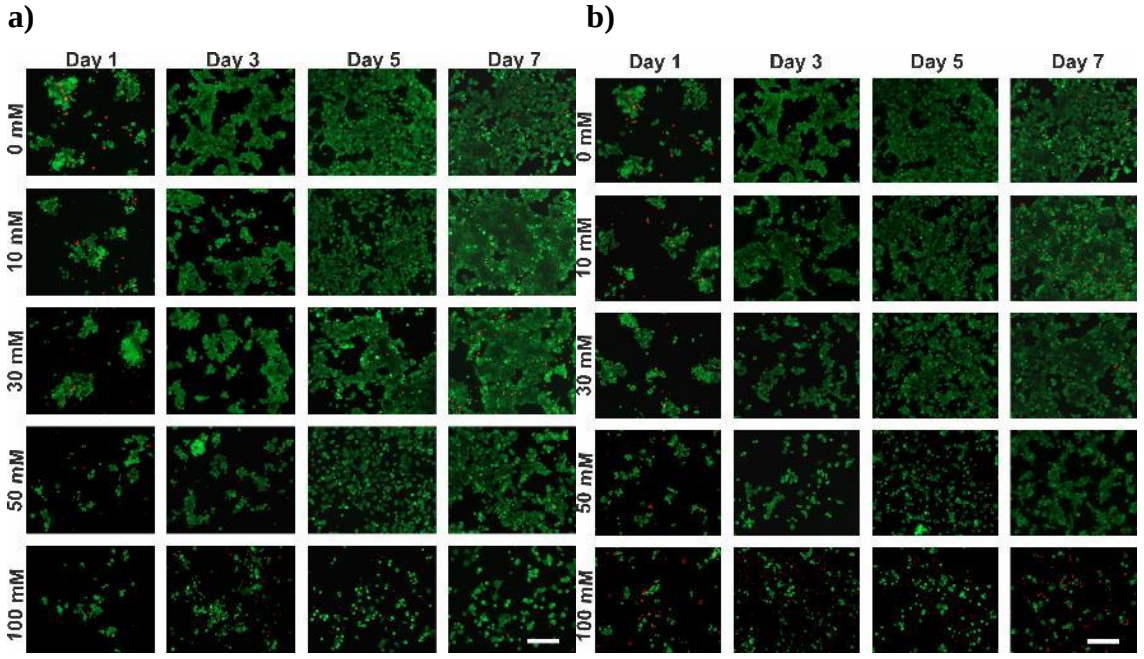


**Figure 17**. Effect of paramagnetic contrast agents on the viability of MCF-7 cells. Viability images obtained as a result of live-dead analysis **a)** Gx effect **b)** Dx effect (scale size: 200 μm).

The live-dead test results given in Figure 17 are compatible with MTT and Alamar blue analysis. Like the results obtained in other cell lines, the highest cell viability was seen in the control groups without paramagnetic agents and in the groups containing 10 mM paramagnetic agents. The increase in paramagnetic contrast agent concentration caused a general decrease in cell viability. According to these results, it is possible to say that 100 mM paramagnetic agent concentrations have a toxic effect on the MCF-7 cell line.

## 3.2. Creation and Characterization of In Vitro 3D Tumor Spheroid Model with Magnetic Levitation Method

In this step, the 3D cell culturing process was started based on the previous studies done by the biomimetics research group (Bilginer Kartal & Arslan Yildiz, 2024; Onbas & Arslan Yildiz, 2021). Optimizations have been completed for 3D culturing of cancer cells using hanging drop and MagLev methods. NdFeB magnets, 40×5 mm in size and placed in an anti-helmholtz configuration, providing a 0.4 T magnetic field, were used for 3D cell culture with the MagLev method.

**a)** **b)**

…. 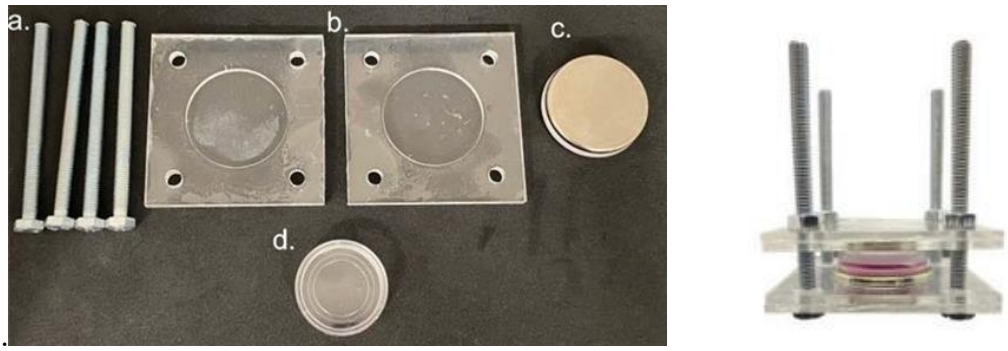


**Figure 18**. **a)** Components of the high volume magnetic levitation set-up produced and developed for 3D cell culture **b)** assembled set-up.

For 3D cell culture, special petri dishes (ibidi petri dishes) with a volume of 800 μL, which are not coated on the cell surface, prevent cell adhesion, and do not form spheroids spontaneously, were preferred. The MagLev set-up components and the completed set-up are shared in Figure 18. The most important advantage of the system is that the medium can be changed to provide optimum living conditions for cells for long-term culturing.

### 3.2.1. Optimization of Parameters for 3D Cell Culture Studies with the Magnetic Levitation Method and In Vitro 3D Cell Culturing

After the first studies using the MagLev system, it was observed that aggregations occurred for some cell lines within a 24-hour period, but compact spheroid structures were not obtained. To obtain clearer and more compact cellular structures before moving on to drug screening studies, spheroid formation was examined over a 7-day period and optimized for each cell line. Although it varies from cell to cell, cell numbers in the range of 5-25 x $10^3$ were tried to obtain the appropriate spheroid structure. Optimization was made to determine the amount of Gx that would enable the cells to levitate (suspend) until they formed a spheroid. Due to its low toxic effect, the concentration ranged from 10 mM up to a maximum of 50 mM. Culturing was continued for 7 days, and light microscope images were taken at 0, 24, 48, 72, 96, and 168 hours. At the end of day 7, the viability of the spheroid and spheroid-like structures obtained was checked by performing a live-dead test. The results obtained for each cell line are shared in figures 19-22. Fluorescence images of light microscopy and live/dead analysis were obtained with a Zeiss Axio Observer microscope.

In 3D cell culture studies with HeLa cells using the magnetic levitation method, successful spheroid structures could be obtained after the 96th hour (Figure 19). Optimized values are 15 x $10^3$ cell number and 30 mM Gx concentration. The obtained spheroids were observed for a period of 7 days, and with the live-dead analysis, it was determined that the viability level was 90% and above, regardless of the drug.

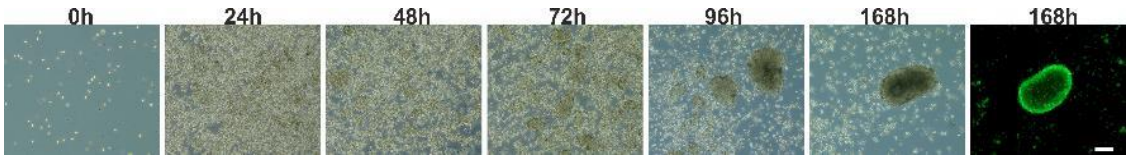


**Figure 19**. Light and viability analysis images of HeLa spheroids during the 7-day culture period. (Scale size:200 μm).

In 3D cell culture studies with SH-SY5Y cells using the magnetic levitation method, successful spheroid structures were obtained after the 48$^{th}$ hour (Figure 20), and the spheroid structure became more clear day by day. Optimized values are 50 x 10$^3$ cell number and 30 mM Gx concentration. The obtained spheroids were observed for a period of 7 days, and with the live/dead analysis, it was determined that the viability level was 80% and above, regardless of the drug.

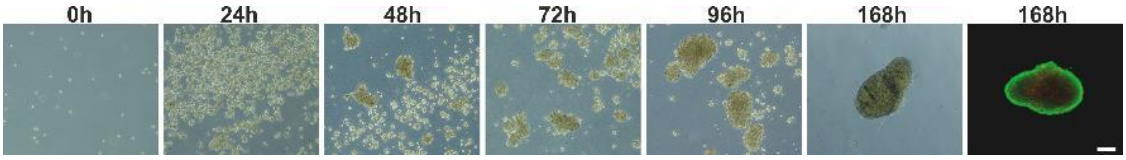


**Figure 20**. Light and viability analysis images of SH-SY5Y spheroids during the 7-day culture period. (Scale size:200 μm).

Spheroid-like 3D cellular structures could be obtained in 3D cell culture studies with HepG2 cells using the magnetic levitation method. Since there is no study on this method and this cell line in the literature, there are no examples and optimization conditions to take as a basis. As shared in Figure 21, the optimized values as of the 168$^{th}$ hour are 10 x 10$^3$ cell number and 30 mM Gx concentration. The resulting spheroid-like structures were observed over a 7-day period, and with the live/dead analysis, it was determined that the viability level was 75% and above, regardless of the drug.

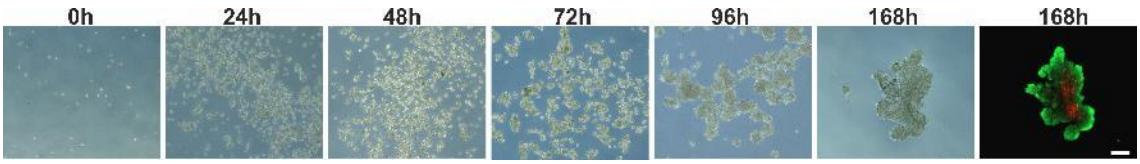


**Figure 21**. Light and viability analysis images of HepG2 spheroids during the 7-day culture period. (Scale size:200 μm).

In 3D cell culture studies with MCF-7 cells using the magnetic levitation method, successful spheroid structures could be obtained after the 96$^{th}$ hour (Figure 22), and the spheroid structure became more evident day by day. Optimized values are 30 x 10$^3$ cell number and 30 mM Gx concentration. The resulting spheroid-like structures were observed over a 7-day period, and through live/dead analysis, it was determined that the viability level dropped to 50% on the 7$^{th}$ day, regardless of the drug. To prevent this situation in the later stages of the research and to conduct drug screening in a reliable way, spheroid-like structures that were smaller in size and obtained at an early stage (72-96 hours) were preferred.


**Figure 22**. Light and viability analysis images of MCF-7 spheroids during the 7-day culture period. (Scale size:200 μm)

### 3.2.2. Characterization of in vitro 3D Tumor Spheroid Models Produced by Magnetic Levitation Method

The characterization results of HeLa spheroids obtained with the MagLev method after 1 and 7 days of culturing are shared in Figure 23. In the results obtained, actin and dapi signals are seen from the first day. It can be seen from actin and nucleus staining that

the cells stand together in a compact manner. Additionally, it is seen that this structure did not deteriorate at the end of the 7-day culturing process. While a very low amount of signal is seen in the collagen signal on the first day, it is seen that there is an increase on the 7$^{th}$ day. This situation is compatible with the literature (Onbas & Arslan Yildiz, 2021). It can be interpreted that extracellular matrix secretion from cells increases day by day, and a structure closer to real tissue physiology is obtained.

**a)** **b)**

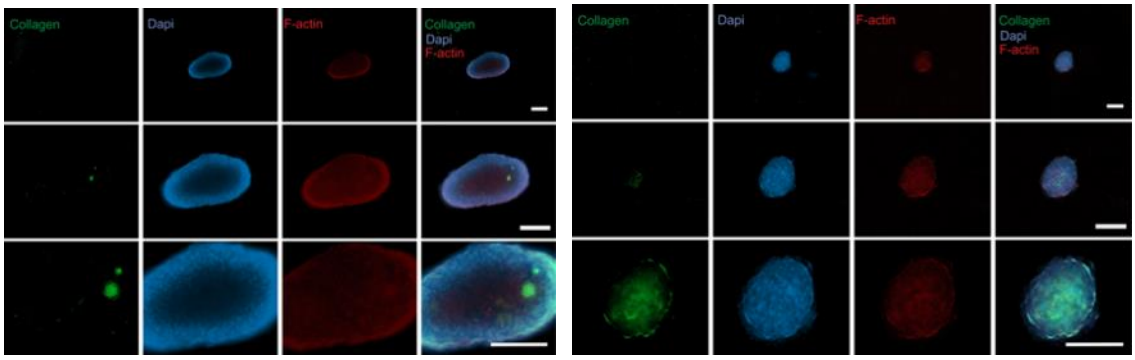


**Figure 23**. Collagen, Actin and Dapi Staining Results of 3D HeLa Tumor Spheroid Models obtained by MagLev method **a)** 1st day **b)** 7th day (5x, 10x and 20x Magnification from top to bottom).

Figure 24 shows the characterization results of SH-SY5Y spheroids obtained with the MagLev method after 1 and 7 days of culturing. In the results obtained, actin and dapi signals are seen from the first day. It can be seen from actin and nucleus staining that the cells stand together in a compact manner. Additionally, it is seen that this structure did not deteriorate at the end of the 7-day culturing process. While there is a very low amount of signal in the collagen signal on the first day, it is seen that there is an increase on the 7$^{th}$ day. This situation is compatible with the literature. It can be interpreted that extracellular matrix secretion from cells increases day by day, and a structure closer to real tissue physiology is obtained.

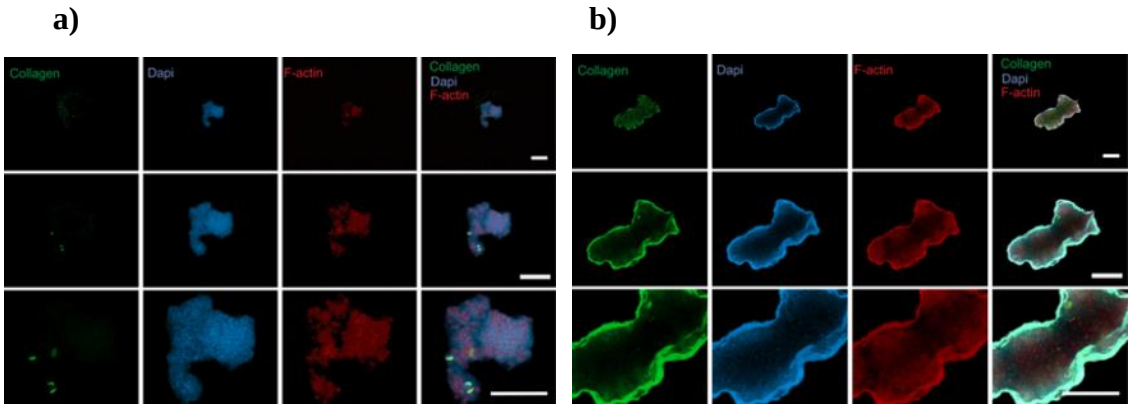


**Figure 24**. Collagen, Actin and Dapi Staining Results of 3D SH-SY5Y Tumor Spheroid Models obtained by MagLev method **a)** 1st day **b)** 7th day (5x, 10x and 20x Magnification from top to bottom).

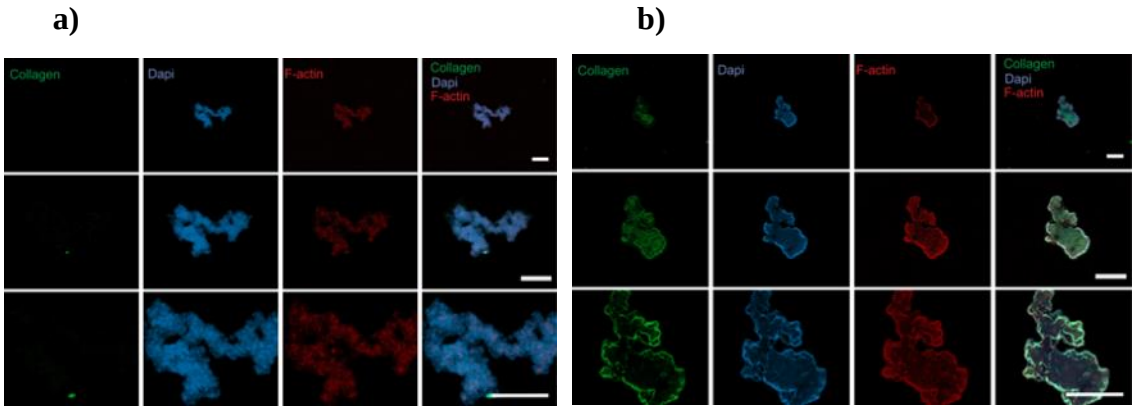


**Figure 25**. Collagen, Actin and Dapi Staining Results of 3D HepG2 Tumor Spheroid Models obtained by MagLev method **a)** 1st day **b)** 7th day (5x, 10x and 20x Magnification from top to bottom).

Figure 25 shows the characterization results of HepG2 spheroids obtained by the MagLev method after 1 and 7 days of culturing. In the results obtained, actin and dapi signals are seen from the first day. It can be seen from actin and nucleus staining that the cells stand together in a compact manner. Additionally, it is seen that this structure did not deteriorate at the end of the 7-day culturing process. While there is a very low amount

of signal in the collagen signal on the first day, it is seen that there is an increase on the 7th day. This situation is compatible with the literature. It can be interpreted that extracellular matrix secretion from cells increases day by day, and a structure closer to real tissue physiology is obtained.

Figure 26 shows the characterization results of MCF-7 spheroids obtained by the MagLev method after 1 and 7 days of culturing. In the results obtained, actin and dapi signals are seen from the first day. It can be seen from actin and nucleus staining that the cells stand together in a compact manner. Additionally, it is seen that this structure did not deteriorate at the end of the 7-day culturing process. While there is a very low amount of signal in the collagen signal on the first day, it is seen that there is an increase on the 7th day. This situation is compatible with the literature. It can be interpreted that the secretion of extracellular matrix from cells increases day by day, and a structure closer to real tissue physiology is obtained.

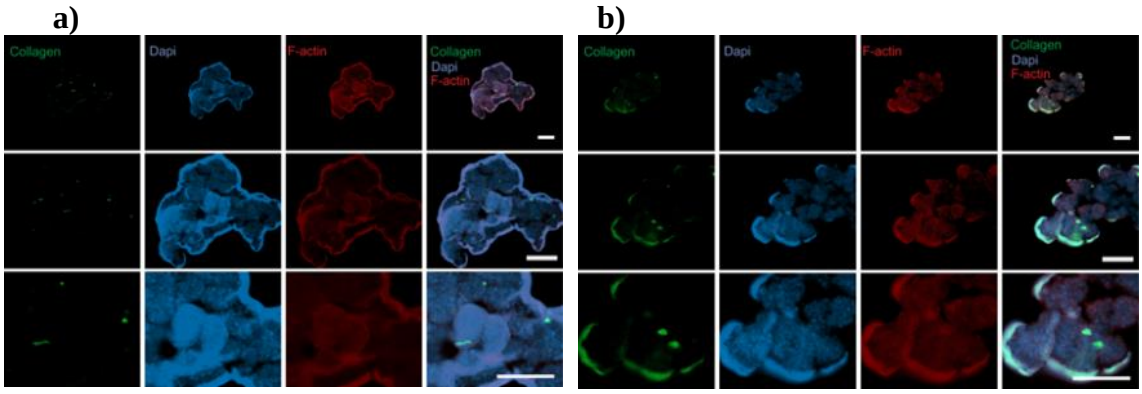


**Figure 26**. Collagen, Actin and Dapi Staining Results of 3D MCF-7 Tumor Spheroid Models obtained by MagLev method **a)** 1st day **b)** 7th day (5x, 10x and 20x Magnification from top to bottom).

## 3.3. Creation and Characterization of 3D Tumor Spheroid Model with the Hanging Drop Method

At this stage, in order to make better comparisons with spheroids obtained by the MagLev method, the parameters required to produce spheroids from different cell lines using the hanging drop method were optimized, and characterization studies were carried out.

### 3.3.1. Optimization of Parameters for 3D Cell Culture Studies with the Hanging Drop Method and In Vitro 3D Cell Culturing

Different cell numbers were tried in studies to obtain spheroids with HeLa cells using the hanging drop method. In Figure 27, the results of 5-10 x $10^3$ cell count experiments in a 24-hour period are shared. Apart from these experiments, different cell numbers (1000, 2500, 15000, and 20000) and incubation times (48 hours and 72 hours) were tried, and similar results were obtained. In addition, the drop volume, which is one of the most basic parameters in the hanging drop method, was changed, but the targeted spheroid structure could not be achieved with HeLa cells. To perform drug trials and viability analyses, the obtained cellular structures must be transferred to 96-well plates. However, since the resulting cellular structures were not compact and were very weak aggregates, the transportation process could not be carried out and the structures dispersed.

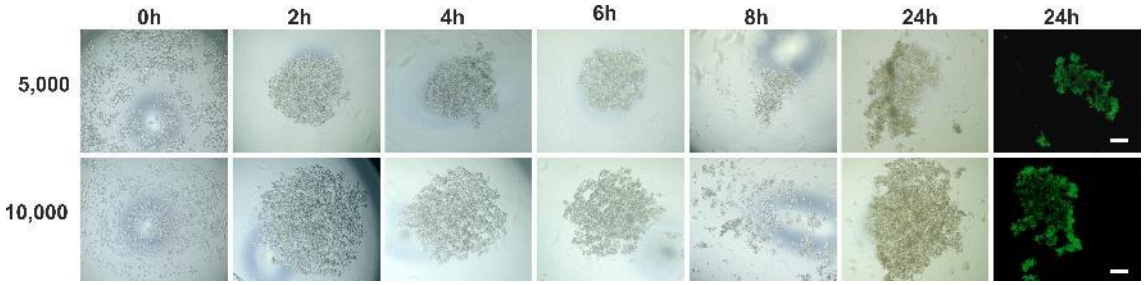


**Figure 27**. Light and viability analysis images of HeLa spheroids during the 24-hour culture period. (Scale size:200 µm)

Different cell numbers were tried in studies to obtain spheroids with SH-SY5Y cells using the hanging drop method. In Figure 28, the results of 25-50 x $10^3$ cell number trials in a 24-hour period are shared. When 50 x $10^3$ cell number is used, the spheroid structures obtained required density and shape. The resulting structures could be successfully transferred to 96-well plates for drug trials and viability analyses. Live-dead analysis performed after 24 hours shows that the viability of the spheroid structures is 90% and above. This allows drug screening studies to be carried out successfully (Namkaew et al., 2018).

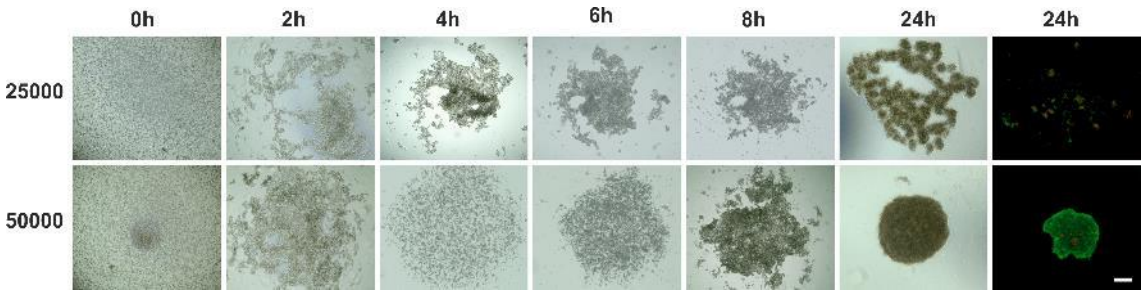


**Figure 28**. Light and viability analysis images of SH-SY5Y spheroids during the 24-hour culture period. (Scale size:200 µm).

Different cell numbers were tried in studies to obtain spheroids with HepG2 cells using the hanging drop method. In Figure 29, the results of 5-10 x $10^3$ cell number trials in a 24-hour period are shared. Successful results were obtained in experiments with both

cell numbers. It has been observed that the success rate is higher in spheroids produced with a cell number of 10 x $10^3$ for multiple productions. The obtained spheroids were successfully transferred to 96-well plates for drug trials and viability analyses. Live-dead analysis performed after 24 hours shows that the viability of the spheroid structures is 90% and above.

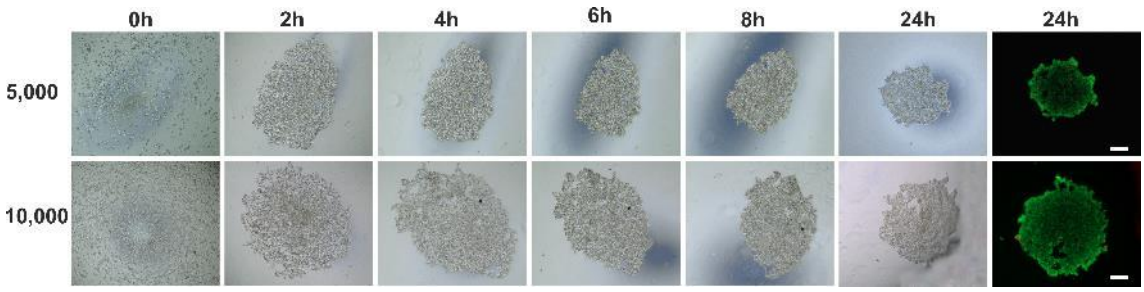


**Figure 29**. Light and viability analysis images of HepG2 spheroids during the 24-hour culture period. (Scale size:200 μm).

Different cell numbers were tried in studies to obtain spheroids with MCF-7 cells using the hanging drop method. In Figure 30, the results of 5-10 x $10^3$ cell number trials in a 24-hour period are shared. Successful results were obtained in experiments with both cell numbers. It has been observed that the success rate is higher in spheroids produced with a cell count of 10 x $10^3$ for multiple productions. The obtained spheroids were successfully transferred to 96-well plates for drug trials and viability analyses. Live-dead analysis performed after 24 hours shows that the viability of the spheroid structures is 90% and above.

For viability analyses to be performed in 3D cell culture, the stability of the spheroid structure free from chemical factors and its viability in long-term culturing are important. Spheroid size, compactness, and circularity have a direct impact on spheroid viability (Leung et al., 2015; Raghavan et al., 2016). In addition, the diffusion limit is another important factor affecting the viability of the spheroid in 3D cell culture (Boucherit et al., 2020; Gerlee et al., 2010; Grimes et al., 2014; Zhu et al., 2022). As time passes, the access of the cells in the inner part of the spheroids to nutrients and oxygen is restricted, thus, the number of dead cells in the inner part of the spheroid increases. This

situation is explained in the literature as necrotic core formation. (Huang et al., 2020; Zanoni et al., 2016) To examine this effect on the produced spheroids, roundness and area analyses were performed, and the results are shared in Figures 31 and 32.

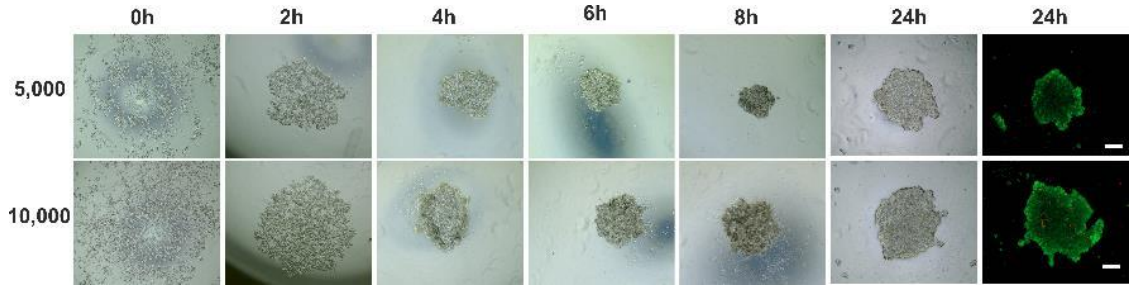


**Figure 30**. Light and viability analysis images of MCF-7 spheroids during the 24-hour culture period. (Scale size:200 µm).

It is known that the number of cells used in spheroids produced by the hanging drop method is directly proportional to the spheroid size, in addition to growth kinetic factors. (Nath & Devi, 2016) The sizes of spheroids belonging to different cells that could be produced in the targeted structure are shared as area analysis results in Figure 31. The results were compared with each other and with the literature, and the ideal number of cells for the spheroid size to be used in drug screening studies was determined. As shared in the results of the optimization studies, successful production at the desired level could not be achieved with HeLa cells. For SH-SY5Y cells, 25000 and 50000 cell numbers were tested, and in the experiments with 25000 cells, it was observed that the spheroid structure was weak and dispersed during the incubation and transferring processes. For this reason, data could not be shared in the area analysis graph. The results of the areas of HepG2 and MCF-7 spheroids according to the number of cells used are compatible with the literature results (Hurrell et al., 2018). Due to the need for many spheroid structures in drug screening studies, it was decided to continue production with 10000 cells for both cell lines, based on the success rate of the spheroids obtained.

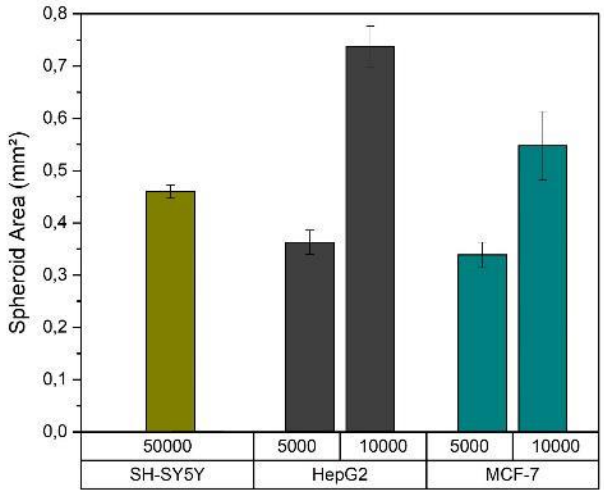


**Figure 31**. Cell line-specific area analysis graph in spheroids obtained by the hanging drop method.

Circularity is used to express the distance from any point of the spheroid structure to the surface. Spheroid circularity is directly related to the diffusion limit (Ermis et al., 2023). Studies in the literature have compared oxygen diffusion in circle and elliptical spheroid structures, and it has been observed that nutrient and oxygen constraints remain at lower levels in spheroid structures with higher circularity values. In the results shared in Figure 32, the circularity values of cell type-specific spheroids obtained by magnetic levitation and the hanging drop method are compared. Analyses were made with the help of the ImageJ program. The ideal circularity value was accepted as 1, and the results were compared with this value (Onbas & Arslan Yildiz, 2021). There is some difference between the circularity values of the spheroids obtained by magnetic levitation and the hanging drop method. In the literature, the circularity of the spheroid structures produced by the hanging drop method is explained as an advantage of the method. The circularity values of the spheroid structures obtained in the studies carried out within the scope of the study are within the acceptable range according to the literature (Leung et al., 2015; Raghavan et al., 2016).

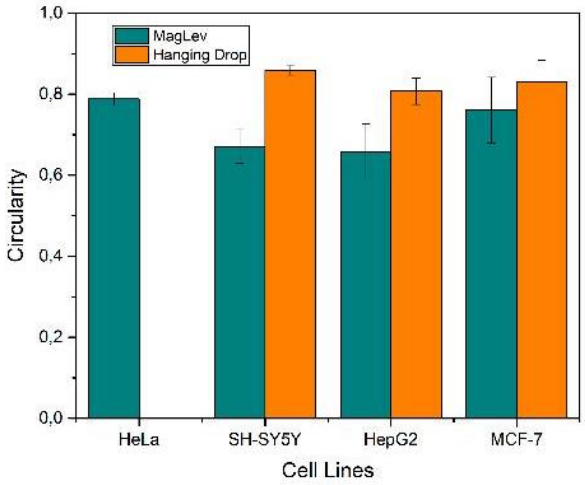


**Figure 32**. Cell line-specific circularity analysis graph in spheroids obtained by hanging drop and MagLev method.

### 3.3.2. Characterization of in vitro 3D Tumor Spheroid Models Produced by Hanging Drop Method

Characterization studies of tumor spheroid models obtained by the hanging drop method were carried out. At this stage, the tumor spheroid models obtained by the hanging drop method were fixed using 4% PFA (paraformaldehyde) on Day 1, then Collagen I (stains the collagens released in the extracellular matrix green), Phalloidin (F-actin) (stains the actin filaments red), and DAPI (stains cell nuclei blue) immunofluorescence staining was performed. In this way, cell nucleus, cell scaffold formation and extracellular matrix formation were observed (Yildirim-Semerci et al., 2024).

The immunofluorescent staining results of spheroid models formed by SH-SY5Y cells are shared in Figure 33. There is a collagen, f-actin, and dapi signal at the 24$^{th}$ hour after obtaining the spheroids. It is understood that collagen I was synthesized in the resulting spheroid structures by the 24$^{th}$ hour. This can be interpreted as the formation of an extracellular matrix-cell complex, similar to real tissue physiology, as expected in the spheroid structure.

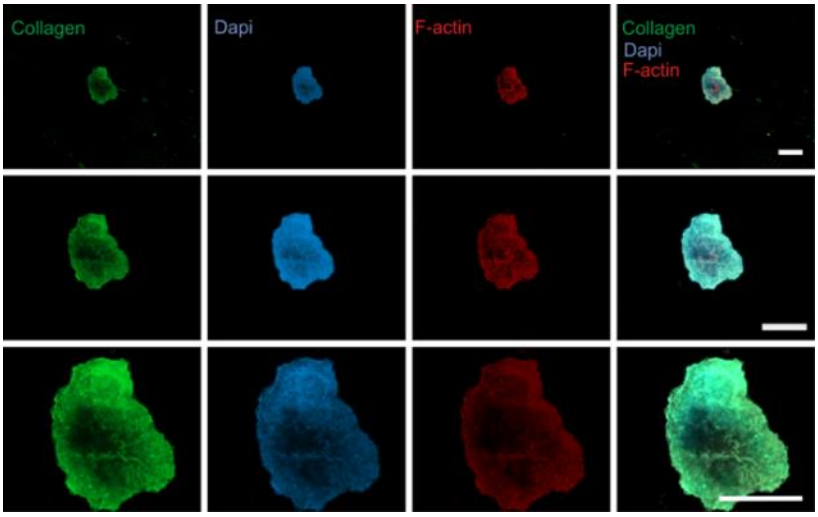


**Figure 33**. Collagen, Actin and Dapi Staining Results of 3D SH-SY5Y Tumor Spheroid Models obtained by hanging drop method (5x, 10x and 20x Magnification from top to bottom).

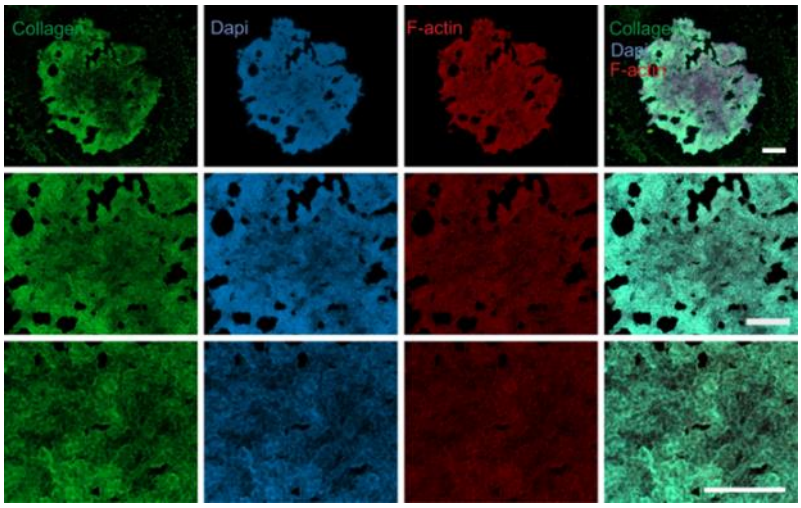


**Figure 34**. Collagen, Actin and Dapi Staining Results of 3D HepG2 Tumor Spheroid Models obtained by hanging drop method. (5x, 10x and 20x Magnification from top to bottom).

Immunofluorescent staining results of spheroid models formed by HepG2 cells are shared in Figure 34. There is a collagen, f-actin, and dapi signal at the 24$^{th}$ hour after obtaining the spheroids. It is understood that collagen was synthesized in the resulting spheroid structures by the 24$^{th}$ hour. This can be interpreted as the formation of an extracellular matrix-cell complex, similar to real tissue physiology, as expected in the spheroid structure.

Immunofluorescent staining results of spheroid models formed by MCF-7 cells are shared in Figure 35. There is a collagen, f-actin, and dapi signal at the 24$^{th}$ hour after obtaining the spheroids. It is understood that collagen was synthesized in the resulting spheroid structures by the 24$^{th}$ hour. This can be interpreted as the formation of an extracellular matrix-cell complex, similar to real tissue physiology, as expected in the spheroid structure.

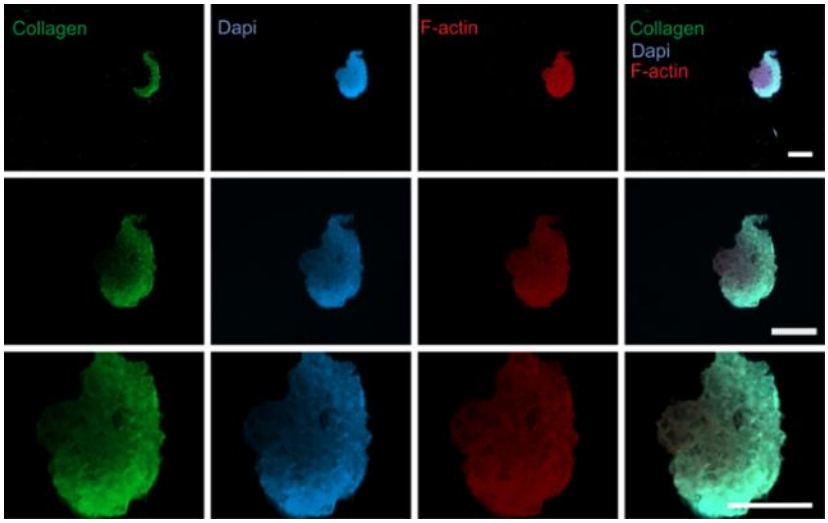


**Figure 35**. Collagen, Actin and Dapi Staining Results of 3D MCF-7 Tumor Spheroid Models obtained by hanging drop method (5x, 10x and 20x Magnification from top to bottom).

## 3.4. Drug Activity Screening of Sapogenol Derived Molecules and Paclitaxel Anticancer Drug

Before obtaining 3D tumor spheroid models, the toxic effects of the PTX and sapogenol-derived molecules (AG-04, AG-08, CG-03, and CG-04), which will be used in drug screening, were investigated in 2D cell culture. AG-08, the target molecule whose effects on 3D tumor spheroid models were investigated, improves proteolysis in cancer cell lines, changes lysosomal functions and physiology, and causes controlled necrosis (Üner et al., 2020). Another molecule known to have anticancer effects with its chemical structure, like this one is CG-03. In order to fully evaluate the results, AG-04 and CG-04 molecules, which have similar chemistry but are not cytotoxic, were used as negative controls. To evaluate the results comparatively, Ptx, which is frequently used in the literature and whose effect is known, was preferred as a positive control. The PTX accumulates in cells and causes inhibition of microtubules, which triggers the apoptotic pathway in cells and causes a decrease in the viability level (Kumar et al., 2010).

In this step, the toxic effects of paramagnetic agents were compared, and it was decided to continue with the 10 mM Gx paramagnetic agent, which has low cytotoxicity, for 3D cell studies. Also, whether this paramagnetic agent caused a possible negative effect when used with Ptx and others was examined.

### 3.4.1 Drug Activity Screening of Sapogenol Derived Molecules in Standard 2D Cell Culture

In Figure 36, the MTT graph for viability analysis after Ptx application for HeLa cells is shared. Ptx cytotoxicity in the presence and absence of Gx was investigated over a 48-hour period. The applied Ptx concentration range was used as 0-200 nM, similar to previous studies based on the literature. According to MTT results, it showed a serious toxic effect at 5 nM and above, and its cytotoxicity on cells increases day by day, and accordingly, there is a decreasing trend in viability values. It is seen that the presence of

10 mM Gx does not create an extra toxic effect, and the viability results in the presence and absence of Gx are at similar values in both graphs.

**a)** **b)**

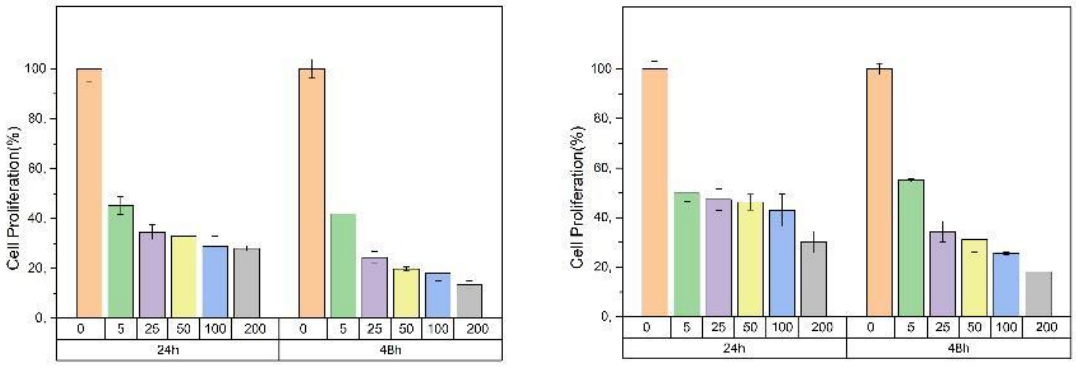


**Figure 36**. 48-hour MTT analysis results showing cytotoxicity of PTX on HeLa cells **a)** in the absence of 10 mM Gx paramagnetic contrast agent **b)** in the presence of 10 mM Gx paramagnetic contrast agent (unit of Ptx concentration: nM)

In Figure 37, the results of live-dead analysis after Ptx application for HeLa cells are shared. Ptx cytotoxicity in the presence and absence of Gx was investigated over a 48-hour period. The applied Ptx concentration range was determined as 0-200 nM, similar to previous studies using the literature. According to the live-dead test results, it showed a toxic effect at concentrations of 25 nM and above, and the decrease in cell viability is clearly seen after 48 hours. In addition to the decrease in the amount of viability, it is observed that due to the increasing drug concentration, the cells cannot adhere to the surface, and they lose their original morphology and remain in a circular morphology. Additionally, no extra toxic effect was observed in the presence of 10 mM Gx, and similar results were obtained. Finally, when the results of MTT and live-dead analysis are compared, it is seen that the results of both analyses are generally consistent with each other.

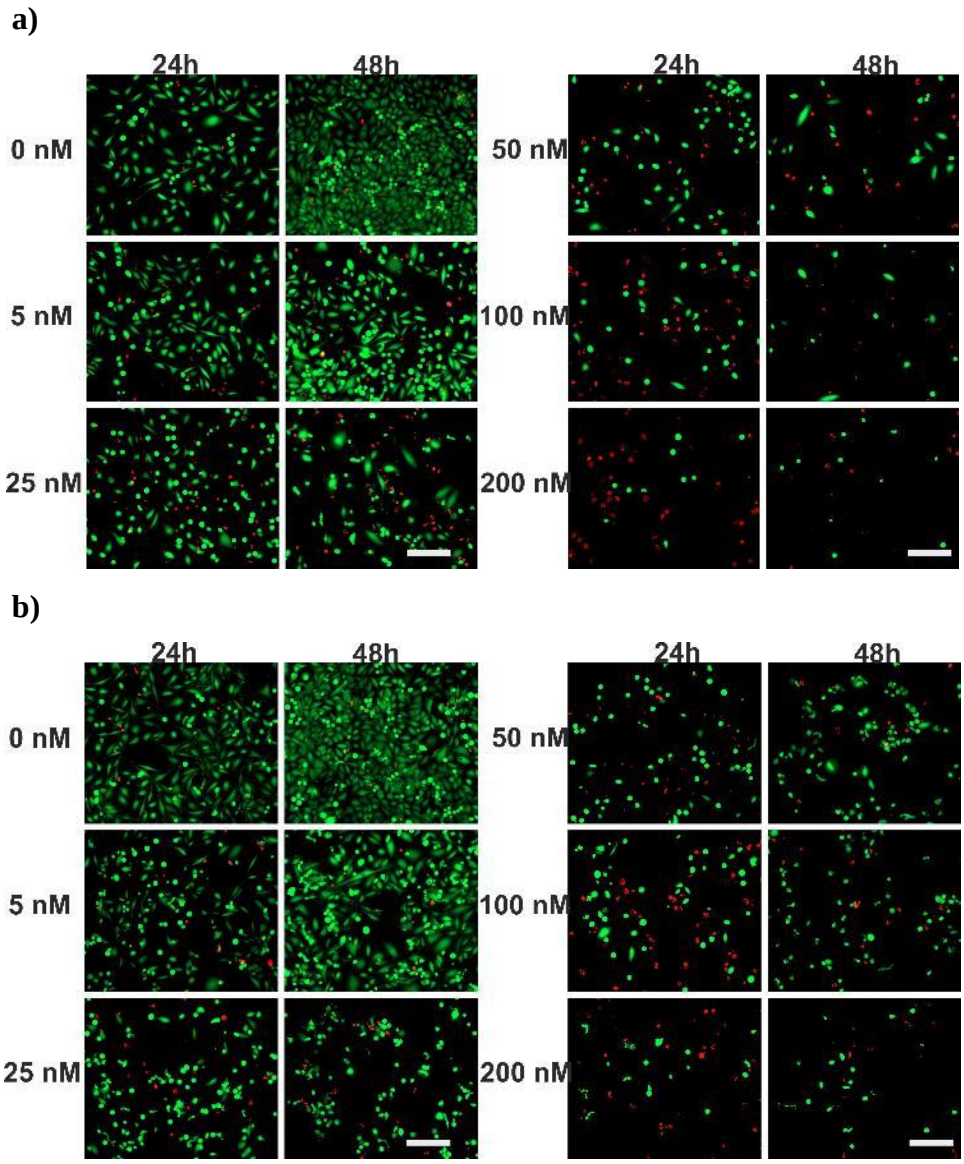


**Figure 37**. 48h live-dead analysis results showing cytotoxicity of PTX on HeLa cells **a)** absence **b)** presence of 10 mM Gx paramagnetic contrast agent.

In Figure 38, the MTT graph for viability analysis after AG-08 application to HeLa cells is shared. In the presence and absence of Gx, the toxic effect of the AG-08 molecule synthesized by Prof. Bedir and his group was investigated over a 48-hour period. The concentration range of sapogenol-derived molecules applied in 2D cell culture was detected by using literature close to previous studies as a range of 0-30 µM to allow comparisons to be made in all cell lines. (Üner et al., 2020, 2022). According to MTT results, a serious toxic effect was observed at concentrations between 5-10 µM and

above, and the cytotoxic effect on cells increases over time. Accordingly, there is a decreasing trend in viability values. It is seen that the presence of 10 mM Gx does not create an extra toxic effect, and the viability results are at similar values in both graphs.

**a)** **b)**

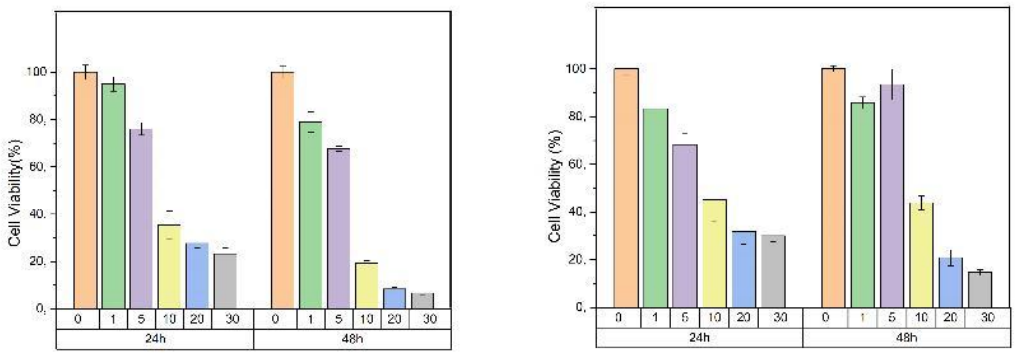


**Figure 38**. 48h MTT analysis results showing the cytotoxicity of AG-08 on HeLa cells in **a)** absence **b)** presence of 10 mM Gx paramagnetic contrast agent (unit of AG-08 concentration: μM).

In Figure 39, the results of live-dead analysis after AG-08 application for HeLa cells are shared. In the presence and absence of Gx, the cytotoxicity of the AG-08 molecule synthesized by Prof. Bedir and his group was investigated over a 48-hour period. According to the live-dead test results, a serious toxic effect occurred at 10 μM and above, and the decrease in cell viability was clearly seen. In addition to the decrease in the amount of viability, it is observed that due to the increasing drug concentration, the rare surviving cells lose their original morphology and remain in a circular morphology. Also, it is seen that the presence of 10 mM Gx does not cause any extra toxic effects, and the results regarding viability are similar. Finally, when the results of MTT and live-dead analysis are compared, it is seen that the results of both analyses are generally consistent with each other.

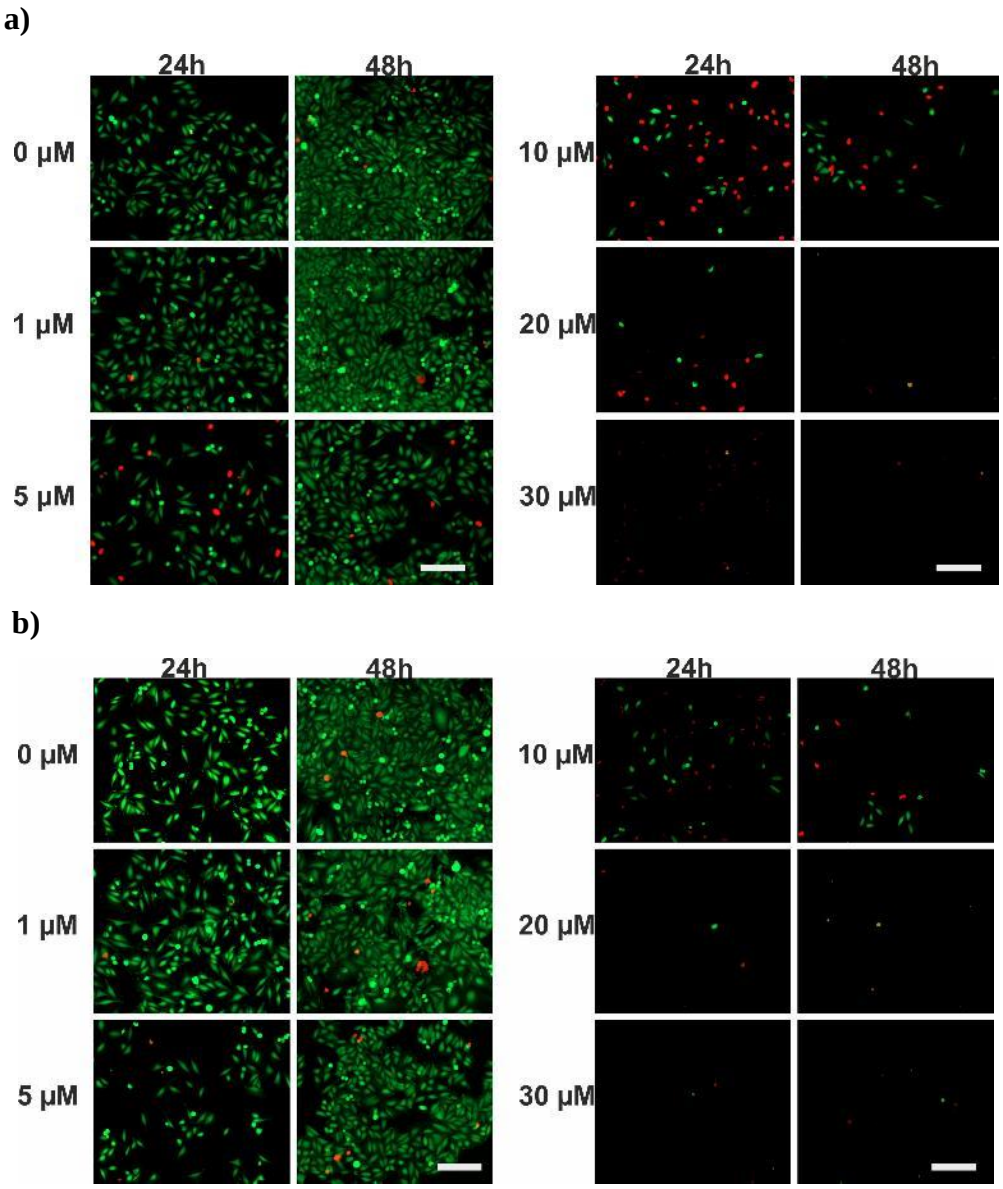


**Figure 39**. 48h live-dead analysis results showing the cytotoxicity of AG-08 on HeLa cells in **a)** absence **b)** presence of 10 mM Gx paramagnetic contrast agent. (unit of AG-08 concentration: µM).

MTT graphs for viability analysis after AG-04 application to HeLa cells are shared in Figure 40. In the presence and absence of Gx, the toxic effect of the AG-04, which is one of the analogues of the AG-08 molecule synthesized by Prof. Bedir and his group, was investigated over a 48-hour period. The applied concentration range of AG-04 is in the range of 0-30 µM, as in the AG-08 molecule. Depending on the chemical structure of the AG-04 molecule, it is not expected to have any toxic effects on cells,

unlike AG-08 (Üner et al., 2022). It was determined to be the negative control group within the research. For this reason, viability values are expected to be 60% and above. When the results were examined, there was a decrease in the viability level in the presence and absence of Gx after 30 µM application. It can be interpreted that the toxic effect caused by the AG-08 molecule on cells occurs at lower concentrations compared to AG-04. The presence of 10 mM Gx did not create an extra toxic effect, and the viability results were generally similar in both graphs.

**a)** **b)**

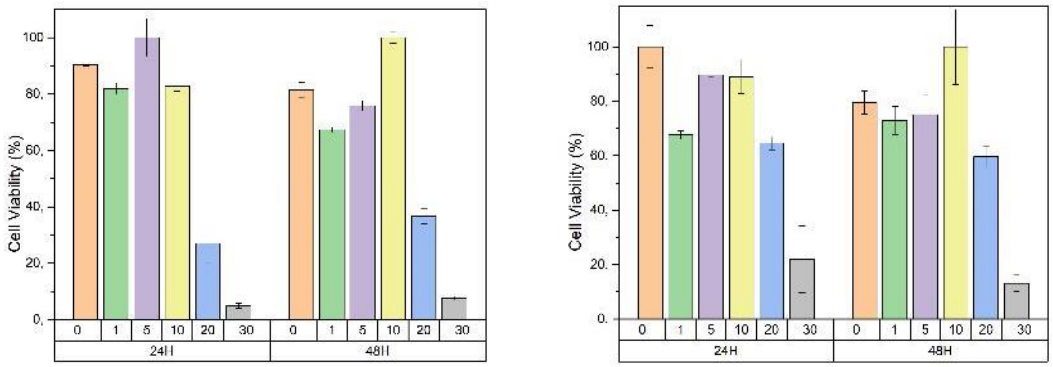


**Figure 40**. 48h MTT analysis results showing the cytotoxicity of AG-04 on HeLa cells in **a)** absence **b)** presence of 10 mM Gx paramagnetic contrast agent (unit of AG-08 concentration: µM).

In Figure 41, the results of live-dead analysis after AG-04 application for HeLa cells are shared. The toxic effect of the AG-04 in the presence and absence of Gx was investigated over a 48-hour period. According to the results obtained, the viability is at a high level, and there is a decrease in cell viability starting with a 30 µM application. However, unlike the AG-08 molecule, there was no change in the adhesion and morphology of the cells to the surface as the applied molecule concentration increased. It also appears that the presence of 10 mM Gx does not create an extra toxic effect, and the results regarding viability are similar. Finally, when the results of MTT and live-dead analysis are compared, it is seen that the results of both analyses support each other.

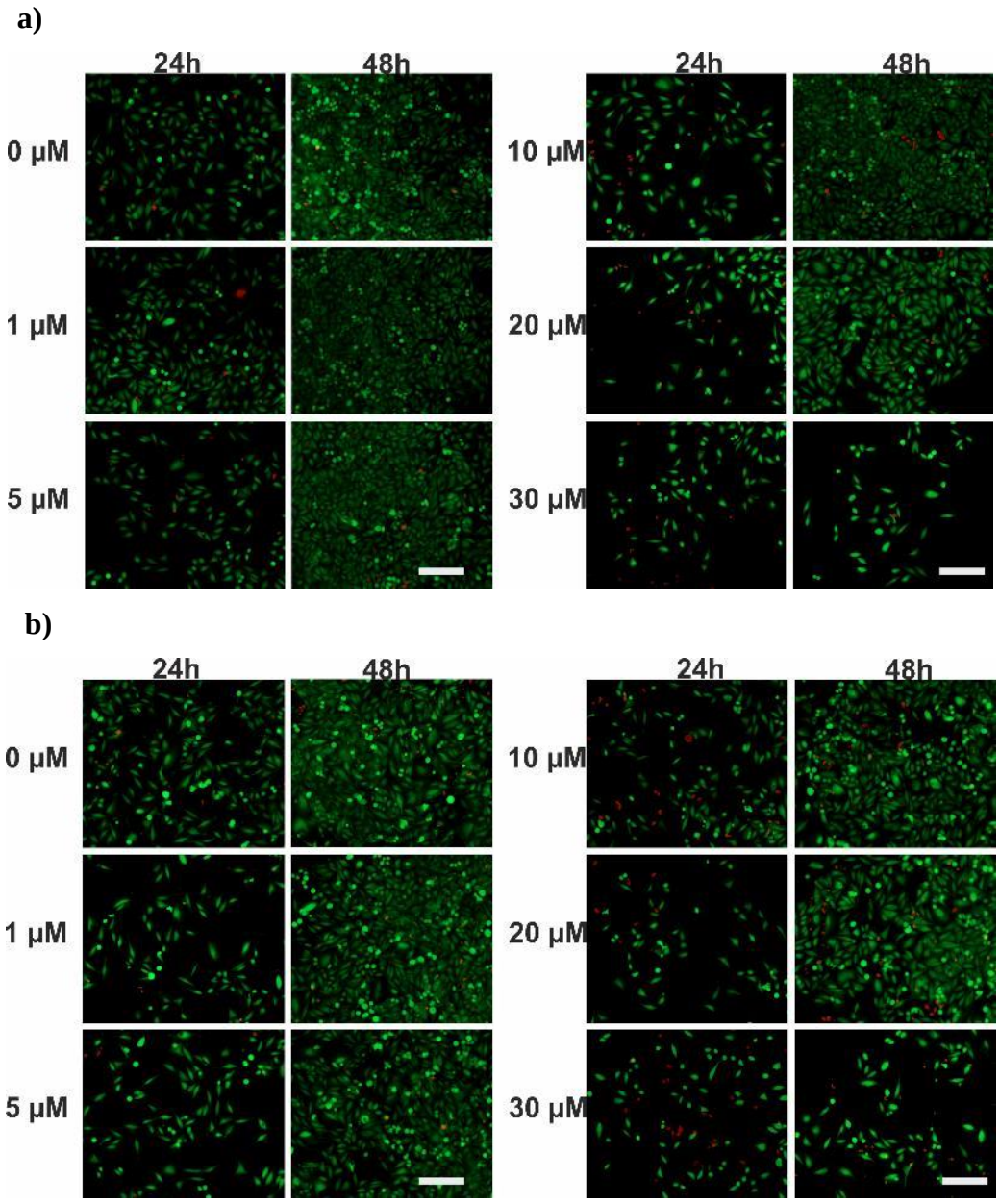


**Figure 41**. 48h live-dead analysis results showing the cytotoxicity of AG-04 on HeLa cells in the **a)** absence **b)** presence of 10 mM Gx paramagnetic contrast agent (scale unit 100 µm).

Figure 42 shows the MTT graph for viability analysis after CG-03 molecule application to HeLa cells. In the presence and absence of Gx, the toxic effect of the CG-03 , one of the analogues of the AG-08 molecule synthesized by Prof. Bedir and his group, was investigated over a 48-hour period. The chemical structure of the CG-03 molecule is like AG-08; therefore, it causes controlled necrosis in a similar way to the AG-08

molecule (Üner et al., 2022). It is expected to cause toxic effects on cancer cell lines in future trials. The applied concentration range of CG-03 is in the range of 0-30 µM, as in AG-08 and AG-04 molecules. According to the results of MTT analysis, a toxic effect was observed at concentrations of 10 µM and higher, resulting in a decreasing trend in viability values. Additionally, the presence of 10 mM Gx did not cause any extra toxic effects, and the viability results were consistent with each other in both graphs.

**a)** **b)**

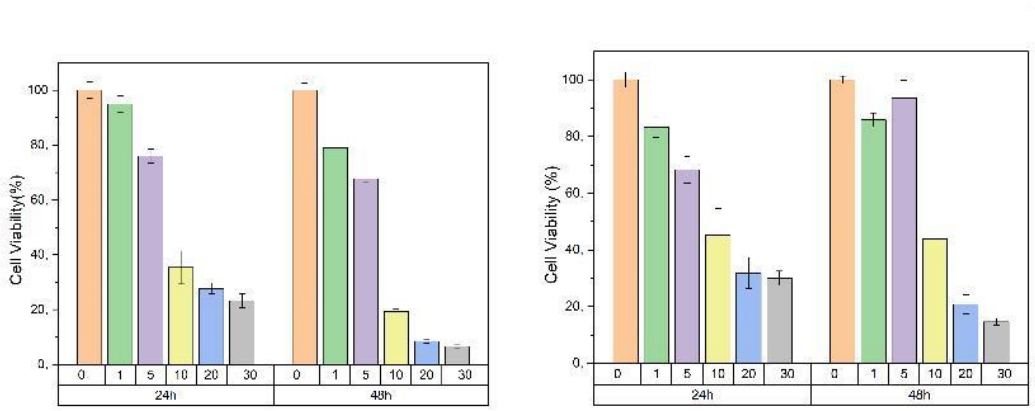


**Figure 42**. 48h MTT analysis results showing the cytotoxicity of CG-03 on HeLa cells in the **a)** absence **b)** presence of 10 mM Gx paramagnetic contrast agent.

In Figure 43, the results of the live-dead analysis after the application of the CG-03 molecule to HeLa cells are shared. The toxic effect of the CG-03 in the presence and absence of Gx was investigated over a 48-hour period. According to the results obtained, serious toxic effects occurred in applications at concentrations of 10 µM and above. Moreover, a decreasing trend in cell viability was observed. In addition to the decrease in the amount of viability due to the increasing molecule concentration, it is observed that the rare surviving cells lose their original morphology and remain in a circular morphology. On the other hand, it is seen that the presence of 10 mM Gx does not cause any extra cytotoxicity, and the viability results are similar. Finally, when the results of MTT and live-dead analysis are compared, it can be said that the results of both analyses generally support each other.

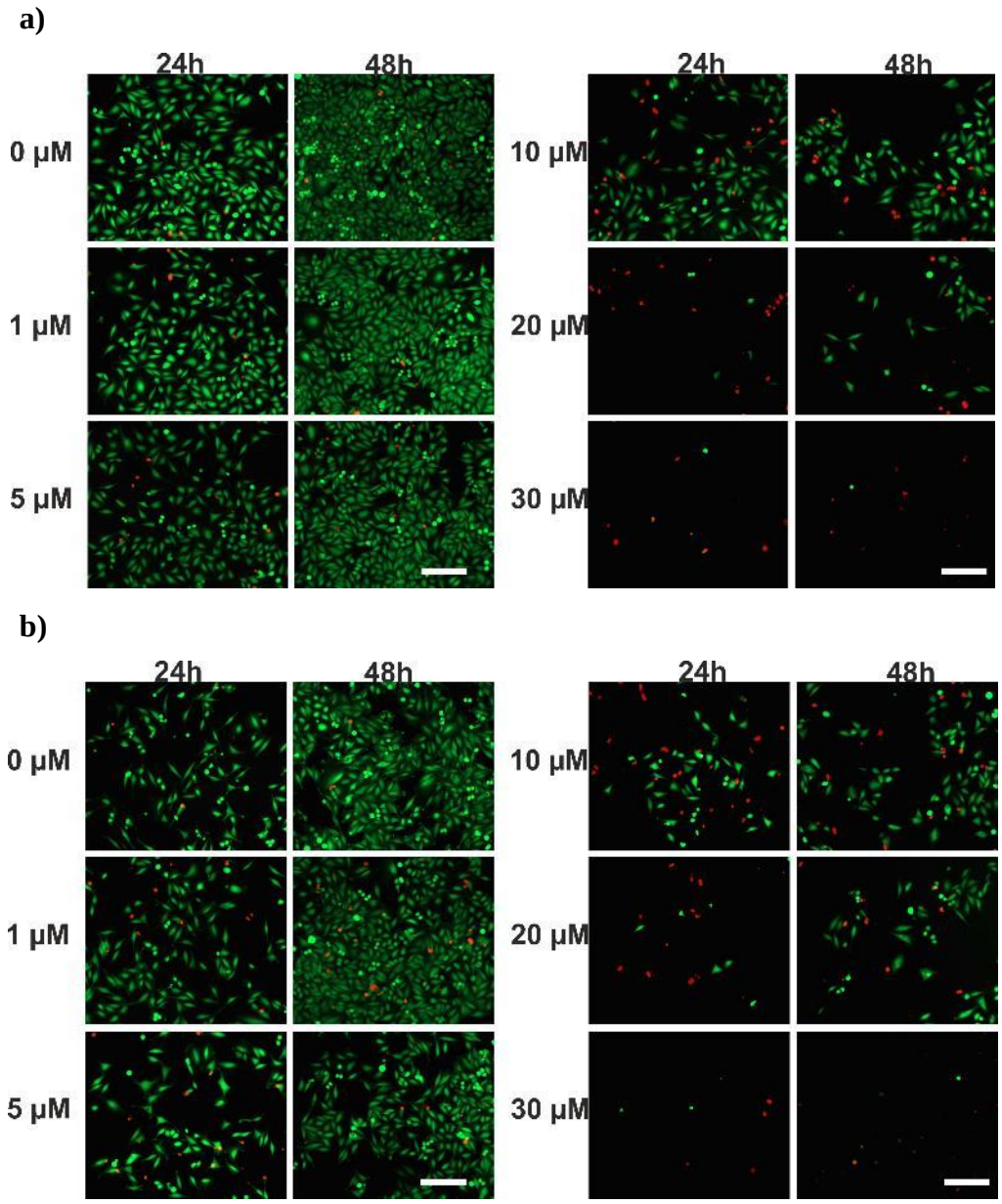


**Figure 43**. 48h live-dead analysis results showing the cytotoxicity of CG-03 on HeLa cells in the **a)** absence **b)** presence of 10 mM Gx paramagnetic contrast agent (scale unit 100 µm).

MTT graphs for viability analysis after CG-04 molecule application to HeLa cells are shared in Figure 44. In the presence and absence of Gx, the toxic effect of the CG-04 , one of the analogues of the AG-08 molecule synthesized by Prof. Bedir and his group, was investigated over a 48-hour period. The applied CG-04 concentration range is 0-30 µM, as with the other three molecules. The chemical structure of the CG-04 molecule is

like AG-04. Unlike AG-08 and CG-03 molecules, it is expected to not cause any toxic effects on cells or to have very low levels of cytotoxicity. (Viability values are expected to be 60% and above.) When the results obtained are examined, it is evident that they are compatible with the expectations. Despite the increased CG-04 molecule concentration, the cell viability level is 60% and above. The presence of 10 mM Gx did not cause any extra cytotoxicity, and the viability values were close in both graphs.

**a)** **b)**

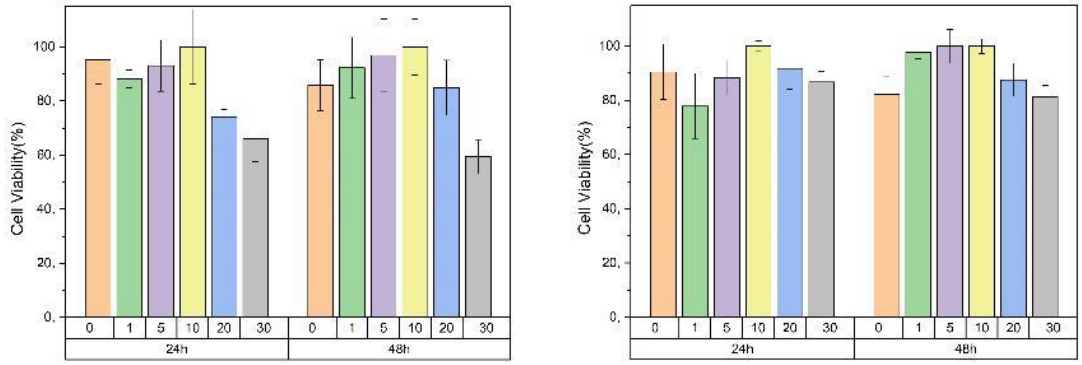


**Figure 44**. 48h MTT analysis results showing the cytotoxicity of CG-04 on HeLa cells in the **a)** absence **b)** presence of 10 mM Gx paramagnetic contrast agent.

In Figure 45, the results of live-dead analysis after CG-04 molecule application for HeLa cells are shared. The cytotoxicity of the CG-04 in the presence and absence of Gx was investigated over a 48-hour period. The results obtained show that cell viability remains at a high level despite the increasing CG-04 molecule concentration. Unlike AG-08 and CG-03 molecules, which have high cytotoxicity, there was no change in the morphology of the cells as the concentration of the applied CG-04 molecule increased. It also appears that the presence of 10 mM Gx does not cause any extra cytotoxicity, and the viability results are similar. Finally, when the results of MTT and live-dead analysis are compared, it can be said that the results of both analyses support each other.

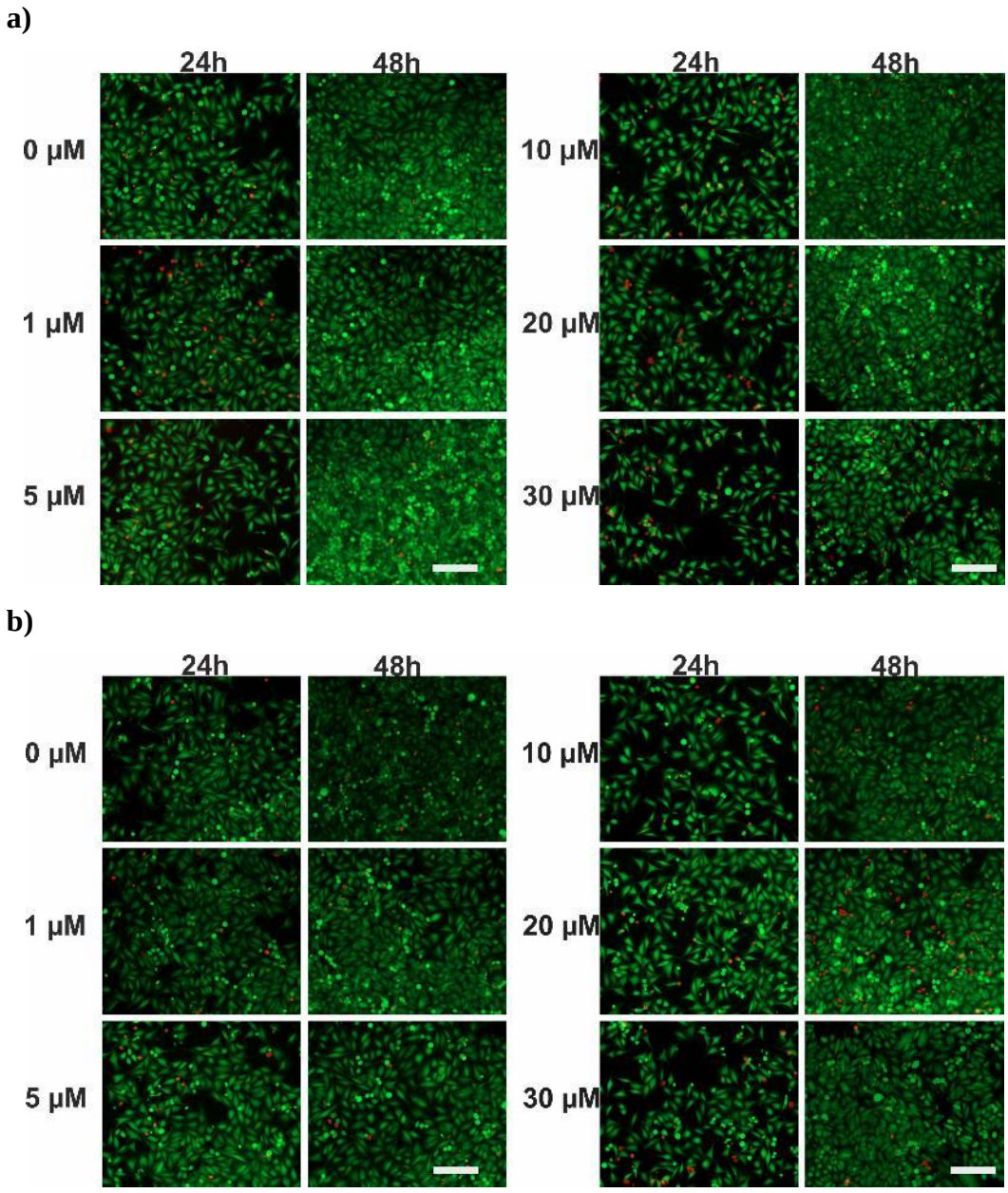


**Figure 45**. 48h live-dead analysis results showing the cytotoxicity of CG-04 on HeLa cells in the **a)** absence **b)** presence of 10 mM Gx paramagnetic contrast agent (scale unit 100 µm).

In Figure 46, MTT graphs for viability analysis are shared for SH-SY5Y cells after PTX application. Ptx cytotoxicity in the presence and absence of Gx was investigated over a 48-hour period. The applied Ptx concentration range is 0-200 nM, like previous studies, using the literature. According to the MTT analysis results, the viability value decreased to the expected level (50% and below) at the 200 nM concentration

application. In addition, there is a decreasing trend in cell viability day by day due to the toxic effects caused by the drug. It is also seen that the presence of 10 mM Gx does not create an extra toxic effect, and the viability results are at similar values in both graphs.

**a)** **b)**

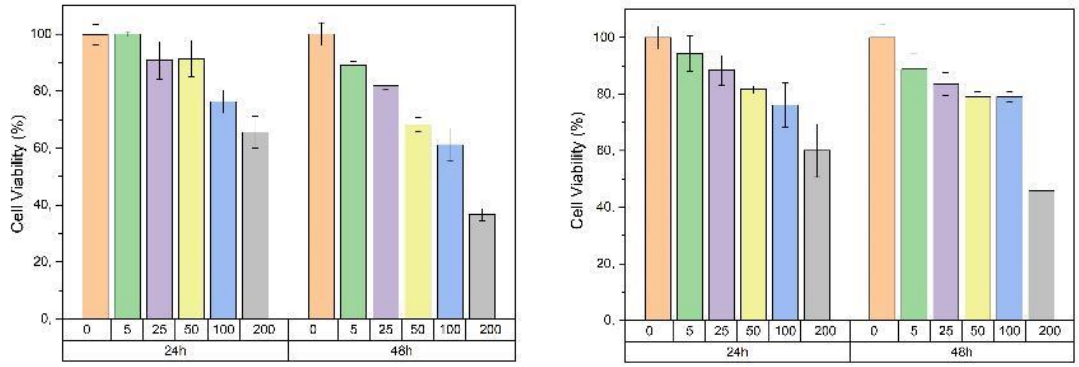


**Figure 46**. 48h MTT analysis results showing the cytotoxicity of PTX on SH-SY5Y cells in the **a)** absence **b)** presence of 10 mM Gx paramagnetic contrast agent.

In Figure 47, the results of live-dead analysis after Ptx application for SH-SY5Y cells are shared. Ptx cytotoxicity in the presence and absence of Gx was investigated over a 48-hour period. The applied Ptx concentration range is 0-200 nM, similar to previous studies using the literature. According to the live-dead analysis results, a high toxic effect was observed in applications at 25 nM and increasing concentrations, and the decrease in cell viability is clearly seen after 48 hours. In addition to the decrease in cell viability, it is observed that due to increasing drug concentration, the cells lose their original morphology and remain in a circular morphology. It also appears that the presence of 10 mM Gx does not create an extra toxic effect, and the viability results are similar. Finally, when the results of MTT and live-dead analysis are compared, it can be said that the results of both analyses are generally consistent with each other.

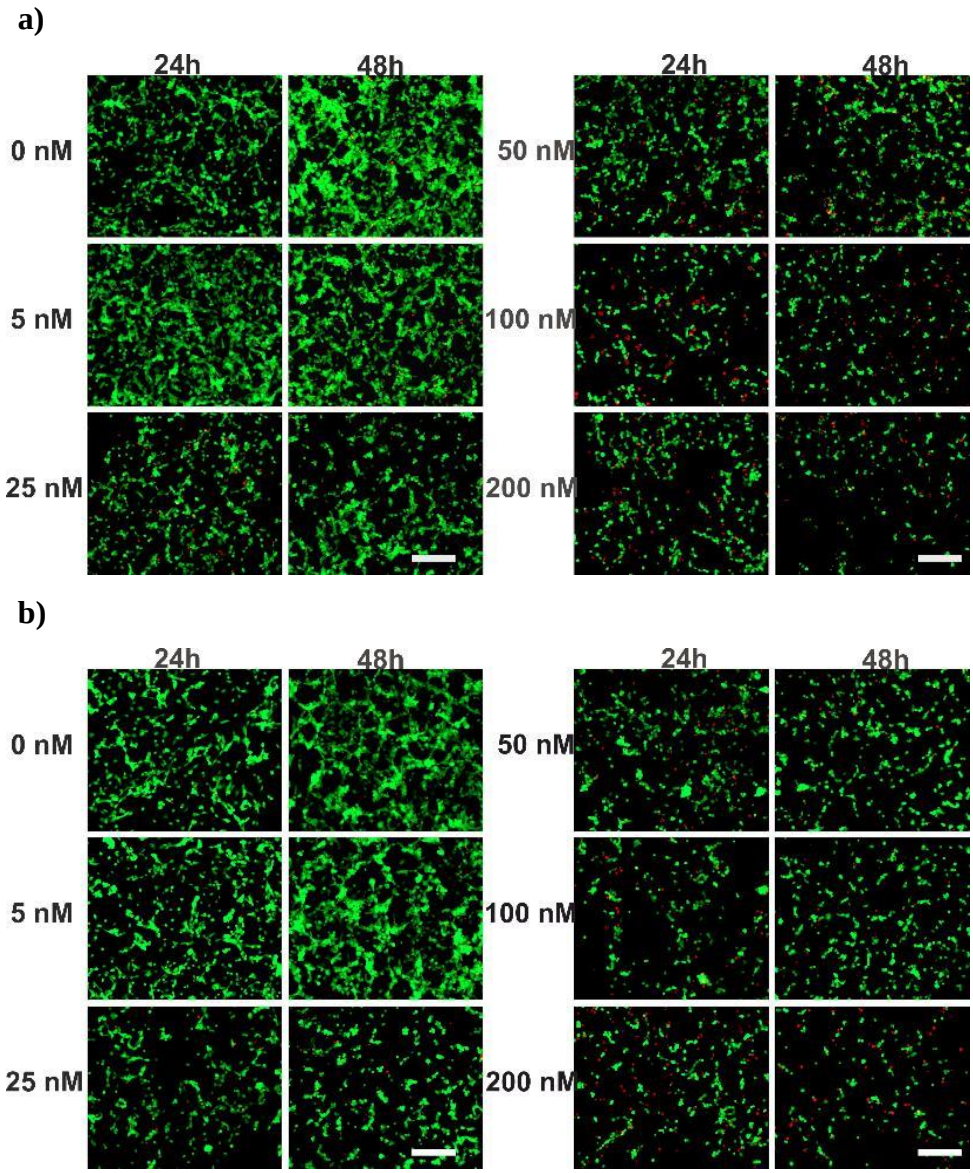


**Figure 47**. 48h live-dead analysis results showing the cytotoxicity of PTX on SH-SY5Y cells in the **a)** absence **b)** presence of 10 mM Gx paramagnetic contrast agent (scale unit 100 μm).

Figure 48 shows MTT graphs for viability analysis after AG-08 molecule application for SH-SY5Y cells. The toxic effect of the AG-08 in the presence and absence of Gx was investigated over a 48-hour period. According to the MTT results obtained, it is seen that there is a decreasing trend in the viability values in applications starting from 10 μM and increasing concentrations due to the cytotoxicity occurring on the cells. It was

also concluded that the presence of 10 mM Gx did not cause any extra cytotoxicity, and the viability levels were at similar values in both graphs.

**a)** **b)**

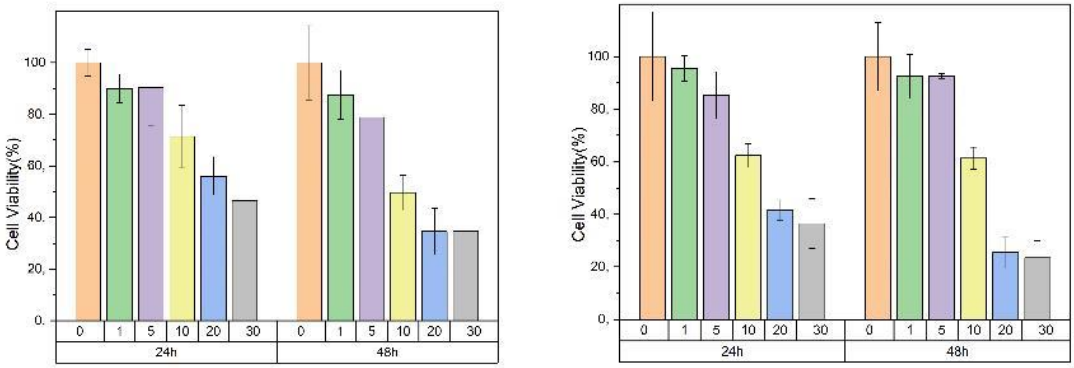


**Figure 48**. 48h MTT analysis results showing the cytotoxicity of AG-08 on SH-SY5Y cells in the **a)** absence **b)** presence of 10 mM Gx paramagnetic contrast agent.

In Figure 49, the results of live-dead analysis after the application of the AG-08 molecule to SH-SY5Y cells are shared. The cytotoxicity of the AG-08 in the presence and absence of Gx was investigated over a 48-hour period. According to the live-dead analysis results, a toxic effect on the cells was observed at 10 μM, and with increasing molecule concentrations, a decrease in cell viability occurred after 48 hours. In addition to the decrease in cell viability, it is observed that due to the increasing molecule concentration, rare surviving cells lose their original morphology and remain in a circular morphology. It also appears that the presence of 10 mM Gx does not cause any extra cytotoxicity, and the viability results are similar. When the results of MTT and live-dead analysis are compared, it can be said that the results of both analyses are generally consistent with each other.

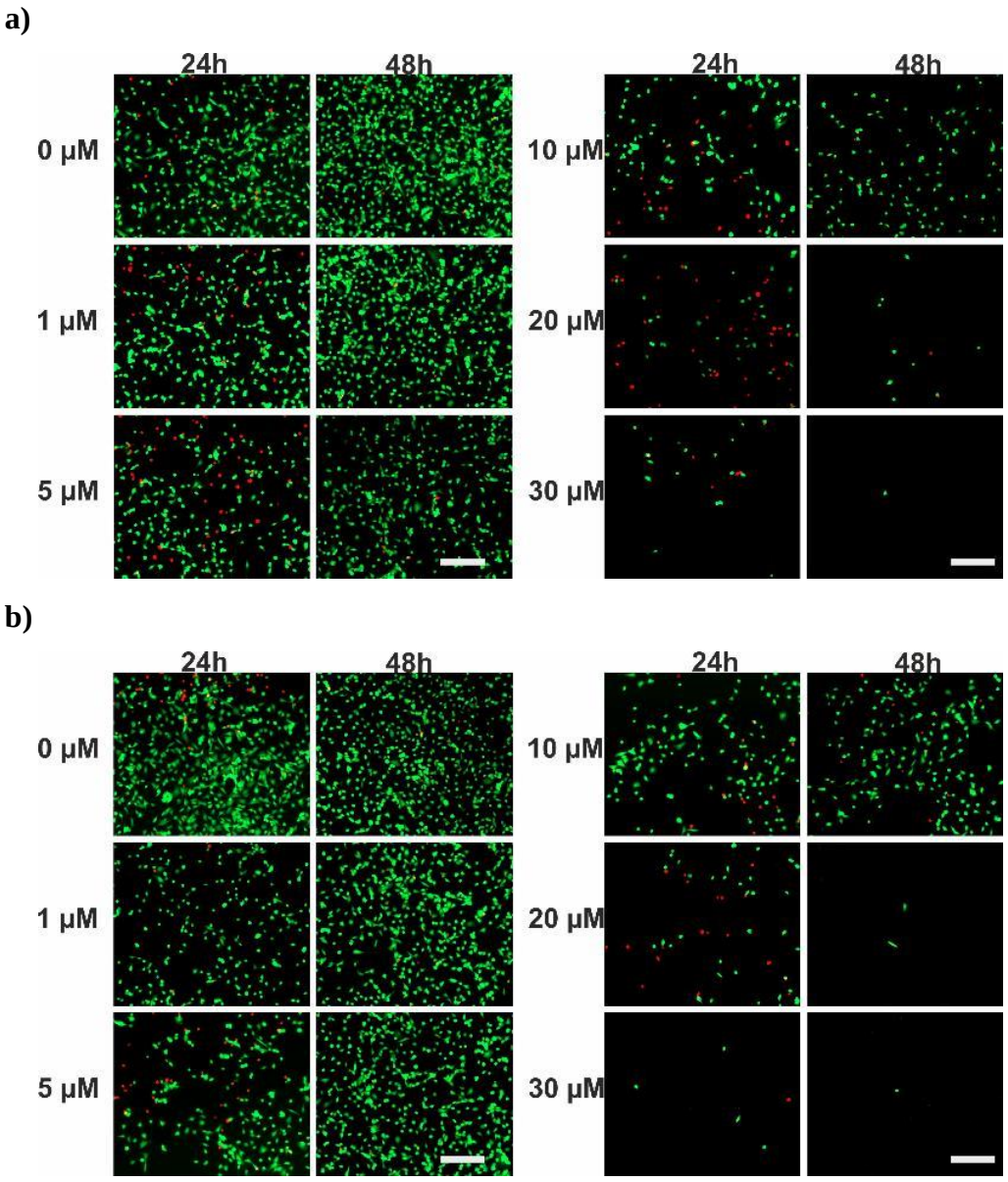


**Figure 49**. 48h live-dead analysis results showing the cytotoxicity of AG-08 on SH-SY5Y cells in the **a)** absence **b)** presence of 10 mM Gx paramagnetic contrast agent (scale unit 100 µm).

In Figure 50, MTT graphs for viability analysis are shared for SH-SY5Y cells after AG-04 application. The toxic effect of the AG-04 in the presence and absence of Gx was investigated over a 48-hour period. When the MTT results obtained are examined, it is seen that the cell viability is at a high level as expected and drops below 50% in the presence and absence of Gx only at 30 µM application. This result can be interpreted as the cytotoxicity of the AG-04 molecule, as in the results of the HeLa cell line, occurring

when applied at much higher concentrations compared to the AG-08 molecule. Additionally, the presence of 10 mM Gx did not cause any extra cytotoxicity, and the viability results were similar in both graphs.

**a)** **b)**

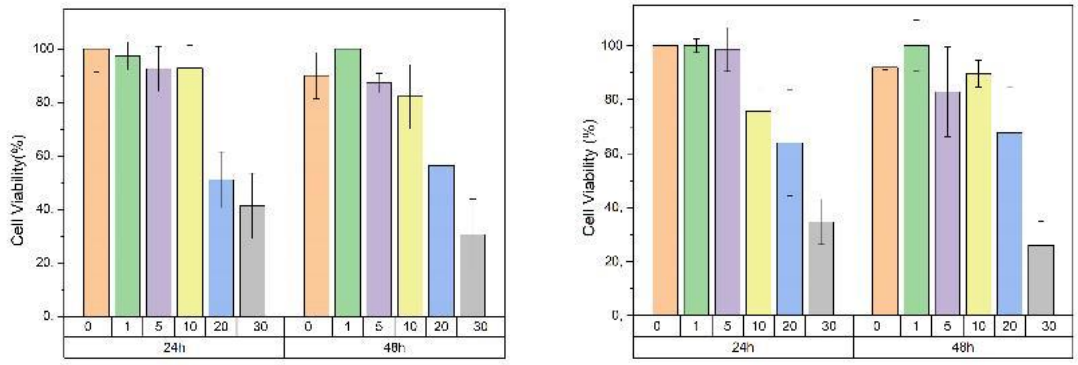


**Figure 50**. 48h MTT analysis results showing the cytotoxicity of AG-04 on SH-SY5Y cells in the **a)** absence **b)** presence of 10 mM Gx paramagnetic contrast agent.

In Figure 51, the results of live-dead analysis after the application of the AG-04 molecule to SH-SY5Y cells are shared. The cytotoxicity of the AG-04 in the presence and absence of Gx was investigated over a 48-hour period. According to the analysis results obtained, cell viability is at a high level despite the increasing molecule concentration. It is observed that there is a decrease in viability only after 30 µM application. However, unlike the AG-08 molecule, as the concentration increased, there was no change in the morphology of the cells. In addition, it is seen that the presence of 10 mM Gx does not cause an extra toxic effect, and the viability results are similar. Finally, when the results of MTT and live-dead analysis are compared, it is seen that the results of both analyses support each other.

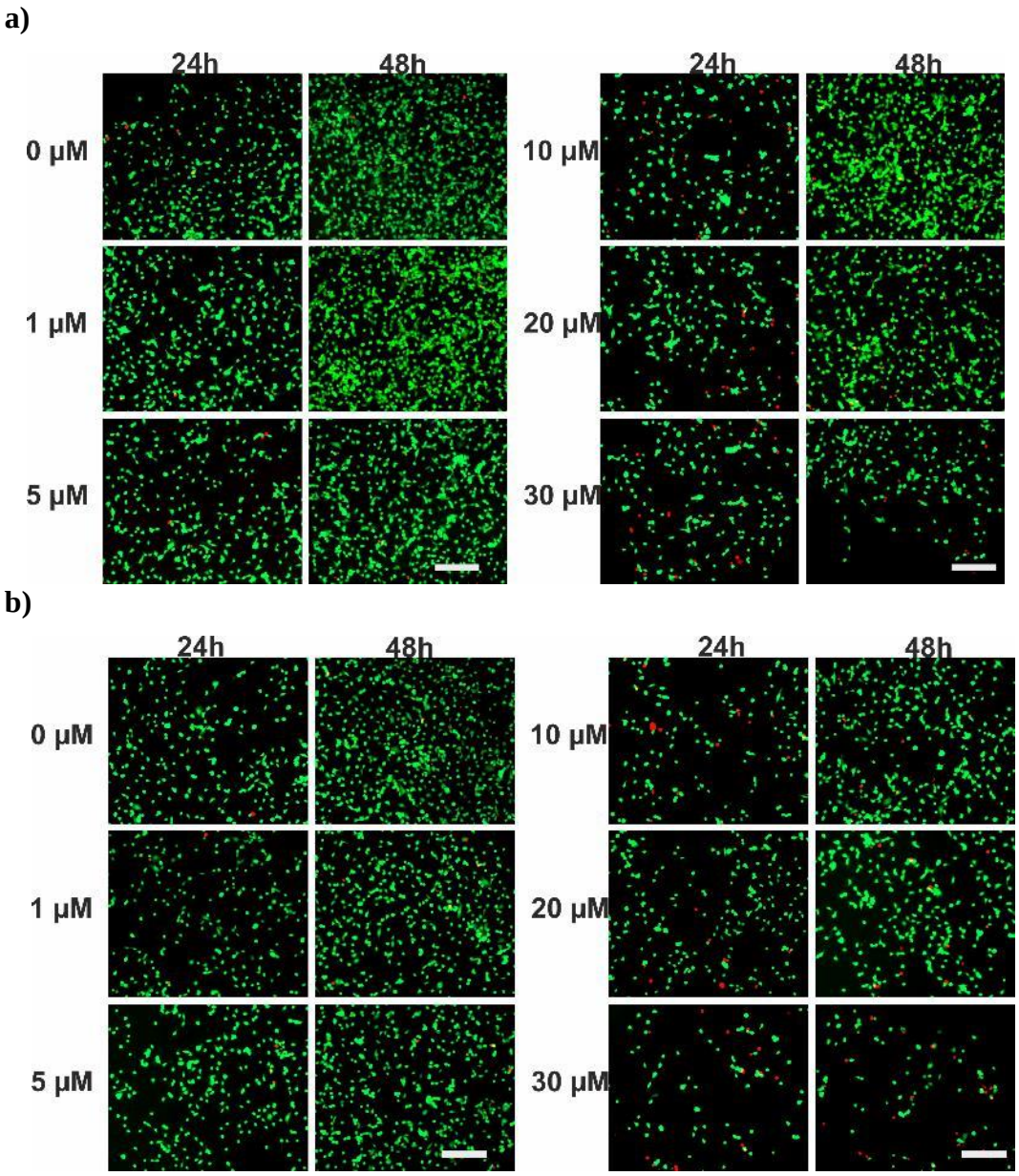


**Figure 51**. 48h live-dead analysis results showing the cytotoxicity of AG-04 on SH-SY5Y cells in the **a)** absence **b)** presence of 10 mM Gx paramagnetic contrast agent (scale unit 100 µm).

In Figure 52, MTT graphs for viability analysis after CG-03 application to SH-SY5Y cells are shared. The toxic effect of the CG-03 in the presence and absence of Gx was investigated over a 48-hour period. According to the MTT results obtained, a high toxic effect occurred at 10 µM and increasing concentrations. Also, a decreasing trend in viability values was observed. The results obtained are like the AG-08 molecule

application, in line with expectations. The presence of 10 mM Gx did not cause any extra cytotoxicity, and the viability results were similar in both graphs.

**a)** **b)**

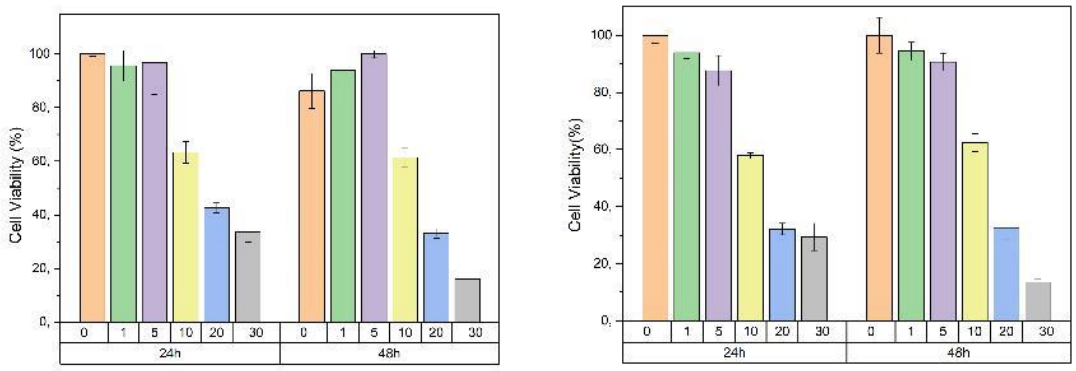


**Figure 52**. 48h MTT analysis results showing the cytotoxicity of CG-03 on SH-SY5Y cells in the **a)** absence **b)** presence of 10 mM Gx paramagnetic contrast agent.

In Figure 53, the results of live-dead analysis after CG-03 application for SH-SY5Y cells are shared. The cytotoxicity of the CG-03 in the presence and absence of Gx was investigated over a 48-hour period. According to the live-dead analysis results, a toxic effect was observed on the cells at 20 μM, and increasing concentrations, a serious decrease in cell viability also occurred. In addition to the decrease in cell viability due to the increasing molecule concentration, it is observed that rare surviving cells lose their original morphology and remain in a circular morphology. Moreover, it is seen that the presence of 10 mM Gx does not cause any extra cytotoxicity, and the viability results are similar. Finally, when the results of MTT and live-dead analysis are compared, it can be said that the results of both analyses generally support each other.

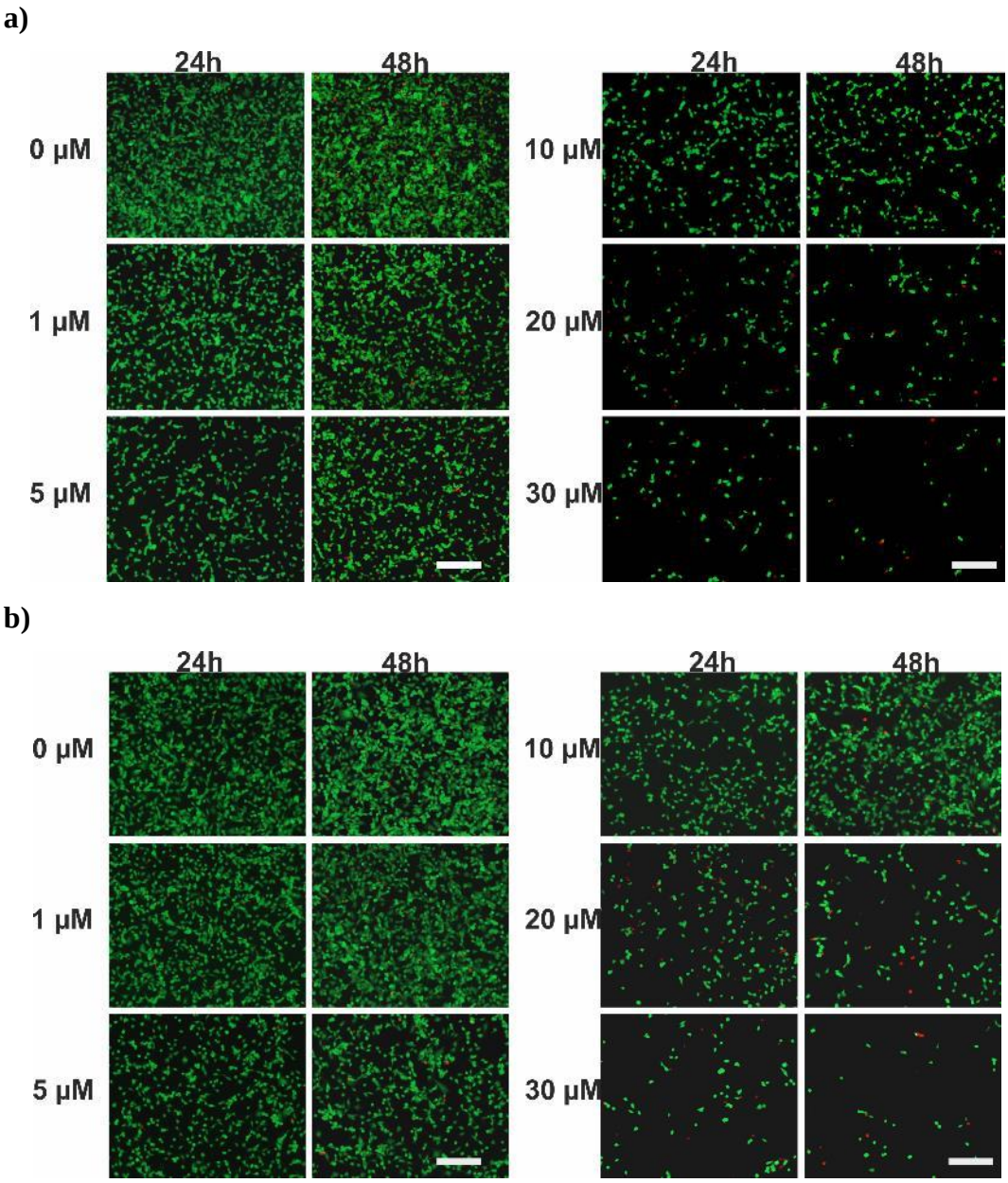


**Figure 53**. 48h live-dead analysis results showing the cytotoxicity of CG-03 on SH-SY5Y cells in the **a)** absence **b)** presence of 10 mM Gx paramagnetic contrast agent (scale unit 100 µm).

Figure 54 shows MTT graphs for viability analysis after CG-04 application to SH-SY5Y cells. The toxic effect of the CG-04 in the presence and absence of Gx was investigated over a 48-hour period. Despite the increasing molecule concentration, viability values are at 60% and above, as expected. The presence of 10 mM Gx did not cause any additional cytotoxicity. Viability values are at similar levels in both graphs.

**a)** **b)**

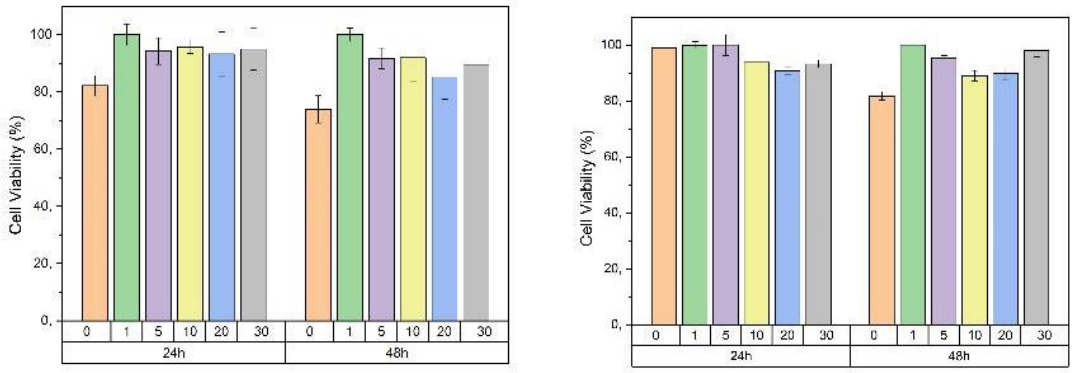


**Figure 54**. 48h MTT analysis results showing the cytotoxicity of CG-04 on SH-SY5Y cells in the **a)** absence **b)** presence of 10 mM Gx paramagnetic contrast agent.

In Figure 55, the results of live-dead analysis after the application of the CG-04 molecule to SH-SY5Y cells are shared. The cytotoxicity of the CG-04 in the presence and absence of Gx was investigated over a 48-hour period. According to the live-dead analysis results, the cell viability level is stable despite the increasing molecule concentration. Unlike the toxic molecules AG-08 and CG-03, no change occurred in cell morphology as the molecule concentration increased. Additionally, the presence of 10 mM Gx did not cause extra cytotoxicity, and the viability level is close to each other in both experiments. Finally, when the results of MTT and live-dead analysis are compared, it can be said that the results of both analyses support each other.

In Figure 56, MTT graphs for viability analysis after Ptx application for HepG2 cells are shared. Ptx cytotoxicity in the presence and absence of Gx was investigated over a 48-hour period. The applied Ptx concentration range is 0-200 nM, similar to previous studies using the literature. According to the MTT results obtained, cytotoxicity was observed in the cells at 25 nM and increasing drug concentrations, and the viability decreased to 60%. In order to reach lower levels for viability, the drug concentration should be increased, or the application process should be extended. Additionally, the presence of 10 mM Gx did not cause any extra cytotoxicity, so it was concluded that the viability level was at similar values in both graphs.

**a)**

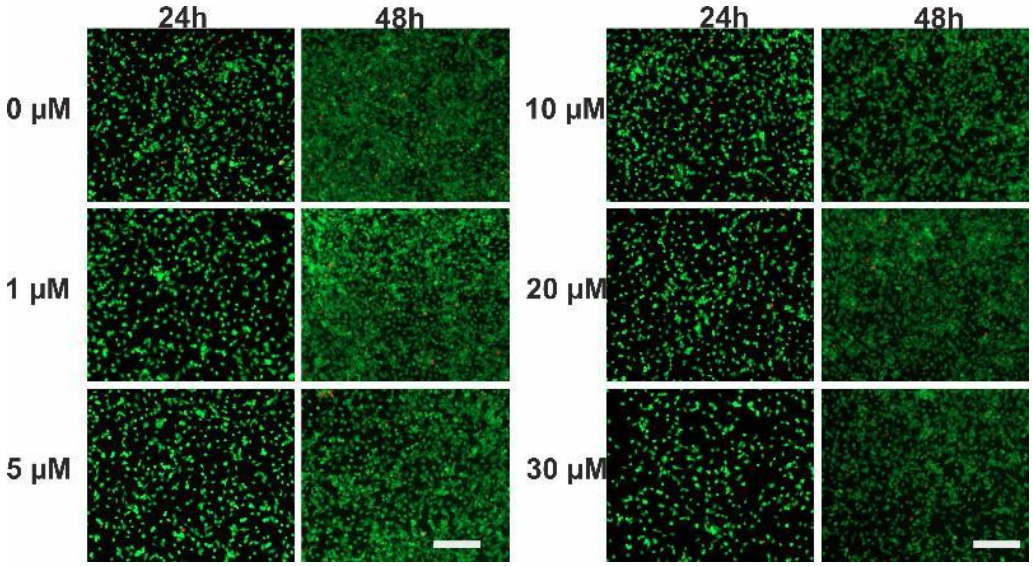


**b)**

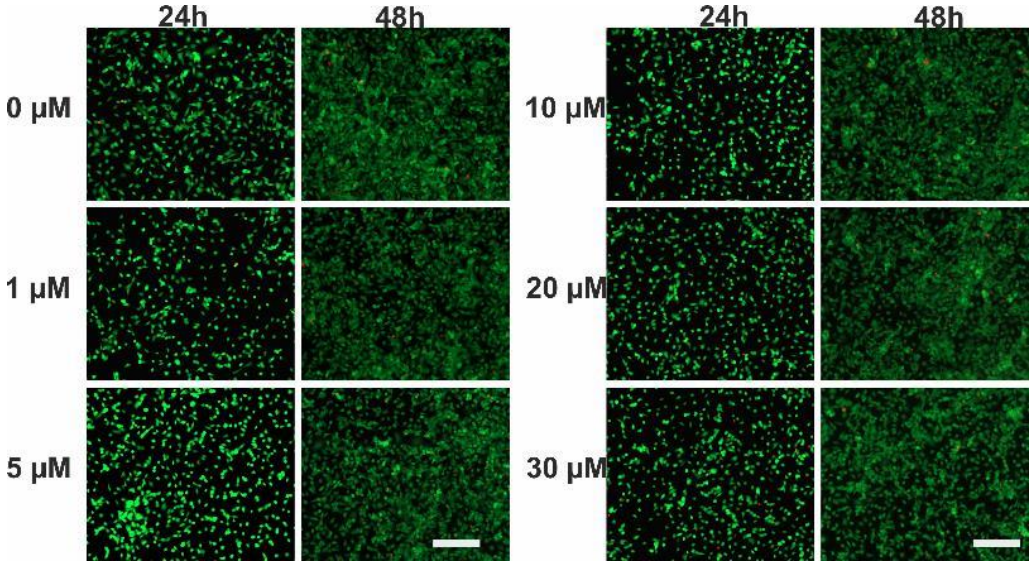


**Figure 55**. 48h live-dead analysis results showing the cytotoxicity of CG-04 on SH-SY5Y cells in the **a)** absence **b)** presence of 10 mM Gx paramagnetic contrast agent (scale unit 100 µm).

**a)** **b)**

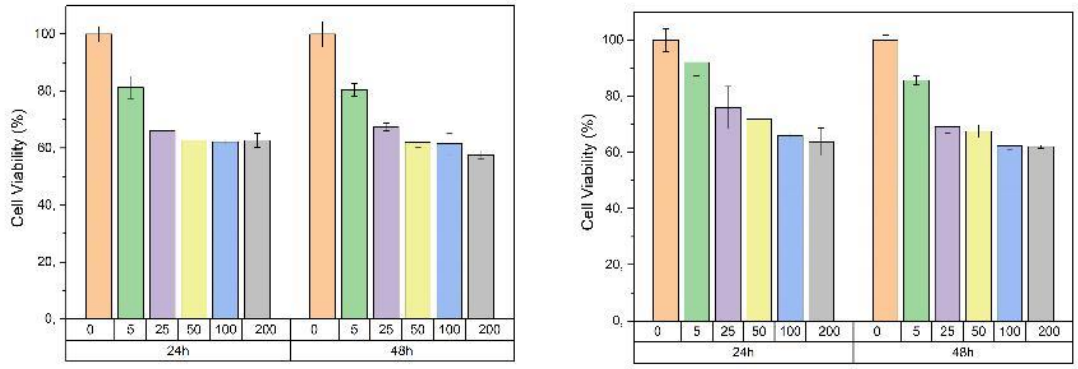


**Figure 56**. 48h MTT analysis results showing the cytotoxicity of PTX on HepG2 cells in the **a)** absence **b)** presence of 10 mM Gx paramagnetic contrast agent.

In Figure 57, the results of live-dead analysis after Ptx application for HepG2 cells are shared. Ptx cytotoxicity in the presence and absence of Gx was investigated over a 48-hour period. The applied Ptx concentration range is 0-200 nM, similar to previous studies using the literature. According to the live-dead analysis results, it was understood that although 50 nM and increasing drug concentration applications had a toxic effect on the cells, it was at a lower level compared to the results obtained with other cell lines. It is known in the literature and in studies conducted in previous work packages that healthy HepG2 cells exist in clusters (Hurrell et al., 2018). It is observed that as the drug concentration applied is increased, this aggregation is disrupted, and the cells remain separated. Additionally, the presence of 10 mM Gx did not cause any extra toxic effects, and the viability results were similar. Finally, when the results of MTT and live-dead analysis are compared, it can be said that the results of both analyses are consistent with each other.

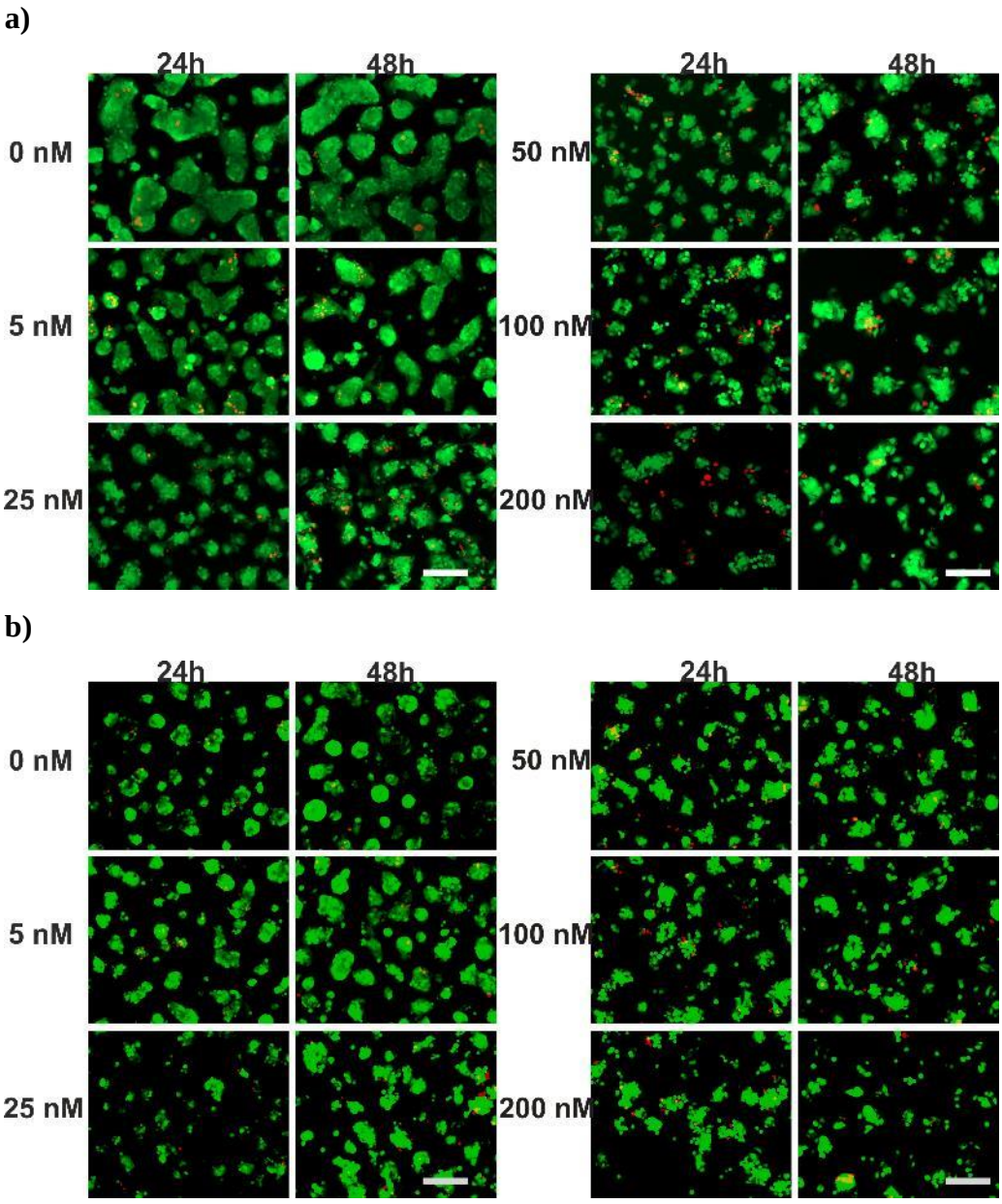


**Figure 57**. 48h live-dead analysis results showing the cytotoxicity of PTX on HepG2 cells in the **a)** absence **b)** presence of 10 mM Gx paramagnetic contrast agent (scale unit 100 μm).

In Figure 58, MTT graphs for viability analysis are shared for HepG2 cells after AG-08 application. The toxic effect of the AG-08 in the presence and absence of Gx was investigated over a 48-hour period. According to the MTT results obtained, a toxic effect on the cells was observed at 20 μM and increasing molecular concentrations, and the cytotoxic effect on the cells increases day by day. Accordingly, there is a decreasing trend

in vitality values. In addition, the presence of 10 mM Gx did not cause any extra cytotoxicity, and it was concluded that the viability levels were at similar values in both graphs.

**a)** **b)**

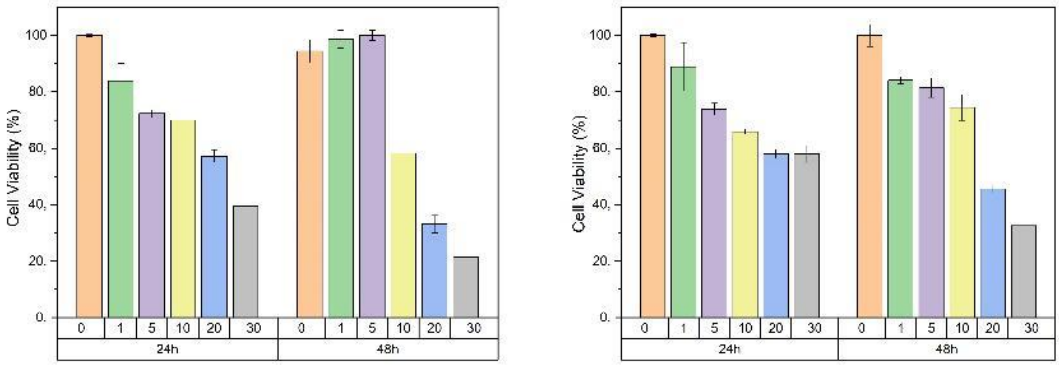


**Figure 58**. 48h MTT analysis results showing the cytotoxicity of AG-08 on HepG2 cells in the **a)** absence **b)** presence of 10 mM Gx paramagnetic contrast agent.

In Figure 59, the results of live-dead analysis after AG-08 application to HepG2 cells are shared. The cytotoxicity of the AG-08 in the presence and absence of Gx was investigated over a 48-hour period. According to the live-dead analysis results, a high level of toxic effects was observed in 10 µM and increasing molecule concentration applications, and a decrease in cell viability was observed. In addition to the decrease in cell viability, it is observed that the cells with impaired aggregation, which is a characteristic feature of the HepG2 cell line, are dispersed in an unhealthy manner. There is no negative effect on the proliferation of cells in experiments carried out in the 0-5 µM concentration range. As seen in the MTT graphs, the amount of viability increases in direct proportion to the incubation period. In addition, the presence of 10 mM Gx did not cause any extra toxic effects, and the viability results appeared to be similar. Finally, when the results of MTT and live-dead analysis are compared, it can be said that the results of both analyses are generally consistent with each other.

**a)**

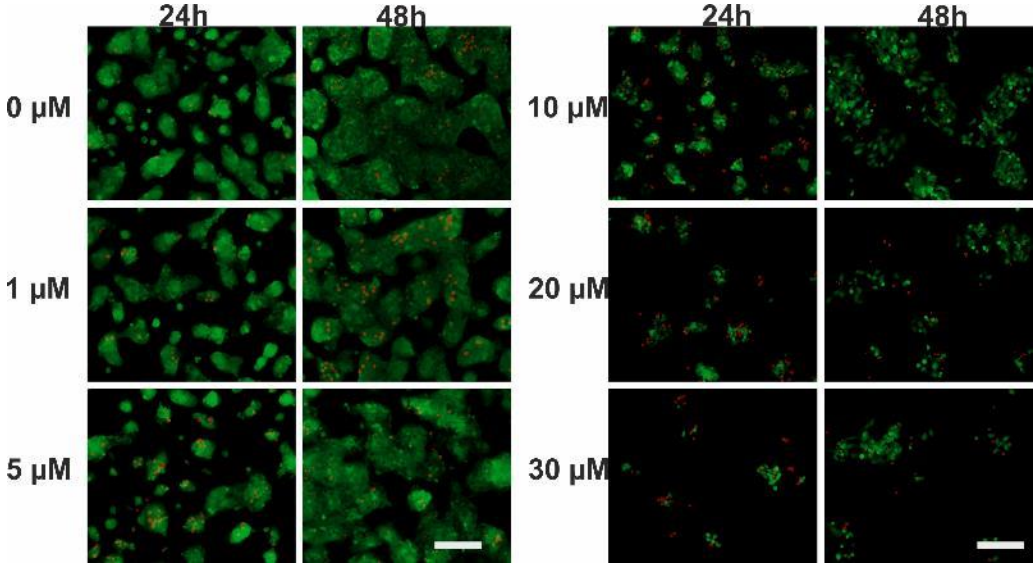


**b)**

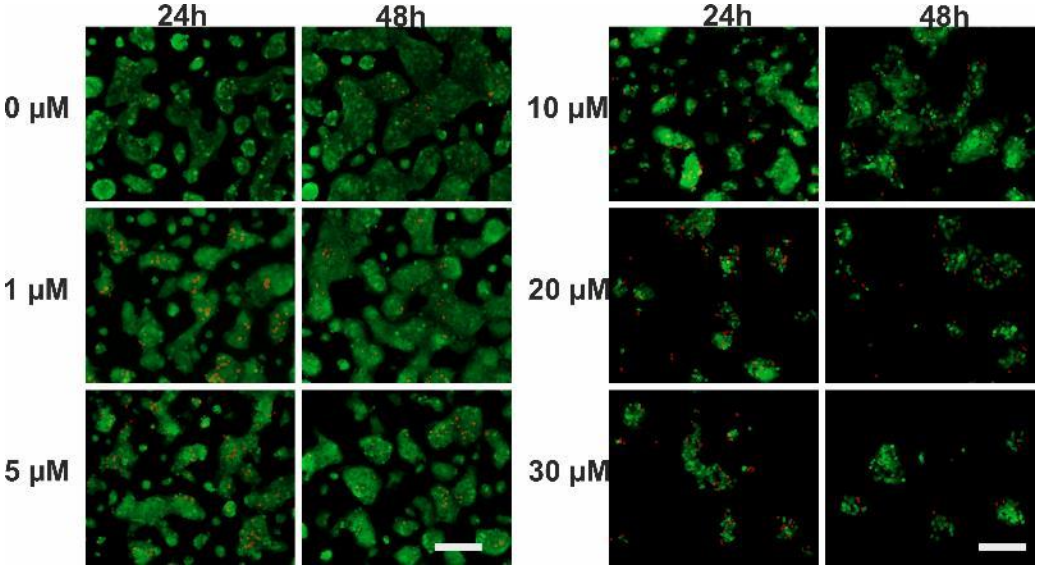


**Figure 59**. 48h live-dead analysis results showing the cytotoxicity of AG-08 on HepG2 cells in the **a)** absence **b)** presence of 10 mM Gx paramagnetic contrast agent. (scale unit 100 µm)

In Figure 60, MTT graphs for viability analysis after the application of the AG-04 molecule to HepG2 cells are shared. The toxic effect of the AG-04 in the presence and absence of Gx was investigated over a 48-hour period. When the MTT results obtained are examined, it is seen that the viability level is at a high level (60% and above) at all concentrations, as expected. It is possible that viability values will decrease if higher

AG-04 concentrations are tried. Additionally, the presence of 10 mM Gx did not cause any additional toxic effects, and the viability levels were in a similar range in both graphs.

**a)** **b)**

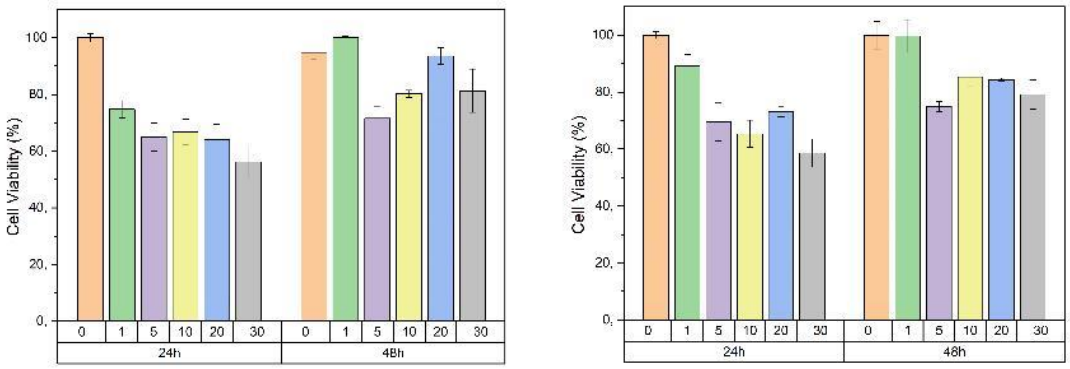


**Figure 60**. 48h MTT analysis results showing the cytotoxicity of AG-04 on HepG2 cells in the **a)** absence **b)** presence of 10 mM Gx paramagnetic contrast agent.

In figure 61, the results of live-dead analysis after AG-04 application for HepG2 cells are shared. The cytotoxicity of the AG-04 in the presence and absence of Gx was investigated over a 48-hour period. According to the analysis results, viability is at a high level despite the increasing molecule concentration, and there is a slight decrease in viability in the presence of Gx with the application of 30 μM AG-04. However, unlike AG-08, there was no disruption in the aggregation characteristic of HepG2 cells. If the results obtained in live-dead analysis after the application of both molecules (AG-08 and AG-04) are compared, it can be said that AG-04 affects the viability value much less than AG-08. Finally, when the results of MTT and live-dead analysis are compared, it can be said that the results of both analyses support each other.

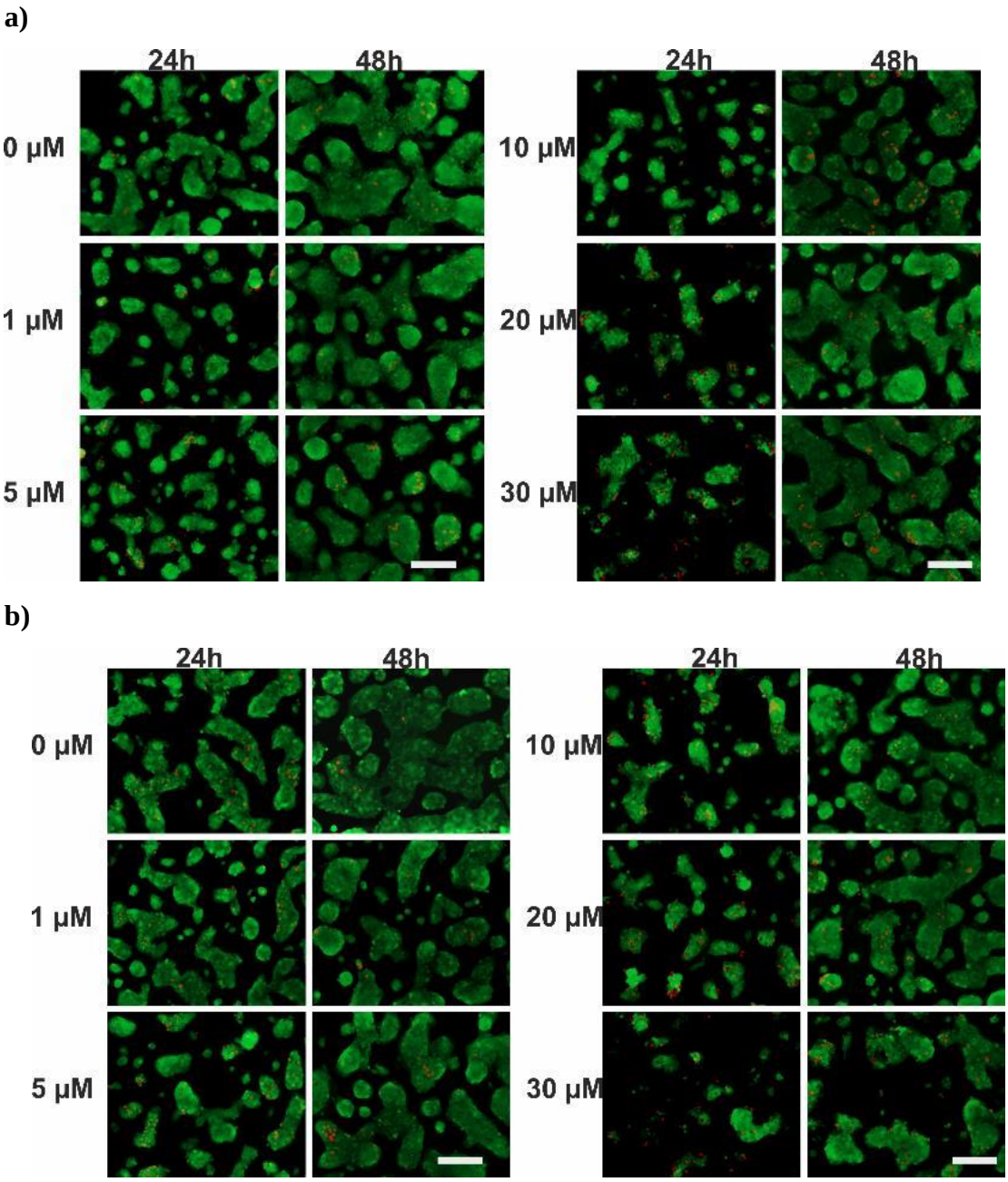


**Figure 61**. 48h live-dead analysis results showing the cytotoxicity of AG-04 on HepG2 cells in the **a)** absence **b)** presence of 10 mM Gx paramagnetic contrast agent. (scale unit 100 µm)

MTT graphs for viability analysis after CG-03 application to HepG2 cells are shared in Figure 62. The toxic effect of the CG-03 in the presence and absence of Gx was investigated over a 48-hour period. According to the MTT results obtained, there is a decreasing trend in cell viability due to increasing molecule concentrations. It is

observed that the viability decreases to 50% and below at 20 µM and 30 µM concentration applications. As expected, the results are like those of the AG-08 molecule application. Additionally, the presence of 10 mM Gx did not cause any extra cytotoxicity, and the viability values were at similar levels in both graphs.

**a)** **b)**

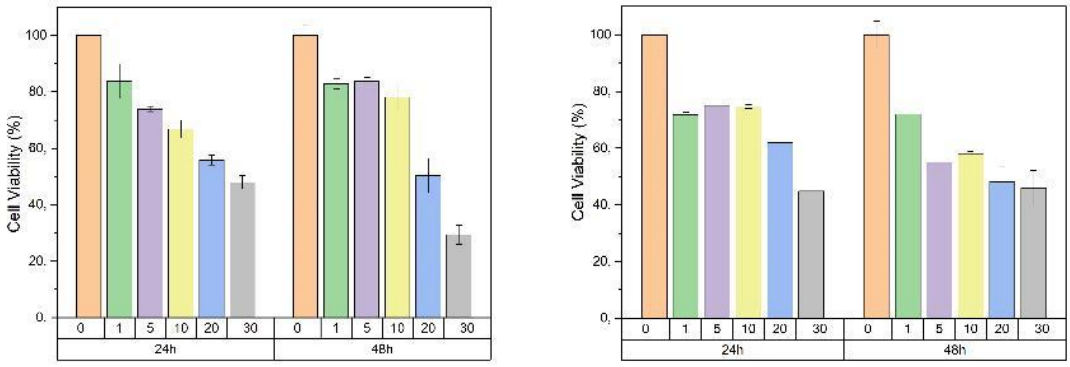


**Figure 62**. 48h MTT analysis results showing the cytotoxicity of CG-03 on HepG2 cells in the **a)** absence **b)** presence of 10 mM Gx paramagnetic contrast agent.

In Figure 63, the results of live-dead analysis after the application of the CG-03 molecule to HepG2 cells are shared. The cytotoxicity of the CG-03 in the presence and absence of Gx was investigated over a 48-hour period. According to the live-dead analysis results, a high level of toxic effects was observed in 10 µM and increasing concentration molecule applications, and the decrease in cell viability is clearly seen. In addition to the decrease in cell viability, it is observed that the cells with impaired aggregation, which is a characteristic feature of the HepG2 cell line, are dispersed in an unhealthy manner. There is no negative effect on the proliferation of cells in experiments performed in the 0-5 µM range. As seen in the MTT graphs, the amount of viability increases in direct proportion to the incubation period. Additionally, the presence of 10 mM Gx did not cause any extra toxic effects, and the viability results were similar. Finally, when the results of MTT and live-dead analysis are compared, it is seen that the results of both analyses generally support each other.

**a)**

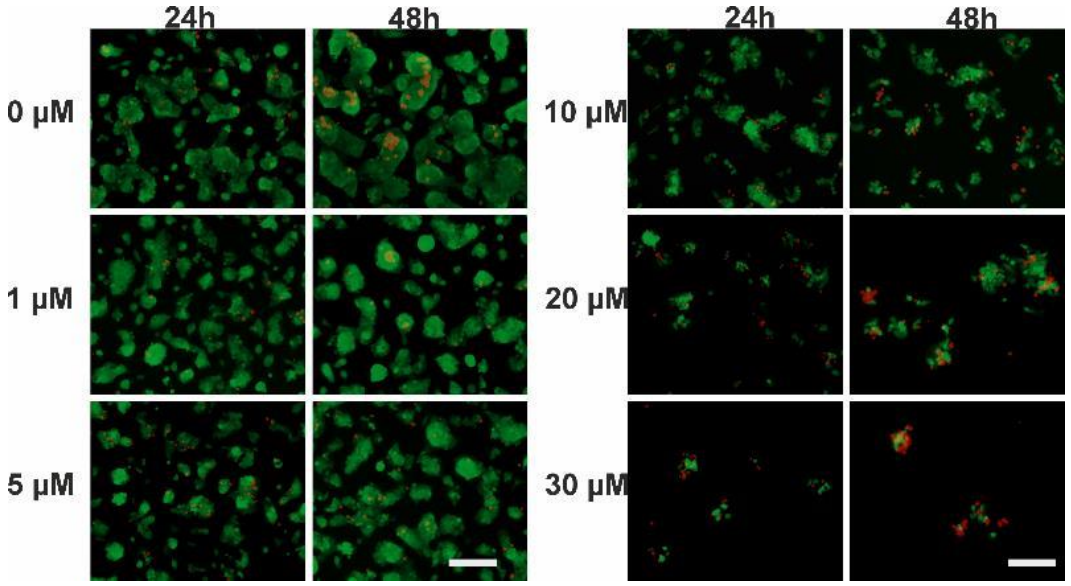


**b)**

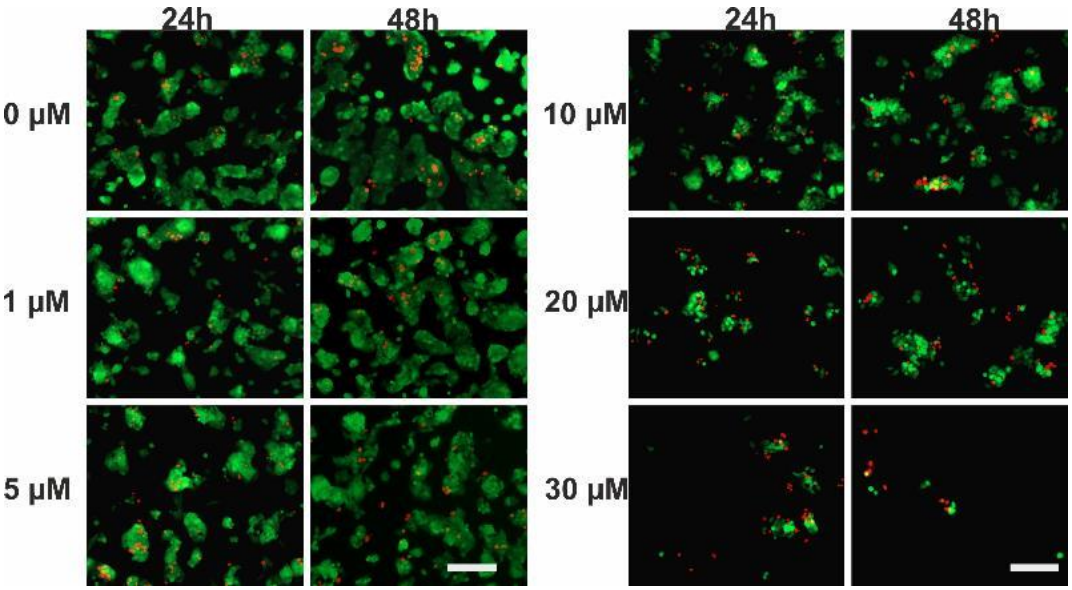


**Figure 63**. 48h live-dead analysis results showing the cytotoxicity of CG-03 on HepG2 cells in the **a)** absence **b)** presence of 10 mM Gx paramagnetic contrast agent. (scale unit 100 µm).

In Figure 64, MTT graphs for viability analysis after the application of the CG-04 molecule to HepG2 cells are shared. The toxic effect of the CG-04 in the presence and absence of Gx was investigated over a 48-hour period. Viability values at all applied molecule concentrations are high (70% and above), as expected. The results obtained can

be interpreted as indicating that the toxic effects will probably occur at much higher concentrations compared to the experiments conducted with AG-08 and CG-03 molecules, which have high toxic effects. Additionally, the presence of 10 mM Gx did not cause any extra toxic effects, and the viability values were at similar levels in both graphs.

**a)** **b)**

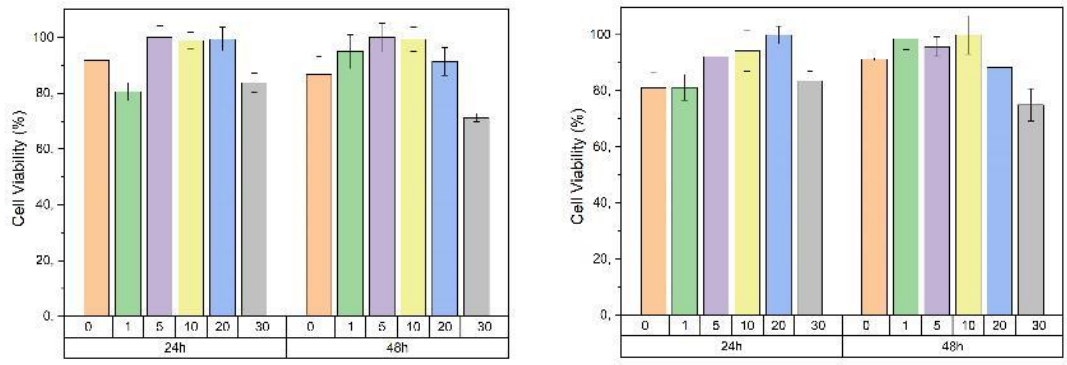


**Figure 64**. 48h MTT analysis results showing the cytotoxicity of CG-04 on HepG2 cells in the **a)** absence **b)** presence of 10 mM Gx paramagnetic contrast agent.

In Figure 65, the results of live-dead analysis of HepG2 cells after CG-04 molecule application are shared. The cytotoxicity of the CG-04 in the presence and absence of Gx was investigated over a 48-hour period. According to the analysis results, viability is at a high level despite the increased molecule concentration. Contrary to the experiments with AG-08 and CG-03 molecules, which are known to have a high toxic effect, no dispersion occurred in the aggregation characteristic of HepG2 cells after CG-04 application. In addition, the presence of 10 mM Gx did not cause any extra toxic effects, and the viability results were similar. Finally, when the results of MTT and live-dead analysis are compared, it can be said that the results of both analyses are compatible with each other.

**a)**

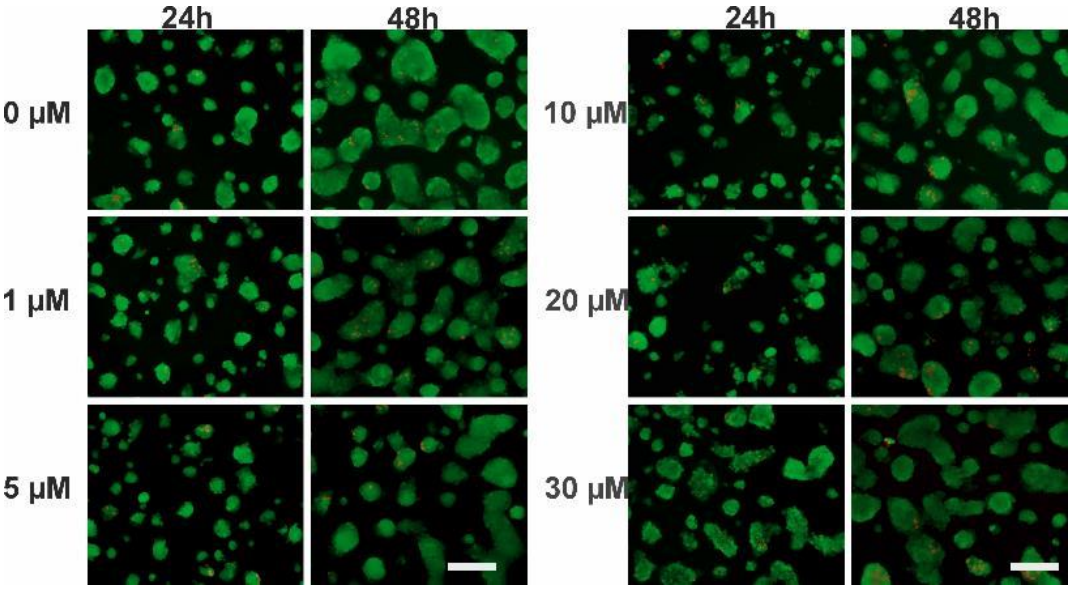


**b)**

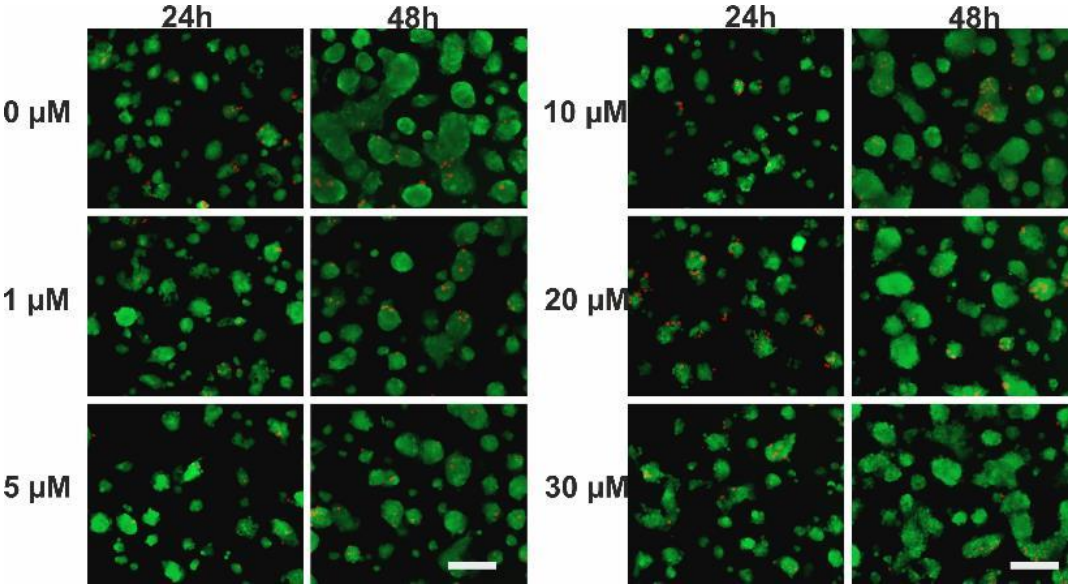


**Figure 65**. 48h live-dead analysis results showing the cytotoxicity of CG-04 on HepG2 cells in the **a)** absence **b)** presence of 10 mM Gx paramagnetic contrast agent. (scale unit 100 µm).

MTT graphs for viability analysis after Ptx application for MCF-7 cells are shared in Figure 66. Ptx cytotoxicity in the presence and absence of Gx was investigated over a 48-hour period. The applied Ptx concentration range is 0-200 nM, similar to previous studies using the literature. According to the MTT results obtained, a toxic effect was

observed in 25 nM and increasing concentration applications; also, the cytotoxicity on the cells increases day by day, and accordingly, there is a decreasing trend in the viability values. In addition, the presence of 10 mM Gx did not cause an extra toxic effect, and it was concluded that the viability results were at similar levels in both graphs.

**a)** **b)**

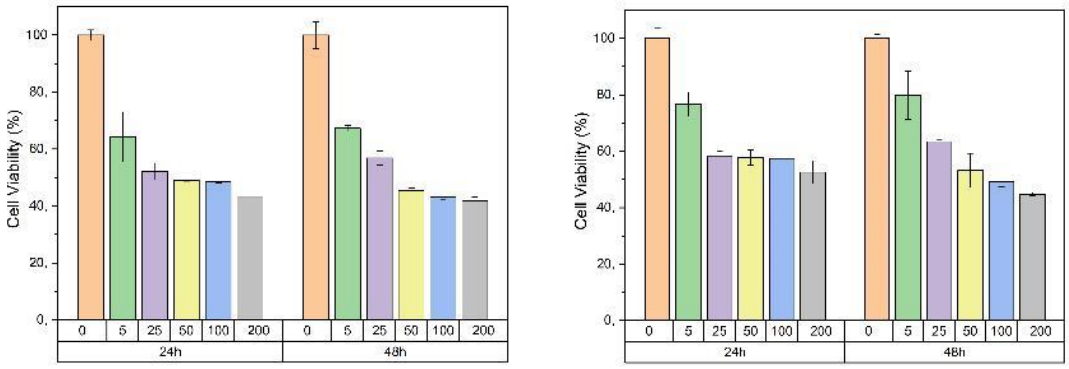


**Figure 66**. 48h MTT analysis results showing the cytotoxicity of PTX on MCF-7 cells in the **a)** absence **b)** presence of 10 mM Gx paramagnetic contrast agent.

In Figure 67, the results of live-dead analysis after Ptx application for MCF-7 cells are shared. Ptx cytotoxicity in the presence and absence of Gx was investigated over a 48-hour period. The applied Ptx concentration range is 0-200 nM, like previous studies using the literature. According to the results obtained, a high level of toxic effects was observed in applications at 25 nM and increasing molecule concentrations, and cell viability decreased after 48 hours. In addition to the decrease in cell viability, it is observed that due to increasing drug concentration, the surviving cells lose their original morphology and remain in a circular morphology. Additionally, the presence of 10 mM Gx did not cause any extra toxic effects, and the viability results were similar in both cases. When the results of MTT and live-dead analysis are compared, it can be interpreted that the results of both analyses support each other.

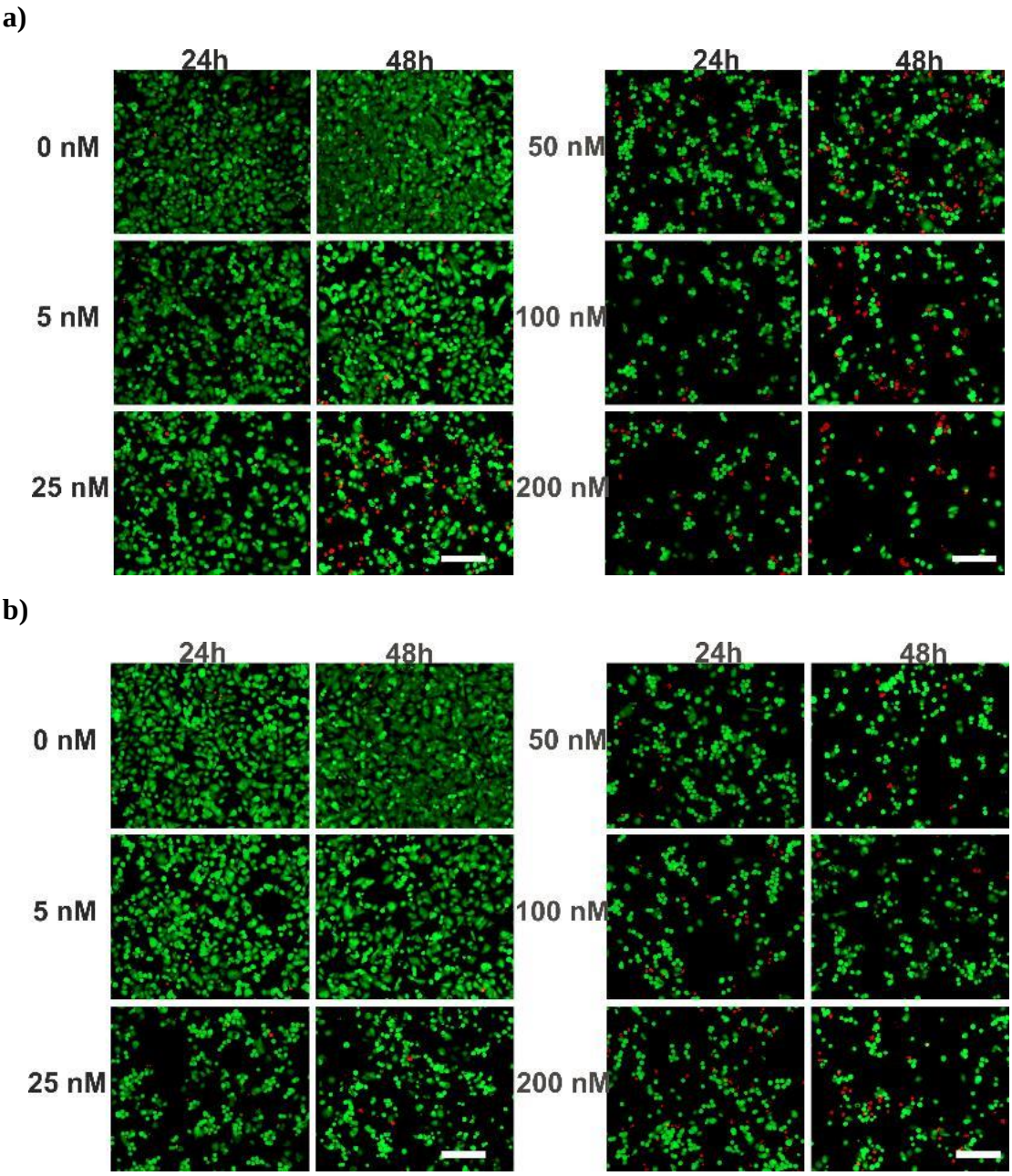


**Figure 67**. 48h live-dead analysis results showing the cytotoxicity of PTX on MCF-7 cells in the **a)** absence **b)** presence of 10 mM Gx paramagnetic contrast agent. (scale unit 100 μm).

In Figure 68, MTT graphs for viability analysis after the application of the AG-08 molecule to MCF-7 cells are shared. The toxic effect of the AG-08 in the presence and absence of Gx was investigated over a 48-hour period. According to the MTT results obtained, a toxic effect was observed in applications at 10 μM and increasing molecule

concentrations, and the cytotoxicity on the cells increased day by day. So, there is a decreasing trend in the viability values. In addition, the presence of 10 mM Gx did not cause an extra toxic effect, and it was concluded that the viability values were at similar levels in both graphs.

**a)** **b)**

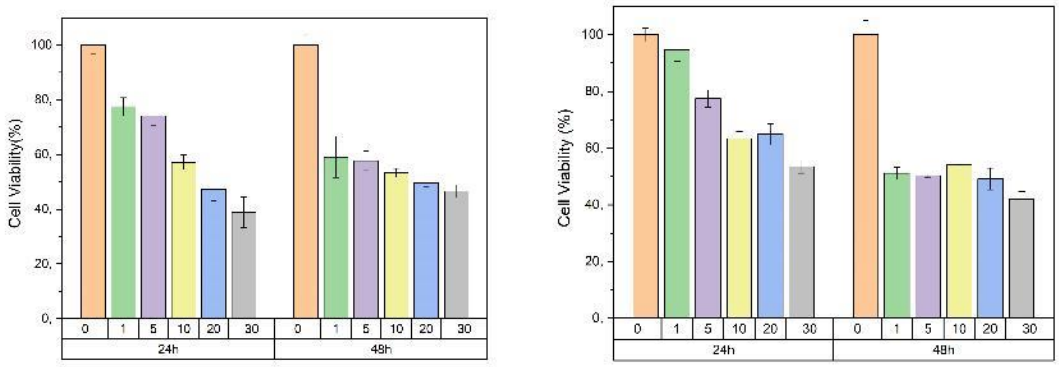


**Figure 68**. 48h MTT analysis results showing the cytotoxicity of AG-08 on MCF-7 cells in the **a)** absence **b)** presence of 10 mM Gx paramagnetic contrast agent.

In Figure 69, the results of live-dead analysis after the application of the AG-08 molecule to MCF-7 cells are shared. The cytotoxicity of the AG-08 in the presence and absence of Gx was investigated over a 48-hour period. According to the live-dead analysis results, a high level of toxic effects was observed at 10 µM, and increasing molecule concentration applications and cell viability decreased. In addition to the decrease in cell viability, it is observed that due to the increasing molecule concentrations, rare surviving cells lose their original morphology and remain in a circular morphology. On the other hand, the presence of 10 mM Gx did not cause any extra cytotoxicity, and the viability results in both samples were similar. Finally, when the results of MTT and live-dead analysis are compared, it is seen that the results of both analyses are generally consistent with each other.

**a)**

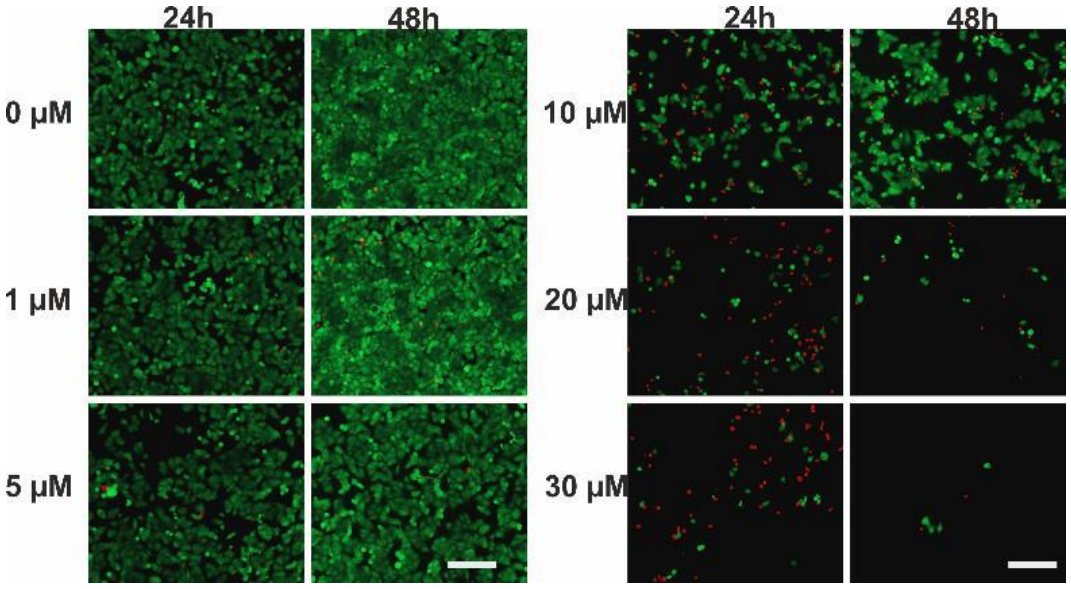


**b)**

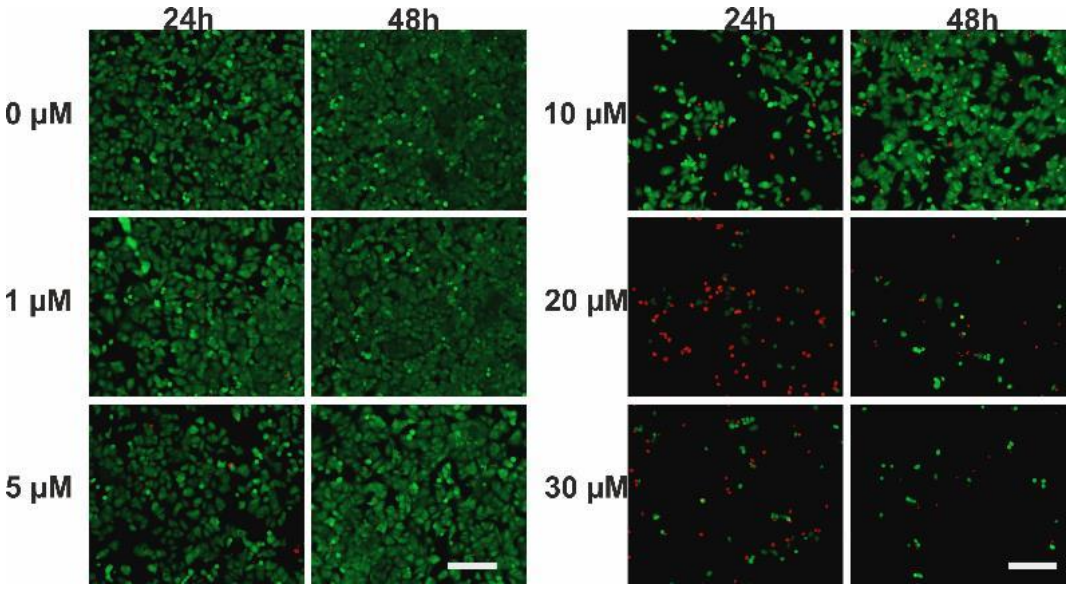


**Figure 69**. 48h live-dead analysis results showing the cytotoxicity of AG-08 on MCF-7 cells in the **a)** absence **b)** presence of 10 mM Gx paramagnetic contrast agent. (scale unit 100 µm).

In Figure 70, MTT graphs for viability analysis after the application of the AG-04 molecule to MCF-7 cells are shared. The toxic effect of the AG-04 in the presence and absence of Gx was investigated over a 48-hour period. Viability values at all applied molecule concentrations are high (80% and above), as expected. The results obtained can

be interpreted as indicating that the toxic effects will probably occur at much higher concentrations compared to the experiments conducted with AG-08 and CG-03 molecules, which have high toxic effects. Additionally, the presence of 10 mM Gx did not cause any extra toxic effects, and the viability values were at similar levels in both graphs.

**a)** **b)**

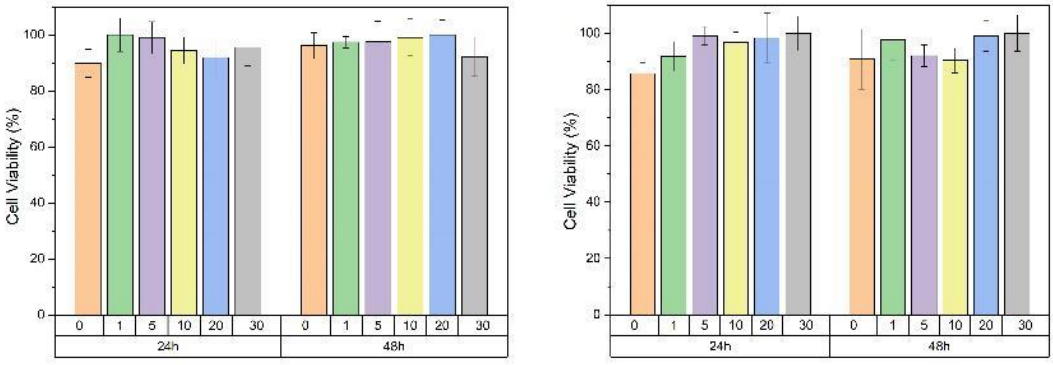


**Figure 70**. 48h MTT analysis results showing the cytotoxicity of AG-04 on MCF-7 cells in the **a)** absence **b)** presence of 10 mM Gx paramagnetic contrast agent.

In Figure 71, the results of the live-dead analysis after the application of the AG-04 molecule to MCF-7 cells are shared. The cytotoxicity of the AG-04 in the presence and absence of Gx was investigated over a 48-hour period. According to the live-dead analysis results, the viability is at a high level in line with expectations, but there is a decrease in cell viability only after the application of 30 µM. However, unlike the toxic molecule AG-08, there was no change in the morphology of the cells as the applied molecule concentration increased. In addition, while the presence of 10 mM Gx does not cause an extra toxic effect, the viability results in both experiments are similar. In the live-dead analysis results, it is seen that cell viability decreases starting from 30 µM molecule application, in accordance with the literature.

**a)**

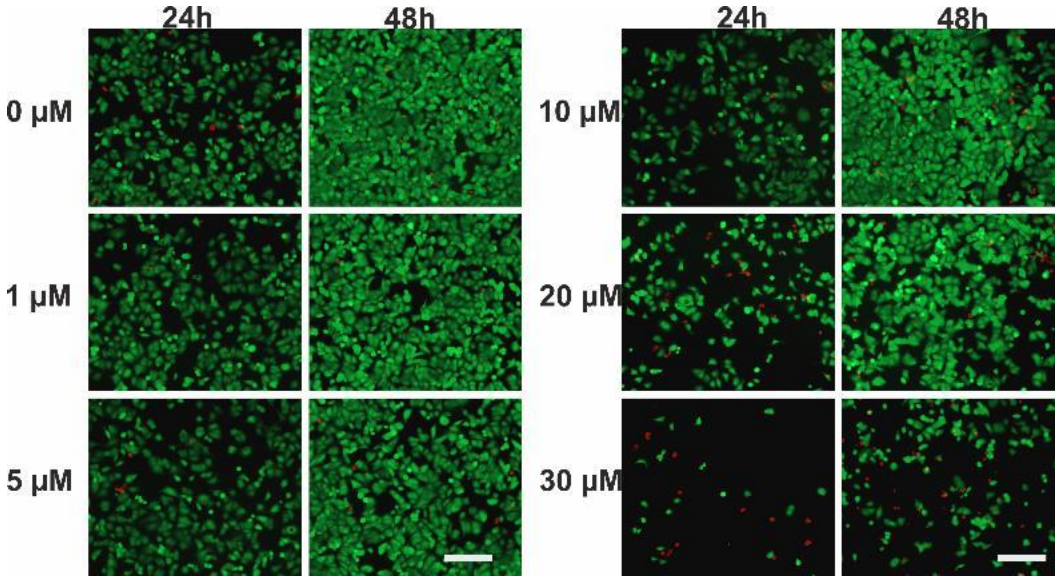


**b)**

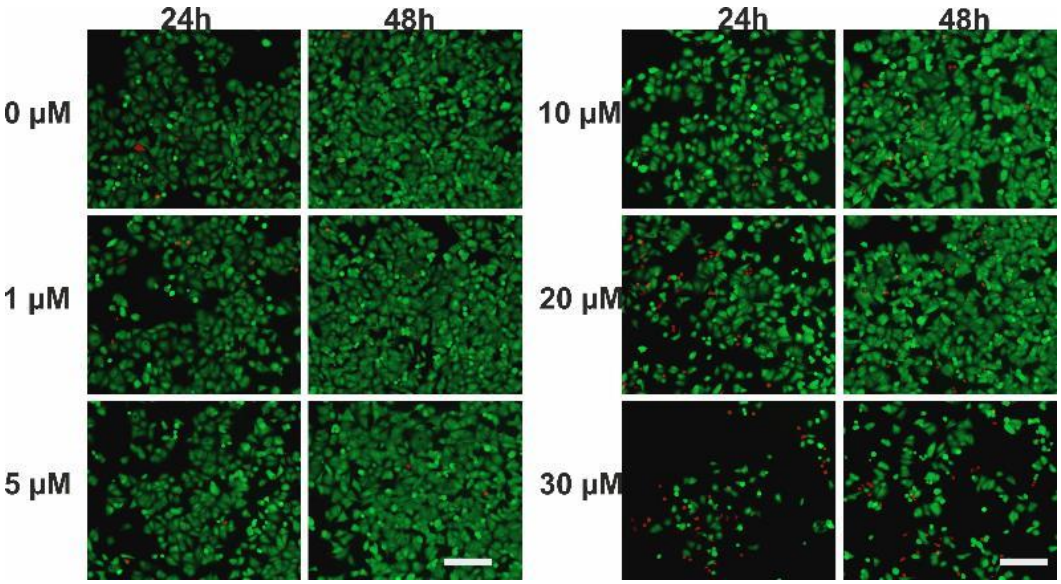


**Figure 71**. 48h live-dead analysis results showing the cytotoxicity of AG-04 on MCF-7 cells in the **a)** absence **b)** presence of 10 mM Gx paramagnetic contrast agent. (scale unit 100 µm).

In Figure 72, MTT graphs for viability analysis are shared after the application of the CG-03 molecule to MCF-7 cells. The toxic effect of the CG-03 in the presence and absence of Gx was investigated over a 48-hour period. According to the MTT results obtained, there is a decreasing trend in the amount of viability depending on the increasing

molecule concentration. Viability values decreased to 50% and below at 20 µM and 30 µM concentration applications. As expected, the results are similar to the application of AG-08, another toxic molecule. Additionally, the presence of 10 mM Gx did not cause any extra toxic effects, and the viability results were similar in both graphs.

**a)** **b)**

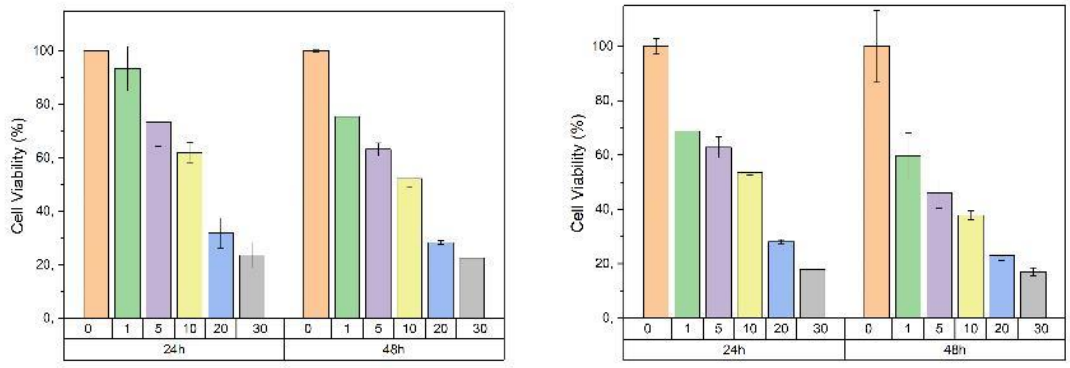


**Figure 72**. 48h MTT analysis results showing the cytotoxicity of CG-03 on MCF-7 cells in the **a)** absence **b)** presence of 10 mM Gx paramagnetic contrast agent.

In Figure 73, the results of the live-dead analysis after the application of the CG-03 molecule to MCF-7 cells are shared. The cytotoxicity of the CG-03 in the presence and absence of Gx was investigated over a 48-hour period. According to the live-dead analysis results, a high level of toxic effect was observed at 10 µM and above, and the decrease in cell viability was distinct. In addition to the decrease in cell viability due to the increasing molecule concentration, it is observed that the rare surviving cells lose their original morphology and remain in a circular morphology. Moreover, it is seen that the presence of 10 mM Gx does not cause an extra toxic effect, and the results regarding viability are similar in both cases. Finally, when the results of MTT and live-dead analysis are compared, it is concluded that the results of both analyses generally support each other.

**a)**

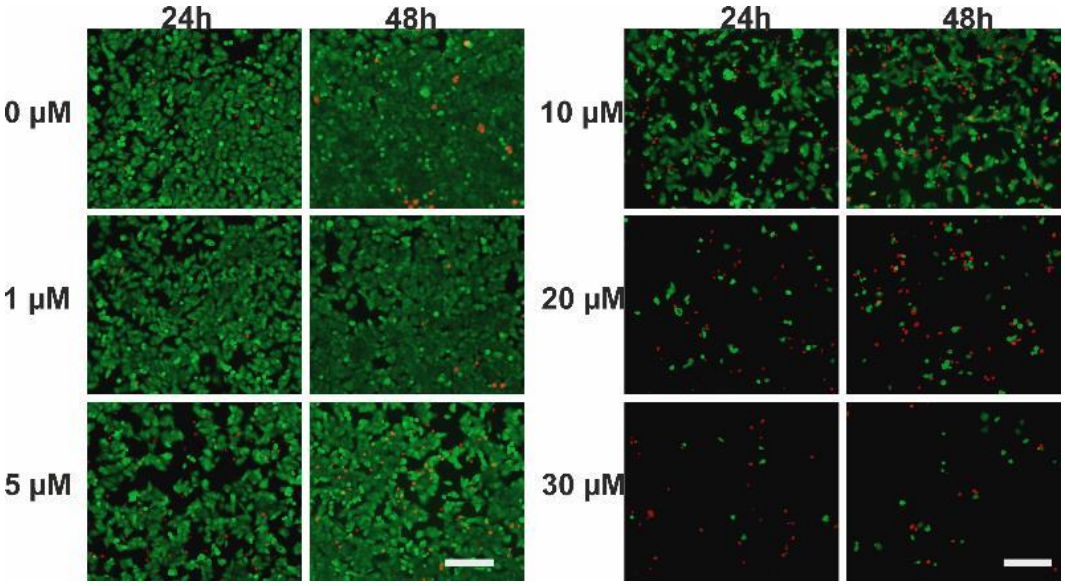


**b)**

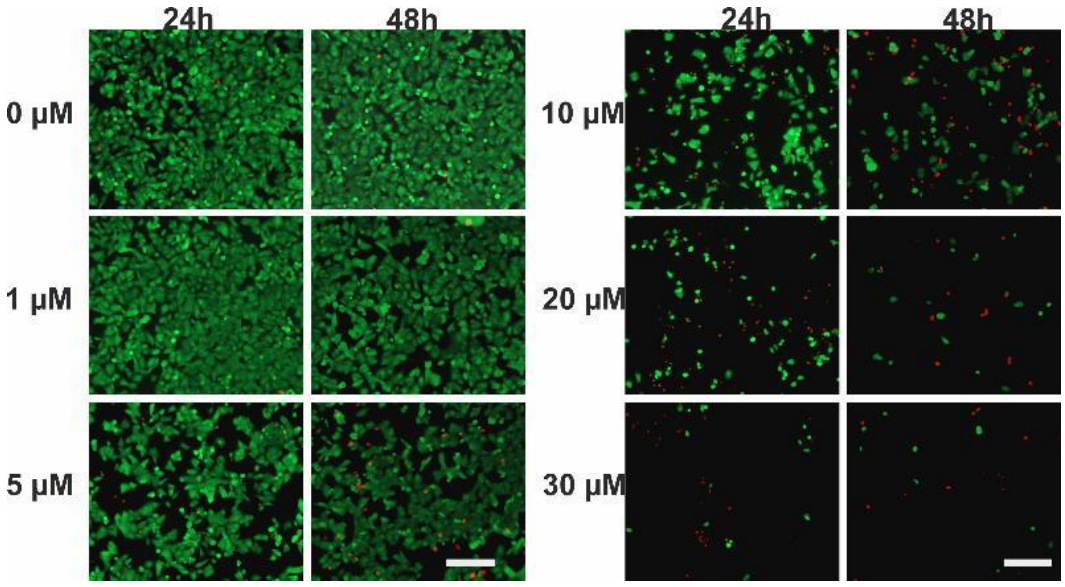


**Figure 73**. 48h live-dead analysis results showing the cytotoxicity of CG-03 on MCF-7 cells in the **a)** absence **b)** presence of 10 mM Gx paramagnetic contrast agent. (scale unit 100 µm).

In Figure 74, MTT graphs for viability analysis after CG-04 molecule application for MCF-7 cells are shared. The toxic effect of the CG-04 in the presence and absence of Gx was investigated over a 48-hour period. Despite the increasing molecule concentration, viability values are at 60% and above at all concentration applications, as

expected. The presence of 10 mM Gx did not cause any additional toxic effects, and the viability results were at similar levels in both graphs.

**a)** **b)**

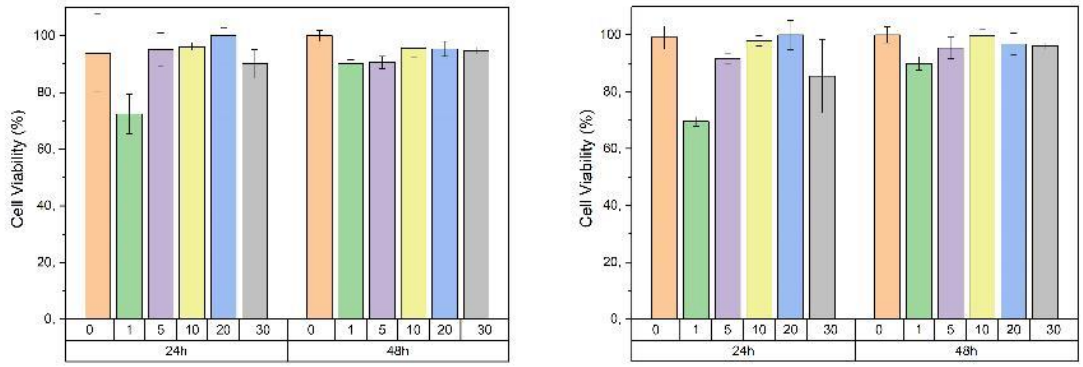


**Figure 74**. 48h MTT analysis results showing the cytotoxicity of CG-04 on MCF-7 cells in the **a)** absence **b)** presence of 10 mM Gx paramagnetic contrast agent.

In Figure 75, the results of the live-dead analysis after the application of the CG-04 molecule to MCF-7 cells are shared. The cytotoxicity of the CG-04 in the presence and absence of Gx was investigated over a 48-hour period. According to the analysis results, viability is at a high level despite the increased molecule concentration. Contrary to the effect of toxic molecules, no change in the original morphology of the cells was observed as the molecule concentration increased after CG-04 application. Moreover, while the presence of 10 mM Gx does not cause any extra cytotoxicity, the results on viability are similar. Finally, when the results of MTT and live-dead analysis are compared, it is seen that the results of both analyses support each other.

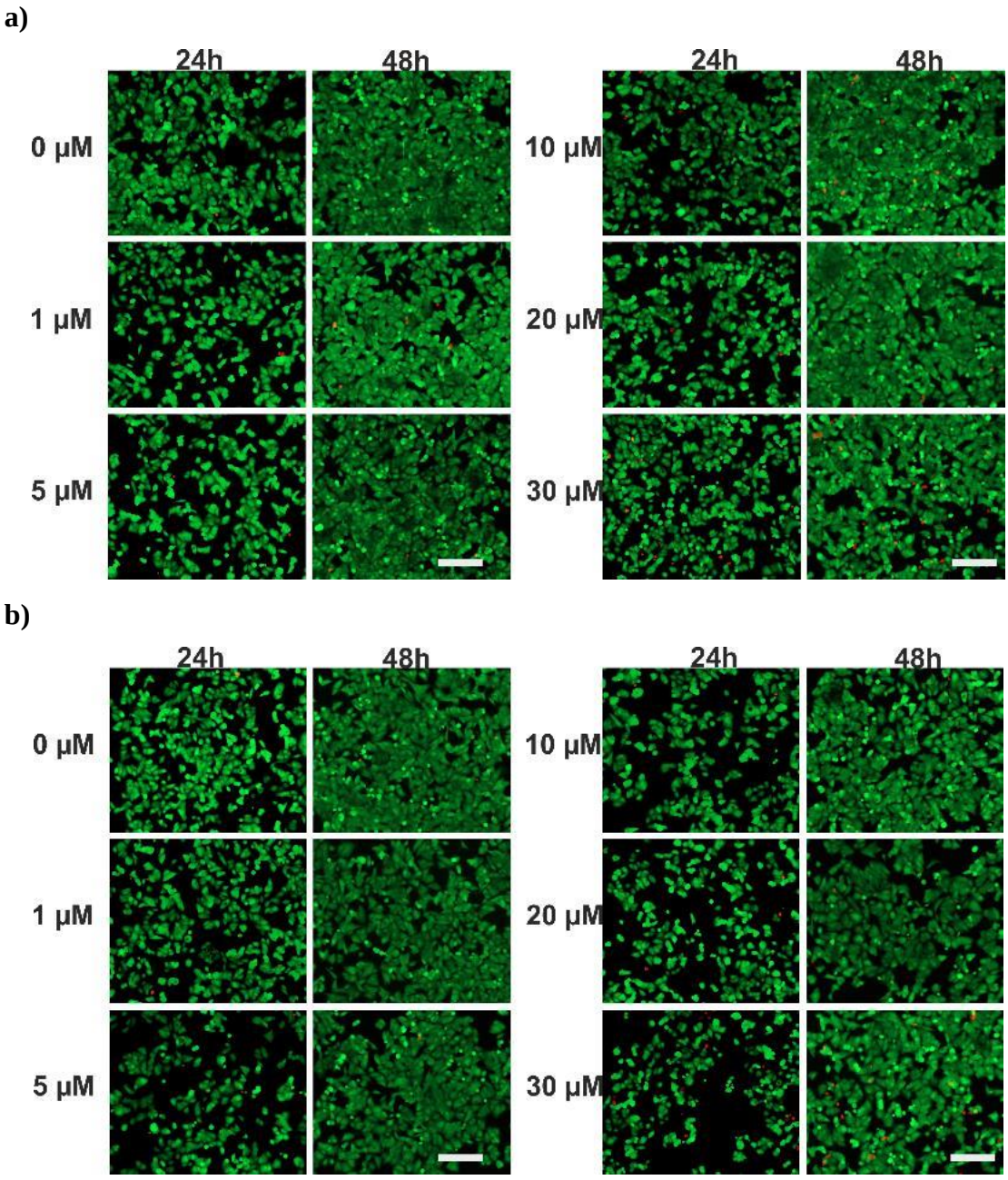


**Figure 75**. 48h live-dead analysis results showing the cytotoxicity of CG-04 on MCF-7 cells in the **a)** absence **b)** presence of 10 mM Gx paramagnetic contrast agent. (scale unit 100 µm)

With these results, toxic concentrations of the FDA-approved anticancer drug Ptx and sapogenol-derived molecules were determined for four cell lines. In general, the results of MTT and live-dead analysis are compatible with each other. The results are parallel to the literature. The values obtained in this completed step were used to

determine the concentration range for drug screening, which was performed on subsequent 3D tumor spheroid models.

### 3.4.2 Drug Activity Screening in 3D Tumor Spheroids Produced by the Hanging Drop Method

Drug screening on 3D tumor spheroid models, which is the main target of the thesis topic, has started. To perform drug screening on spheroid models produced with the hanging drop model, the results of the optimization studies carried out in the previous stage were used to produce at least three spheroids for each trial with different drug concentrations, as well as each cell line to be used in drug experiments. In addition, the results of drug activity screenings in 2D cell culture were used to determine the molecule and anticancer drug Ptx concentrations to be tested. Since 3D structures are much more compact and can better mimic tissue physiology, and the interactions of cells with each other and the extracellular complex are more intense, the concentrations applied in 2D studies need to be increased in this step (Fontoura et al., 2020; Imamura et al., 2015). The Ptx concentration range to be applied was determined as 0-400 nM (0, 20, 100, 200, and 400 nM), and the concentration range of sapogenol-derived molecules was determined as 0-60 μM (0, 20, 40, and 60 μM). Viability values were determined using MTT and live-dead analysis. Spheroids produced in a volume of 10 μL in the Petri dish lid were transferred to a 96-well plate. A 48-hour incubation period is planned after the drug application. However, since the viability level remained very high in the 48-hour period in the first trials, the incubation period was increased to 72 hours. After 72 hours of incubation, the medium in the wells was collected with the help of a micropipette without damaging the spheroid structures, and imaging was performed under a fluorescence microscope for a live-dead assay. The resulting figures were analysed in the ImageJ program, and viability graphs were prepared. Similarly, cell viability analysis was performed using the MTT method using spheroid structures, and graphs were prepared. The results obtained are shared below, separately for each cell line and drug.

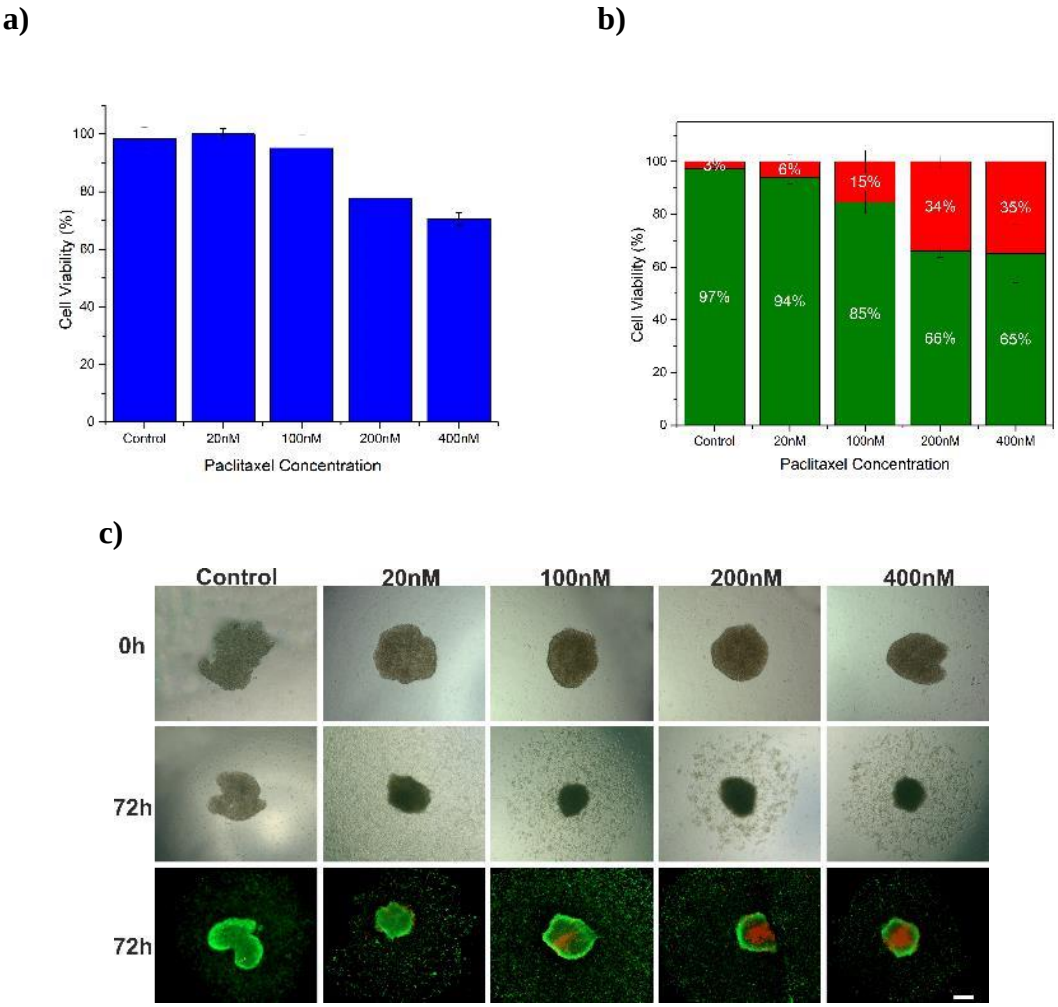


**Figure 76**. Analysis results of Ptx toxicity in SH-SY5Y spheroids obtained by hanging drop method **a)** MTT **b-c)** Live-dead analysis (Ptx concentration unit: nM) (scale size 200µm).

In Figure 76, the effects of the FDA-approved Ptx drug on viability in 3D tumor spheroid models obtained with SH-SY5Y cells are shown by MTT and live-dead analyses. Ptx has been used in the concentration range of 60-250 mg/mm2 in different clinical studies (Kumar et al., 2010). As seen in the results, the expected effect appeared to be a decreasing trend in viability in tumor models produced with SH-SY5Y cells, so the maximum concentration for this study was 400 nM. The concentrations used are within the reference range. The results of the MTT and living dead analysis overlap with each other. In Figure 76-c, 72-hour images showing the change and vitality in the morphology of spheroids due to the molecule effect are shared together for different Ptx

concentrations. It is seen that the increase in the applied Ptx concentration increases the number of dead cells in the spheroids. In addition, in the control group and in low concentrations, it was observed that some of the cells in the spheroid adhered to the surface. This can be interpreted as meaning that the toxic effect is low, the cells are not suppressed by the drug, and cell proliferation continues.

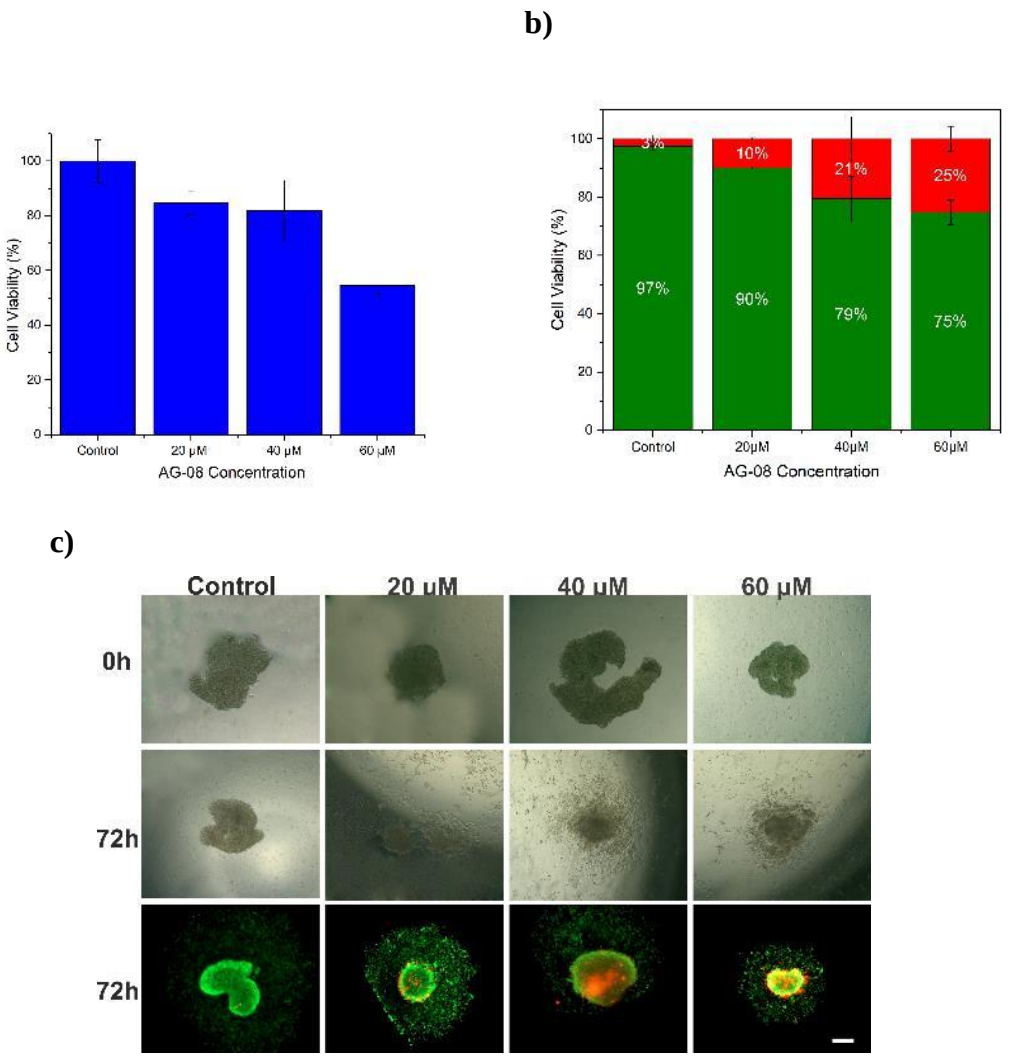


**Figure 77**. Analysis results of AG-08 toxicity in SH-SY5Y spheroids obtained by hanging drop method **a)** MTT **b-c)** Live-dead analysis (AG-08 concentration unit: µM) (scale size 200µm).

The effects of the AG-08 molecule synthesized by Prof. Bedir and his group on viability on 3D tumor spheroid models obtained with SH-SY5Y cells are shown in Figure

77 with MTT and live-dead analyses. As a result of cytotoxicity studies conducted in 2D cell culture for the AG-08 molecule in the literature, the $IC_{50}$ value for SH-SY5Y cells is 3.5 -4 μM (Üner et al., 2019), and within the scope of this study, the $IC_{50}$ value was in the range of 5-10 μM. Since these molecules are being tested for the first time in 3D cell culture studies, there is no concentration range for 3D models in the literature. The experiments will add significant data to the literature. The concentration range for 3D experiments was chosen in the higher concentration range, as previously described. As can be seen from the results, viability decreases if the concentration applied to 3D tumor models produced with SH-SY5Y cells is increased. It is seen that the increase in the applied AG-08 concentration increases the number of dead cells in the spheroids. The results of MTT and live-dead analysis overlap with each other. In Figure 77-c, 72-hour microscope images showing the morphological change and viability of spheroids due to the molecule effect are shared for different concentrations. In addition, in the control group and at low concentrations of application, it is observed that some of the cells in the spheroid continue to proliferate and adhere to the surface, preserving their viability. This can be interpreted as the toxic effect being low and cell viability continuing at a high level.

The effects of the AG-04 molecule, one of the analogues of the AG-08 molecule synthesized by Prof. Bedir and his group, in viability on 3D tumor spheroid models obtained with SH-SY5Y cells are shown in figure 78 with MTT and live-dead analyses. In the literature, studies conducted in 2D cell culture have proven that the $IC_{50}$ value of the molecule is >50 μM (Üner et al., 2019). For this reason, the molecule was preferred for controlling AG-08, which has a high cytotoxic effect. This result was also supported in the 2D studies carried out within the scope of this study. The concentration range for 3D experiments was chosen to be the same as for the toxic AG-08 molecule to enable accurate comparisons. As seen in the results, the expected effect is that the viability level in tumor models produced with SH-SY5Y cells is quite high. The results of MTT and live-dead analysis overlap with each other. In Figure 78-c, 72-hour images showing the morphological change and viability of spheroids due to the molecule effect are shared for different concentrations. There is no evidence that the increase in the applied AG-04 concentration causes a clear change in the number of dead cells in the spheroids.

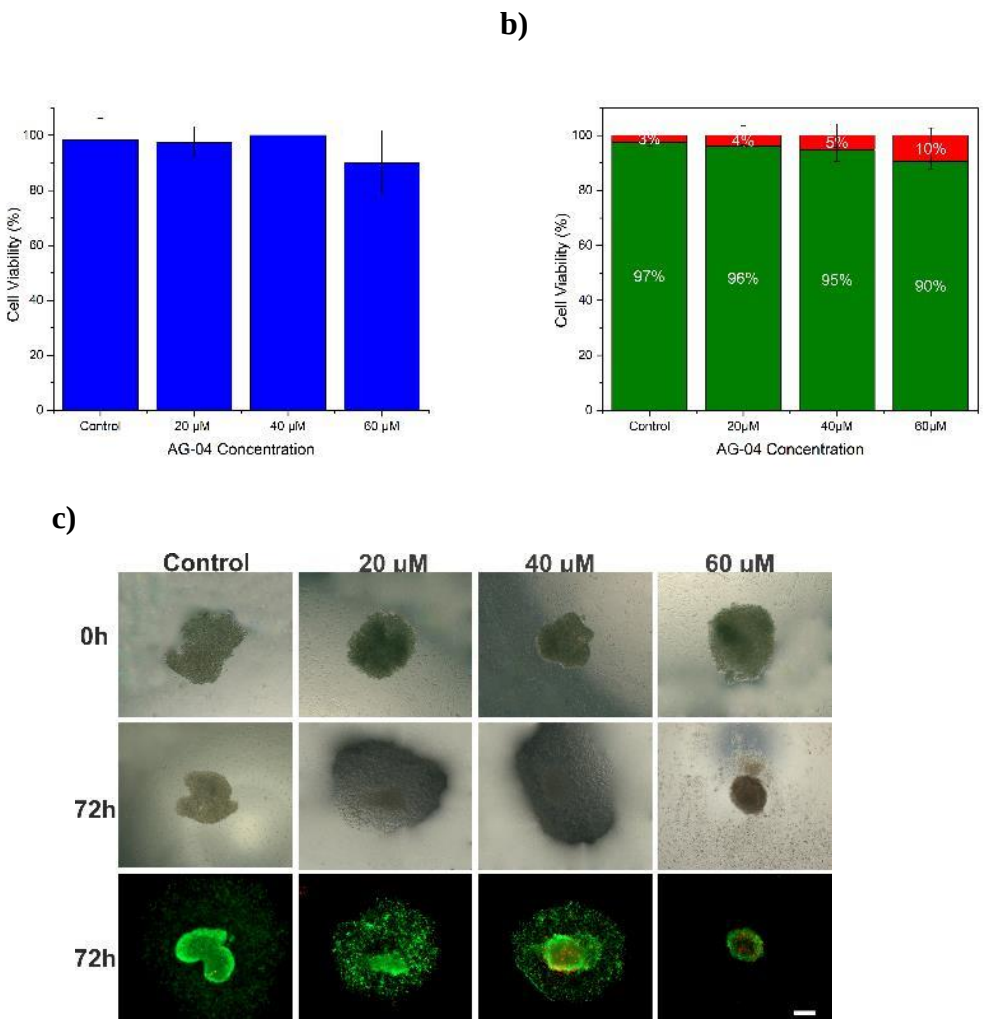


**Figure 78**. Analysis results of AG-04 toxicity in SH-SY5Y spheroids obtained by hanging drop method **a)** MTT **b-c)** Live-dead analysis (AG-04 concentration unit: µM) (scale size 200µm).

The effects of CG-03, one of the analogues of the AG-08 molecule synthesized by Prof. Bedir and his group, on viability on 3D tumor spheroid models obtained with SH-SY5Y cells are shown in Figure 79 with MTT and live-dead analyses. Similar to the AG-08 molecule, the CG-03 molecule causes controlled necrosis in cancer cell lines by improving proteolysis and changing lysosomal functions and physiology (Üner et al., 2022). As a result of the viability tests performed in 2D cell culture in the literature on the CG-03 molecule, the $IC_{50}$ value in SH-SY5Y cells was calculated to be in the range of 3.5 -12 µM (Üner et al., 2019). In the 2D experiments carried out within the scope of

this study, it was found to be in the range of 5-10 μM. The concentration range for 3D experiments was chosen at higher values, as previously described. As seen in the results, the expected effect appeared as a decreasing trend in viability in tumor models produced with SH-SY5Y cells. The results of the MTT and live-dead analyses overlap with each other. In Figure 79-c, 72-hour images showing the morphological change and viability of spheroids due to the molecule effect are shared for different concentrations. It is seen that the increase in the applied CG-03 concentration increases the dead cells within the spheroid. The red color begins to dominate on the spheroids. In the control group and at low concentrations, it is expected that some of the cells in the spheroid will adhere to the surface. Here it can be seen that there is cell attachment at all applied concentrations. This can be interpreted as the toxic effect being lower than AG-08. Studies in the literature have also proven that AG-08 has a higher toxic effect.

The effects of the CG-04 molecule, one of the analogues of the AG-08 molecule synthesized by Prof. Bedir and his group, in viability on 3D tumor spheroid models obtained with SH-SY5Y cells are shown in figure 80 with MTT and live-dead analyses. In the literature, studies conducted in 2D cell culture have proven that the $IC_{50}$ value of the molecule is >50 μM (Üner et al., 2019). For this reason, the molecule CG-04 was preferred for control purposes over CG-03, which has a high cytotoxic effect. This result was also supported in the 2D studies carried out within the scope of this study. The concentration range for 3D experiments was chosen to be the same as the toxic CG-03 molecule to enable accurate comparisons. As can be seen in the results, the expected effect is at high levels of viability in tumor models produced with SH-SY5Y cells. The results of MTT and live-dead analysis overlap with each other. In Figure 80-c, 72-hour images showing the morphological change and viability of spheroids due to the molecule effect are shared for different concentrations. There is no evidence that the increase in the applied CG-04 concentration causes a clear change in the number of dead cells in the spheroids. In addition, it is seen that some of the cells in the spheroid adhere to the surface in the control group and in applications at different concentrations. This can be interpreted as the toxic effect being low and the proliferation continuing at a high level.

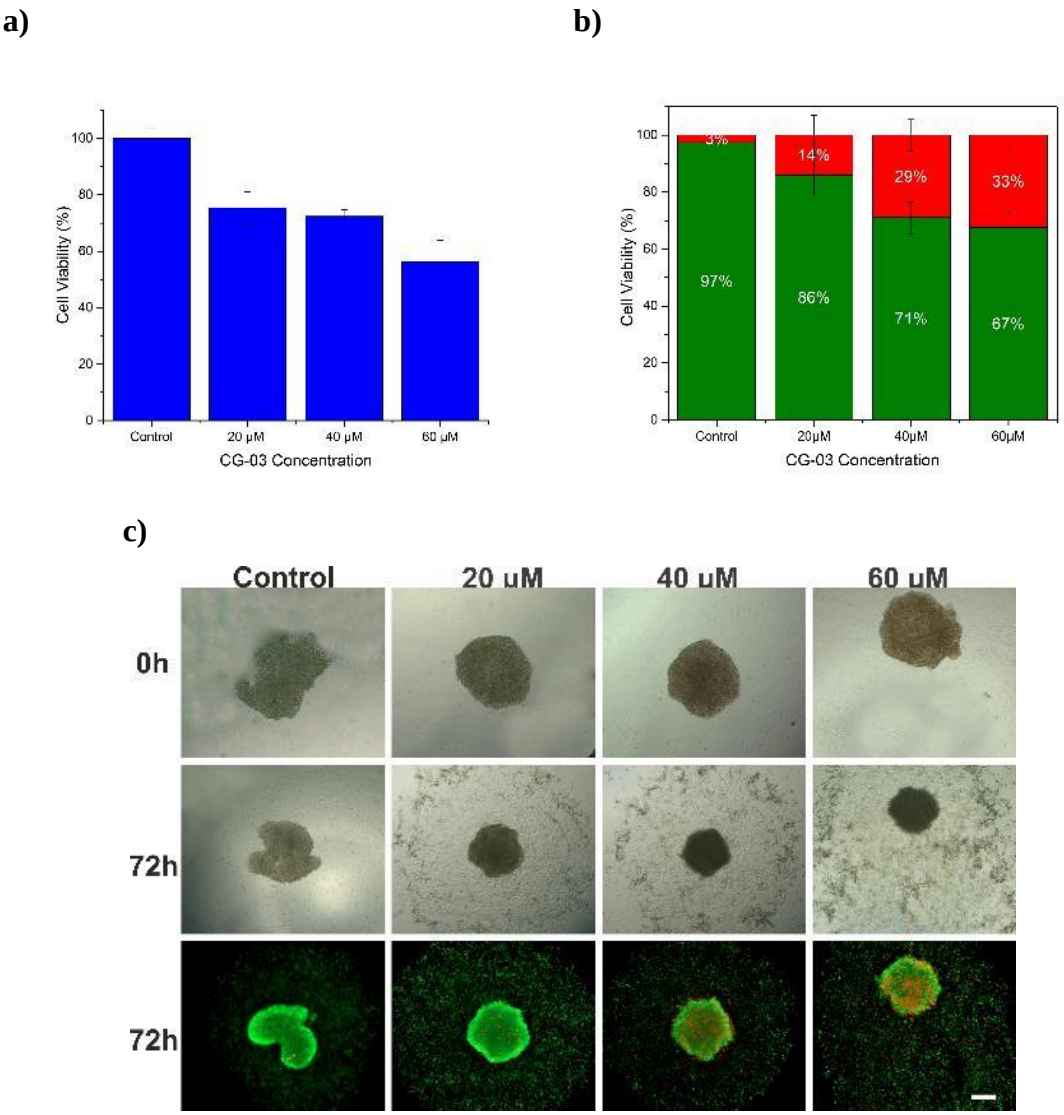


**Figure 79**. Analysis results of CG-03 toxicity in SH-SY5Y spheroids obtained by hanging drop method **a)** MTT **b-c)** Live-dead analysis (CG-03 concentration unit: μM) (scale size 200μm).

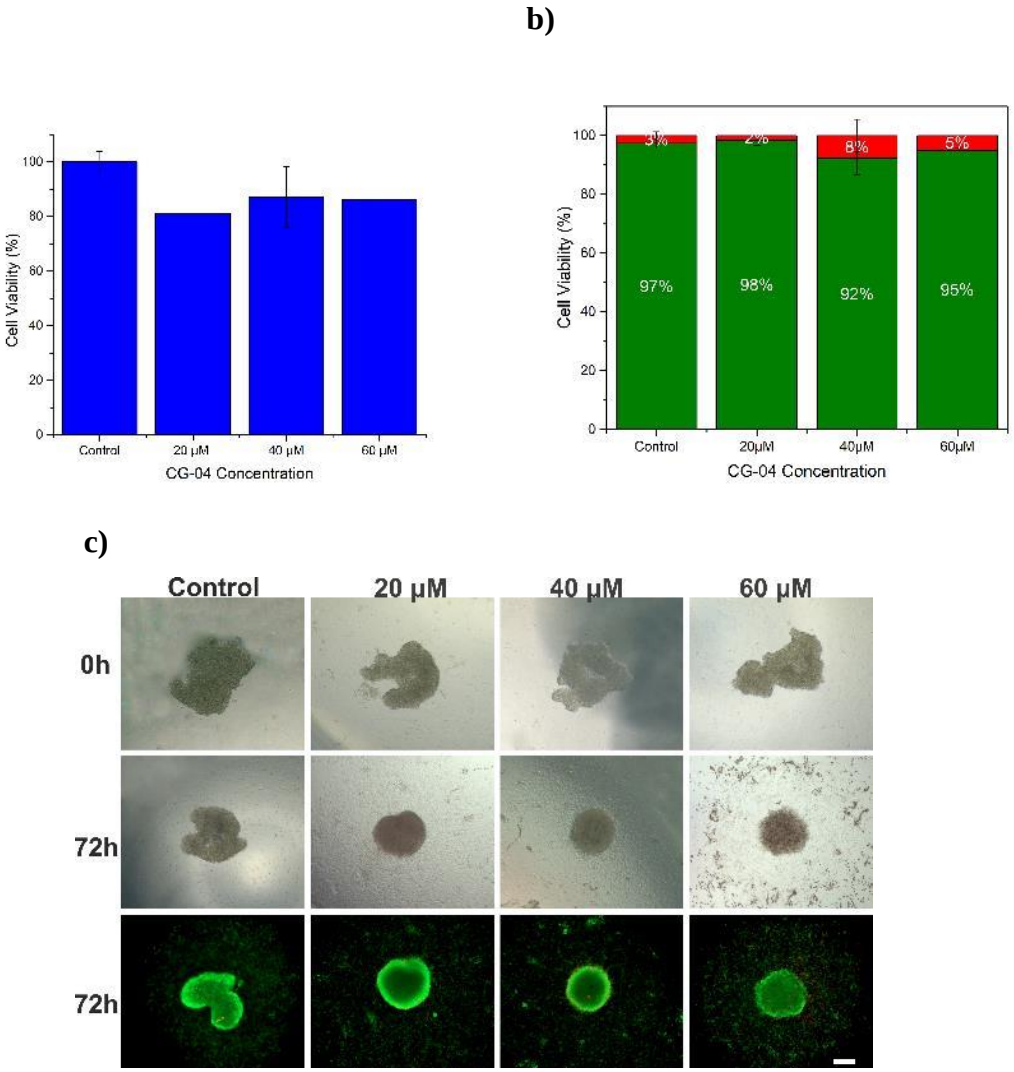


**Figure 80**. Analysis results of CG-04 toxicity in SH-SY5Y spheroids obtained by hanging drop method **a)** MTT **b-c)** Live-dead analysis (CG-04 concentration unit: µM) (scale size 200µm).

The effects of the FDA-approved Ptx drug on viability on 3D tumor spheroid models obtained with HepG2 cells are shown in Figure 81 with MTT and live-dead analyses. The concentration range for 3D experiments was chosen at higher values, as previously described. In the study investigating the toxic effect of Ptx on HepG2 cells at the 2D level, it was observed that there was a certain decrease in cell viability in the 5-25 nM concentration range, while viability remained at similar levels at higher concentrations. The expected result at this stage is a significant decrease in cell viability in the 20-100 nM drug concentration range. MTT and live-dead analysis results support

this situation. As seen in the results, the expected effect appeared to be a decreasing trend in viability in tumor models produced with HepG2 cells. It is seen that the increase in the applied Ptx concentration increases the dead cells within the spheroid. The red color begins to dominate on the spheroids. 72-hour images showing the morphological change and viability of 3D spheroids due to the Ptx effect are shared together in Figure 81-c for different concentrations. In addition, in the drug screening studies conducted with SH-SY5Y, it was observed that the cells separated from the spheroid adhered to the surface, whereas such a result was not obtained in the experiments conducted with HepG2, and it can be said that the spheroid structures were obtained more tightly and the cells on the surface of the spheroid were not affected much by the drug application.

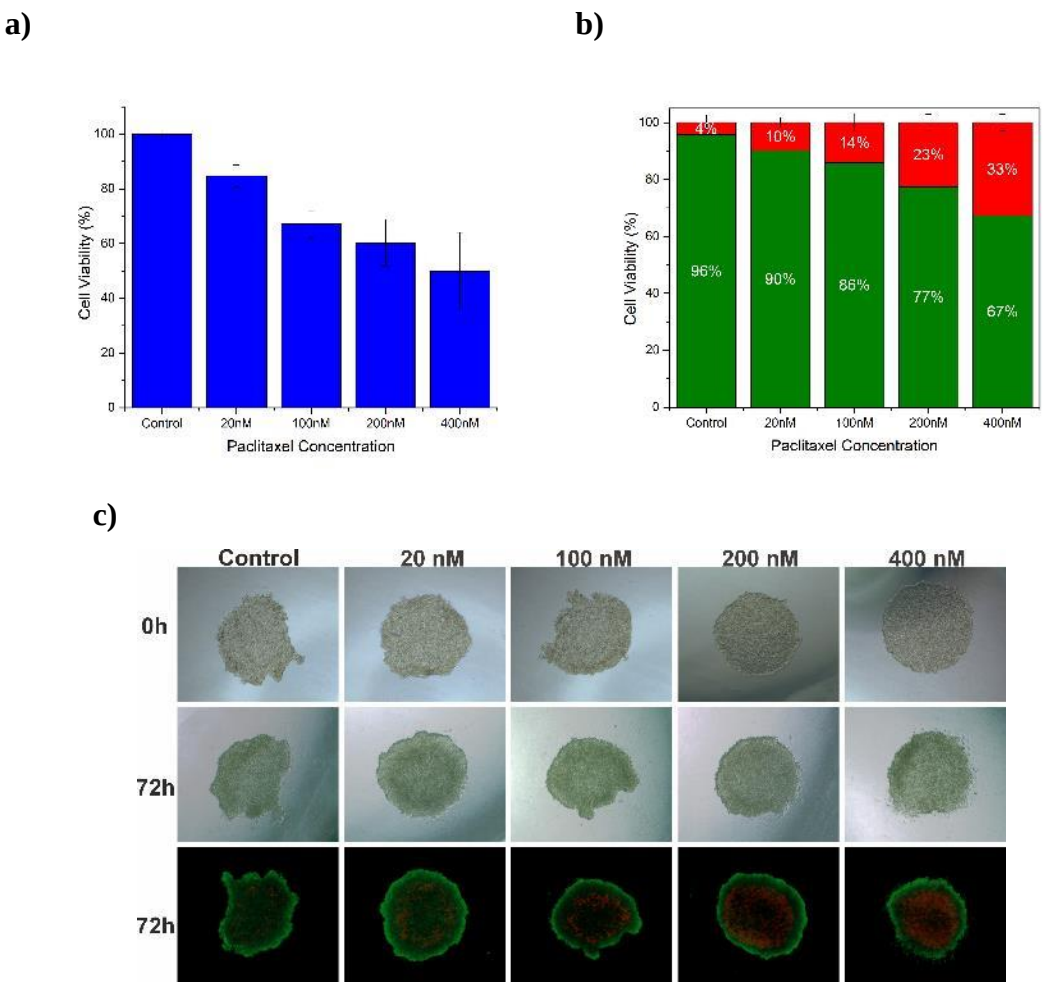


**Figure 81**. Analysis results of Ptx toxicity in HepG2 spheroids obtained by hanging drop method **a)** MTT **b-c)** Live-dead analysis (Ptx concentration unit: nM) (scale size 200µm).

The effects of the AG-08 molecule on viability in 3D tumor spheroid models obtained with HepG2 cells are shown in figure 82 with MTT and live-dead analyses. As a result of the viability tests performed in 2D cell culture in the literature on the AG-08 molecule, the $IC_{50}$ value in HepG2 cells was calculated as 5.5 -7 μM (Üner et al., 2019). In the 2D experiments carried out within the scope of this study, it was found to be in the range of 5-10 μM. The concentration range for 3D experiments is 0-60 μM, as in other studies. As seen in the results, the expected effect appeared to be a decreasing trend in viability in tumor models produced with HepG2 cells. The results of MTT and live-dead analysis overlap with each other. The decrease in viability value is seen more clearly in the results of MTT. 72-hour images showing the morphological change and viability of spheroids due to the molecule effect are shared together for different concentrations in Figure 82-c. It is seen that the increase in the applied AG-08 concentration increases the number of dead cells in the spheroids, and the green colour is replaced by red.

The effects of the AG-04 molecule, one of the analogues of the AG-08 molecule, on viability in 3D tumor spheroid models obtained with HepG2 cells are shown in figure 83 with MTT and live-dead analyses. In the literature, studies conducted in 2D cell culture have proven that the $IC_{50}$ value of the molecule is >50 μM for the HepG2 cell line (Üner et al., 2019). This result was also supported by the 2D studies carried out within the scope of this project. For this reason, the molecule was preferred for control purposes to AG-08, which has a high cytotoxic effect. The concentration range for 3D experiments was chosen to be the same as for the toxic AG-08 molecule to enable accurate comparisons. As seen in the results, the expected effect is at high levels of viability in tumor models produced with HepG2 cells. The results of MTT and live- dead analysis overlap with each other. 72-hour images showing the morphological change and viability of spheroids due to the molecular effect are shared together for different concentrations in Figure 83-c. As expected, there is no clear change in the number of dead cells in the spheroids despite the increase in the applied AG-04 concentration.

**a)** **b)**

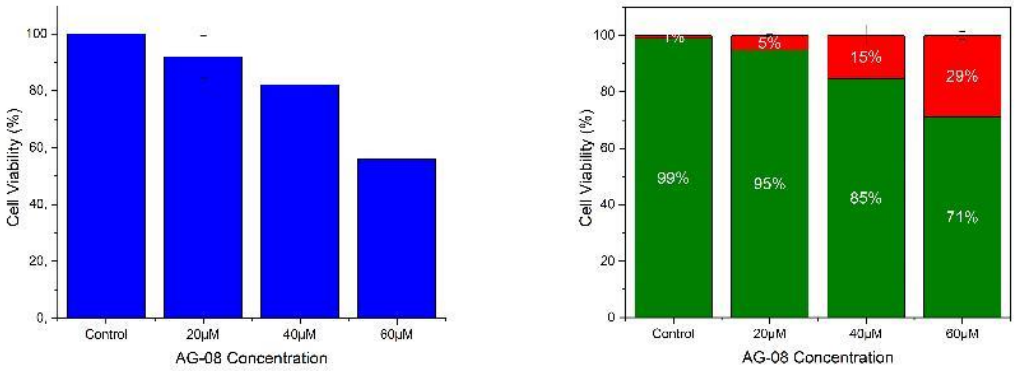


**c)**

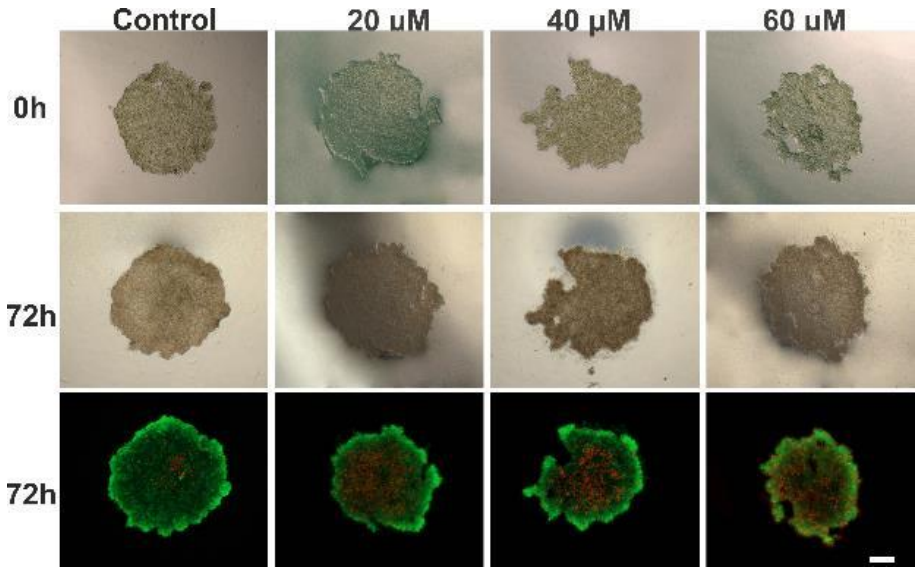


**Figure 82**. Analysis results of AG-08 toxicity in HepG2 spheroids obtained by hanging drop method **a)** MTT **b-c)** Live-dead analysis (AG-08 concentration unit: μM) (scale size 200μm).

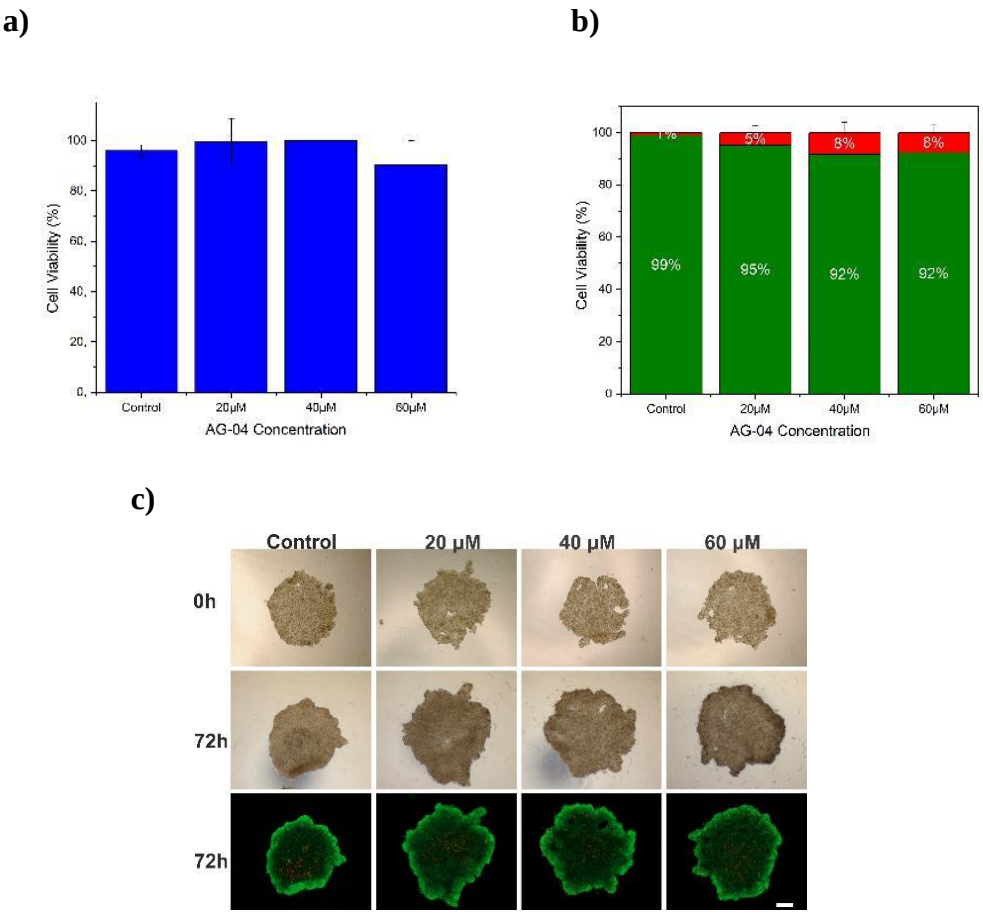


**Figure 83**. Analysis results of AG-04 toxicity in HepG2 spheroids obtained by hanging drop method **a)** MTT **b-c)** Live-dead analysis (AG-04 concentration unit: µM) (scale size 200µm).

The effects of CG-03, one of the analogues of the AG-08 molecule, on viability on 3D tumor spheroid models obtained with HepG2 cells are shown in figure 84 with MTT and live-dead analyses. As a result of viability tests performed in 2D cell culture in the literature on the CG-03 molecule, the $IC_{50}$ value in HepG2 cells was calculated to be approximately 10 µM (Üner et al., 2019). In the 2D experiments carried out within the scope of this study, it was found to be in the range of 5-10 µM. The concentration range for 3D experiments was chosen at higher values compared to 2D experiments, as described previously. When the results are examined, it is seen that there are partial differences in the results of MTT and live-dead analysis. The expected result is fully compatible with the MTT chart. As seen in Figure 84-c, as the molecule concentration increased, the change in the number of dead cells remained limited, and no major change

in spheroid morphologies due to the increasing molecule concentration could be observed. A similar situation was seen in the AG-08 application, although there were decreases in viability levels after the AG-08 application, the expected effect was limited. It is thought that this may be due to the fact that the 3D structures of this cell line adhere to each other very firmly, preventing the diffusion of the molecules or the remaining dead cells in the interior of the spheroids.

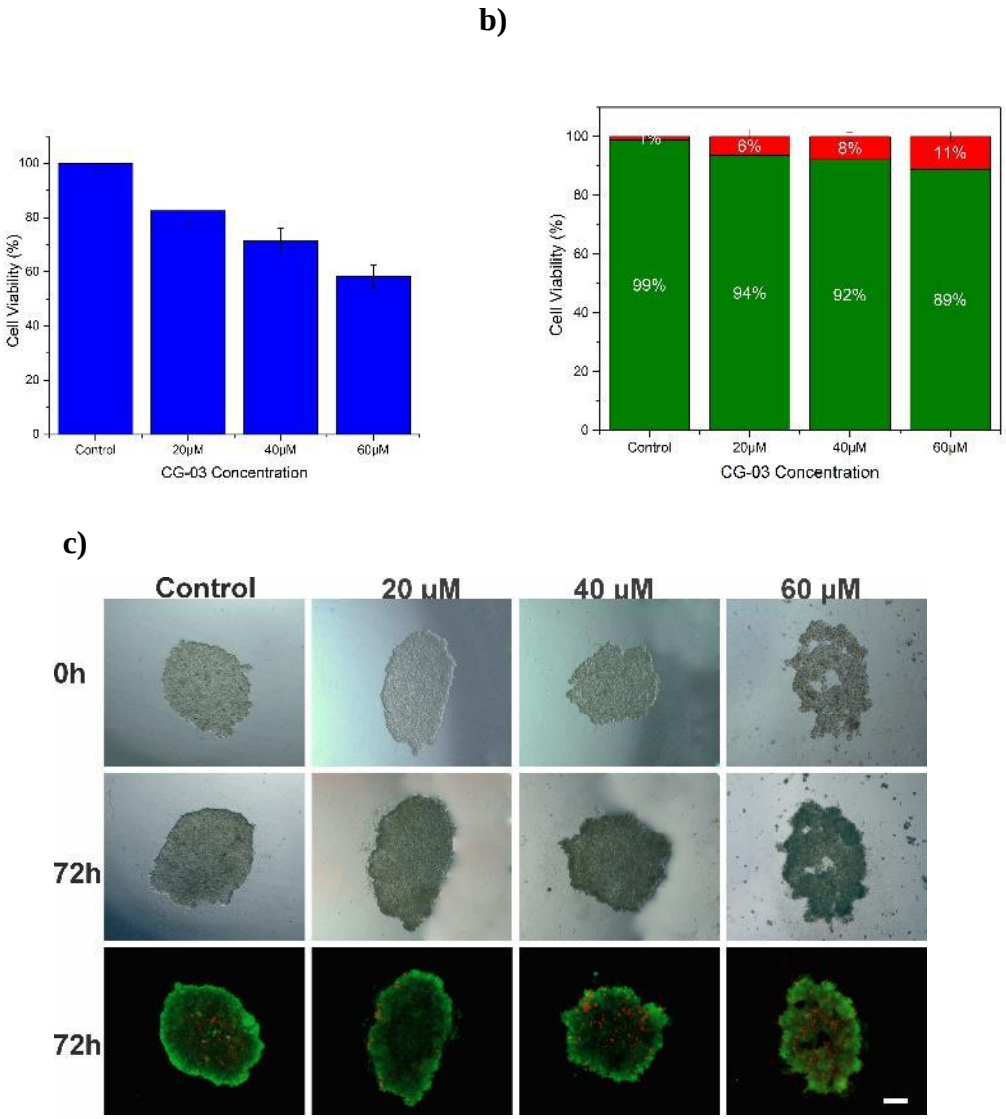


**Figure 84**. Analysis results of CG-03 toxicity in HepG2 spheroids obtained by hanging drop method **a)** MTT **b-c)** Live-dead analysis (CG-03 concentration unit: µM) (scale size 200µm).

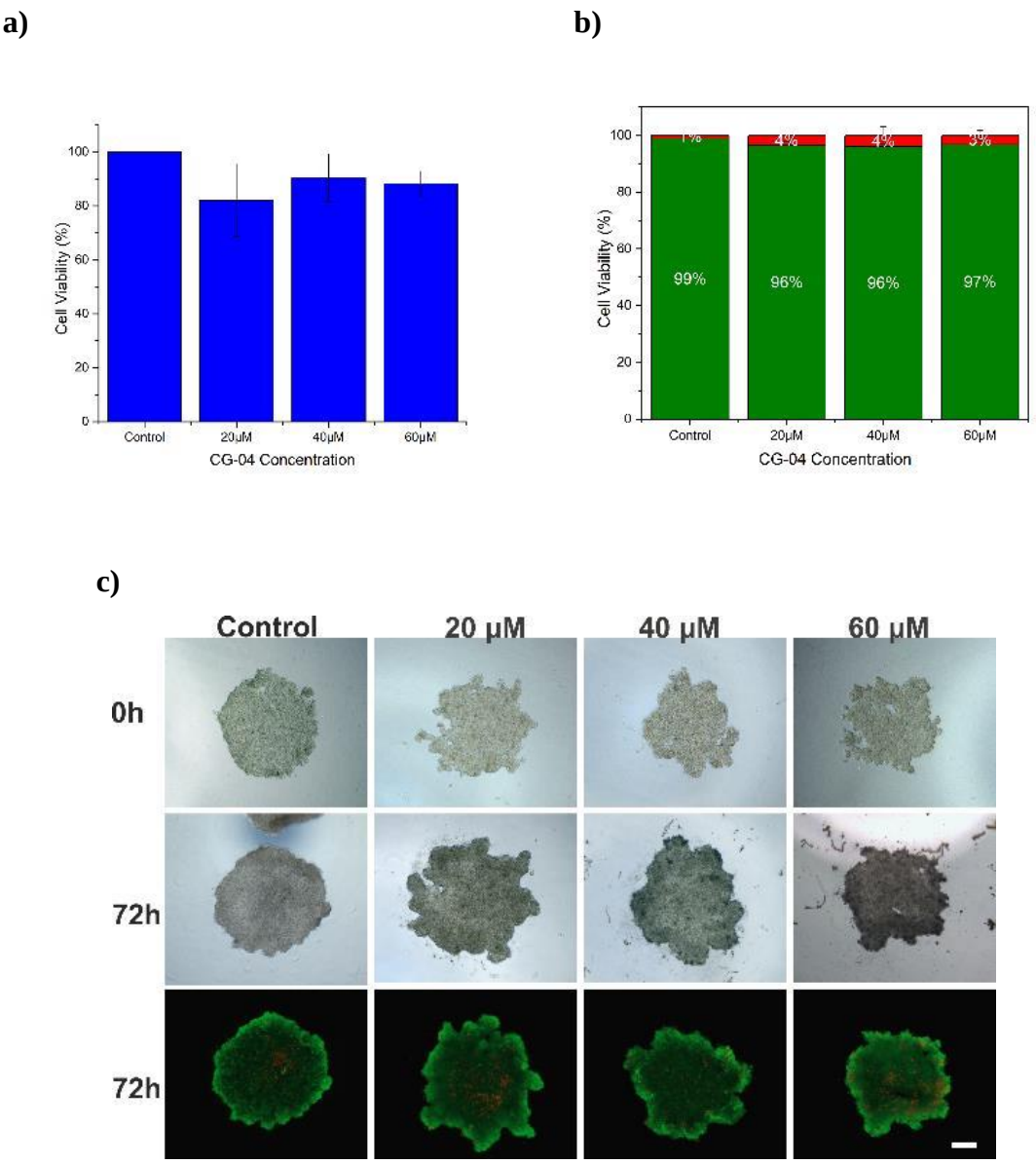


**Figure 85**. Analysis results of CG-04 toxicity in HepG2 spheroids obtained by hanging drop method **a)** MTT **b-c)** Live-dead analysis (CG-04 concentration unit: µM) (scale size 200µm).

The effects of the CG-04 molecule, one of the analogues of the AG-08 molecule, on viability in 3D tumor spheroid models obtained with HepG2 cells are shown in figure 85 with MTT and live-dead analyses. In the literature, studies conducted with HepG2 cells in 2D cell culture have proven that the $IC_{50}$ value of this molecule is >50 µM (Üner et al., 2019). This result was also supported in the 2D studies carried out within the scope of this study. For this reason, the molecule was preferred for control purposes to CG-03,

which has a high cytotoxic effect. The concentration range for 3D experiments was chosen to be the same as the toxic CG-03 molecule to enable accurate comparisons. The results are as expected, and the viability values are high in tumor models produced with HepG2 cells. The results of MTT and live-dead analysis overlap with each other. 72-hour images showing the change and viability in the morphology of spheroids due to the molecule effect are shared together for different concentrations in Figure 85-c. Despite the increase in the applied CG-04 concentration, there is no clear change in the number of dead cells in the spheroids. In addition, spheroids preserved their morphological structure under the influence of molecules.

**a)** **b)**

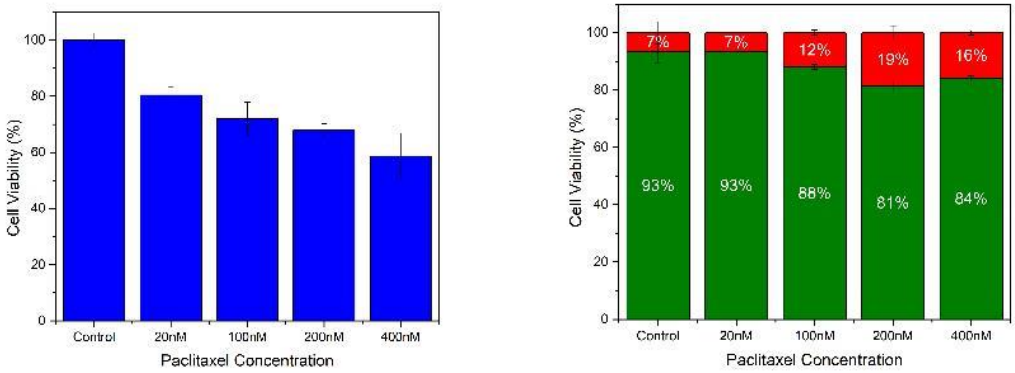


**c)**

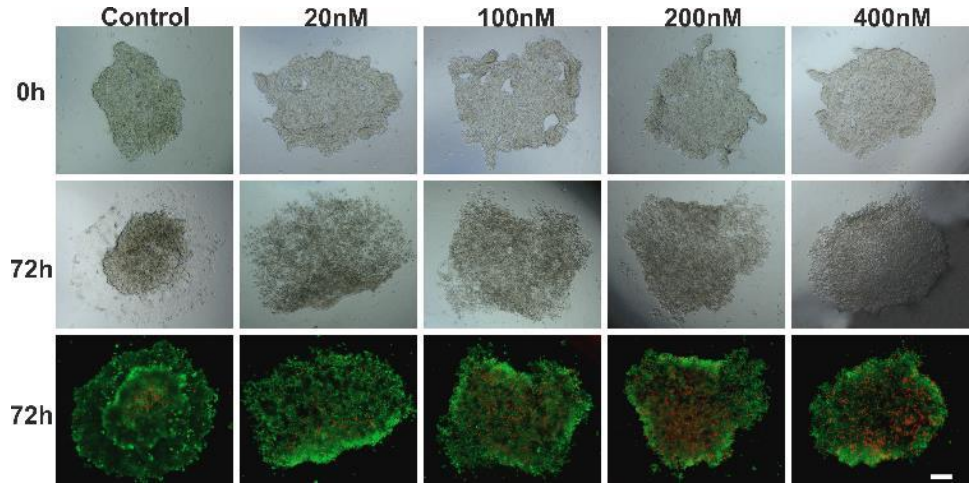


**Figure 86**. Analysis results of Ptx toxicity in MCF-7 spheroids obtained by hanging drop method **a)** MTT **b-c)** Live-dead analysis (Ptx concentration unit: nM) (scale size 200µm).

The effects of the FDA-approved Ptx drug on viability on 3D tumor spheroid models obtained with MCF-7 cells are shown in Figure 86 with MTT and live-dead analyses. As a result of the viability experiments in the 2D culture of MCF-7 cells in the studies carried out within the scope of the study, the toxic effect of Ptx, which will reduce the viability value to 50% or below, is in the range of 25-50 nM. Although there is a decreasing trend in the MTT and live-dead test results of the drug screening performed after 3D culturing, there is some difference. The decreasing rate of cell viability was limited in the live-dead graph. In Figure 86-c, 72-hour images showing the morphological change and viability of spheroids due to the molecule effect are shared for different concentrations. Looking at Figure 101-b of the live-dead analysis, there is a partial increase in the number of dead cells, with the red color indicating dead cells. Additionally, it can be seen in Figure 86-c that the cells separated from the spheroid surface in drug screening studies carried out with MCF-7 3D tumor spheroid models. Similar to the SH-SY5Y characteristic, it adhered to the surface and continued to proliferate. This indicates that the viability of the cells on the outer surface of the spheroid remains at a high level.

When the spheroids obtained by the hanging drop method are evaluated together, it is seen that the viability level does not decrease as much as expected in the results of the three cell lines (SH-SY5Y, HepG2, and MCF-7), especially in the live-dead test results with the Ptx effect. It is envisaged that this situation can be solved by increasing the drug concentration or increasing the incubation period.

The effects of the AG-08 molecule on viability on 3D tumor spheroid models obtained with MCF-7 cells are shown in figure 87 with MTT and live-dead analyses. As a result of the viability tests performed in 2D cell culture in the literature on the AG-08 molecule, the $IC_{50}$ value in MCF-7 cells was calculated as 3.5 -4 μM (Üner et al., 2022). In the 2D experiments carried out within the scope of this study, it was found to be in the range of 10-20 μM. Since these molecules are being tested for the first time in 3D cell culture studies, there is no effective concentration range specific to the cell line in the literature. The concentration range is the same as for experiments in other cell lines (0-60 μM). As seen in the results, the expected effect appeared to be a decreasing trend in viability in tumor models produced with MCF-7 cells. The results of MTT and live- dead analysis overlap with each other. 72-hour images showing the morphological change and viability of spheroids due to the molecular effect are shared together for different concentrations in Figure 87-c. It is seen that the increase in the applied concentration of AG-08 increases the number of dead cells in the spheroids, and the color red dominates

in the figures. Additionally, it is observed that there is deterioration in the spheroid structure with the incubation process starting from the 20 µM application and that there is no obvious structure left after the 60 µM concentration application. Moreover, in the control group and in low concentrations, it was observed that some of the cells in the spheroid separated from the spheroid, adhered to the surface, and continued the proliferation process.

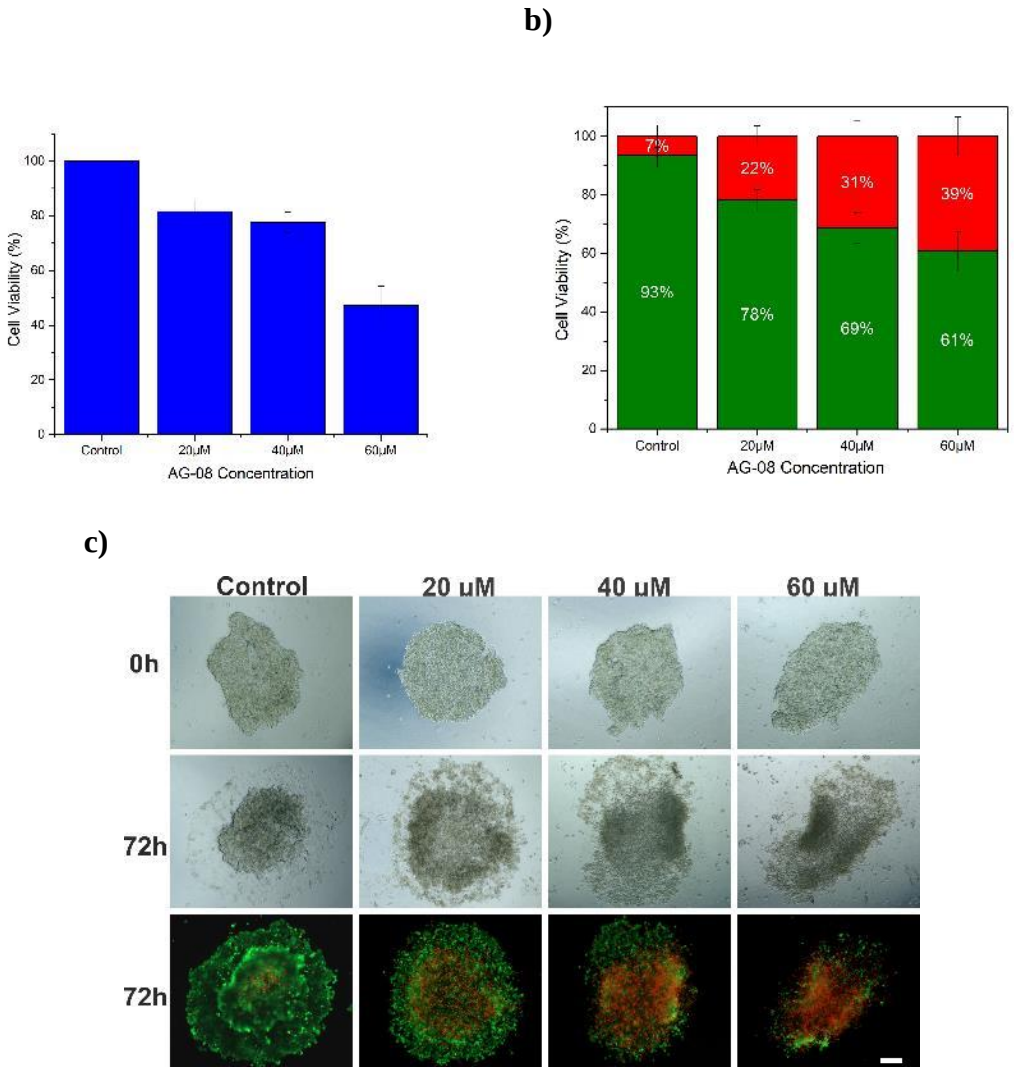


**Figure 87**. Analysis results of AG-08 toxicity in MCF-7 spheroids obtained by hanging drop method **a)** MTT **b-c)** Live-dead analysis (AG-08 concentration unit: µM) (scale size 200µm).

The effects of the AG-04 molecule, one of the analogues of the AG-08 molecule, on viability in 3D tumor spheroid models obtained with MCF-7 cells are shown in figure 88 with MTT and live-dead analyses. As a result of the viability tests performed in 2D cell culture in the literature on the AG-04 molecule, the $IC_{50}$ value in MCF-7 cells was calculated as 22.05 μM (Üner et al., 2022). In the 2D experiments carried out within the scope of this study, it is seen that the viability level decreases in the 20-30 μM concentration range. Since these molecules are being tested for the first time in 3D cell culture studies, there is no effective concentration range specific to the cell line in the literature. The concentration range is the same as for experiments in other cell lines (0-60 μM). As seen in the results, the viability level remained at 70% and above in the AG-04 concentration range applied in MCF-7 3D tumor spheroid models. The results of MTT and live-dead analysis overlap with each other. 72-hour images showing the morphological change and viability of spheroids due to the molecular effect are shared together for different concentrations in Figure 88-c. It seems that the increase in the applied AG-04 concentration does not affect the number of dead cells in the spheroids. During the incubation process, in the control group and in the molecule applications, it is observed that some of the cells separate from the spheroid, adhere to the surface, and continue the proliferation process. Although the spheroid structure deteriorates over time, vitality is high.

The effects of the CG-03 molecule, one of the analogues of the AG-08 molecule, on viability in 3D tumor spheroid models obtained with MCF-7 cells are shown in figure 89 with MTT and live-dead analyses. As a result of viability tests performed in 2D cell culture in the literature on the CG-03 molecule, the $IC_{50}$ value in MCF-7 cells was calculated as 5.5 μM (Üner et al., 2022). In the 2D experiments carried out within the scope of this research, it was found to be close to 10 μM. Since these molecules are being tested for the first time in 3D cell culture studies, there is no effective concentration range specific to the cell line in the literature. The concentration range is the same as for experiments in other cell lines (0-60 μM). As seen in the results, the expected effect appeared to be a decreasing trend in viability in tumor models produced with MCF-7 cells. In the live-dead results, the viability level was expected to be slightly lower at a 60 μM molecule concentration. The results of MTT and live-dead analysis coincide with each other in a decreasing trend. 72-hour images showing the morphological change and viability of spheroids due to the molecular effect are shared together for different concentrations in Figure 89-c. It is seen that the increase in the applied concentration of

CG-03 increases the number of dead cells in the spheroids, and the green color indicating living cells turns red. It is observed that there are changes in the spheroid shape with the incubation process starting from 20 µM application. In addition, it is seen that some of the cells in the spheroid in the control group detach from the spheroid, attach to the surface, and continue the proliferation process.

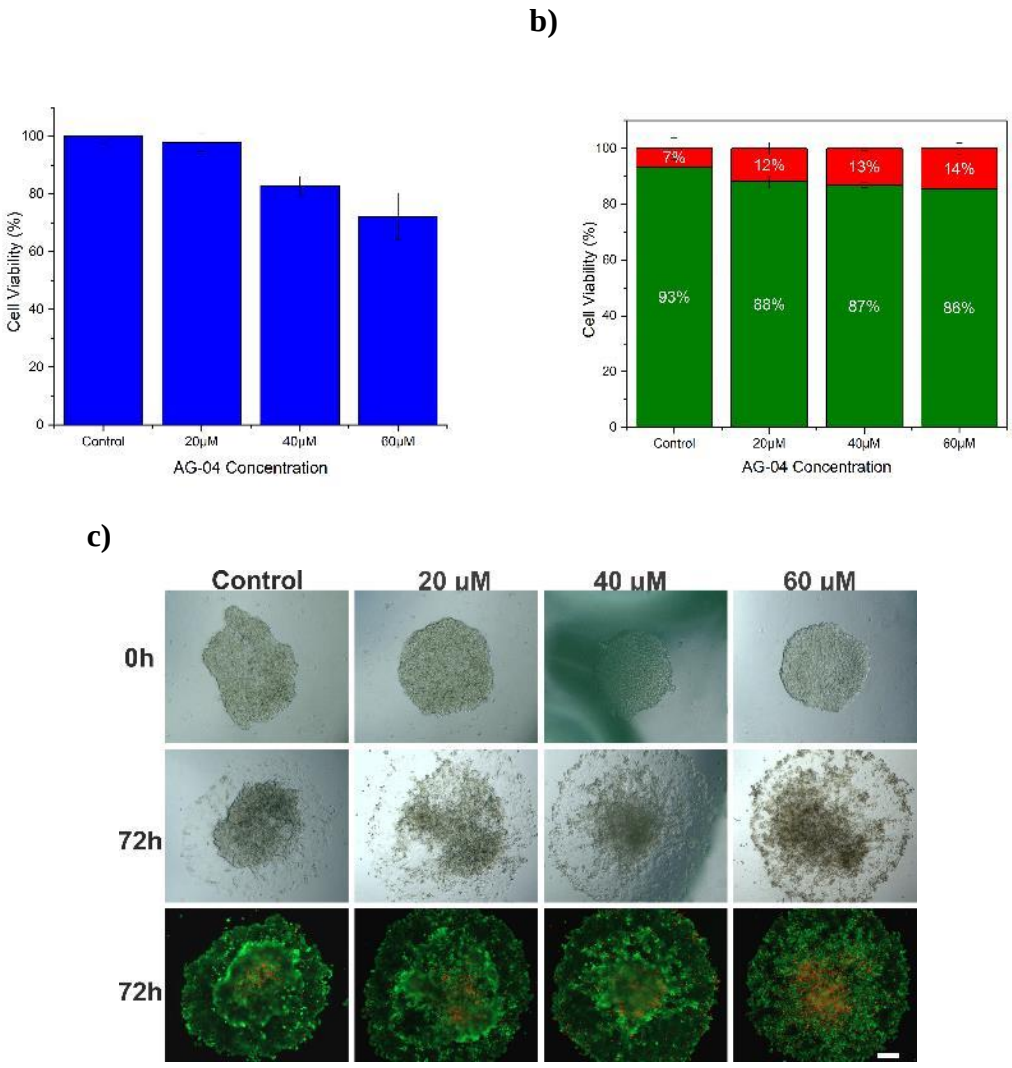


**Figure 88**. Analysis results of AG-04 toxicity in MCF-7 spheroids obtained by hanging drop method **a)** MTT **b-c)** Live-dead analysis (AG-04 concentration unit: µM) (scale size 200µm).

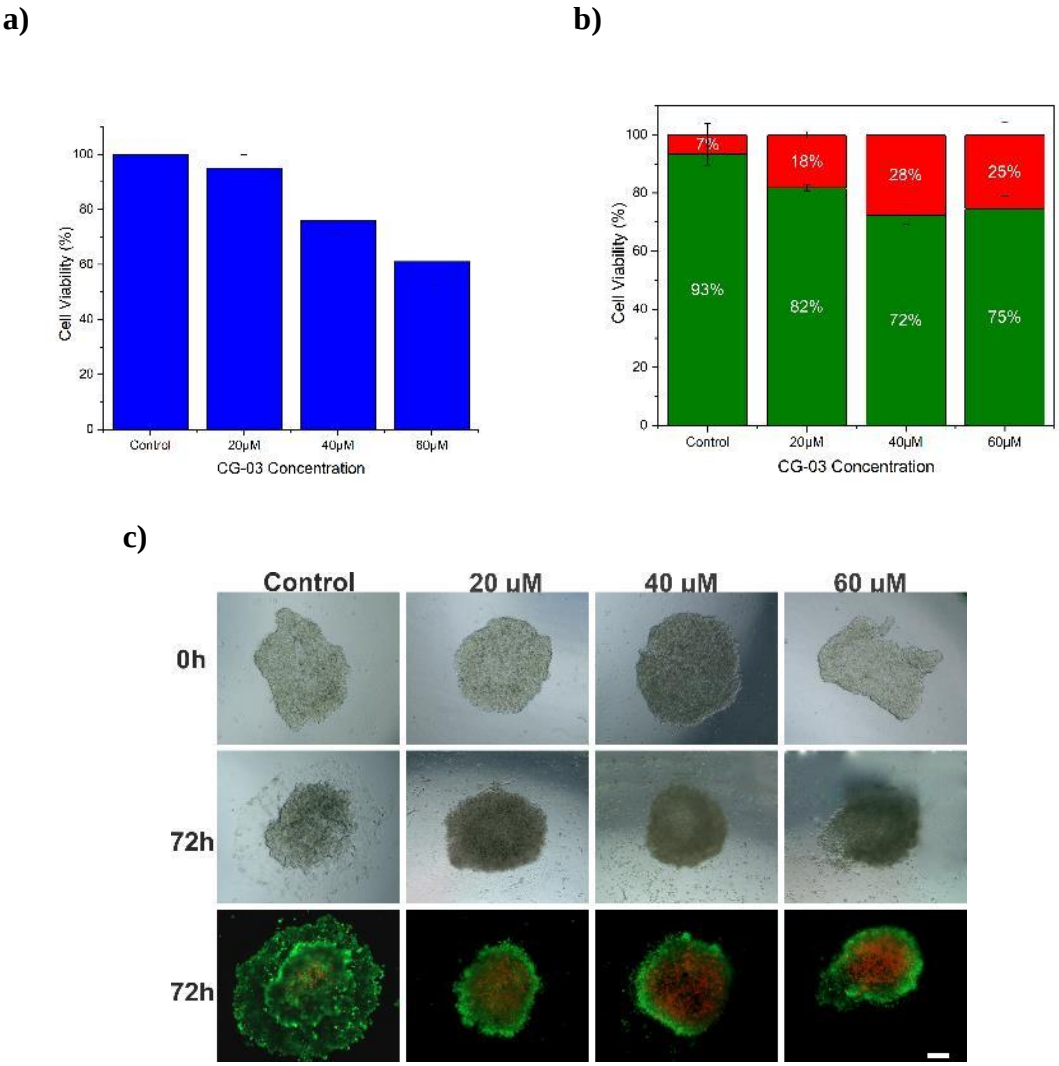


**Figure 89**. Analysis results of CG-03 toxicity in MCF-7 spheroids obtained by hanging drop method **a)** MTT **b-c)** Live-dead analysis (CG-03 concentration unit: µM) (scale size 200µm).

The effects of the CG-04 molecule, one of the analogues of the AG-08 molecule, on viability in 3D tumor spheroid models obtained with MCF-7 cells are shown in figure 90 with MTT and live-dead analyses. As a result of viability tests performed in 2D cell culture in the literature on the CG-04 molecule, the $IC_{50}$ value in MCF-7 cells was calculated as > 50 µM (Üner et al., 2022). In the 2D experiments carried out within the scope of this study, a maximum concentration of 30 µM was applied, and it was observed that the viability values remained at 80% and above. Since these molecules are being tested for the first time in 3D cell culture studies, there is no effective concentration range

specific to the cell line in the literature. The concentration range is the same as for experiments in other cell lines (0-60 µM).

**a)** **b)**

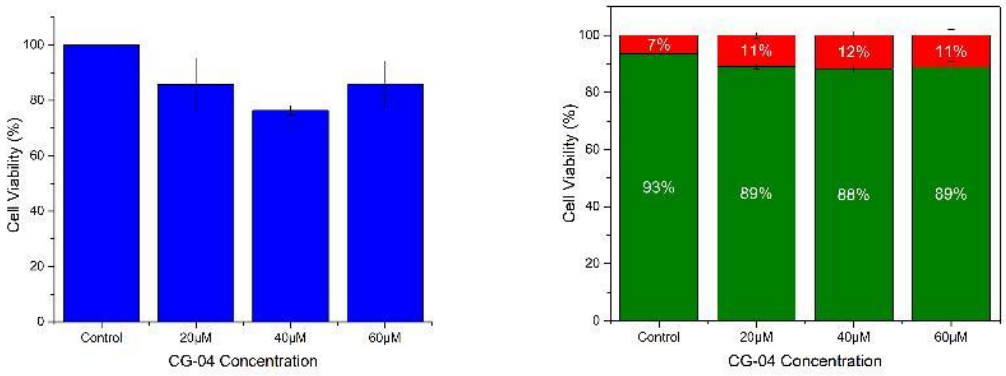


**c)**

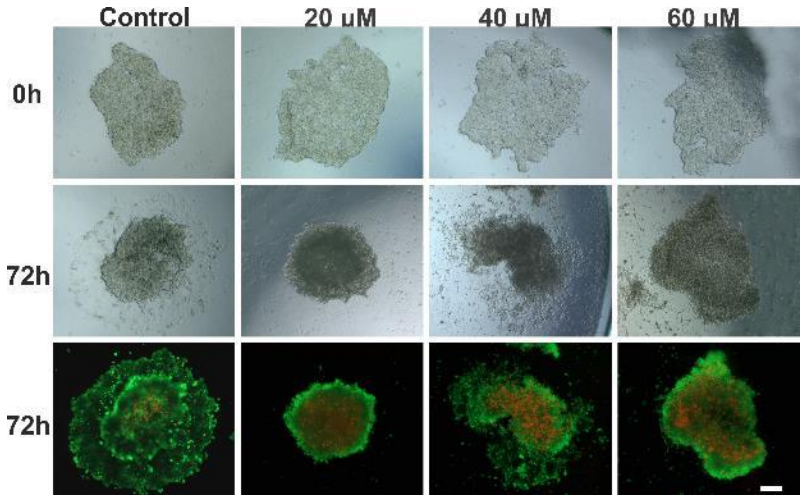


**Figure 90**. Analysis results of CG-04 toxicity in MCF-7 spheroids obtained by hanging drop method **a)** MTT **b-c)** Live-dead analysis (CG-04 concentration unit: µM) (scale size 200µm)

As seen in the results, the cell viability level remained at 70% and above in the CG-04 concentration range applied in MCF-7 3D tumor spheroid models. The results of MTT and live-dead analysis overlap with each other. 72-hour images showing the change and vitality in the morphology of spheroids due to the molecular effect are shared together

for different concentrations in Figure 90-c. There appear to be some dead cells in each spheroid, which is thought to be independent of the increase in the applied CG-04 concentration. Although there have been changes in spheroid structures over time, they are highly preserved.

### 3.4.3. Drug Activity Screening in 3D Tumor Spheroids Produced by the Magnetic Levitation Method

After the completion of drug screening studies on 3D tumor spheroid models obtained by the hanging drop method, drug screenings were carried out on 3D tumor spheroid models produced by the magnetic levitation method, an innovative method that has recently entered the literature (Bilginer Kartal & Arslan Yildiz, 2024; Durmus et al., 2015; Onbas & Arslan Yildiz, 2021; Parfenov et al., 2020; Sözmen & Arslan-Yildiz, 2024; Sözmen & Arslan-Yıldız, 2022; Tseng et al., 2013; Türker et al., 2018; Turker & Arslan-Yildiz, 2018). The results were compared with the viability values obtained after drug screening in 3D tumor spheroid models obtained by the hanging drop method, which was selected as the control group. In order to perform drug screening on spheroid models produced by the magnetic levitation method, the optimization results made within the scope of the previous step were used to produce at least three spheroids for each trial at different drug concentrations to be used in drug trials for each cell line. Before viability tests were performed, similar sized spheroids were preferred, and drugs were applied. The drug concentrations to be tested are in the same concentration range as the values optimized by the hanging drop method. Viability values were measured using MTT and live-dead analysis as in the previous step.

For the viability test, the spheroid/spheroid-like structures produced in special ‘ibidi’ petri dishes in the presence of 10-30 mM Gx in the 3-4 day incubation period are first collected without damaging the spheroid structures. The drug concentration was adjusted using DMSO and added to each petri dish by mixing it with the medium to a maximum volume of 800 µL. After 72 hours of incubation, the medium in the wells was collected with the help of a micropipette without damaging the spheroid structures, and live-dead analysis was performed. Similarly, MTT analysis was performed for 3D tumor

spheroids obtained with the MagLev method, and the results were compared both within themselves and with the hanging drop method. The results obtained are shared below, separately for each cell line and drug molecule.

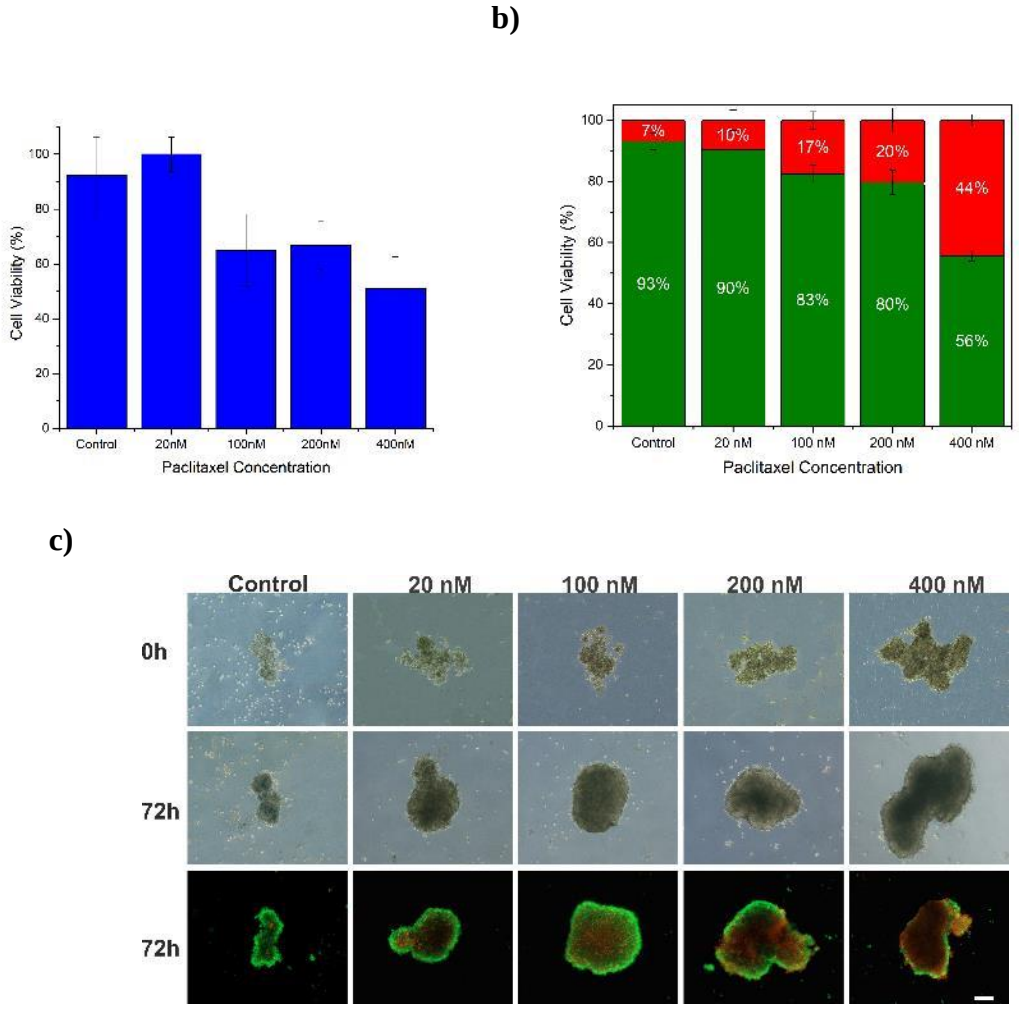


**Figure 91**. Analysis results of Ptx toxicity in HeLa spheroids obtained by MagLev method **a)** MTT **b-c)** Live-dead analysis (Ptx concentration unit: nM) (scale size 200µm).

While starting drug screening on HeLa spheroid models produced with the MagLev method, it is known that HeLa spheroids begin to form after the 96$^{th}$ hour, thanks to optimization studies. It was thought that drug screening could not be performed properly after 168 hours due to diffusion problems and low viability, and drug trials were carried out on 3D HeLa spheroid models obtained by the MagLev method at the 96$^{th}$ hour.

Drug screening studies could not be carried out due to the weak structure of HeLa spheroids produced by the hanging drop method, which was determined as the control method, but the concentration range used in drug screenings with other cell spheroids was the same at this stage, and a higher concentration range was determined from 2D cell culture trials. In this regard, the toxic effect of the FDA-approved anticancer drug Ptx is shared with MTT and live-dead analysis in figure 91. Since spheroids were not obtained in the hanging drop method with HeLa cells, a comparison could not be made on these results, but it was observed that results were obtained that support drug screening studies carried out in 2D cell culture. In the 400 nM Ptx experiment, it was observed that the viability value reached 50% as expected, and the number of dead cells in the spheroids increased due to the increasing drug concentration. MTT and live-dead analysis results support each other. Analyses were completed on three spheroid models for measurements of each concentration. In addition, the fact that a 3D tumor model could not be obtained with the hanging drop method but could be created with the MagLev method demonstrates the advantages of the method used.

The effects of the AG-08 molecule synthesized by Prof. Bedir and his group on 3D tumor spheroid models obtained with HeLa cells on viability are shown in Figure 92 by MTT and live-dead analyses. As a result of the viability tests performed in 2D cell culture in the literature on the AG-08 molecule, the $IC_{50}$ value in HeLa cells was calculated as 5.2 -6 μM (Üner et al., 2022), and in the 2D experiments carried out within the scope of this study, it was in the range of 5-10 μM. Since these molecules are being tested for the first time in 3D cell culture studies, there is no concentration range in the literature, and important data will be accumulated in the literature with the trials. Drug screening studies could not be carried out due to the weak structure of HeLa spheroids produced by the hanging drop method, which was determined as the control method, but the concentration range used in drug screenings with other cell line spheroids was the same at this point and was chosen at higher values than 2D experiments. 72-hour drug screening images showing the morphological change and vitality of spheroids under the influence of the drug molecule are shared together for different concentrations in Figure 92-c. Despite the increase in the applied AG-08 concentration, there was no change in the cytotoxic effect or the number of dead cells. The difference between MTT and live-dead analysis graphs has also been seen in some experiments obtained with the hanging drop method. It is thought that this may be due to the diffusion problem caused by the compact structure of the spheroid, or it may be related to the inability to visualize dead cells

because they remain in the inner part of the spheroid structure. When the results are evaluated, the expected toxic effect and decrease in viability values are not fully seen in the 3D HeLa tumor models produced with the Maglev method, and it is considered that the drug resistance of 3D tumor models is much higher compared to 2D models.

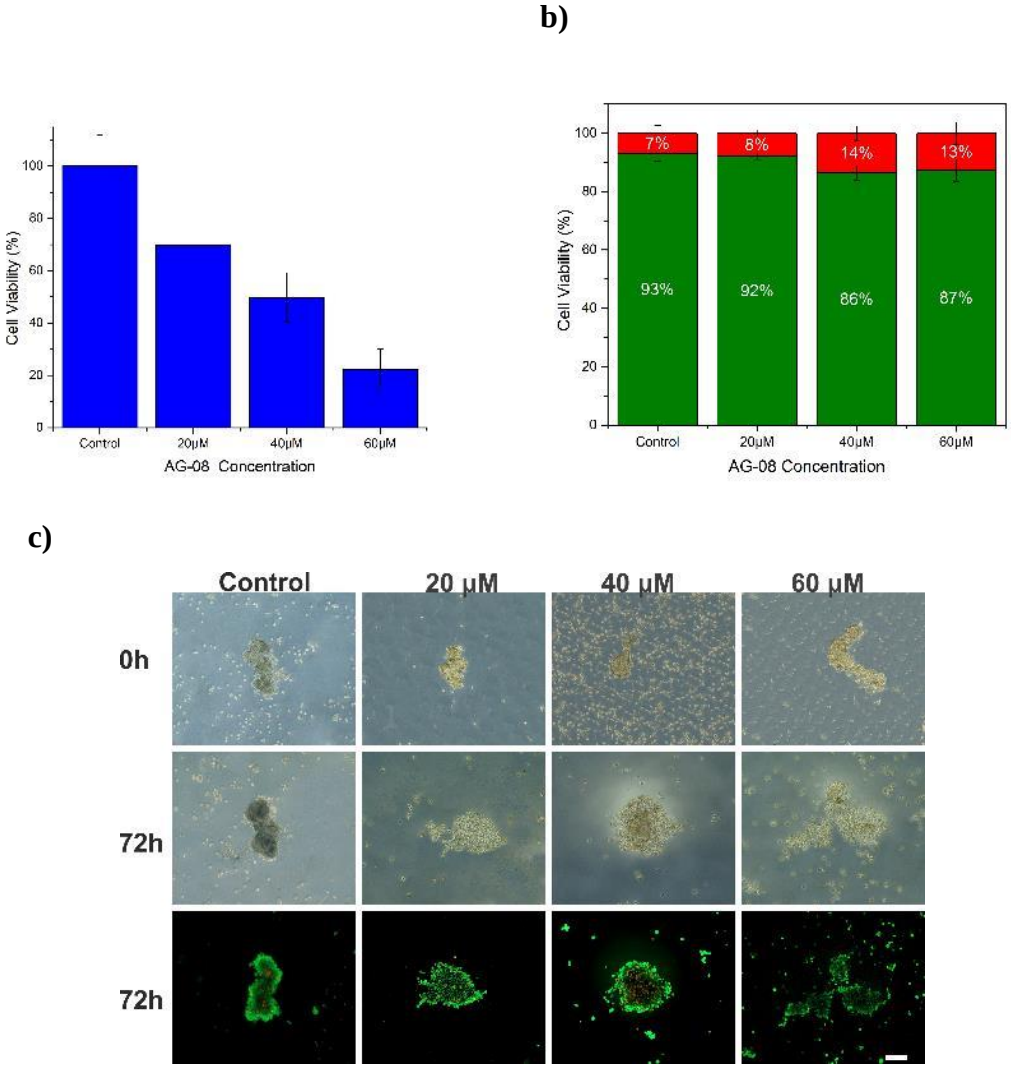


**Figure 92**. Analysis results of AG-08 toxicity in HeLa spheroids obtained by MagLev **a)** MTT **b-c)** Live-dead analysis (AG-08 concentration unit: µM) (scale size 200µm).

The effects of the AG-04 molecule, one of the analogues of the AG-08 molecule synthesized by Prof. Bedir and his group, on viability in 3D tumor spheroid models obtained with HeLa cells are shown in Figure 93 with MTT and live-dead analyses. In

the literature, studies conducted in 2D cell culture have proven that the $IC_{50}$ value of the molecule is >50 µM (Üner et al., 2022). For this reason, the molecule was preferred for control purposes to AG-08, which has a high cytotoxic effect. The concentration range for 3D experiments was chosen to be the same as for the toxic AG-08 molecule to enable accurate comparisons. When the results are examined, it is seen that the viability values in tumor models produced with HeLa cells are at high levels. MTT and live-dead analyses support each other. 72-hour images showing the morphological change and viability of spheroids due to the molecule effect are shared together for different concentrations in Figure 93-c. Despite the increase in the applied AG-04 concentration, there was no change in the number of dead cells. In line with the data obtained, it is known that the AG-04 does not have a toxic effect on cancer cells in 2D studies, as explained in the literature. The same results were seen in HeLa spheroid models produced by the magnetic levitation method, but a comparison was not made between the two molecules because the toxic effect of the toxic AG-08 molecule remained at a lower level than expected, especially in the live-dead assay.

The effects of the CG-03 molecule, one of the derivatives of the AG-08 molecule synthesized by Prof. Bedir and his group, on viability in 3D tumor spheroid models obtained with HeLa cells are shown in Figure 94 with MTT and live-dead analyses. As a result of viability tests performed in 2D cell culture in the literature on the CG-03 molecule, the $IC_{50}$ value in HeLa cells was calculated as 12.87 µM (Üner et al., 2022). In the 2D experiments carried out within the scope of this study, it was found to be in the range of 5-10 µM. Since these molecules are being tested for the first time in 3D cell culture studies, there is no concentration range available in the literature. With the experiments carried out, important data will be added to the literature. When the results in Figure 94 are examined, it is seen in the MTT and live-dead graphs that as the CG-03 molecule concentration increases, the viability of the cells in the spheroids decreases. Both graphs support each other. 72-hour images showing the morphological change and viability of spheroids due to the molecular effect are shared together for different concentrations in Figure 94-c. It is seen that there is an increase in the red color, which represents dead cells, in the images in proportion to the increase in the applied CG-03 concentration. Due to the weak structure of HeLa spheroids with the hanging drop method, which was determined to be the control method, it was not possible to make a comparison of the spheroids obtained by both methods for this cell line and this molecule.

**a)** **b)**

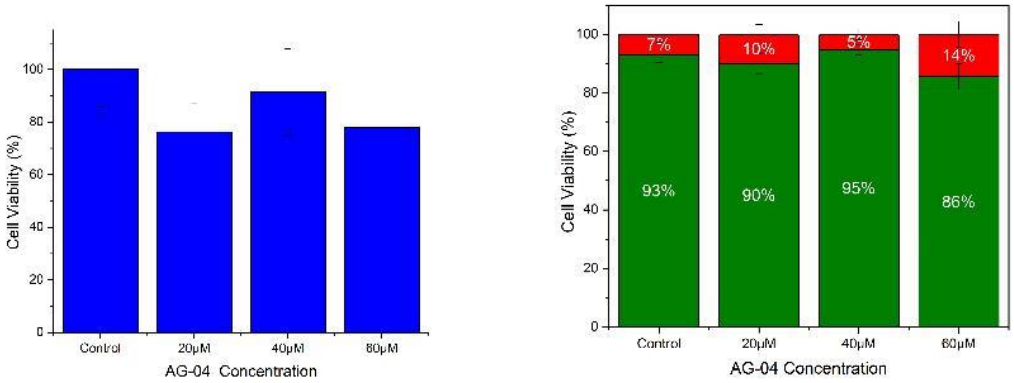


**c)**

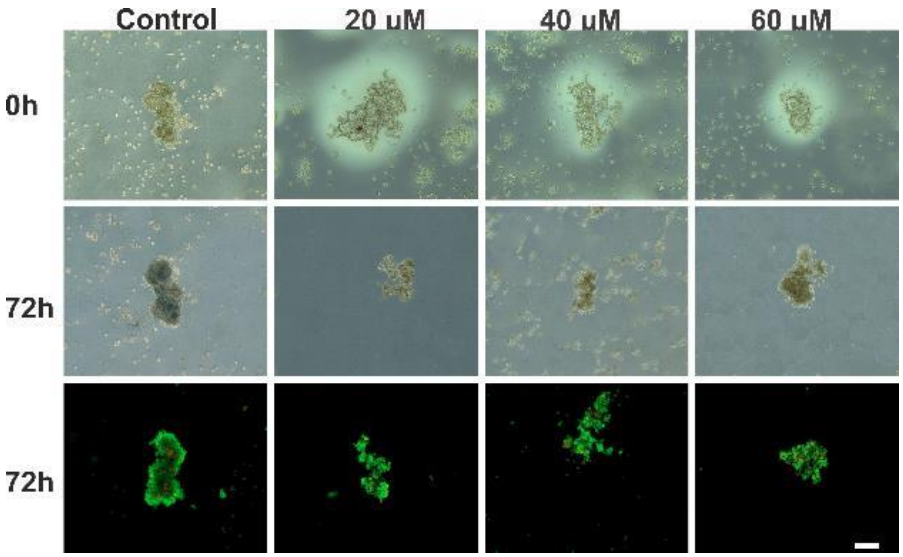


**Figure 93**. Analysis results of AG-04 toxicity in HeLa spheroids obtained by MagLev **a)** MTT **b-c)** Live-dead analysis (AG-04 concentration unit: μM) (scale size 200μm).

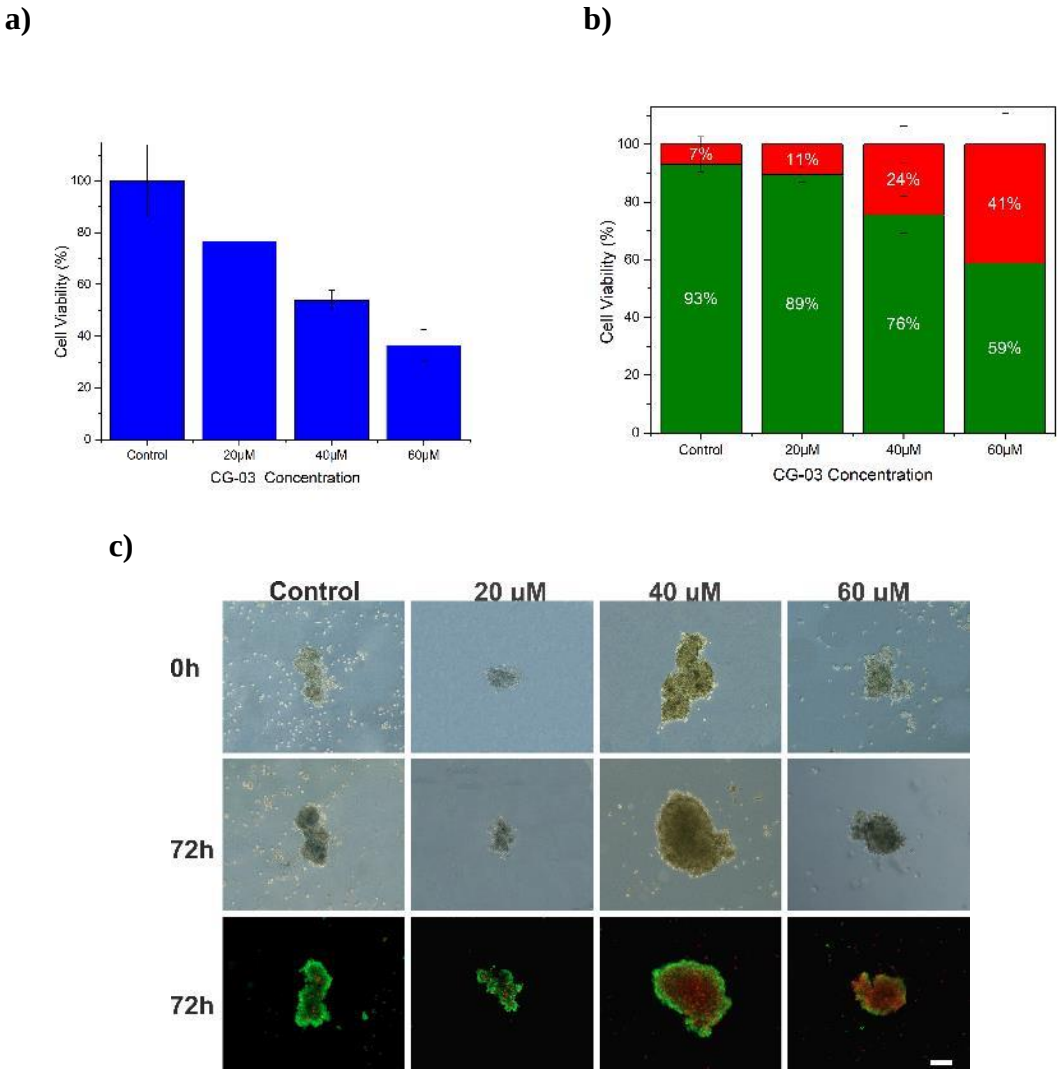


**Figure 94**. Analysis results of CG-03 toxicity in HeLa spheroids obtained by MagLev **a)** MTT **b-c)** Live-dead analysis (CG-03 concentration unit: µM) (scale size 200µm).

The effects of the CG-04 molecule, one of the analogues of the AG-08 molecule synthesized by Prof. Bedir and his group, on viability in 3D tumor spheroid models obtained with HeLa cells are shown in Figure 95 with MTT and live-dead analyses. In the literature, studies conducted in 2D cell culture have proven that the $IC_{50}$ value of the molecule is >50 µM (Üner et al., 2022). For this reason, the molecule CG-03, which has a high cytotoxic effect, was preferred for control purposes. The concentration range for 3D experiments was chosen to be the same as the toxic CG-03 molecule to enable accurate comparisons. As expected from the results, the viability level of tumor models produced with HeLa cells is quite high. 72-hour images showing the change and vitality in the

morphology of spheroids due to the molecular effect are shared together for different concentrations in Figure 95-c. Despite the increase in the applied CG-04 concentration, there was no change in the number of dead cells. In line with the data obtained, it is known that the CG-04 does not have a toxic effect on cancer cells in 2D studies, as explained in the literature. The same results were seen in HeLa spheroid models produced by the magnetic levitation method.

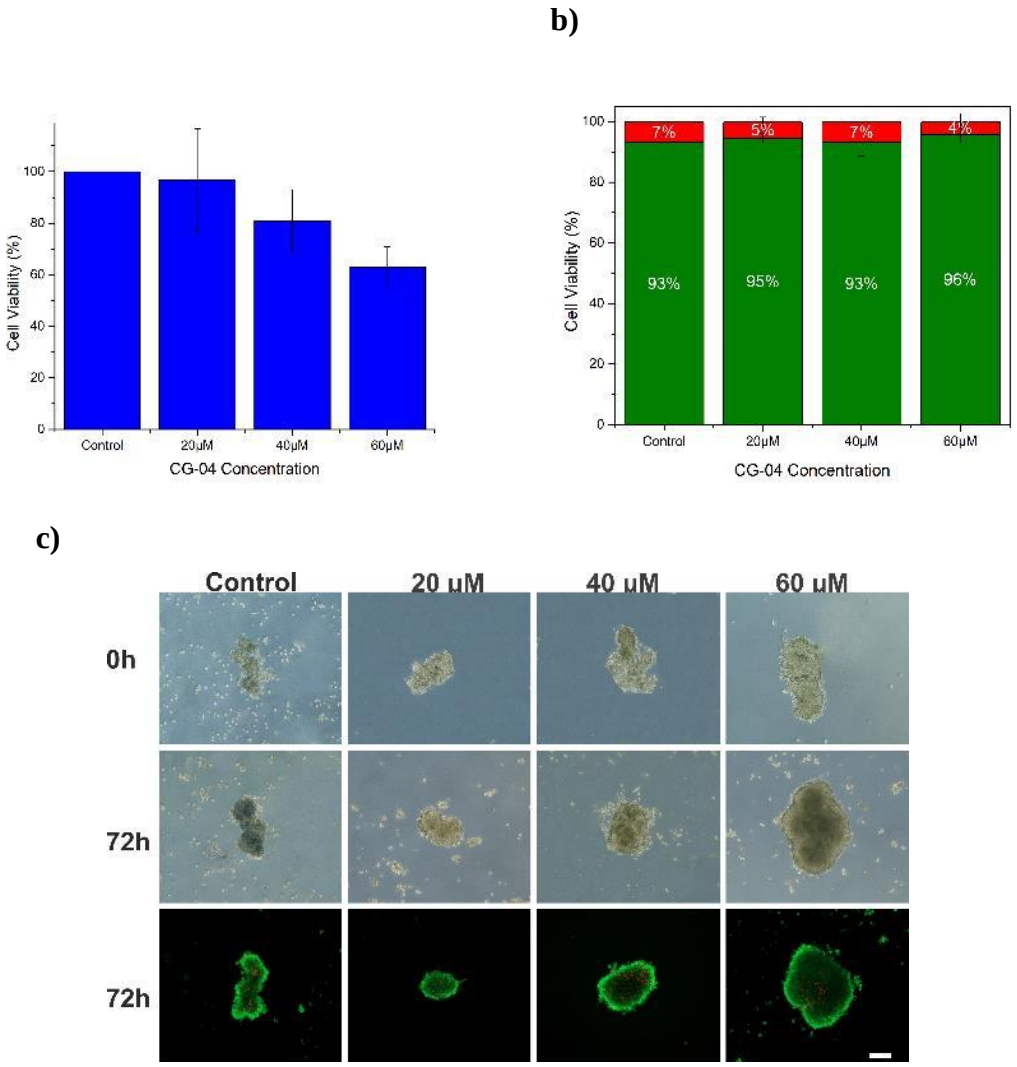


**Figure 95**. Analysis results of CG-04 toxicity in HeLa spheroids obtained by MagLev **a)** MTT **b-c)** Live-dead analysis (CG-04 concentration unit: µM) (scale size 200µm).

With these results, AG-04 and CG-04 molecules have a low toxic effect on HeLa spheroids obtained by magnetic levitation, and cell viability is at a high level, while the toxic effects of previously proven (with this research experiment) Ptx and CG-03 molecules are relatively higher. It was observed that the viability level decreased depending on the concentration.

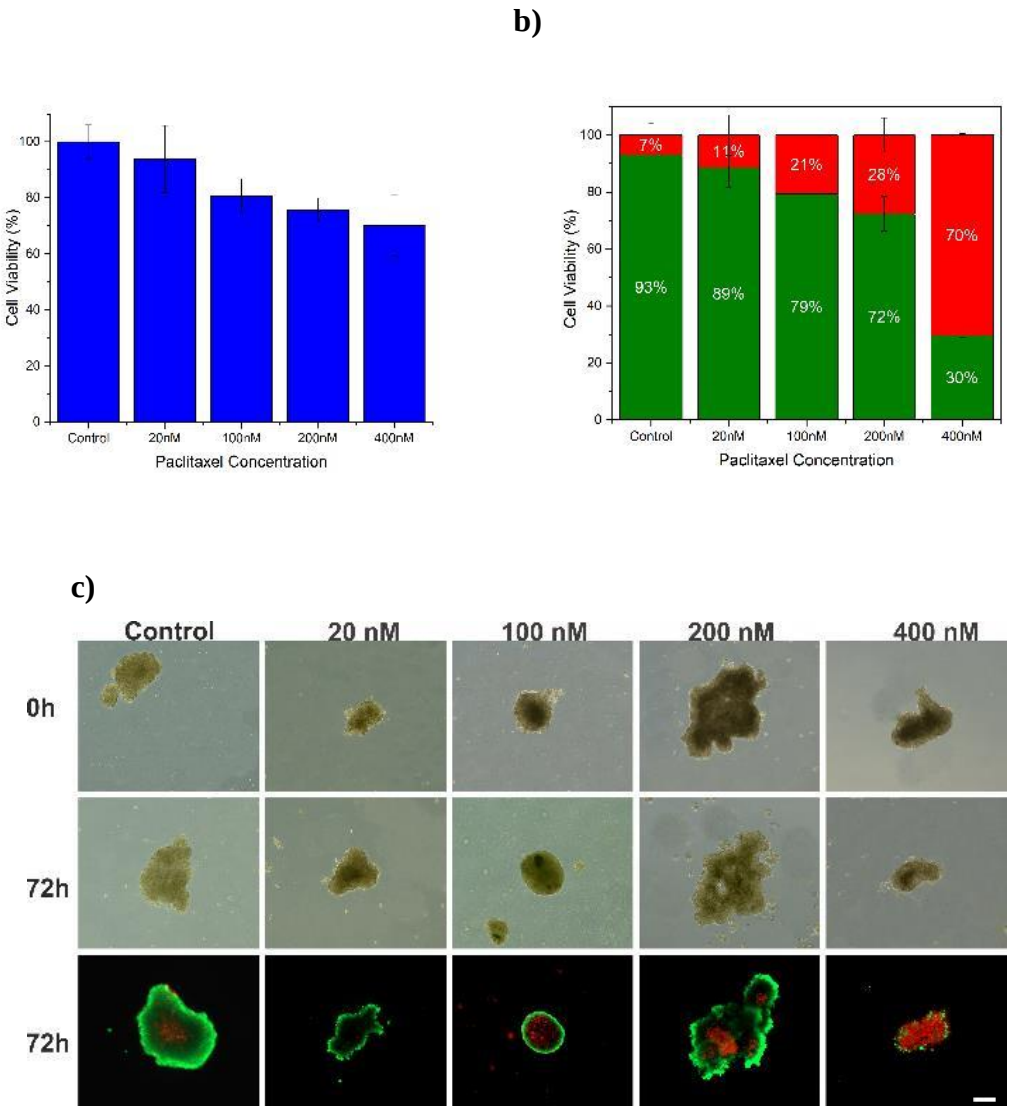


**Figure 96**. Analysis results of Ptx toxicity in SH-SY5Y spheroids obtained by MagLev method **a)** MTT **b-c)** Live-dead analysis (Ptx concentration unit: nM) (scale size 200µm).

The effects of the FDA-approved Ptx molecule on viability on SH-SY5Y 3D tumor spheroid models obtained by the MagLev method are shown in Figure 96 with MTT and live-dead analyses. As seen in the results, the expected effect appeared as a decreasing trend in viability in SH-SY5Y 3D tumor models. The decreasing trend seen in the results of MTT, and live-dead analysis coincides with each other. 72-hour images showing the change and vitality in the morphology of spheroids due to the molecular effect are shared together for different concentrations in Figure 96-c. It is seen that the increase in the applied Ptx concentration increases the number of dead cells in the spheroids, and there is an increase in the red color indicating dead cells. In addition, when the results obtained with the hanging drop method are compared with the Ptx effect in 3D tumor spheroid models, it is seen that similar results are obtained in both models, and the results obtained with the hanging drop and MagLev method support each other.

The effects of the AG-08 molecule synthesized by Prof. Bedir and his group on the viability of SH-SY5Y 3D tumor spheroid models by the MagLev method are shown in figure 97 with MTT and live-dead analyses. As a result of the viability tests performed in 2D cell culture in the literature on the AG-08 molecule, the $IC_{50}$ value in SH-SY5Y cells was calculated as 3.5 -4 μM (Üner et al., 2019). In the 2D experiments carried out within the scope of this thesis, it was found to be in the range of 5-10 μM. In addition, scans performed on 3D tumor spheroid models obtained by the hanging drop method showed that cell viability decreased as the molecule concentration increased. The preferred concentration range in this step is the same as that investigated by the hanging drop method (0-60 μM). As seen in the results, the expected effect of the AG-08 molecule appeared to be a decreasing trend in viability in tumor models produced with SH-SY5Y cells. The results of MTT and live-dead analysis overlap with each other. AG-08 scanning performed on spheroids produced by the hanging drop method and the MagLev method gives similar results. 72-hour images showing the change and vitality in the morphology of spheroids due to the molecular effect are shared together for different concentrations in Figure 97-c. It is seen that the increase in the applied AG-08 concentration increases the number of dead cells in the spheroids.

**a)** **b)**

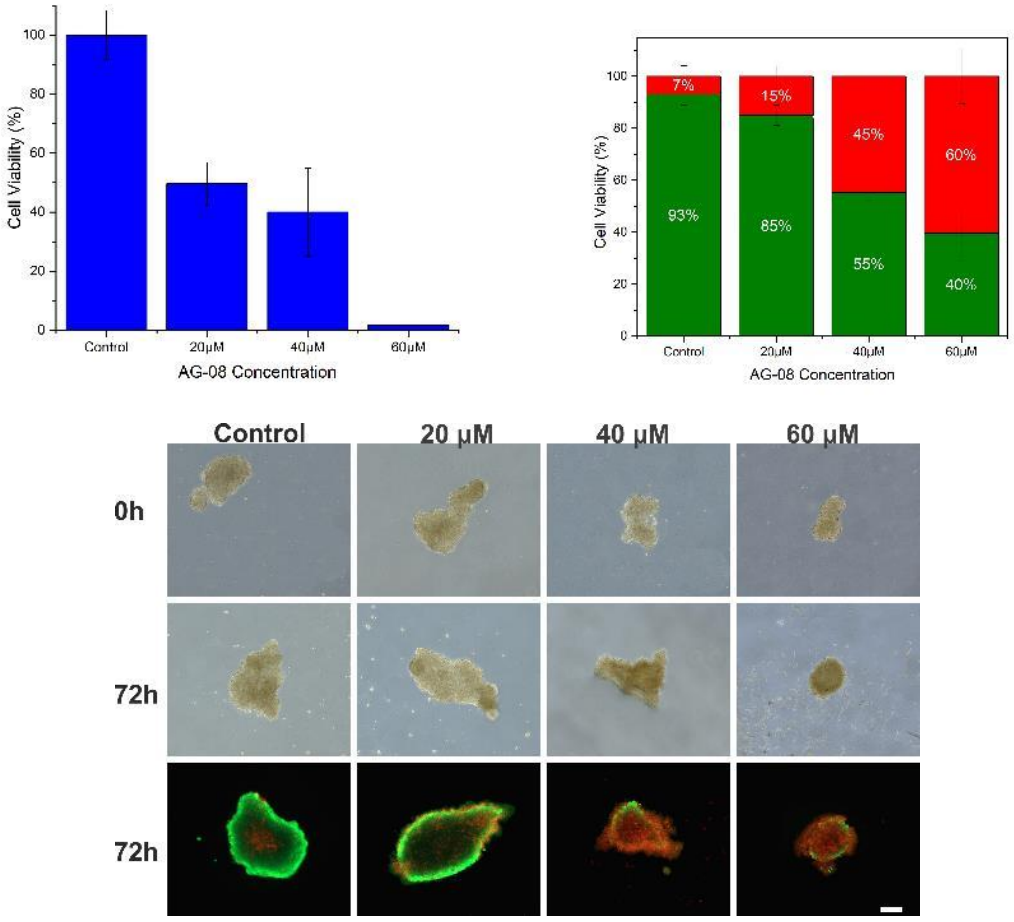


**Figure 97**. Analysis results of AG-08 toxicity in SH-SY5Y spheroids obtained by MagLev **a)** MTT **b-c)** Live-dead analysis (AG-08 concentration unit: µM) (scale size 200µm).

The effects of the AG-04 molecule, one of the derivatives of the AG-08 molecule synthesized by Prof. Bedir and his group, on viability for SH-SY5Y 3D tumor spheroid models with the MagLev method are shown in figure 98 with MTT and live-dead analyses. As a result of the viability tests performed in 2D cell culture in the literature on the AG-04 molecule, the $IC_{50}$ value in SH-SY5Y cells was calculated as >50 µM (Üner et al., 2019). The results of the 2D experiments conducted within the scope of this thesis also support the literature. In addition, in the scans performed on 3D tumor spheroid models obtained by the hanging drop method, the viability level remained at 90% and above despite the increase in molecule concentration. The preferred concentration range

in this step is the same as that investigated by the hanging drop method. As seen in the results, the AG-04 molecule did not cause a toxic effect on tumor models produced with SH-SY5Y cells, as expected.

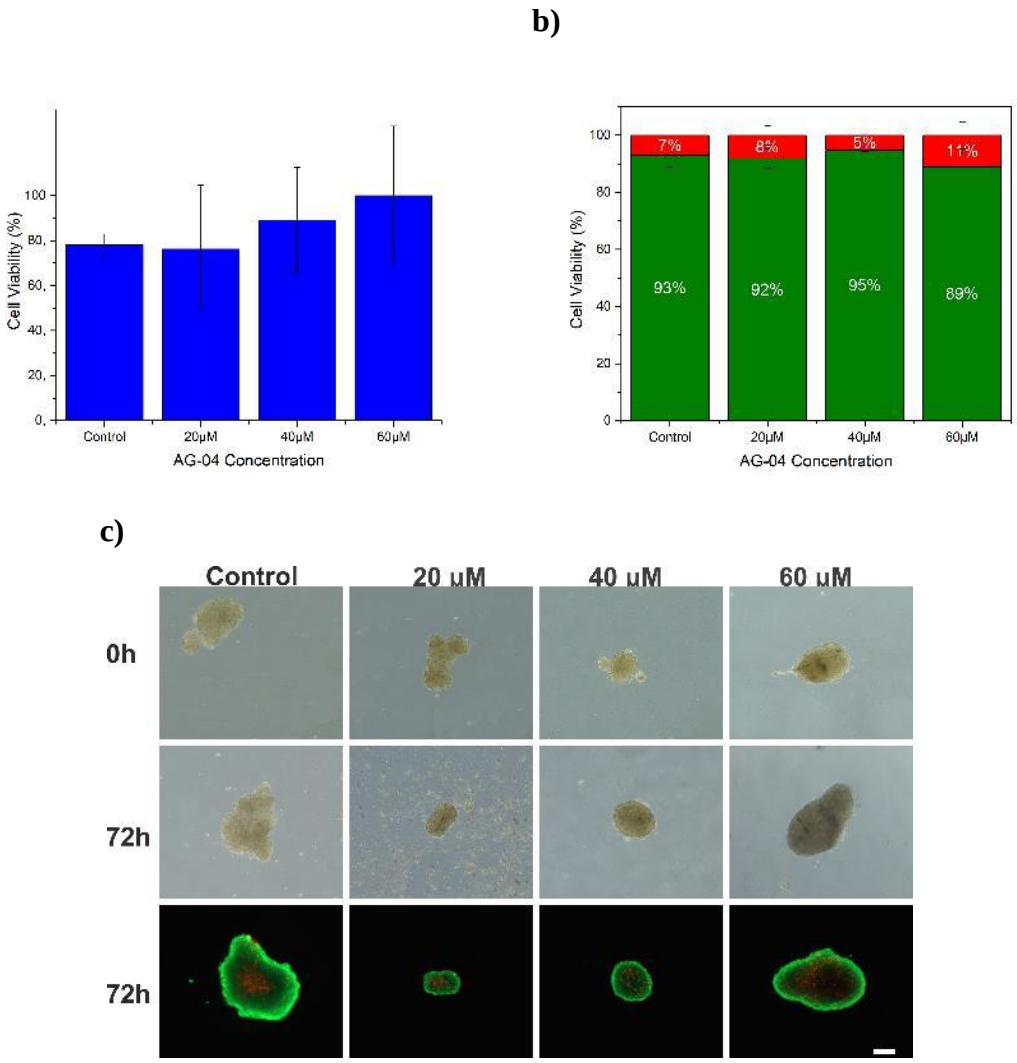


**Figure 98**. Analysis results of AG-04 toxicity in SH-SY5Y spheroids obtained by MagLev **a)** MTT **b-c)** Live-dead analysis (AG-04 concentration unit: µM) (scale size 200µm).

The results of MTT and live-dead analysis overlap with each other. AG-04 scanning performed on spheroids produced by the hanging drop method and the MagLev method gives similar results. 72-hour images showing the change and vitality in the

morphology of spheroids due to the molecular effect are shared together for different concentrations in Figure 98-c. It is seen that the increase in the applied AG-04 concentration does not change the live appearance of the spheroids. Based on the results obtained, the difference in the toxic effects of AG-08 and AG-04 molecules on 3D tumor spheroid models can be seen.

The effects of the CG-03 molecule, one of the derivatives of the AG-08 molecule synthesized by Prof. Bedir and his group, on viability for SH-SY5Y 3D tumor spheroid models by the MagLev method are shown in figure 99 with MTT and live-dead analyses. As a result of the viability tests performed in 2D cell culture in the literature on the CG-03 molecule, the $IC_{50}$ value in SH-SY5Y cells was calculated as 3.5-12 μM (Üner et al., 2019). In the 2D experiments carried out within the scope of this project, it was found to be in the range of 5-10 μM. In addition, scans performed on 3D tumor spheroid models obtained by the hanging drop method showed that cell viability decreased as the molecule concentration increased. The preferred concentration range in this step is the same as that investigated by the hanging drop method. As seen in the results, the expected effect of the CG-03 molecule appeared to be a decreasing trend in viability in tumor models produced with SH-SY5Y cells. The results of MTT and live- dead analysis overlap with each other. CG-03 scanning performed on spheroids produced by the hanging drop method and the MagLev method gives similar results. 72-hour images showing the change and vitality in the morphology of spheroids due to the molecular effect are shared together for different concentrations in Figure 99-c. It is seen that the increase in the applied CG-03 concentration increases the number of dead cells in the spheroids. The results proved that Ptx, AG-08, and CG-03 drug molecules showed similar toxic effects on 3D SH-SY5Y spheroid models produced by hanging drop and MagLev methods. Compared to studies conducted with 2D cell lines, viability values were observed to be at higher levels. This is due to the fact that 3D spheroid structures mimic real tissue physiology much better. The diffusion problem, which is frequently encountered in 3D structures, prevents molecules and drugs from diffusing into the interior; therefore, the cytotoxicity level is much lower. The results obtained support the literature.

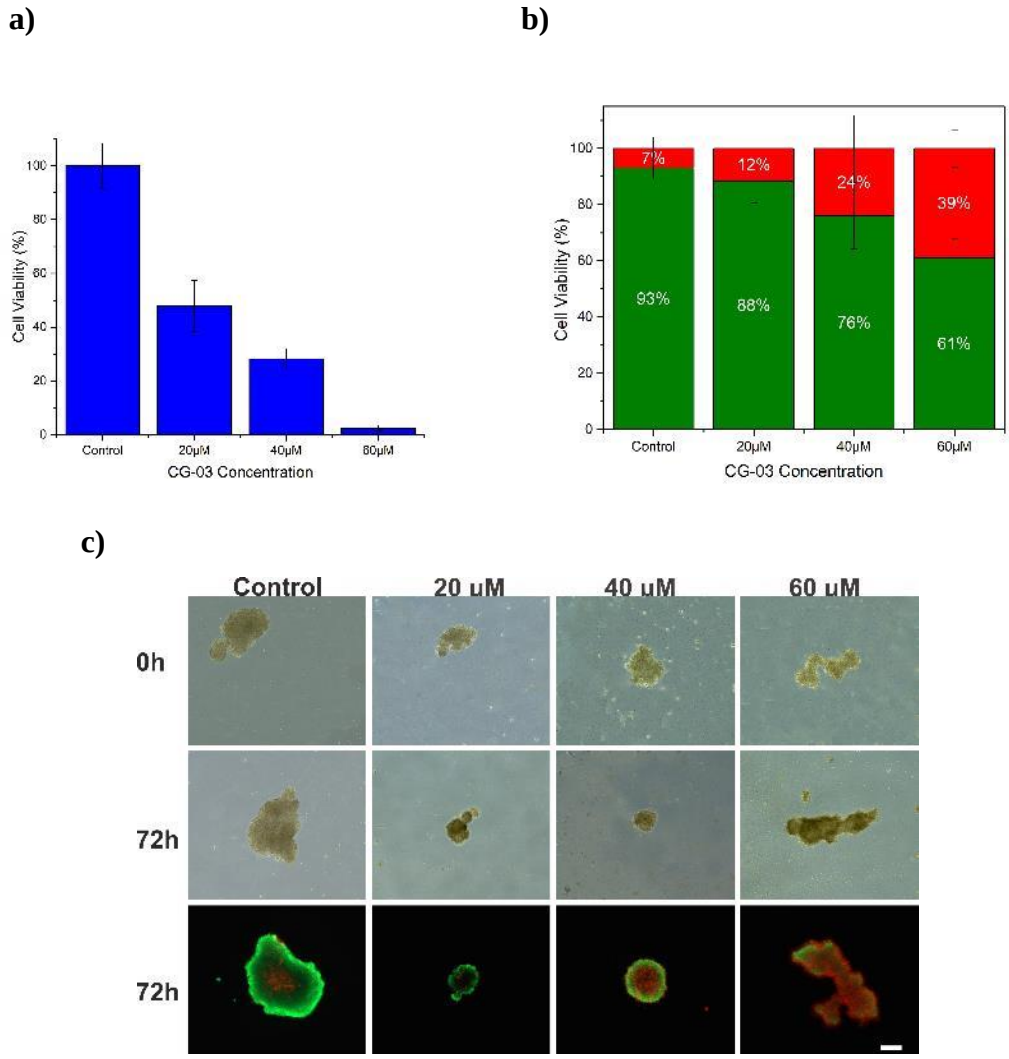


**Figure 99**. Analysis results of CG-03 toxicity in SH-SY5Y spheroids obtained by MagLev **a)** MTT **b-c)** Live-dead analysis (CG-03 concentration unit: µM) (scale size 200µm).

The effects of the CG-04 molecule, one of the derivatives of the AG-08 molecule synthesized by Prof. Bedir and his group, on viability for SH-SY5Y 3D tumor spheroid models with the MagLev method are shown in figure 100 with MTT and live-dead analyses. As a result of the viability tests performed in 2D cell culture in the literature on the CG-04 molecule, the $IC_{50}$ value in SH-SY5Y cells was calculated as >50 µM (Üner et al., 2019). The results of the 2D experiments conducted within the scope of this project also support the literature. In addition, in the scans performed on 3D tumor spheroid models obtained by the hanging drop method, the viability level remained at 80% and

above despite the increase in molecule concentration. The preferred concentration range in this step is the same as that investigated by the hanging drop method. As seen in the results, the CG-04 molecule did not cause a toxic effect on tumor models produced with SH-SY5Y cells, as expected. In the MTT chart, it is seen that there is a decrease in the vitality level of the control and experimental groups. It is thought that this situation is partly due to the difference in spheroid sizes. CG-04 scanning performed on spheroids produced by the hanging drop method and the MagLev method gives similar results. 72-hour images show the change and vitality in the morphology of spheroids due to the molecule effect, which are shared for different concentrations in Figure 100-c. It is seen that the increase in the applied CG-04 concentration does not change the viability of the spheroids. The levels of green are close to each other. Based on the results obtained, the difference in the toxic effects of CG-03 and CG-04 molecules on cancer cells can be clearly seen. It has been proven that AG-04 and CG-04 molecules have similar effects on SH-SY5Y spheroid models produced by hanging drop and MagLev methods. These results support the literature. (Üner et al., 2022)

The effects of the FDA-approved Ptx molecule on viability on 3D tumor spheroid models obtained with HepG2 cells are shown in Figure 101 with MTT and live-dead analyses. In the 2D cell culture studies conducted within the scope of the thesis, Ptx reduced the viability of HepG2 cells below 50% at concentrations of 25 nM and above. Ptx caused a toxic effect on the cells in the concentration range investigated in HepG2 3D tumor spheroid models obtained by the hanging drop method. According to the results obtained in Figure 101, there is a decreasing trend in cell viability. 72-hour images showing the change and vitality in the morphology of spheroids due to the molecular effect are shared together for different concentrations in Figure 116-c. In 3D tumor spheroids obtained by the hanging drop method with the same cell line, Ptx affected cell viability to a lesser extent than expected for hanging drop trials, and the results obtained in this regard support each other for both methods. It is thought that 3D tumor spheroid models obtained with the HepG2 cell line resist drug diffusion, and viability remains high.

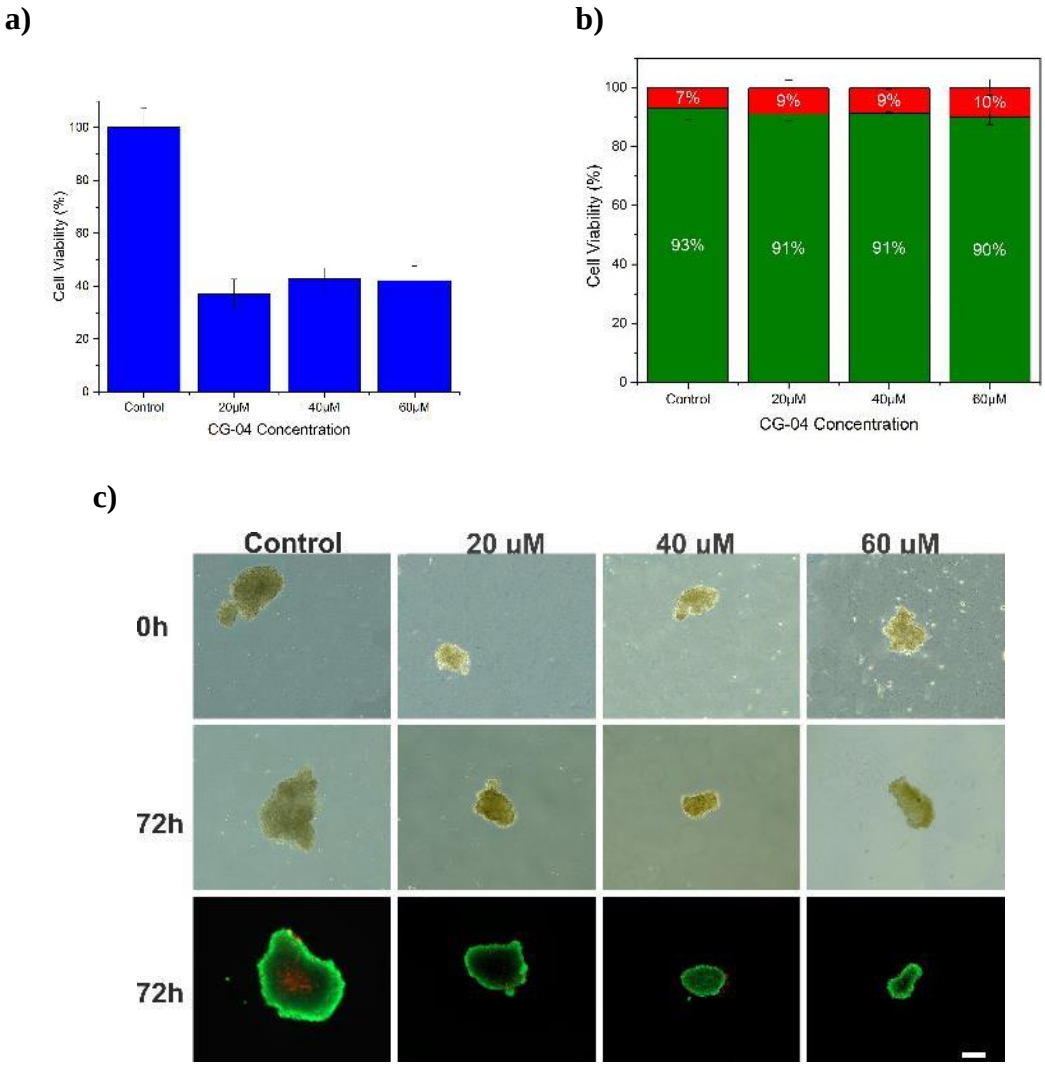


**Figure 100**. Analysis results of CG-04 toxicity in SH-SY5Y spheroids obtained by MagLev **a)** MTT **b-c)** Live-dead analysis (CG-04 concentration unit: μM) (scale size 200μm).

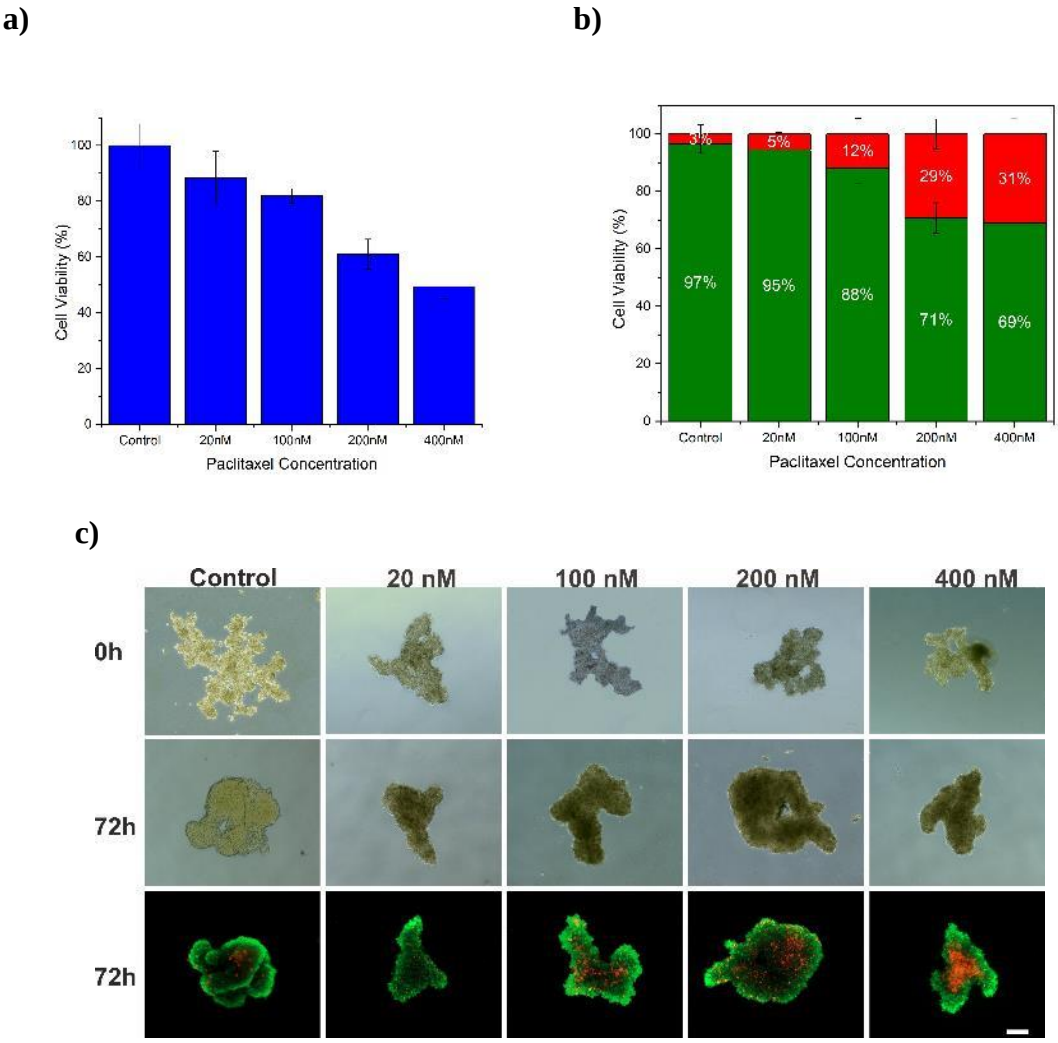


**Figure 101**. Analysis results of PTX toxicity in HepG2 spheroids obtained by MagLev **a)** MTT **b-c)** Live-dead analysis (Ptx concentration unit: nM) (scale size 200µm).

The effects of the AG-08 molecule on viability in 3D tumor spheroid models obtained with HepG2 cells are shown in Figure 102 with MTT and live-dead analyses. As a result of the viability tests performed in 2D cell culture in the literature on the AG-08 molecule, the $IC_{50}$ value in HepG2 cells was calculated as 5.5 -7 µM (Üner et al., 2019). In the 2D experiments carried out within the scope of this project, it was found to be in the range of 5-10 µM. In addition, scans performed on 3D tumor spheroid models obtained by the hanging drop method showed that cell viability decreased as the molecule concentration increased. The preferred concentration range in this step is the same as that investigated by the hanging drop method. As seen in both graphs, the expected effect appeared as a decreasing trend in viability in tumor models produced with HepG2 cells.

72-hour images showing the change and vitality in the morphology of spheroids due to the molecular effect are shared together for different concentrations in Figure 102-c. It is seen that the increase in the applied AG-08 concentration increases the number of dead cells in the spheroids, and the green color is replaced by red. Similar results were obtained in 40 and 60 µM applications, and the viability value remained stable.

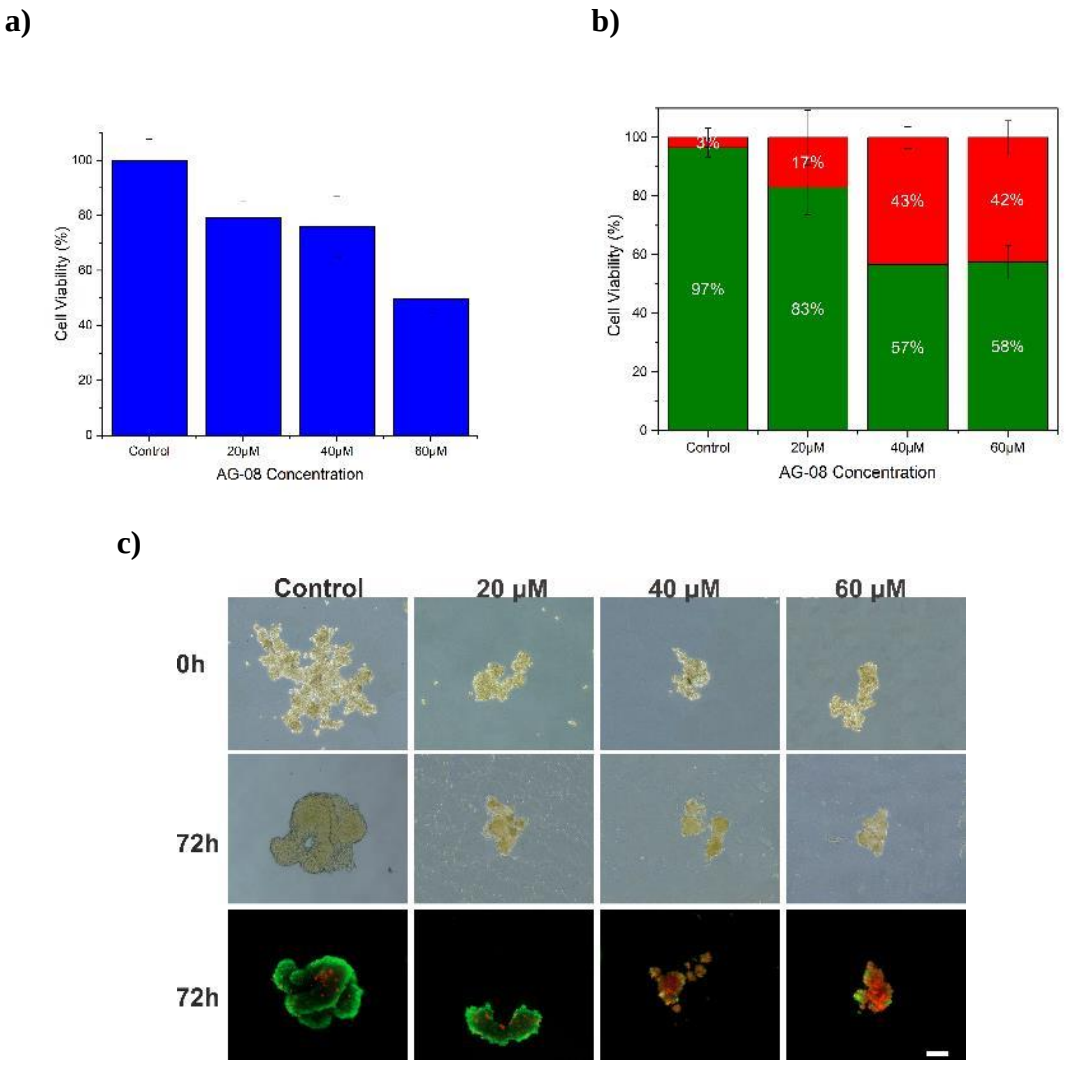


**Figure 102**. Analysis results of AG-08 toxicity in HepG2 spheroids obtained by MagLev **a)** MTT **b-c)** Live-dead analysis (AG-08 concentration unit: µM) (scale size 200µm).

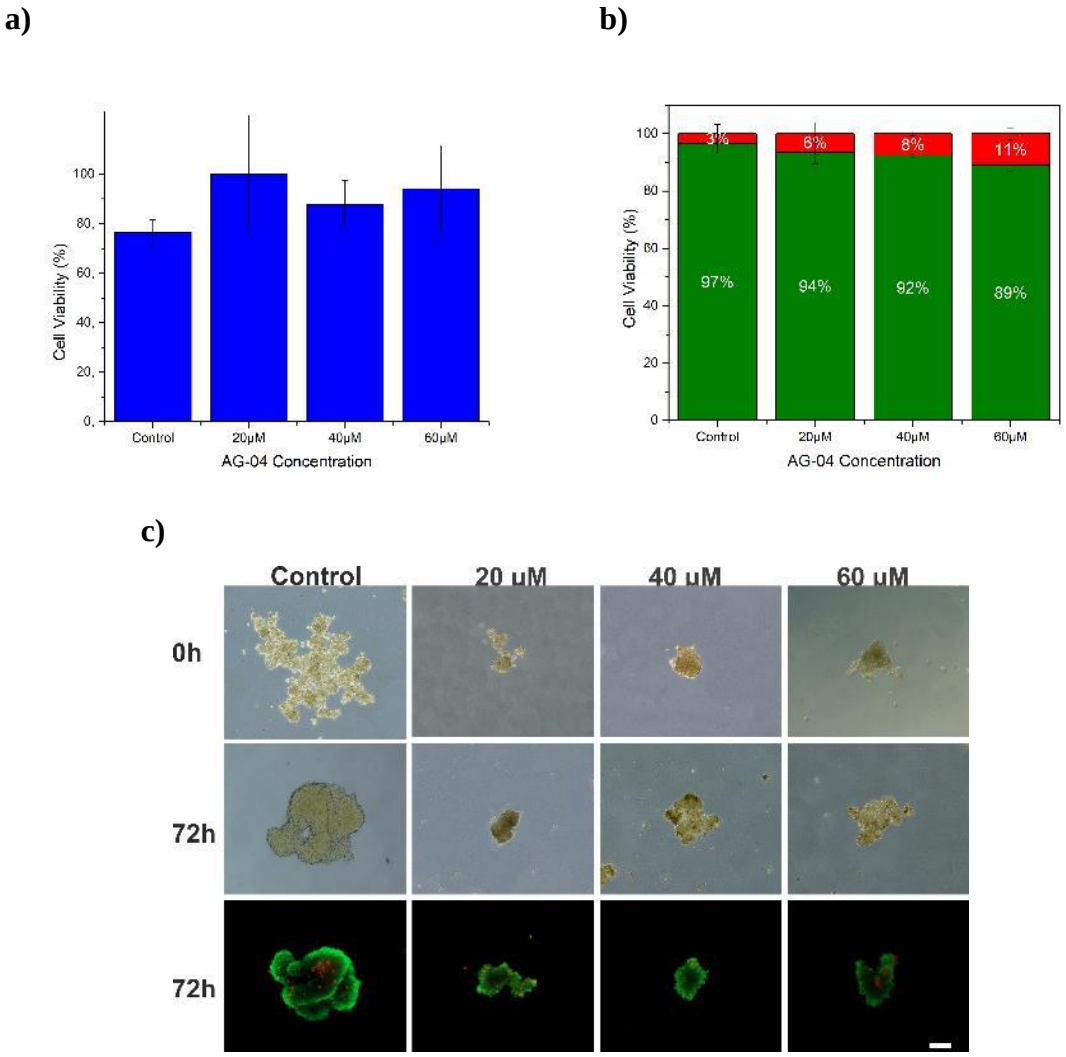


**Figure 103.** Analysis results of AG-04 toxicity in HepG2 spheroids obtained by MagLev **a)** MTT **b-c)** Live-dead analysis (AG-04 concentration unit: µM) (scale size 200µm)

The effects of the AG-04 molecule, one of the analogues of the AG-08 molecule, on viability in 3D tumor spheroid models obtained with HepG2 cells are shown in Figure 103 with MTT and live-dead analyses. In the literature, studies conducted in 2D cell culture have proven that the $IC_{50}$ value of the molecule is >50 µM for the HepG2 cell line (Üner et al., 2019). For this reason, AG-04 was preferred for control purposes to AG-08, which has a high cytotoxic effect. This result was also supported in the 2D studies carried out within the scope of this research. In addition, in the studies performed on 3D tumor spheroid models obtained by the hanging drop method, the viability level remained at

90% and above despite the increase in molecule concentration. The preferred concentration range in this step is the same as that investigated by the hanging drop method. As seen in the results, the AG-04 molecule did not cause a toxic effect on tumor models produced with HepG2 cells, as expected. The viability level in tumor models produced with HepG2 cells is quite high. 72-hour images showing the change and vitality in the morphology of spheroids due to the molecular effect are shared together for different concentrations in Figure 103-c. There is no evidence that the increase in the applied AG-04 concentration causes a change in the number of dead cells in the spheroids. Based on the results obtained, the difference in the toxic effects of AG-08 and AG-04 molecules on cancer cells can be clearly seen.

The effects of CG-03, one of the analogues of the AG-08 molecule, on viability in 3D tumor spheroid models obtained with HepG2 cells are shown in figure 104 with MTT and live-dead analyses. As a result of viability tests performed in 2D cell culture in the literature on the CG-03 molecule, the $IC_{50}$ value in HepG2 cells was calculated to be approximately 10 μM (Üner et al., 2019). In the 2D experiments carried out within the scope of this research, it was found to be in the range of 5-10 μM. The preferred concentration range in this step is the same as that investigated by the hanging drop method. In the results here, the expected effect appeared as a decreasing trend in viability in 3D tumor models produced with HepG2 cells. Figure 104-c shows the change in the morphology and viability of the spheroids under the influence of the drug at different concentrations during the 72-hour drug application. It is seen that the increase in the applied CG-03 concentration increases the number of dead cells in the spheroids, and the green color is replaced by red.

The effects of the CG-04 molecule, one of the analogues of the AG-08 molecule, on viability in 3D tumor spheroid models obtained with HepG2 cells are shown in figure 105 with MTT and live-dead analyses. In the literature, studies conducted with HepG2 cells in 2D cell culture have proven that the $IC_{50}$ value of this molecule is >50 μM (Üner et al., 2019). For this reason, CG-04 was preferred for control purposes to CG-03, which has a high cytotoxic effect. This result was also supported in the 2D studies carried out within the scope of this research. In addition, in the studies performed on 3D tumor spheroid models obtained by the hanging drop method, the viability level remained at 80% and above despite the increase in molecule concentration. As expected from the results, the viability level of 3D tumor models produced with HepG2 cells is quite high. 72-hour images showing the change and vitality in the morphology of spheroids due to

the molecular effect are shared together for different concentrations in Figure 105-c. It was observed that the spheroids maintained their structure and viability despite the increase in the applied CG-04 concentration. Based on the results obtained, the difference in the toxic effects of CG-03 and CG-04 molecules on cancer cells can be seen. It has been proven that AG-04 and CG-04 molecules have similar effects on HepG2 spheroid models produced by the hanging drop and MagLev methods. These results support the literature. (Üner et al., 2022)

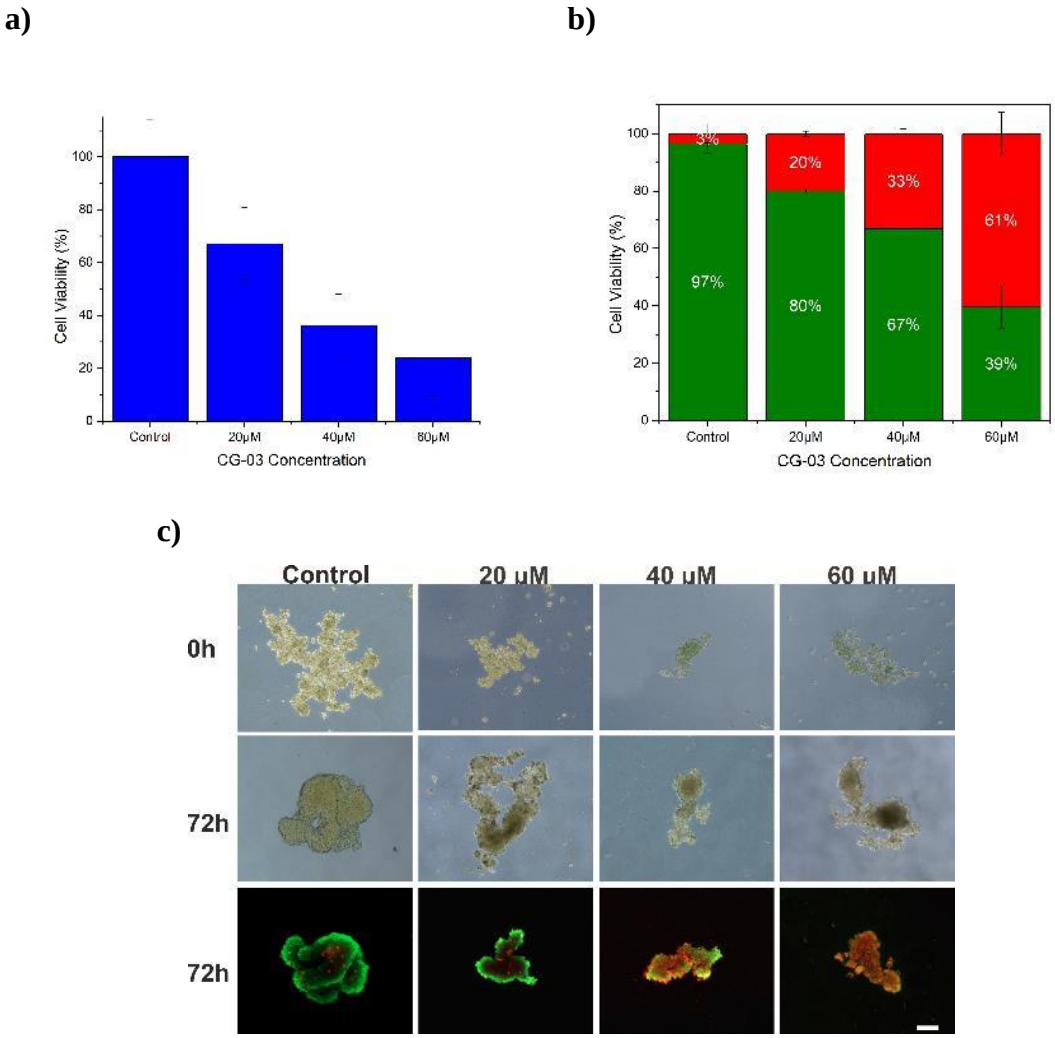


**Figure 104**. Analysis results of CG-03 toxicity in HepG2 spheroids obtained by MagLev **a)** MTT **b-c)** Live-dead analysis (CG-03 concentration unit: µM) (scale size 200µm).

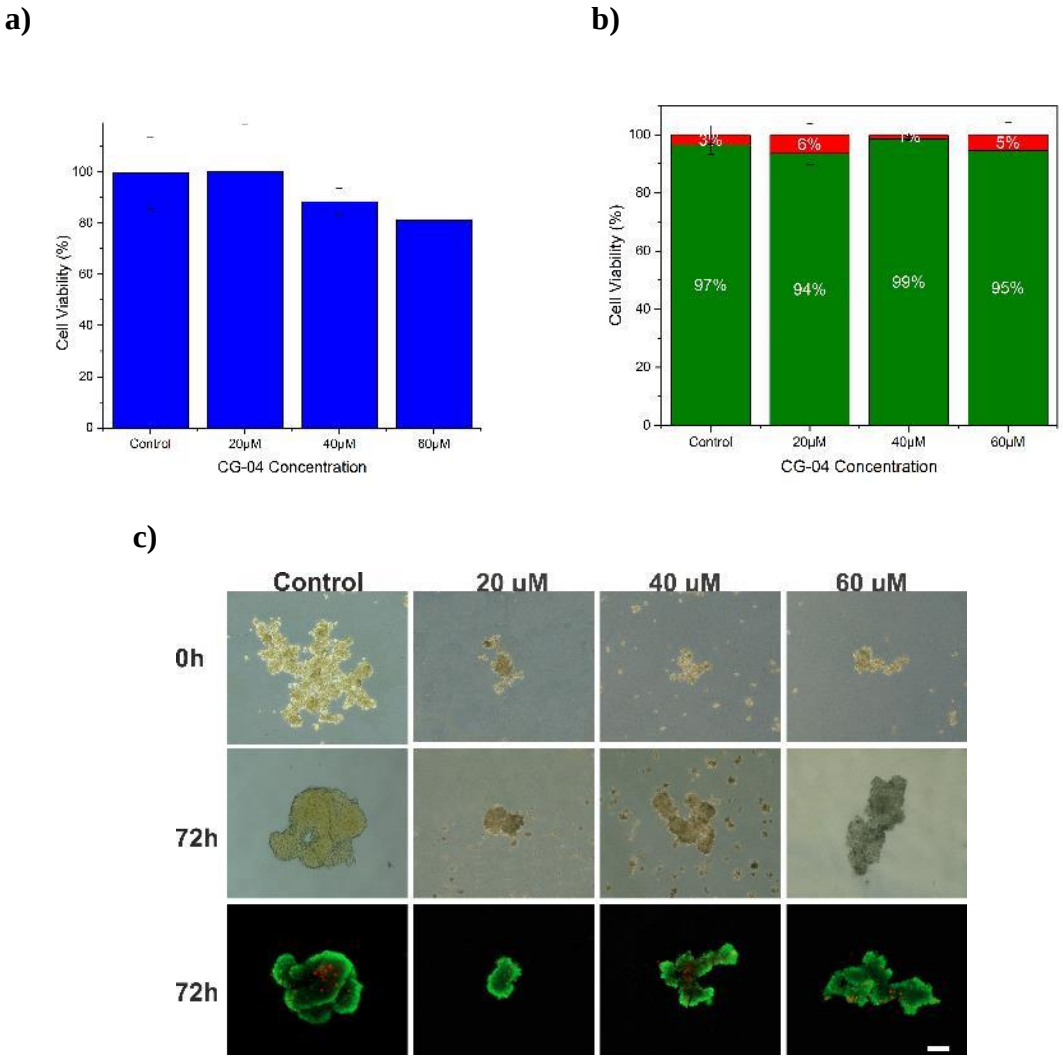


**Figure 105**. Analysis results of CG-04 toxicity in HepG2 spheroids obtained by MagLev **a)** MTT **b-c)** Live-dead analysis (CG-04 concentration unit: µM) (scale size 200µm).

The effects of the FDA-approved Ptx molecule on viability on MCF-7 3D tumor spheroid models with the MagLev method are shown in Figure 106 with MTT and live-dead analyses. As a result of the viability assays in the 2D culture of MCF-7 cells in the studies carried out within the scope of the research, the toxic effect of Ptx, which will reduce the viability value to 50% or below, is in the range of 25-50 nM. As seen in the results of this step, the expected effect appeared to be a decreasing trend in viability in tumor models produced with MCF-7 cells. The decreasing trend seen in the results of MTT and live- dead analysis overlaps with each other. The results are consistent with Ptx scans performed in 3D cell culture in the literature (Imamura et al., 2015; Lugert et al., 2019). 72-hour images showing the change and vitality in the morphology of spheroids

due to the molecule effect are shared together for different concentrations in Figure 106-c. It is seen that the increase in the applied Ptx concentration increases the number of dead cells in the spheroids, and there is an increase in the red color indicating dead cells. In addition, when the results obtained were compared with the Ptx effect in the spheroid models obtained by the hanging drop method, it was observed that while the MTT analysis results were very close to each other, there were partial differences in the live-dead test results.

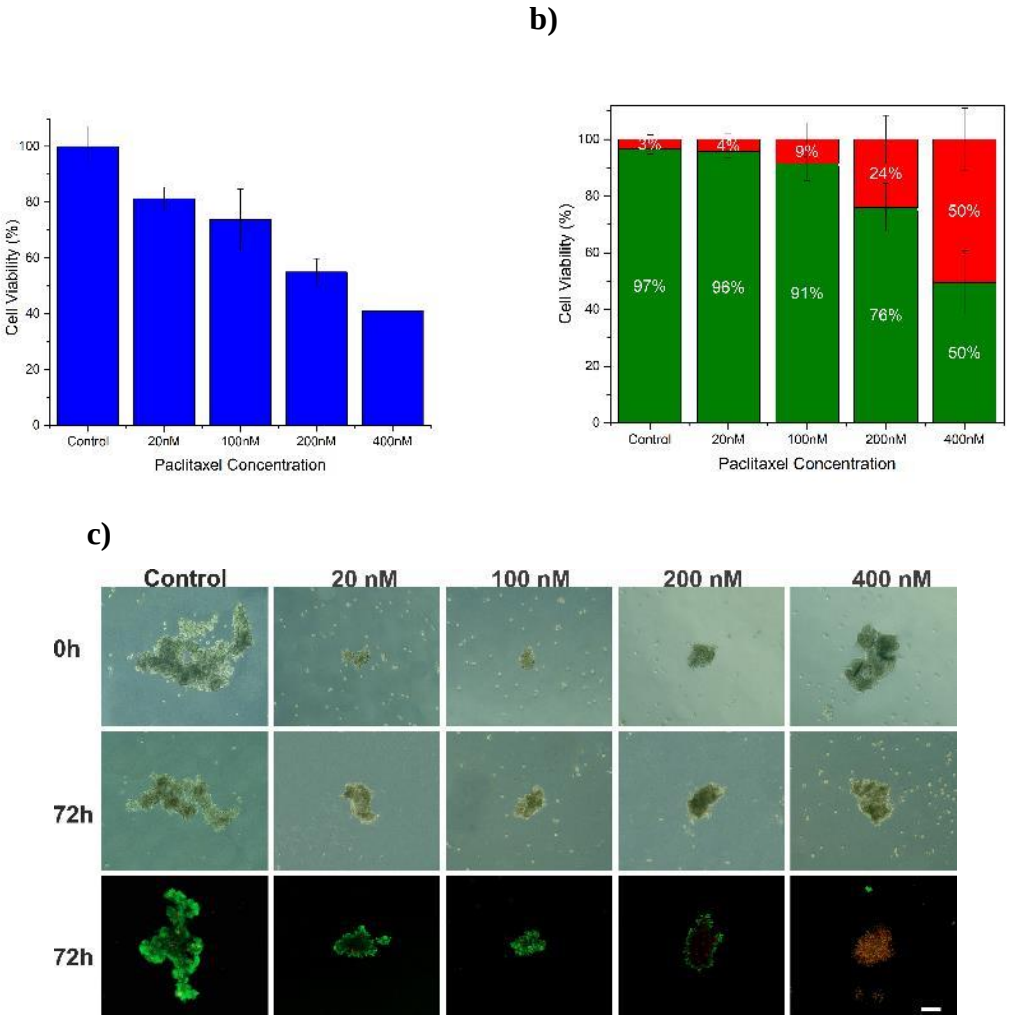


**Figure 106**. Analysis results of Ptx toxicity in MCF-7 spheroids obtained by MagLev method **a)** MTT **b-c)** Live-dead analysis (Ptx concentration unit: nM) (scale size 200µm).

The effects of the AG-08 molecule on viability in 3D tumor spheroid models obtained with MCF-7 cells are shown in figure 107 with MTT and live-dead analyses. As a result of the viability tests performed in 2D cell culture in the literature on the AG-08 molecule, the $IC_{50}$ value in MCF-7 cells was calculated as 3.5 -4 μM (Üner et al., 2022). In the 2D experiments carried out within the scope of this research, it was found to be in the range of 10-20 μM. In addition, tests performed on 3D tumor spheroid models obtained by the hanging drop method showed that cell viability decreased as the molecule concentration increased. As seen in the results, the expected effect appeared to be a decreasing trend in viability in tumor models produced with MCF-7 cells. The results of MTT and live-dead analysis overlap with each other. 72-hour images showing the change and vitality in the morphology of spheroids due to the molecular effect are shared together for different concentrations in Figure 107-c. It is seen that the increase in the applied concentration of AG-08 increases the number of dead cells in the spheroids, and the green color representing living cells is replaced by red representing dead cells.

The effects of the AG-04 molecule, one of the analogues of the AG-08 molecule, on viability on 3D tumor spheroid models obtained with MCF-7 cells are shown in figure 108 with MTT and live-dead analyses. As a result of the viability tests performed in 2D cell culture in the literature on the AG-04 molecule, the $IC_{50}$ value in MCF-7 cells was calculated as 22.05 μM (Üner et al., 2022). In the 2D experiments conducted within the scope of this research, the viability level dropped below 50% in the 20-30 μM concentration range. In addition, in the tests performed on 3D tumor spheroid models obtained by the hanging drop method, the viability level remained at 70% and above despite the increase in molecule concentration. In the results shared here, the AG-04 molecule did not cause a toxic effect on tumor models produced with MCF-7 cells, as expected. The vitality level is 80% and above. The results of MTT and live-dead analysis overlap with each other. 72-hour images show the change and vitality in the morphology of spheroids due to the molecular effect shared together for different concentrations in Figure 108-c. It is seen that the increase in the applied AG-04 concentration does not significantly change the number of dead cells in the spheroids. Based on the results obtained, the difference in the toxic effects of AG-08 and AG-04 molecules on the MCF-7 3D tumor spheroid models obtained by the hanging drop and MagLev methods can be clearly seen.

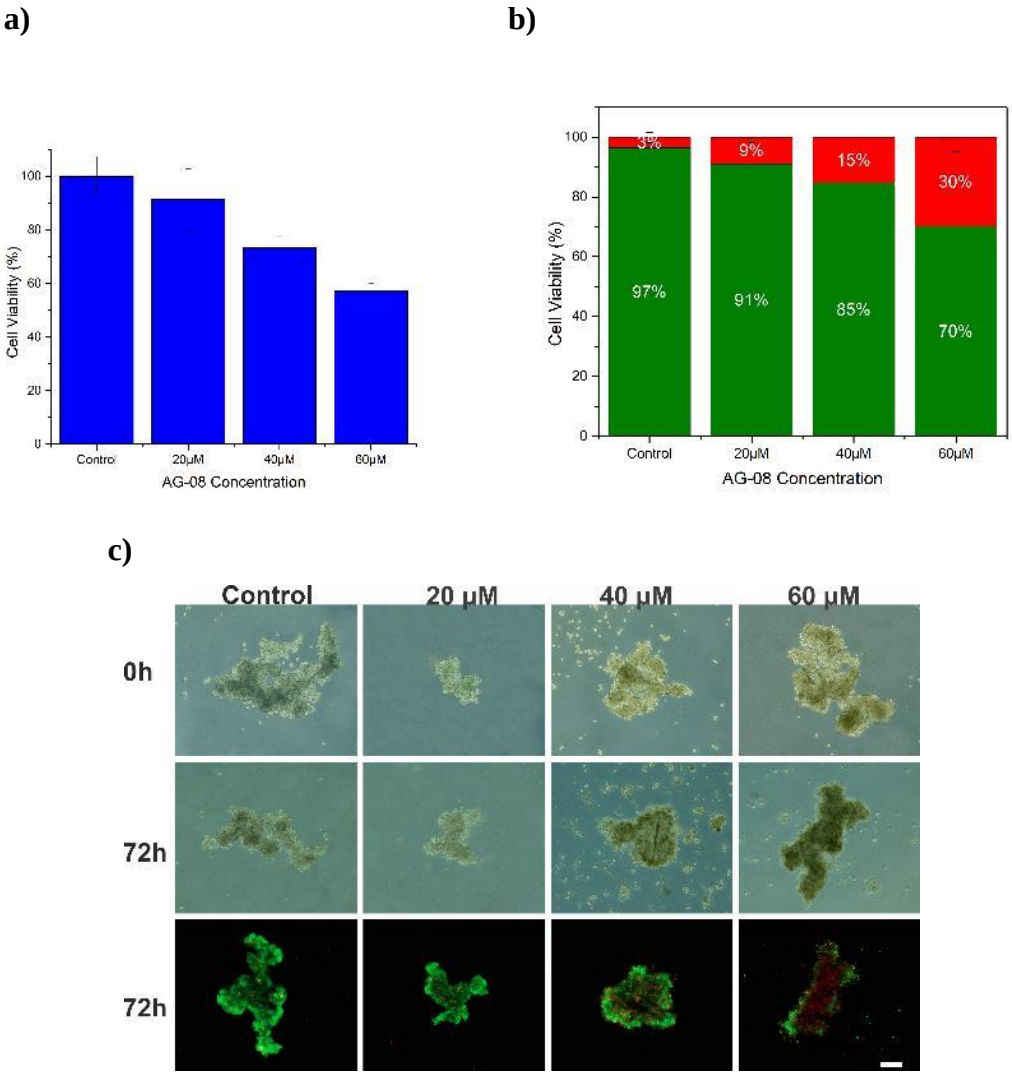


**Figure 107**. Analysis results of AG-08 toxicity in MCF-7 spheroids obtained by MagLev **a)** MTT **b-c)** Live-dead analysis (AG-08 concentration unit: μM) (scale size 200μm).

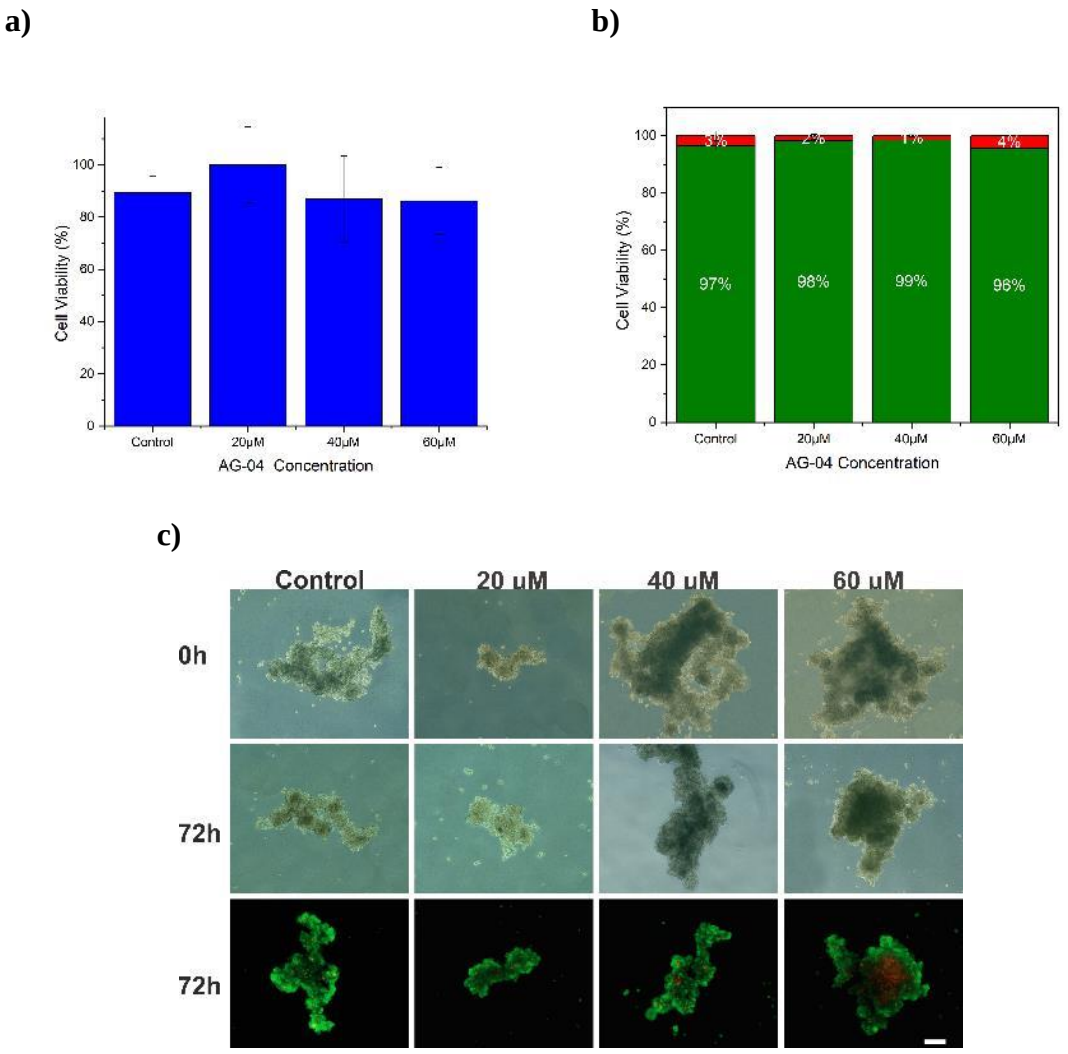


**Figure 108**. Analysis results of AG-04 toxicity in MCF-7 spheroids obtained by MagLev **a)** MTT **b-c)** Live-dead analysis (AG-04 concentration unit: μM) (scale size 200μm)

The effects of CG-03, one of the analogues of the AG-08 molecule, on viability in 3D tumor spheroid models obtained with MCF-7 cells are shown in figure 109 by MTT and live-dead analysis. As a result of the viability tests performed in 2D cell culture in the literature on the CG-03 molecule, the $IC_{50}$ value in MCF-7 cells was calculated as 5.5 μM (Üner et al., 2022). In the 2D experiments carried out within the scope of this research, it was found to be close to 10 μM. Scans performed on 3D tumor spheroid models obtained by the hanging drop method also show that there is a decreasing trend in the viability level as the molecule concentration increases. In the results here, a similar

expected effect appeared as a decreasing trend in viability in both graphs in tumor models produced with MCF-7 cells. 72-hour images showing the change and vitality in the morphology of spheroids due to the molecular effect are shared together for different concentrations in Figure 109-c. It is seen that the increase in the applied CG-03 concentration increases the number of dead cells in the spheroids, and the green color is replaced by red.

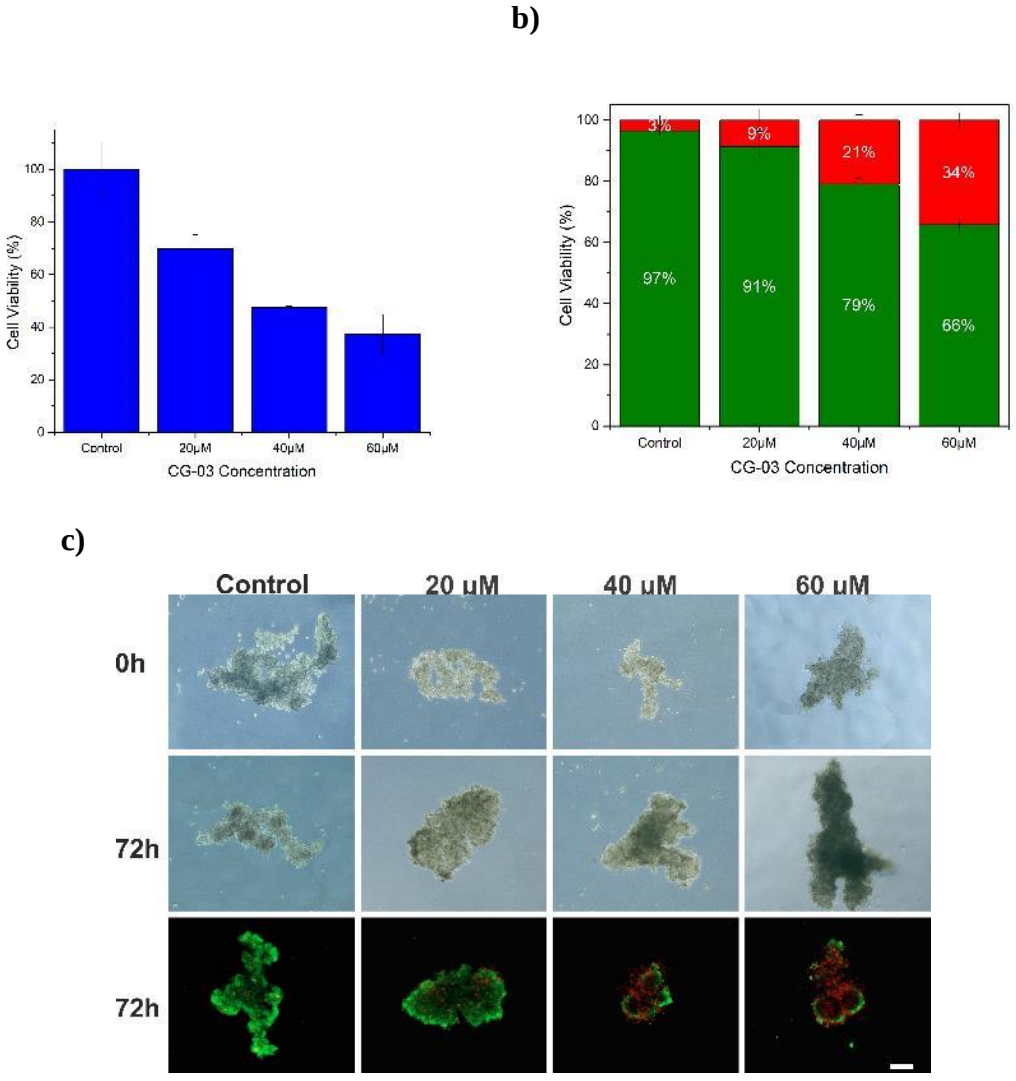


**Figure 109**. Analysis results of CG-03 toxicity in MCF-7 spheroids obtained by MagLev **a)** MTT **b-c)** Live-dead analysis (CG-03 concentration unit: µM) (scale size 200µm).

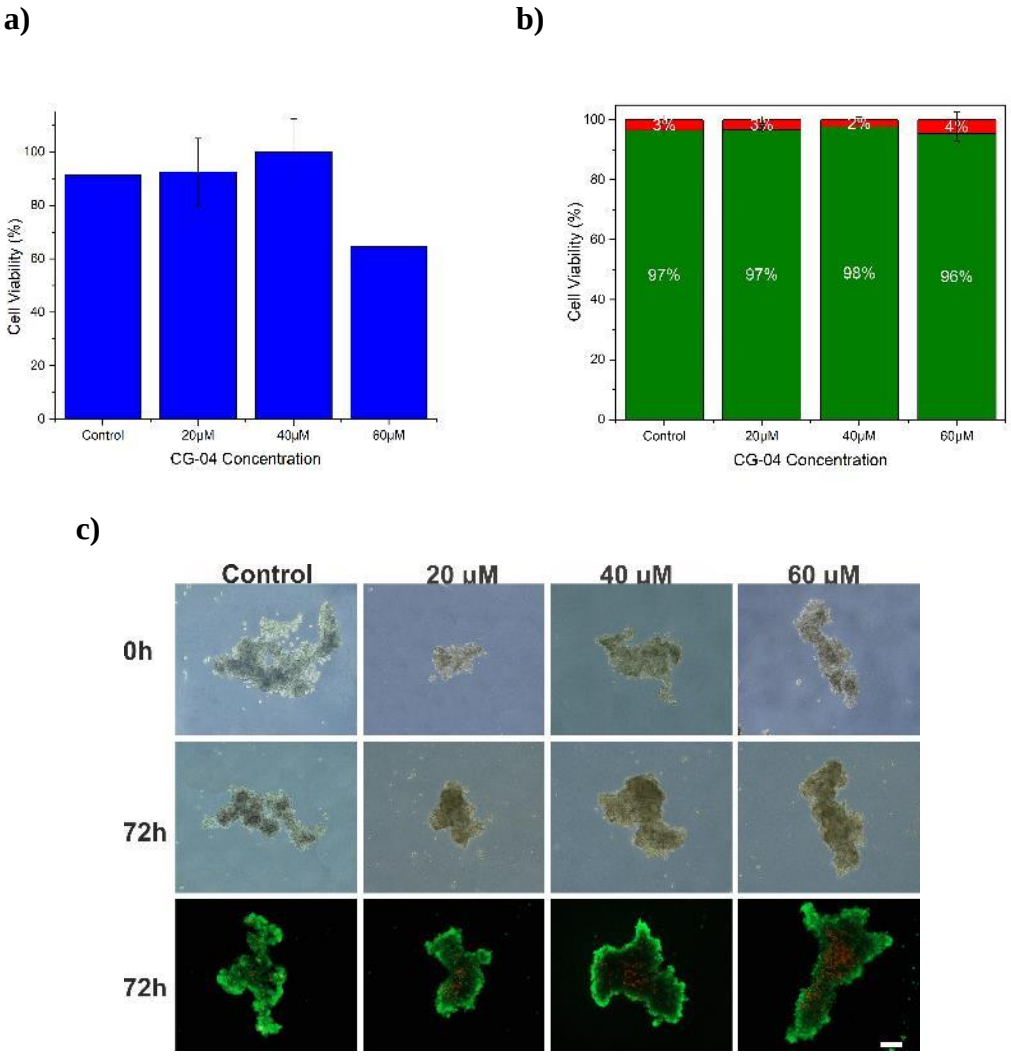


**Figure 110**. Analysis results of CG-04 toxicity in MCF-7 spheroids obtained by MagLev **a)** MTT **b-c)** Live-dead analysis (CG-04 concentration unit: µM) (scale size 200µm).

The effects of the CG-04 molecule, one of the analogues of the AG-08 molecule, on viability in 3D tumor spheroid models obtained with MCF-7 cells are shown in figure 110 by MTT and live-dead analysis. As a result of viability tests performed in 2D cell culture in the literature on the CG-04 molecule, the $IC_{50}$ value in MCF-7 cells was calculated as > 50 µM (Üner et al., 2022). In the 2D experiments carried out within the scope of this research, it was observed that the viability values remained at 80% and above. In addition, in the scans performed on 3D tumor spheroid models obtained by the hanging drop method, the viability level remained at 80% and above despite the increase in molecule concentration. Similarly, in the results shared in the live-dead graph, the viability level remained at 90% and above in the CG-04 concentration range applied in

MCF-7 3D tumor spheroid models. The MTT graph shows a decrease in viability at the 60 μM concentration application, but this value remained above an acceptable level. 72-hour images showing the change and vitality in the morphology of spheroids due to the molecule effect are shared together for different concentrations in Figure 110-c. It was observed that the spheroids maintained their structure and viability despite the increase in the applied CG-04 concentration. Based on the results obtained, the difference in the toxic effects of CG-03 and CG-04 molecules on cancer cells can be clearly seen. It has been proven that AG-04 and CG-04 molecules have similar effects on MCF-7 spheroid models produced by hanging drop and MagLev methods. These results support the literature.

# CHAPTER 4

# CONCLUSION

Within the scope of the completed thesis, different tumor spheroid models were obtained by magnetic levitation, one of the new generations of 3D cell culturing methods. FDA-approved anticancer drug Ptx and sapogenol-derived drug molecules synthesized by Prof. Bedir and his group were screened. Subsequently, the toxicity of paramagnetic contrast agents on four different cancer cell lines (HeLa, SH-SY5Y, HepG2, and MCF-7) was investigated by 2D cell culture analyses. As a result of the toxicity tests, it was determined that concentrations of 50 mM and above caused high toxicity in cells. Due to increased cytotoxicity, paramagnetic agent concentrations of 50 mM and above were not preferred in cell culturing, and low concentrations were used. In the next stage, the necessary parameters (cell number, Gx concentration, and incubation time) were optimized to obtain successful spheroid structures with 3D culturing methods. In addition to the MagLev method, spheroids obtained by the hanging drop method will be used for control purposes as a 3D model. It is known from different studies in the literature that the number of cells used, and the incubation process vary from cell to cell in the formation of spheroids obtained by the hanging drop method (Huang et al., 2020; Hurrell et al., 2018; Shri et al., 2017). Due to this situation, cell number and incubation time were optimized for the four cell lines to be used, based on studies in the literature, and ideal spheroids were obtained to ensure the most accurate results in drug screening studies. In addition to these optimizations, the required paramagnetic agent concentration to obtain spheroids with the MagLev method varies from cell to cell. Whether the number of cells is high or low affects the tendency of cells to cluster together (Jaganathan et al., 2014). Additionally, each cell line can aggregate as a result of a different incubation process. Based on the data from previous studies conducted by our group, optimization studies were carried out for cell number, incubation process, and paramagnetic agent concentration for all four cell lines (Onbas & Arslan Yildiz, 2021; Turker & Arslan-Yildiz, 2018). Due to the characteristic features of the cell lines, much more compact

spheroids could be obtained with HeLa and SH-SY5Y cells. In short and long-term culturing, the viability values of spheroids were examined by live-dead analysis, with the aim of obtaining healthy results independent of time-related deaths in drug trials. Additionally, area, circularity, and viability analyses of the obtained spheroids were performed. Dapi, actin, and collagen immunofluorescence staining of the 3D tumor spheroid models obtained by both methods was performed to observe cell nuclei, cell scaffold formation, and extracellular matrix formation. In the staining results of the models obtained by the hanging drop method, all three signals can be displayed in 24-hour incubated samples, in line with the literature. This confirms that one of the advantages of the hanging drop method is that compact 3D spheroids can be obtained with short-term culturing. In the staining results of the models obtained with the MagLev method, Dapi and Actin signals are marked in 24 hour incubated samples. The collagen signal appears to be very low. After 7 days of incubation, it is seen that the collagen signal increases significantly, while the actin and dapi signals remain approximately at the same level. This situation supports the literature (Onbas & Arslan Yildiz, 2021). It shows that the spheroid structure becomes increasingly compact and a cell-extracellular matrix complex forms over time. It is an important proof that 3D spheroid models obtained with the MagLev method can be used in long-term experiments. One of the important goals of the thesis is to investigate the effects of sapogenol-derived molecules on 3D tumor spheroid models. In order to proceed to this stage, the toxic effects of sapogenol-derived molecules in the 0-30 μM range were investigated in 2D cell culture, and effective concentrations were determined. The $IC_{50}$ values of the sapogenol-derived molecules AG-08, AG-04, CG-03, and CG-04 in 2D cell studies have been shared in the literature (Üner et al., 2019, 2020, 2022). AG-04 and CG-04 molecules were preferred as a negative control to AG-08 and CG-03 molecules, which have been proven to have a toxic effect on cancer cell lines. There are no 3D cell line studies in the literature for the mentioned s. It is known that 3D spheroid models mimic real tissue and tumor physiology much more realistically than 2D cell lines. Upon completion of this study, it is aimed that sapogenol-derived molecules, which have been proven to have toxic effects in 3D tumor spheroid models, will be seen as an important potential drug in cancer treatment. Additionally, the FDA-approved drug Paclitaxel, which has clinically proven anticancer effects, was selected as a positive control for sapogenol-derived molecules. Ptx binds to microtubules and causes inhibition over time, which stops the cell cycle in the G2/M phase and leads to cell death through an apoptotic pathway (Kumar et al., 2010; Riccardi

et al., 1995). In parallel with the literature, the toxic effect of Ptx in the range of 0-200 nM was investigated in 2D cell culture. As a result of sapogenol-derived drug molecules and Ptx screening, different amounts of resistance were encountered in each cell line, and the toxic effects caused by the drugs are at different levels. Based on research in the literature, it is thought that one of the reasons for this situation is cell-molecule interaction. There are differences in the extracellular matrix of each cell, which is likely to affect the toxic effect level of the drug. In addition, receptors that vary from cell to cell may cause differences in the interaction of drug molecules with the cell. This situation also causes the cells to show different levels of resistance to the drug. In the final stage of the project, drug screenings were performed on 3D tumor spheroid models. At this stage, 2D cell culture studies were used in the concentration range, covering the $IC_{50}$ values in the literature, to determine the concentration range investigated. However, 3D cellular models can mimic real tissue physiology much better than 2D models. Therefore, diffusion restriction and high drug resistance are two of the most common situations in 3D cellular models (Dabbagh et al., 2022; Lugert et al., 2019). For this reason, the concentration range of the drug molecules to be investigated was determined at higher concentrations than in 2D studies. In 2D studies conducted in the literature, it has been observed that the expected results were obtained with Ptx in the 0-200 nm concentration range, the viability values decreased to very low levels. The maximum clinical concentration of Ptx is 175 ($mg/m^2$) (Imamura et al., 2015; Riccardi et al., 1995). Based on this, in the calculations made with the area of the petri dishes to be used, screening studies were performed in the 0-400 nM concentration range for Paclitaxel, and the 0-60 μM concentration range was investigated for sapogenol-derived molecules. After obtaining the spheroid structures, molecules/drug were applied, and incubation was performed for 72 hours. Afterwards, toxic effects were measured by the MTT assay and the live-dead test. The results obtained are generally compatible with 2D studies and expectations in the literature. Paclitaxel, AG-08, and CG-03 molecules cause toxic effects in 3D tumor spheroid models and reduce the viability level. As the molecular concentration increases, the strength of this toxic effect also increases. In the statistical analysis results shared in the MTT graphs, it was observed that there was a significant decrease in the cell viability level as the concentration of toxic molecules increased. High viability values were obtained in the analyses performed after the application of AG-04 and CG-04. This situation is compatible with the 2D drug screening data for molecules in the literature. It has been proven that the results of drug screening studies conducted in

2D and 3D cell cultures support each other. With this completed study, a drug screening platform based on Magnetic Levitation, a new generation 3D cell culturing method, was introduced to the literature. Thanks to this method, different cancer models can be investigated in vitro in a 3D model for a longer period of time.

# REFERENCES


Anil-Inevi, M., Delikoyun, K., Mese, G., Tekin, H. C., & Ozcivici, E. 2021. Magnetic levitation assisted biofabrication, culture, and manipulation of 3D cellular structures using a ring magnet based setup. *Biotechnology and Bioengineering*, *118*(12), 4771–4785. https://doi.org/10.1002/bit.27941

Anil-Inevi, M., Yaman, S., Yildiz, A. A., Mese, G., Yalcin-Ozuysal, O., Tekin, H. C., & Ozcivici, E. 2018. Biofabrication of in situ Self Assembled 3D Cell Cultures in a Weightlessness Environment Generated using Magnetic Levitation. *Scientific Reports*, *8*(1). https://doi.org/10.1038/s41598-018-25718-9

Arora, M. 2013. Cell Culture Media: A Review. *Materials and Methods*, *3*. https://doi.org/10.13070/mm.en.3.175

Arslan-Yildiz, A., Yildiz, U. H., Liedberg, B., & Sinner, E. K. 2013. Biomimetic membrane platform: Fabrication, characterization and applications. *Colloids and Surfaces B: Biointerfaces*, *103*, 510–516. https://doi.org/10.1016/j.colsurfb.2012.10.066

Arslan-Yildiz, A., El Assal, R., Chen, P., Guven, S., & Inci, F. 2016. *Towards artificial tissue models: past, present, and future of 3D bioprinting*. https://doi.org/10.1088/1758-5090/8/1/014103

Asghar, W., El Assal, R., Shafiee, H., Pitteri, S., Paulmurugan, R., & Demirci, U. 2015. *Engineering cancer microenvironments for in vitro 3-D tumor models*. https://doi.org/10.1016/j.mattod.2015.05.002

Banerjee, M., & Bhonde, R. R. 2006. Application of hanging drop technique for stem cell differentiation and cytotoxicity studies. *Cytotechnology*, *51*(1), 1–5. https://doi.org/10.1007/s10616-006-9001-z

Bilginer-Kartal, R., & Arslan-Yildiz, A. 2024. Exploring Neuronal Differentiation Profiles in SH-SY5Y Cells through Magnetic Levitation Analysis. *ACS Omega*, *9*(13), 14955–14962. https://doi.org/10.1021/acsomega.3c08962

Bilginer, R., & Arslan Yildiz, A. 2019. Biomimetic Model Membranes as Drug Screening Platform. In *Biomimetic Lipid Membranes: Fundamentals, Applications, and Commercialization* (pp. 225–247). Springer International Publishing. https://doi.org/10.1007/978-3-030-11596-8_10

Bilginer, R., Ozkendir-Inanc, D., Yildiz, U. H., & Arslan-Yildiz, A. 2021. Biocomposite scaffolds for 3D cell culture: Propolis enriched polyvinyl alcohol nanofibers favoring cell adhesion. *Journal of Applied Polymer Science*, *138*(17). https://doi.org/10.1002/app.50287

Boucherit, N., Gorvel, L., & Olive, D. 2020. 3D Tumor Models and Their Use for the Testing of Immunotherapies. In *Frontiers in Immunology* (Vol. 11). Frontiers Media S.A. https://doi.org/10.3389/fimmu.2020.603640

Bumpers, H. L., Janagama, D. G., Manne, U., Basson, M. D., & Katkoori, V. 2015. Nanomagnetic levitation three-dimensional cultures of breast and colorectal cancers. *Journal of Surgical Research*, *194*(2), 319–326. https://doi.org/10.1016/j.jss.2014.12.036

Cortini, M., Macchi, F., Reggiani, F., Vitale, E., Lipreri, M. V., Perut, F., Ciarrocchi, A., Baldini, N., & Avnet, S. 2023. Endogenous Extracellular Matrix Regulates the Response of Osteosarcoma 3D Spheroids to Doxorubicin. *Cancers*, *15*(4). https://doi.org/10.3390/cancers15041221

Crnogorac, M. Đ., Matić, I. Z., Damjanović, A., Janković, N., Krivokuća, A., & Stanojković, T. 2021. 3D HeLa spheroids as a model for investigating the anticancer activity of Biginelli-hybrids. *Chemico-Biological Interactions*, *345*. https://doi.org/10.1016/j.cbi.2021.109565

Dabbagh, S. R., Alseed, M. M., Saadat, M., Sitti, M., & Tasoglu, S. 2022. Biomedical Applications of Magnetic Levitation. In *Advanced NanoBiomed Research* (Vol. 2, Issue 3). John Wiley and Sons Inc. https://doi.org/10.1002/anbr.202100103

Delikoyun, K., Mese, G., Cumhur Tekin, H., & Ozcivici, E. 2021. Axial-circular magnetic levitation assisted biofabrication and manipulation of cellular structures. *BioRxiv*. https://doi.org/10.1101/2021.01.26.428192

Durmus, N. G., Tekin, H. C., Guven, S., Sridhar, K., Yildiz, A. A., Calibasi, G., Ghiran, I., Davis, R. W., Steinmetz, L. M., & Demirci, U. 2015. Magnetic levitation of single cells. *Proceedings of the National Academy of Sciences of the United States of America*, *112*(28), E3661–E3668. https://doi.org/10.1073/pnas.1509250112

Ermis, M., Falcone, N., Roberto de Barros, N., Mecwan, M., Haghniaz, R., Choroomi, A., Monirizad, M., Lee, Y., Song, J., Cho, H. J., Zhu, Y., Kang, H., Dokmeci, M. R., Khademhosseini, A., Lee, J., & Kim, H. J. 2023. Tunable hybrid hydrogels with multicellular spheroids for modeling desmoplastic pancreatic cancer. *Bioactive Materials*, *25*, 360–373. https://doi.org/10.1016/j.bioactmat.2023.02.005

Fennema, E., Rivron, N., Rouwkema, J., van Blitterswijk, C., & De Boer, J. 2013. Spheroid culture as a tool for creating 3D complex tissues. In *Trends in Biotechnology* (Vol. 31, Issue 2, pp. 108–115). https://doi.org/10.1016/j.tibtech.2012.12.003

Ferreira, J. N., Hasan, R., Urkasemsin, G., Ng, K. K., Adine, C., Muthumariappan, S., & Souza, G. R. 2019. A magnetic three-dimensional levitated primary cell culture system for the development of secretory salivary gland-like organoids. *Journal of Tissue Engineering and Regenerative Medicine*, *13*(3), 495–508. https://doi.org/10.1002/term.2809

Fontoura, J. C., Viezzer, C., dos Santos, F. G., Ligabue, R. A., Weinlich, R., Puga, R. D., Antonow, D., Severino, P., & Bonorino, C. 2020. Comparison of 2D and 3D cell culture models for cell growth, gene expression and drug resistance. *Materials Science and Engineering C*, *107*. https://doi.org/10.1016/j.msec.2019.110264

Gerlee, P., A Anderson H Lee, A. R., & A Anderson, A. R. 2010. *DIFFUSION-LIMITED TUMOUR GROWTH: SIMULATIONS AND ANALYSIS*. https://doi.org/10.3934/mbe.2010.7.385

Grimes, D. R., Kelly, C., Bloch, K., & Partridge, M. 2014. A method for estimating the oxygen consumption rate in multicellular tumour spheroids. *Journal of the Royal Society Interface*, *11*(92). https://doi.org/10.1098/rsif.2013.1124

Huang, S. W., Tzeng, S. C., Chen, J. K., Sun, J. S., & Lin, F. H. 2020. A dynamic hanging-drop system for mesenchymal stem cell culture. *International Journal of Molecular Sciences*, *21*(12), 1–22. https://doi.org/10.3390/ijms21124298

Hurrell, T., Ellero, A. A., Masso, Z. F., & Cromarty, A. D. 2018. Characterization and reproducibility of HepG2 hanging drop spheroids toxicology in vitro. *Toxicology in Vitro*, *50*, 86–94. https://doi.org/10.1016/j.tiv.2018.02.013

Idée, J. M., Port, M., Medina, C., Lancelot, E., Fayoux, E., Ballet, S., & Corot, C. 2008. Possible involvement of gadolinium chelates in the pathophysiology of nephrogenic systemic fibrosis: A critical review. In *Toxicology* (Vol. 248, Issues 2–3, pp. 77–88). https://doi.org/10.1016/j.tox.2008.03.012

Imamura, Y., Mukohara, T., Shimono, Y., Funakoshi, Y., Chayahara, N., Toyoda, M., Kiyota, N., Takao, S., Kono, S., Nakatsura, T., & Minami, H. 2015. Comparison of 2D- and 3D-culture models as drug-testing platforms in breast cancer. *Oncology Reports*, *33*(4), 1837–1843. https://doi.org/10.3892/or.2015.3767

Jaganathan, H., Gage, J., Leonard, F., Srinivasan, S., Souza, G. R., Dave, B., & Godin, B. 2014. Three-dimensional in vitro co-culture model of breast tumor using magnetic levitation. *Scientific Reports*, *4*. https://doi.org/10.1038/srep06468

Jensen, C., Shay, C., & Teng, Y. 2022. The New Frontier of Three-Dimensional Culture Models to Scale-Up Cancer Research. *Methods in Molecular Biology*, *2343*, 3–18. https://doi.org/10.1007/978-1-0716-1558-4_1

Jeong, Y. G., Lee, J. S., Shim, J. K., & Hur, W. 2016. A scaffold-free surface culture of B16F10 murine melanoma cells based on magnetic levitation. *Cytotechnology*, *68*(6), 2323–2334. https://doi.org/10.1007/s10616-016-0026-7

Kumar, S., Mahdi, H., Bryant, C., Shah, J. P., Garg, G., & Munkarah, A. 2010. Clinical trials and progress with paclitaxel in ovarian cancer. In *International Journal of Women's Health* (Vol. 2, Issue 1, pp. 411–427). https://doi.org/10.2147/IJWH.S7012

Langer, R., & Vacanti, J. P. 1993. *Tissue Engineering*. https://doi.org/10.1126/science.8493529

Leung, B. M., Lesher-Perez, S. C., Matsuoka, T., Moraes, C., & Takayama, S. 2015. Media additives to promote spheroid circularity and compactness in hanging drop platform. *Biomaterials Science*, *3*(2), 336–344. https://doi.org/10.1039/c4bm00319e

Liebmann, J. E., Cook, J. A., Lipschultz, C., Teague, D., Fisher, J., & Mitchell, J. B. 1993. Cytotoxic studies of pacfitaxel (Taxol®) in human tumour cell lines. In *Br. J. Cancer*. https://doi.org/10.1038/bjc.1993.488

Longhin, E. M., El Yamani, N., Rundén-Pran, E., & Dusinska, M. 2022. The alamar blue assay in the context of safety testing of nanomaterials. *Frontiers in Toxicology*, *4*. https://doi.org/10.3389/ftox.2022.981701

Lugert, S., Unterweger, H., Mühlberger, M., Janko, C., Draack, S., Ludwig, F., Eberbeck, D., Alexiou, C., & Friedrich, R. P. 2019. Cellular effects of paclitaxel-loaded iron oxide nanoparticles on breast cancer using different 2D and 3D cell culture models. *International Journal of Nanomedicine*, *14*, 161–180. https://doi.org/10.2147/IJN.S187886

Marin, V., Kaplanski, G., Gres, S., Farnarier, C., Bongrand´`, P., & Bongrand´`, B. 2001. Endothelial cell culture: protocol to obtain and cultivate human umbilical endothelial cells. In *Journal of Immunological Methods* (Vol. 254). https://doi.org/10.1016/S0022-1759(01)00408-2

Marques, I. A., Fernandes, C., Tavares, N. T., Pires, A. S., Abrantes, A. M., & Botelho, M. F. 2022. Magnetic-Based Human Tissue 3D Cell Culture: A Systematic Review. In *International Journal of Molecular Sciences* (Vol. 23, Issue 20). MDPI. https://doi.org/10.3390/ijms232012681

Muguruma, M., Teraoka, S., Miyahara, K., Ueda, A., Asaoka, M., Okazaki, M., Kawate, T., Kuroda, M., Miyagi, Y., & Ishikawa, T. 2020. Differences in drug sensitivity between two-dimensional and three-dimensional culture systems in triple-negative breast cancer cell lines. *Biochemical and Biophysical Research Communications*, *533*(3), 268–274. https://doi.org/10.1016/j.bbrc.2020.08.075

Namkaew, J., Jaroonwitchawan, T., Rujanapun, N., Saelee, J., & Noisa, P. 2018. Combined effects of curcumin and doxorubicin on cell death and cell migration of SH-SY5Y human neuroblastoma cells. *In Vitro Cellular & Developmental Biology-Animal,*. https://doi.org/10.1007/s11626-018-0288-9

Nath, S., & Devi, G. R. 2016. Three-dimensional culture systems in cancer research: Focus on tumor spheroid model. In *Pharmacology and Therapeutics* (Vol. 163, pp. 94–108). Elsevier Inc. https://doi.org/10.1016/j.pharmthera.2016.03.013

Onbas, R., & Arslan Yildiz, A. 2021. Fabrication of Tunable 3D Cellular Structures in High Volume Using Magnetic Levitation Guided Assembly. *ACS Applied Bio Materials*, *4*(2), 1794–1802. https://doi.org/10.1021/acsabm.0c01523

Onbas, R., & Arslan Yildiz, A. 2023. Biopatterning of 3D Cellular Model by Contactless Magnetic Manipulation for Cardiotoxicity Screening. *Tissue Engineering. Part A*. https://doi.org/10.1089/TEN.TEA.2023.0197

Ozefe, F., & Arslan Yildiz, A. 2020. Smartphone-assisted Hepatitis C detection assay based on magnetic levitation. *Analyst*, *145*(17), 5816–5825. https://doi.org/10.1039/d0an01111h

Özmen, E., Yıldırım, Ö., & Arslan-Yıldız, A. 2023. Bioprinting of hydrogels for tissue engineering and drug screening applications. *Advances in Biomedical Polymers and Composites: Materials and Applications*, 183–221. https://doi.org/10.1016/B978-0-323-88524-9.00028-0

Parant, M., Sohm, B., Flayac, J., Perrat, E., Chuburu, F., Cadiou, C., Rosin, C., & Cossu-Leguille, C. 2019. Impact of gadolinium-based contrast agents on the growth of fish cells lines. *Ecotoxicology and Environmental Safety*, *182*. https://doi.org/10.1016/j.ecoenv.2019.109385

Parfenov, V. A., Khesuani, Y. D., Petrov, S. V, Karalkin, P. A., Koudan, E. V, Nezhurina, E. K., DAS Pereira, F., Krokhmal, A. A., Gryadunova, A. A., Bulanova, E. A., Vakhrushev, I. V, Babichenko, I. I., Kasyanov, V., Petrov, O. F., Vasiliev, M. M., Brakke, K., Belousov, S. I., Grigoriev, T. E., Osidak, E. O., … Mironov, V. A. 2020. *B I O E N G I N E E R I N G Magnetic levitational bioassembly of 3D tissue construct in space*. https://doi.org/10.1126/sciadv.aba4174

Raghavan, S., Mehta, P., Horst, E. N., Ward, M. R., Rowley, K. R., & Mehta, G. 2016. *Comparative analysis of tumor spheroid generation techniques for differential in vitro drug toxicity*. https://doi.org/10.18632/oncotarget.7659

Raghavan, S., Ward, M. R., Rowley, K. R., Wold, R. M., Takayama, S., Buckanovich, R. J., & Mehta, G. 2015. Formation of stable small cell number three-dimensional ovarian cancer spheroids using hanging drop arrays for preclinical drug sensitivity assays. *Gynecologic Oncology*, *138*(1), 181–189. https://doi.org/10.1016/j.ygyno.2015.04.014

Riccardi, A., Servidei, T., Tornesello, A., Puggioni, P., Mastrangelo, S., Rumi, C., & Riccardi, R. 1995. Cytotoxicity of paclitaxel and docetaxel in human neuroblastoma cell lines. *European Journal of Cancer*, *31*(4), 494–499. https://doi.org/10.1016/0959-8049(95)00056-O

Rice, W. R. 1989. ANALYZING TABLES OF STATISTICAL TESTS. *Evolution*, *43*(1), 223–225. https://doi.org/10.1111/j.1558-5646.1989.tb04220.x

Rimann, M., Laternser, S., Gvozdenovic, A., Muff, R., Fuchs, B., Kelm, J. M., & Graf-Hausner, U. 2014. An in vitro osteosarcoma 3D microtissue model for drug development. *Journal of Biotechnology*, *189*, 129–135. https://doi.org/10.1016/j.jbiotec.2014.09.005

Sabino, L. G., Menezes, P. F. C., Bagnato, V. S., Souza, G., Killian, T. C., & Kurachi, C. 2014. Three-dimensional cell culturing by magnetic levitation for evaluating efficacy/toxicity of photodynamic therapy. *Optical Methods for Tumor Treatment and Detection: Mechanisms and Techniques in Photodynamic Therapy XXIII*, *8931*, 893109. https://doi.org/10.1117/12.2040659

Sarigil, O., Anil-Inevi, M., Firatligil-Yildirir, B., Unal, Y. C., Yalcin-Ozuysal, O., Mese, G., Tekin, H. C., & Ozcivici, E. 2021. Scaffold-free biofabrication of adipocyte structures with magnetic levitation. *Biotechnology and Bioengineering*, *118*(3), 1127–1140. https://doi.org/10.1002/bit.27631

Seo, J. Y., Park, S. Bin, Kim, S. Y., Seo, G. J., Jang, H. K., & Lee, T. J. 2023. Acoustic and Magnetic Stimuli-Based Three-Dimensional Cell Culture Platform for Tissue Engineering. In *Tissue Engineering and Regenerative Medicine* (Vol. 20, Issue 4, pp. 563–580). Korean Tissue Engineering and Regenerative Medicine Society. https://doi.org/10.1007/s13770-023-00539-8

Sevimli-Gur, C., Cetin, B., Akay, S., Gulce-Iz, S., & Yesil-Celiktas, O. 2013. Extracts from Black Carrot Tissue Culture as Potent Anticancer Agents. *Plant Foods for Human Nutrition*, *68*(3), 293–298. https://doi.org/10.1007/s11130-013-0371-z

Shri, M., Agrawal, H., Rani, P., Singh, D., & Onteru, S. K. 2017. Hanging drop, a best three-dimensional (3D) culture method for primary buffalo and sheep hepatocytes. *Scientific Reports*, *7*(1). https://doi.org/10.1038/s41598-017-01355-6

Souza, G. R., Molina, J. R., Raphael, R. M., Ozawa, M. G., Stark, D. J., Levin, C. S., Bronk, L. F., Ananta, J. S., Mandelin, J., Georgescu, M. M., Bankson, J. A., Gelovani, J. G., Killian, T. C., Arap, W., & Pasqualini, R. 2010. Three-dimensional tissue culture based on magnetic cell levitation. *Nature Nanotechnology*, *5*(4), 291–296. https://doi.org/10.1038/nnano.2010.23

Sözmen, A. B., & Arslan-Yildiz, A. 2024. Utilizing Magnetic Levitation to Detect Lung Cancer-Associated Exosomes. *ACS Sensors*. https://doi.org/10.1021/acssensors.4c00011

Sözmen, A. B., & Arslan-Yıldız, A. 2022. Sensitive and rapid protein assay via magnetic levitation. *Biosensors and Bioelectronics: X*, *10*. https://doi.org/10.1016/j.biosx.2022.100137

Tavafoghi, M., Sheikhi, A., Tutar, R., Jahangiry, J., Baidya, A., Haghniaz, R., & Khademhosseini, A. 2020. Engineering Tough, Injectable, Naturally Derived, Bioadhesive Composite Hydrogels. *Advanced Healthcare Materials*, *9*(10). https://doi.org/10.1002/adhm.201901722

Tepe, U., Aslanbay Guler, B., & Imamoglu, E. 2023. Applications and sensory utilizations of magnetic levitation in 3D cell culture for tissue Engineering. In *Molecular Biology Reports* (Vol. 50, Issue 8, pp. 7017–7025). Springer Science and Business Media B.V. https://doi.org/10.1007/s11033-023-08585-0

Timmins, N. E., & Nielsen, L. K. 2007. *Generation of Multicellular Tumor Spheroids by the Hanging-Drop Method*. https://doi.org/10.1007/978-1-59745-443-8_8

Tseng, H., Gage, J. A., Raphael, R. M., Moore, R. H., Killian, T. C., Grande-Allen, K. J., & Souza, G. R. 2013. Assembly of a three-dimensional multitype bronchiole coculture model using magnetic levitation. *Tissue Engineering - Part C: Methods*, *19*(9), 665–675. https://doi.org/10.1089/ten.tec.2012.0157

Turker, E., & Arslan-Yildiz, A. 2018. Recent Advances in Magnetic Levitation: A Biological Approach from Diagnostics to Tissue Engineering. In *ACS Biomaterials Science and Engineering* (Vol. 4, Issue 3, pp. 787–799). American Chemical Society. https://doi.org/10.1021/acsbiomaterials.7b00700

Türker, E., Demirçak, N., & Arslan-Yildiz, A. 2018. Scaffold-free three-dimensional cell culturing using magnetic levitation. *Biomaterials Science*, *6*(7), 1745–1753. https://doi.org/10.1039/c8bm00122g

Üner, G., Bedir, E., Serçinoğlu, O., & Kırmızıbayrak, P. B. 2022. Non-apoptotic cell death induction via sapogenin based supramolecular particles. *Scientific Reports* |, *12*. https://doi.org/10.1038/s41598-022-17977-4

Üner, G. 2019. Preparation Of Some Semi-Synthetic Saponin Analogs and Investigation Of Their Mechanism Of Action On Necrotic Cell Death (Master's thesis, Izmir Institute of Technology (Turkey))

Üner, G., Tag`, Ö., Erzurumlu, Y., Kirmizibayrak, P. B., & Bedir, E. 2020. Identification of a Noncanonical Necrotic Cell Death Triggered via Enhanced Proteolysis by a Novel Sapogenol Derivative. *Chemical Research in Toxicology*, *33*(11), 2880–2891. https://doi.org/10.1021/acs.chemrestox.0c00339

Van Tonder, A., Joubert, A. M., & Cromarty, A. D. 2015. Limitations of the 3-(4,5-dimethylthiazol-2-yl)-2,5-diphenyl-2H-tetrazolium bromide (MTT) assay when compared to three commonly used cell enumeration assays. *BMC Research Notes*, *8*(1). https://doi.org/10.1186/s13104-015-1000-8

Wang, S., Wang, X., Boone, J., Wie, J., Yip, K. P., Zhang, J., Wang, L., & Liu, R. 2017. Application of Hanging Drop Technique for Kidney Tissue Culture. *Kidney and Blood Pressure Research*, *42*(2), 220–231. https://doi.org/10.1159/000476018

Yesil-Celiktas, O., Hassan, S., Miri, A. K., Maharjan, S., Al-kharboosh, R., Quiñones-Hinojosa, A., & Zhang, Y. S. 2018. Mimicking Human Pathophysiology in Organ-on-Chip Devices. In *Advanced Biosystems* (Vol. 2, Issue 10). Wiley-VCH Verlag. https://doi.org/10.1002/adbi.201800109

Yesil-Celiktas, O., Sevimli, C., Bedir, E., & Vardar-Sukan, F. 2010. Inhibitory effects of rosemary extracts, carnosic acid and rosmarinic acid on the growth of various human cancer cell lines. *Plant Foods for Human Nutrition*, *65*(2), 158–163. https://doi.org/10.1007/s11130-010-0166-4

Yildirim, Ö., & Arslan-Yildiz, A. 2022. Development of a hydrocolloid bio-ink for 3D bioprinting. *Biomaterials Science*, *10*(23), 6707–6717. https://doi.org/10.1039/d2bm01184k

Yildirim-Semerci, Ö., Bilginer-Kartal, R., & Arslan-Yildiz, A. 2024. Arabinoxylan-based psyllium seed hydrocolloid: Single-step aqueous extraction and use in tissue engineering. *International Journal of Biological Macromolecules*, *270*, 131856. https://doi.org/10.1016/J.IJBIOMAC.2024.131856

Yilmaz, Ö., & Sakarya, S. 2018. Is 'Hanging Drop' a Useful Method to Form Spheroids of Jimt, Mcf-7, T-47d, Bt-474 That are Breast Cancer Cell Lines. *Single Cell Biology*, *07*(01). https://doi.org/10.4172/2168-9431.1000170

Zanoni, M., Piccinini, F., Arienti, C., Zamagni, A., Santi, S., Polico, R., Bevilacqua, A., & Tesei, A. 2016. 3D tumor spheroid models for in vitro therapeutic screening: A systematic approach to enhance the biological relevance of data obtained. *Scientific Reports*, *6*. https://doi.org/10.1038/srep19103

Zhu, Y., Kang, E., Wilson, M., Basso, T., Chen, E., Yu, Y., & Li, Y.-R. 2022. 3D Tumor Spheroid and Organoid to Model Tumor Microenvironment for Cancer Immunotherapy. *Organoids*, *1*(2), 149–167. https://doi.org/10.3390/organoids1020012